



AECENAR

Association for **Economical and Technological Cooperation**
in the **Euro-Asian and North-African Region**

www.aecenar.com



مركز أبحاث تكنولوجيا العمليات الكيميائية

Institute for Chemical Process Technology (ICPT)
<http://aecenar.com/institutes/icpt>

ICPT

ANNUAL REPORT 2022

Editor:

Maryam EL REZ

With contribution of:

Abdullah Kassem	Othman Dhaybi
Ihab Wahbi	Abdel Rahman Hammoud
Jana Hammoud	Abdullah Mourad

Last Update:

02.01.2023 13:08

Table of Contents

Preface.....	1
Introduction.....	2
Project 1: Multistage electrolysis (ICPT - MSE).....	3
1.1. Position of Multistage electrolysis project.....	3
1.2. Mechanical design.....	3
1) Electrolysis multistage design overview.....	4
2) Design of electrolysis for steps 1, 2 & 3 and for steps 4 & 5.....	4
1.3. What's Next.....	11
Project 2: Water electrolysis (ICPT - WE).....	13
2.1. Electrolyser introduction.....	13
2.2. PCS design.....	13
2.3. Calculating the current and the voltage for the existing cells.....	14
1) The bigger cells in which the distance between the electrodes is 3.6 cm.....	14
2) The smaller cells in which the distance between the electrodes is 1.8 cm.....	14
2.4. Calculating the current the voltage and the distance between electrodes of the multistage electrolyser cell.....	14
2.5. Realization / implementation - Mechanical realization.....	15
1) System overview.....	15
2) Pipe installation from O ₂ and H ₂ condenser to fuel burner with filters and expansion tanks.....	16
3) H ₂ burning kit.....	21
4) Nitrogen can pipe installation.....	21
5) Level sensor.....	22
2.6. Process control system realization (PLC + GUI).....	23
1) Process control system for the Electrolyzer system.....	24
2) PLC panel.....	25
3) PLC Control Panel - Wiring Diagram.....	27
4) Instruments (Valves, Level Control Sensors).....	27

5) GUI- Electrolyzer Design	29
2.7. Electrolysis system test specifications	31
1) Pre-starting	31
2) Electrolysis operation method	32
2.8. Electrolyser system test.....	32
1) Test 22.06.2022 – Hydraulic test of pipes.....	32
2) Test 04.07.2022 – Electrolysis	34
3) Test 04.07.2022 – Electrolysis whole system test	35
4) 05.07.2022 – Electrolysis whole system test	37
5) Test #2: 05.07.2022 – Electrolysis whole system.....	39
6) 19.07.2022 – Whole system test with another power supply	40
7) 05.07.2022 – All system test with only one cell connected	43
8) 29.07.2022 – Test whether the membrane is ruptured	45
9) 14.11.2022 – Electrolysis test	48
10) 15/12/2022 - System test.....	52
2.9. What's new	56

Project 3: Ammonia production (ICPT - AP)..... 58

3.1. Position of AP project.....	58
3.2. Introduction.....	58
1) General Introduction.....	58
2) Properties	59
3) Structure.....	60
4) Amphotericity.....	60
5) Self-dissociation	61
6) Combustion	61
7) Formation of other compounds	62
8) History	62
3.3. Applications	63
1) Fertilizer.....	63
2) Precursor to nitrogenous compounds.....	64
3) Fuel	64
4) Solvent.....	67
5) Cleansing agent	67
6) Fermentation.....	67
7) Antimicrobial agent for food products	67

8) What prospects does green ammonia have?.....	65
3.4. Electrochemical Synthesis of Ammonia	68
1) Electrochemical Production (Electrolysis).....	68
2) Electrochemical synthesis of High temperatures.....	79
3) Electrochemical synthesis at intermediate temperature	70
4) Electrochemical synthesis at Low temperatures	74
5) Factor that effect the production	76
3.5. AP system concept.....	88
1) FreeCAD design.....	88
2) Flow chart.....	90
3.6. Characterization: Ammonia synthesis and measurement.....	91
3.7. AP System Realization	91
1) Anode Preparation	91
2) Cathaode preparation.....	93
3.8. AP Requirements / Experimental.....	94
1) Materials and apparatus	94
2) Preparation of cathode and anode and assembly of the single cell	91
3.9. What's next	93
Project 4: Liquefaction of Oxygen (ICPT - LOx).....	98
4.1. Position of LOx project.....	98
4.2. LOx introduction	98
4.3. Cooling component	99
4.4. Project overview	99
1) Overview flow chart	99
2) Pipe sizing.....	100
3) LOx cycle calculation.....	101
4) Yield factor.....	101
4.5. Heat exchanger	102
1) Type of heat exchanger	102
2) Material of Helical Coil Heat Exchanger.....	105
3) Design of heat exchanger	105
4) HX FreeCAD design and size (v0.17)	106
5) Heat exchanger - Thermal calculation	110
6) Design calculation	110

7) Measurement summary of the Helical coil heat exchanger	113
8) List of HX prices	113
4.6. Cooling pipes (Inside kelvinator refrigerator).....	114
1) Sizing calculation	114
2) Freecad Design	115
4.7. Compressor	118
1) Specifications of compressor	118
2) Calculation of rated capacity.....	118
4.8. Expansion valve	118
1) Pressure sensor	119
2) Solenoid valve	119
3) Principle of two phase separator	121
4) Separator calculation	121
5) Sizing of separator	122
6) Design of separator	123
4.9. Cryogenic insulation material for LOx prototype	125
1) Flexible EPDM pipe insulation [5][6].....	125
2) Cryogenic insulation materials [7][8]	126
4.10. Operating system.....	126
1) Preparing the system for operation:.....	126
2) Operation system	127
4.11. LOx PCS implementation.....	128
1) The process control system for the LOX system.....	128
2) Graphical user interface (version 2022)	125
3) The material used	126
4) Control panel wiring diagram	127
4.12. What's next.....	131
Project 5: Biogas (ICPT - Biogas)	133
5.1. Position of biogas project.....	133
5.2. Méthanisation: Processes, conditions, étapes,	133
1) Model size	133
2) Bilan des matières	133
3) Systèmes de production du biogaz.....	133
4) Biogaz dimensions.....	136
5) Biogas steps	138

6) Features of the agitator.....	144
5.3. Biogas production from municipal waste	148
5.4. Wet digestion	148
5.5. System concept / system design	152
1) Raw materials for biogas production.....	152
2) Advantages of biogas production.....	152
3) Components of biogas plants	153
4) Points to be considered for construction of a biogas plant	153
5.6. 18.10.2022 – Proposal FreeCAD design	154
5.7. Design notes.....	155
5.8. Update design - Version 11-12.11.22	157
5.9. Mechanical Realization.....	159
1) Main Fermenter.....	159
2) Outlet.....	161
3) Flanges	162
5.10. Real design.....	163
5.11. What's next.....	165
Project 6: Gas Turbine for Methane gas (ICPT – GTM)	167
6.1. Position of Gas turbine project.....	167
6.2. Relationship between gas turbine and fuel burner	167
6.3. Fuel Burner Testrig	167
1) FreeCAD design of fuel burner stand.....	167
2) Design of fuel burner stand.....	168
6.4. Gas turbine pieces.....	173
1) Moving blade piece.....	173
2) Stator blade piece.....	173
3) Moving blade holder.....	174
4) Stator blade holder.....	174
5) Spacer ring.....	175
6) Cover.....	175
7) Bridge	176
8) Gas turbine integrated with fuel burner.....	176
6.5. Gas turbine pieces - FreeCAD design.....	177
1) Stator.....	177

2) Turbine cover A.....	177
3) Turbine cover B	178
4) Turbine	179
5) Complete turbine	179
6) Complete turbine expanded	180
7) Assembly.....	180
8) Assembly expanded.....	181
6.6. Gas turbine compressor	179
1) Compressor impeller.....	181
2) Compressor diffuser.....	182
6.7. Combustion chamber parts With FreeCAD design	182
1) Cap.....	182
2) Primary zone	183
3) Intermediate zone	183
4) Dilution zone	184
5) Combustion chamber.....	184
6) Alternative Fuel burner combustion chamber.....	185
6.8. What's next.....	185
Project 7: Ashes Recycling (ICPT – AR)	187
7.1. Position of Ashes recycling project.....	187
7.2. Ashes Recycling PCS Implementation.....	187
1) The process control system for the Ashes Recycling system.....	187
2) The Ashes Recycling system.....	187
3) The Material Used	191
4) PLC Panel	191
5) Terminal Block of Panel.....	192
6) Control Panel Wiring.....	193
7) Operating steps.....	194
8) Algorithm	194
9) Graphical user interface	196
7.3. Ashes Recycling System Test Specifications	198
1) Before using	198
2) Follow these steps	198
7.4. Operation of ashes recycling system	199
7.5. Requirements	199

7.6. What's next.....	199
Project 8: Analytical Chemistry Lab.....	201
Project 9: Metallurgical Lab.....	203
9.1. Position of Metallurgical Lab project.....	203
9.2. Iron melting Test.....	203
References.....	206

Preface



This report contains details of the ICPT Institute projects that we carried out for the year 2022. These projects include the old ones that have been continued, such as the Electrolyser project, the Oxygen liquefaction project and the Ashes recycling project. It also reviews new projects such as the Multistage electrolysis, Ammonia project, the Biogas project, the Gas turbine project, the Analytical Lab and the metallurgical Lab.

Introduction

In 2022, the ICPT Institute will be responsible for **9 projects**; Three of them were started in the past years and this year they were continued, and four new projects were attached to the institute this year.

For projects started in previous years (2021 and earlier) and continued in 2022: **Electrolyser project, Oxygen liquefaction project and Ashes recycling project.**

For the projects added to the ICPT Institute this year (2022): **Multistage electrolyser, Ammonia production project, Gas turbine project, Biogas project, Analytical Lab and Metallurgical Lab.**

In the following sections, we will talk about each project in detail; What is it, where did it arrive before 2022, details that were added this year, and finally what should be completed with it.

Project 1: Multistage electrolysis (ICPT - MSE)

1.1. Position of Multistage electrolysis project

Work on this project will begin this year. The project was studied theoretically, and the first part of the project was designed, but it was not implemented, provided that the first part and the remaining parts will be implemented in the following years.

1.2. Mechanical design

In this paragraph we will present the mechanical design of multistage electrolysis

1) Electrolysis multistage design overview

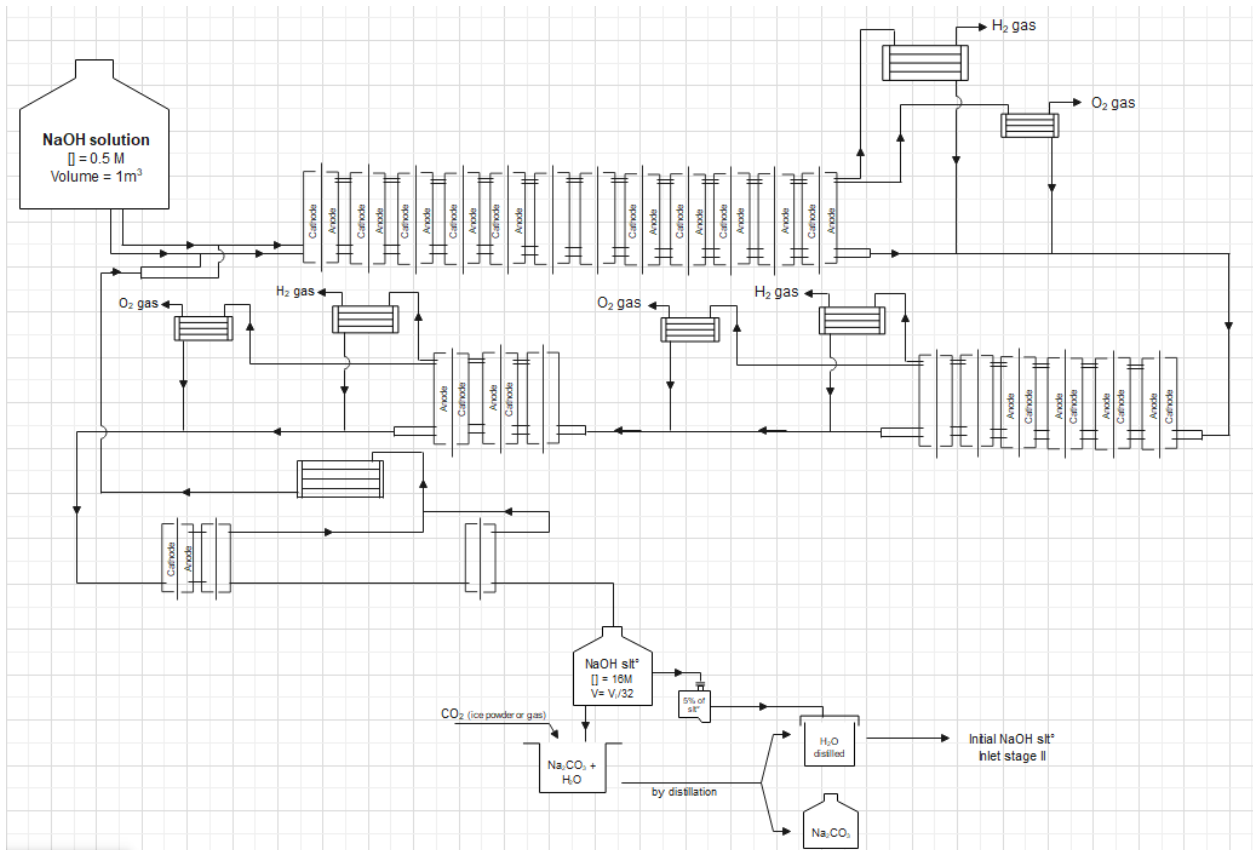
The process is divided into 3 parts:

- Part 1: Multistage electrolysis
- Part 2: Add carbon dioxide to the electrolyte solution
- Part 3: Distillation of the mixture

The multistage of electrolysis, as its name indicates, consists of several successive stages. The first part usually consists of five consecutive stages. The first three stages are similar to each other with a difference in volume as it shrinks to half in the second stage, and again to half in the next stage. As for the other two stages (stage 4 and 5), they are similar to each other and are not similar to the first three stages of design, while maintaining the size reduction in half between each stage and the next.



25052022_multistage-GUI Stage 1.eddx



 **N.B.:**

This Overview is not complete; it lacks pumps, compressors, sanitary installations for cooling water as well as electrical connections.

2) Design of electrolysis for steps 1, 2 & 3 and for steps 4 & 5

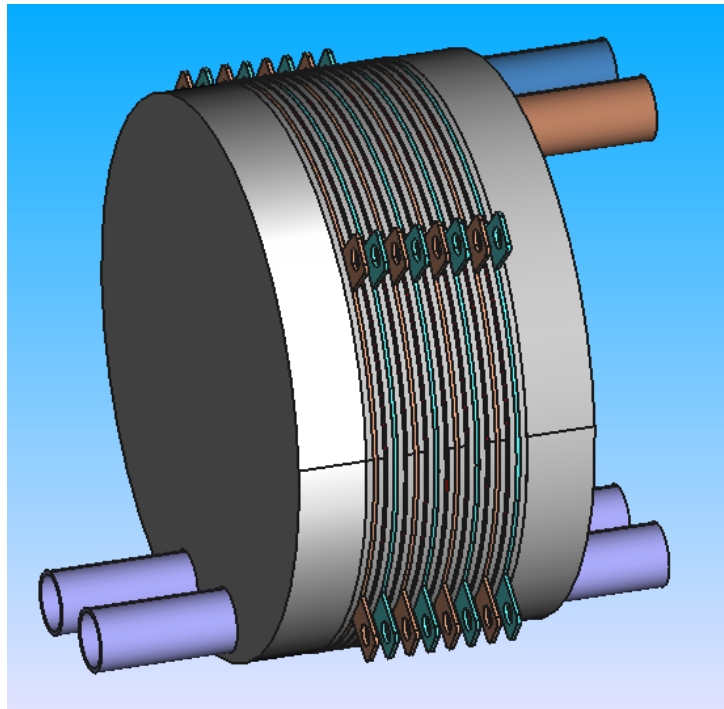
Electrolysis in stage 1 is divided to 5 steps. Step 1, 2 & 3 the production of hydrogen & oxygen separately, while each step 4 & 5 in which produces hydrogen and oxygen mixture to be burned.

In this paragraph, designs for each step of electrolysis multistage will be represented.

a) Electrolysis step 1, 2 & 3 All components -compressed-

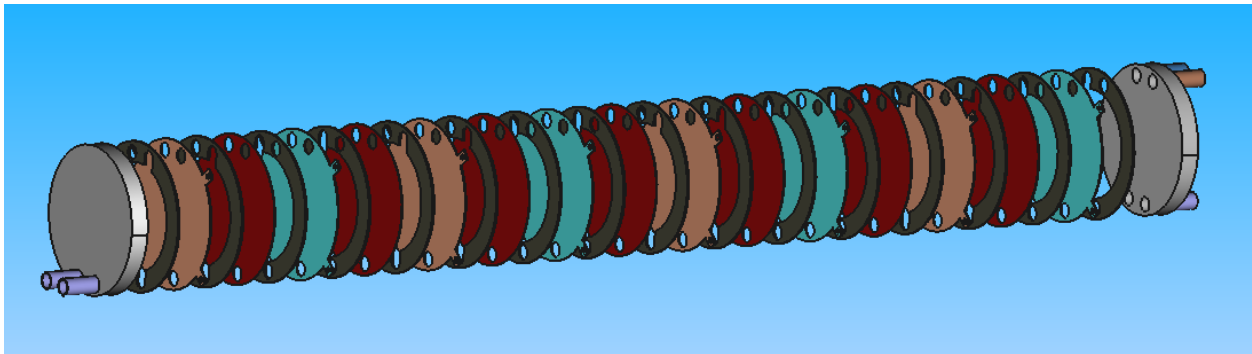


20052022_all components COMPRESSED_step1,2,3.FCStd



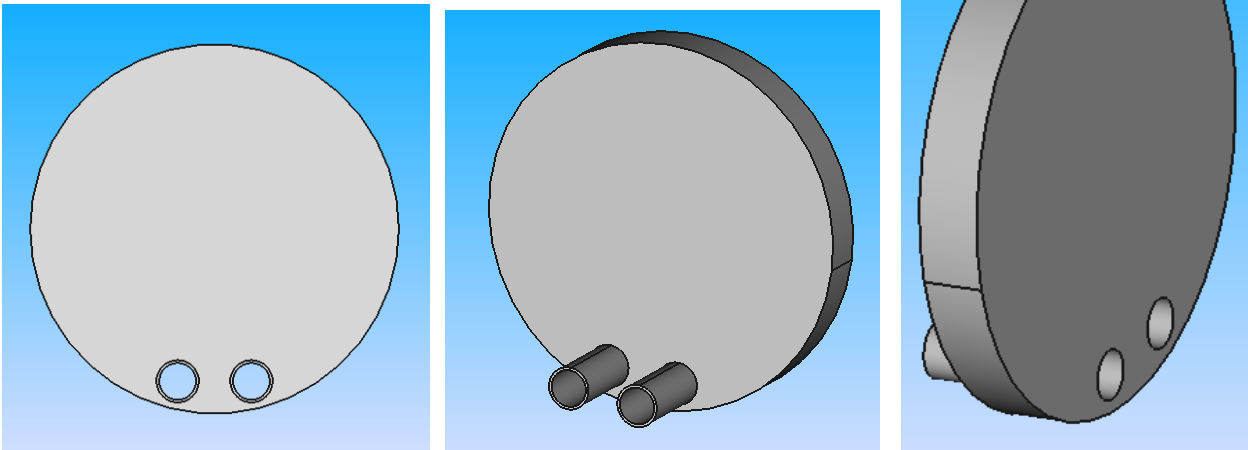
b) Electrolysis step 1, 2 & 3 All components -exploded-


20052022_all
components EXPLO5



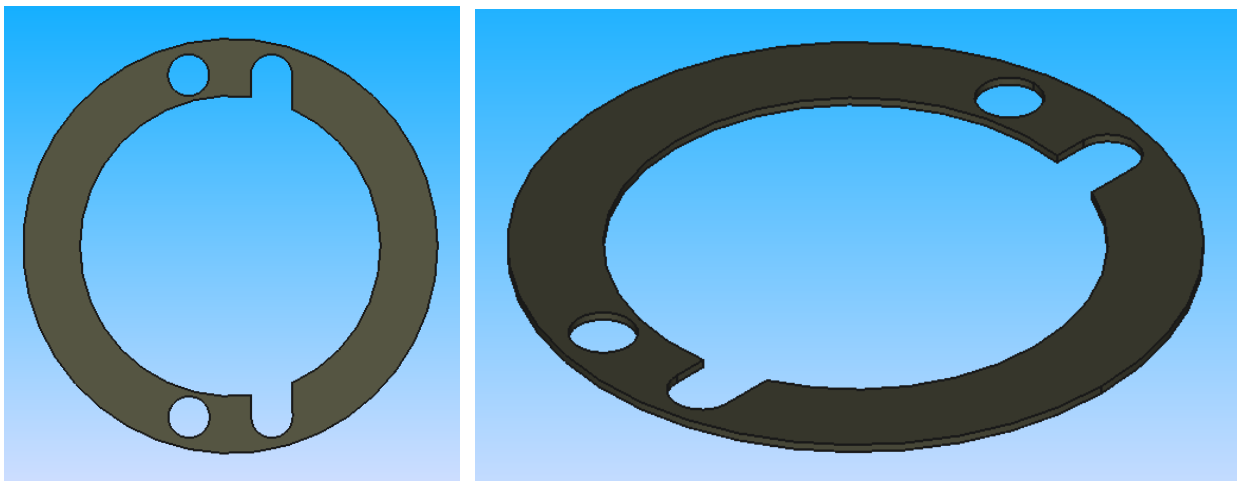
c) Electrolysis step 1, 2 & 3 End plate1 (inlet solution)


12052022_end plate
1 (inlet slit)_step1,2,3



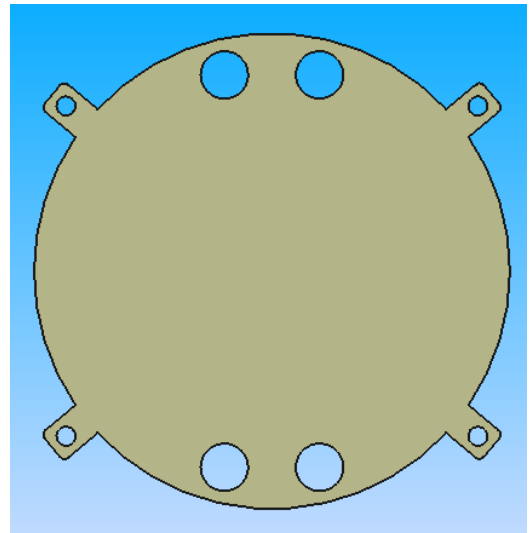
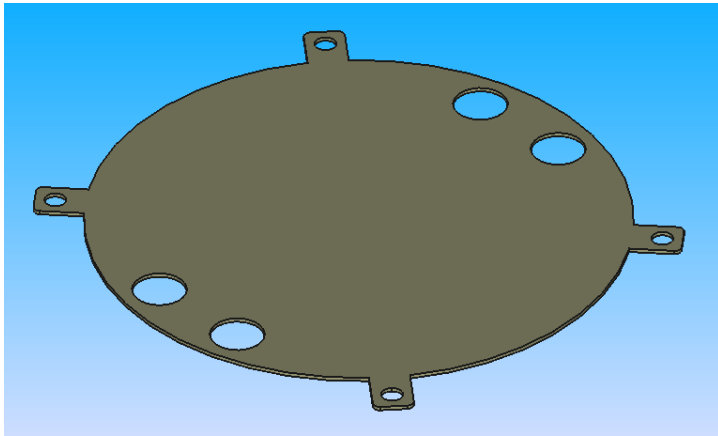
d) Electrolysis step 1, 2 & 3 Gasket


12052022_Gasket
_step1,2,3.FCStd



e) Electrolysis step 1, 2 & 3 Electrode

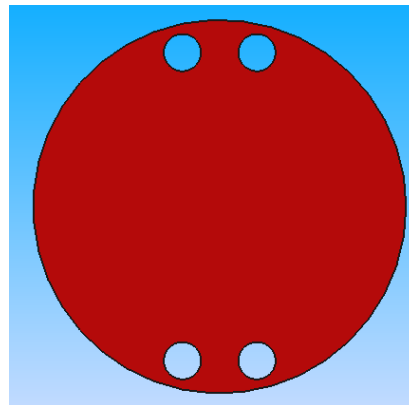
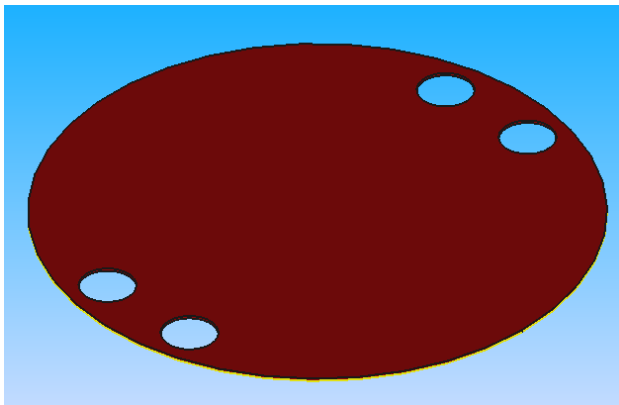

12052022_electrode
plate_step1,2,3.FCS



f) Electrolysis step 1, 2 & 3 Membrane



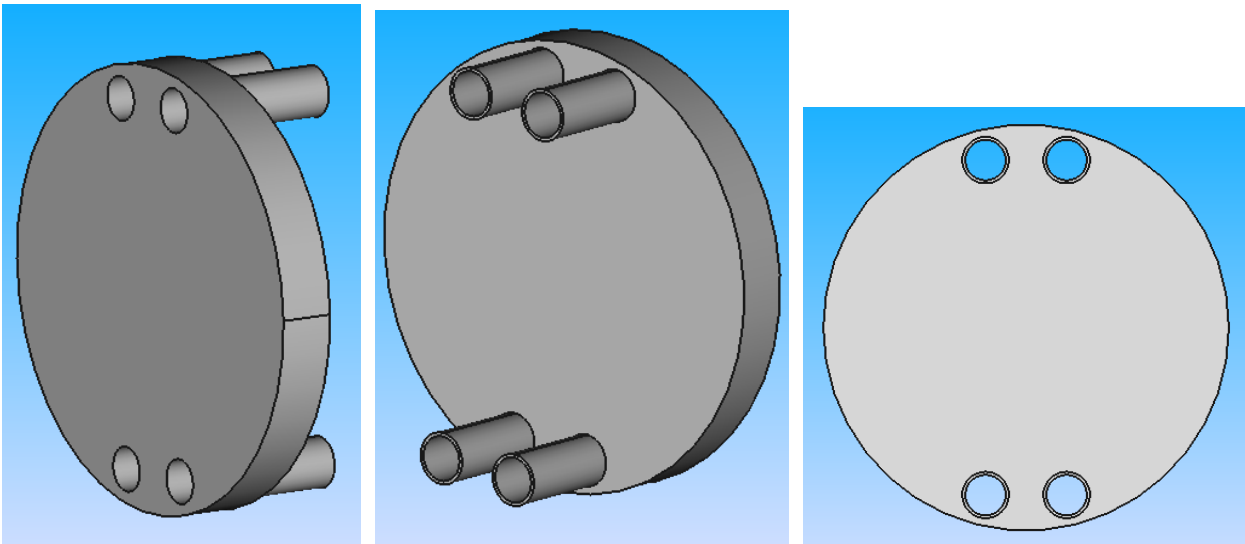
13052022_membrane_step 1,2,3.FCStd



g) Electrolysis step 1, 2 & 3 End plate 2 (Outlet solution)

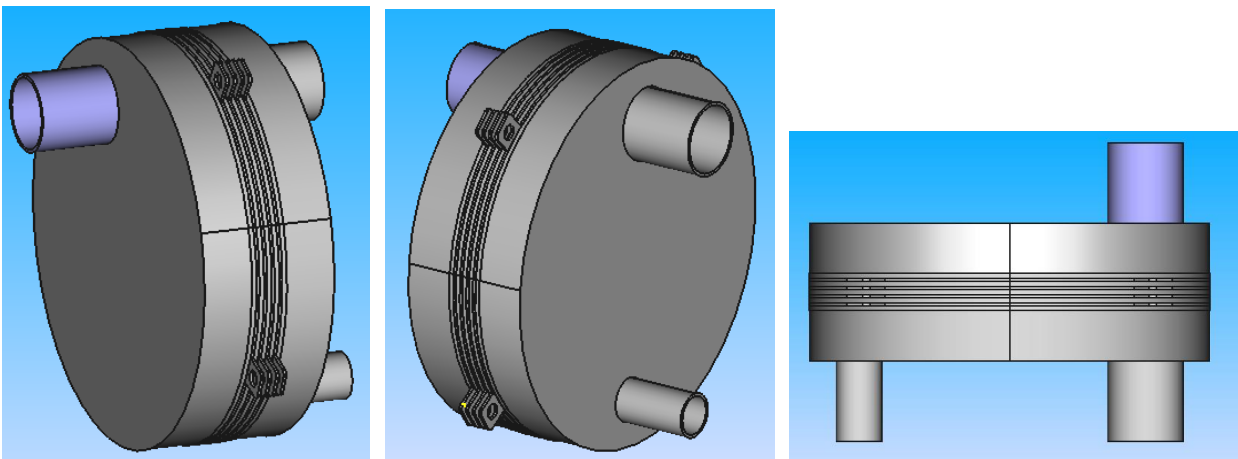


19052022_end plate 2 (outlet slit)_step 1,




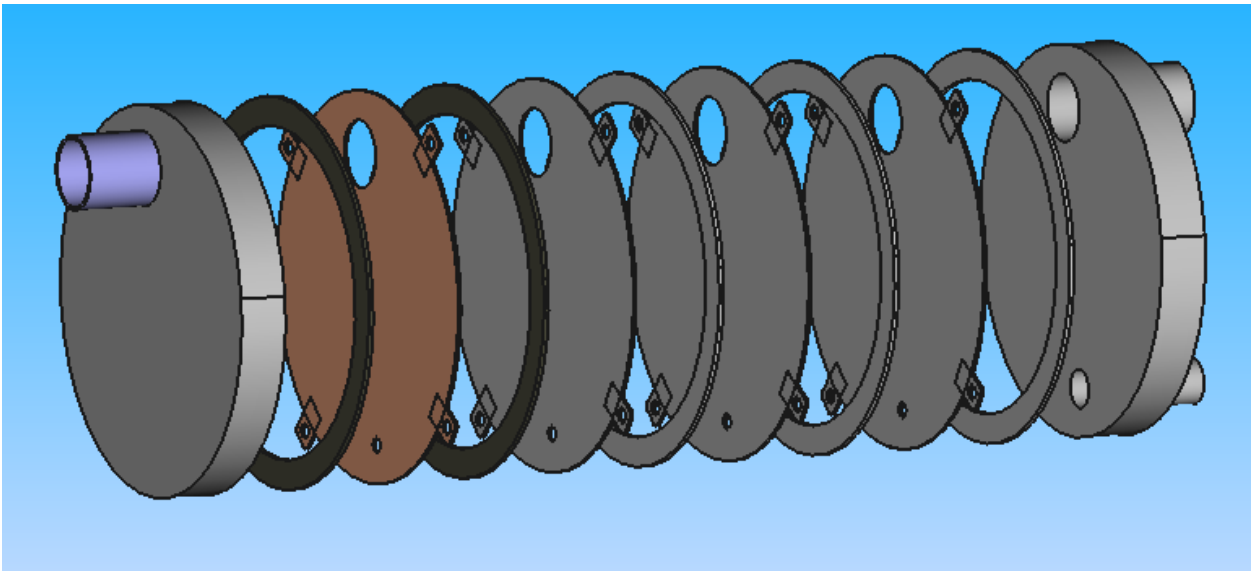
h) Electrolysis step 4 & 5 _ All components -compressed-


27052022_all
components COMPF



i) Electrolysis step 4 & 5 _ All components -Exploded-

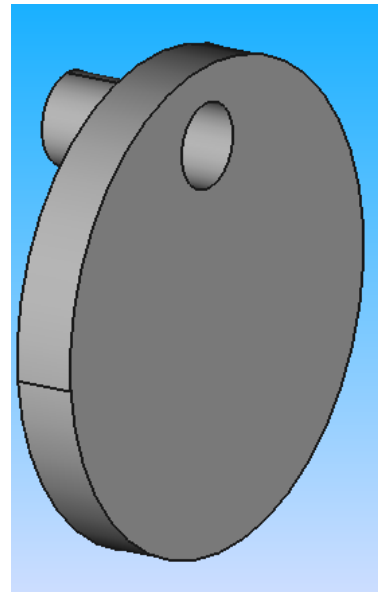
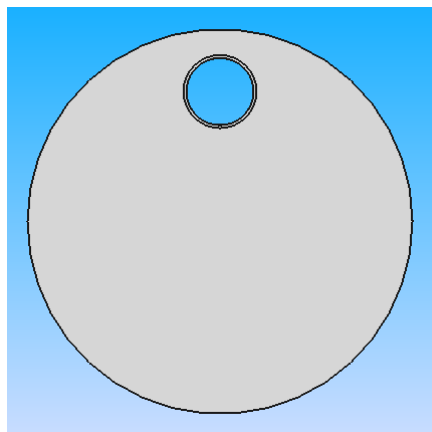
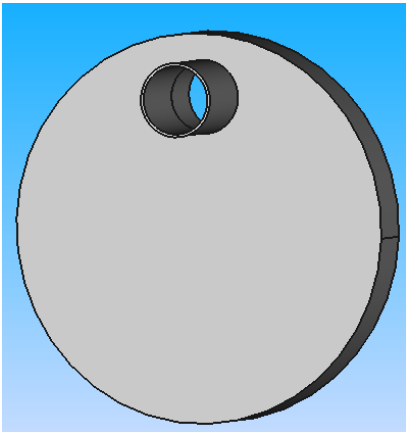

27052022_all
components EXPLOS



j) Electrolysis step 4 & 5 End plate1 (Inlet solution)



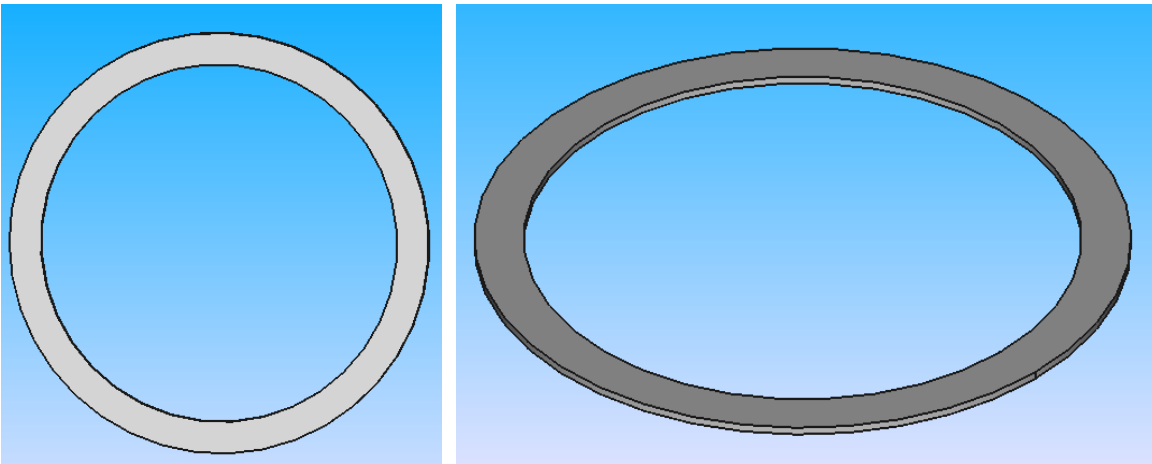
25052022_end plate
1 (inlet slt)_step 4,5.



k) Electrolysis step 4 & 5 Gasket

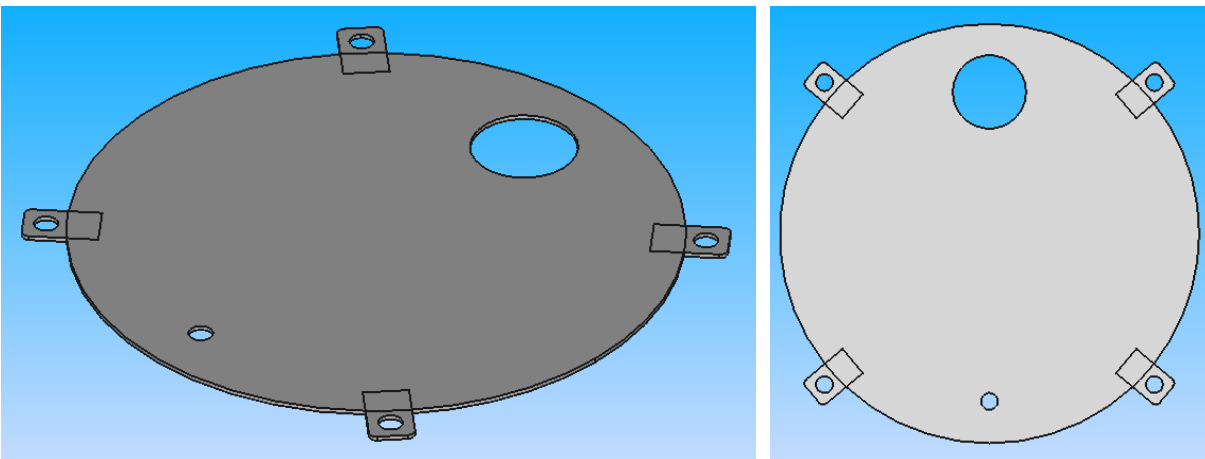


25052022_gasket
_step4,5.FCStd




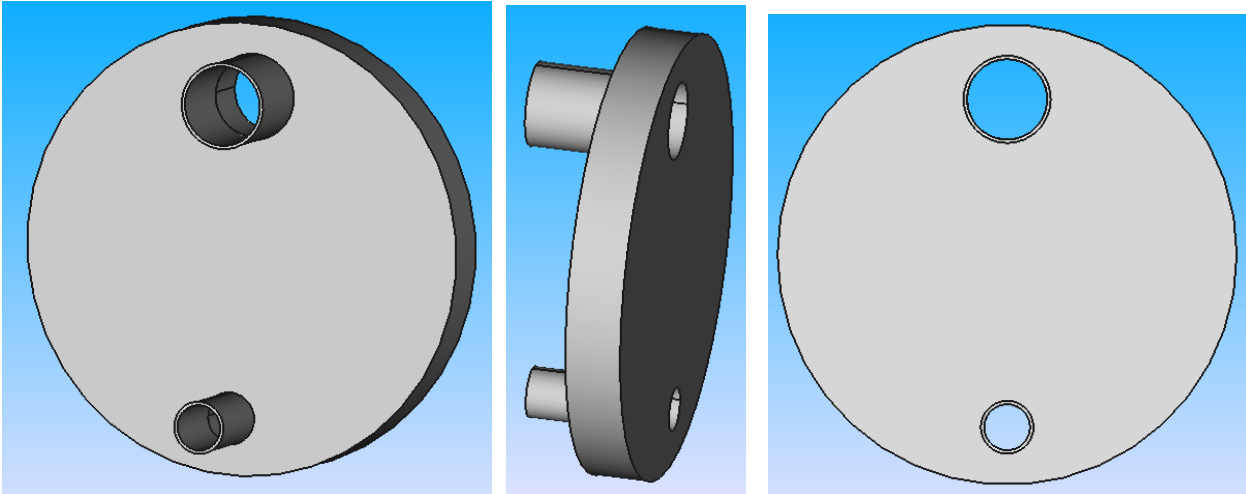
l) Electrolysis step 4 & 5 _ Electrode


25052022_electrode
_step4,5.FCStd



m) Electrolysis step 4 & 5 _ End plate 2 (Outlet solution)


25052022_end plate
2 (outlet slit) _step4,!



1.3. What's Next

After completing the theoretical and design part of the first part of the project, in the future, the practical part must be started, where the required materials are purchased for the purpose of creating and operating the model.

Project 2: Water electrolysis (ICPT - WE)

2.1. Electrolyser introduction

In the past years (2021 and before), and after the theoretical study and the implementation of an applied model, work was done in the year 2022 on the control and automatic system to control the operation of the electrolysis model from a distance. Several operational experiments were also carried out to test the performance of the model.

2.2. PCS design

Needed information for the design and the calculations:

The proposed spaces were 10.65, 9.20, 8.25, 7.25, 6.30, 6.05, 4.35, 4.15, and 3.40 millimeters. From the nine different analyzed distances between electrodes, it can be said that the best performance was reached by one of the smallest distances proposed, 4.15 mm. When the same distance between electrodes was compared (the same and different distance between electrodes and separator), the one that had almost twice the distance (negative compartment) presented an increase in current density of approximately 33% with respect to that where both distances (from electrodes to separator) are the same. That indicates that the stichometry of the electrolysis reaction influenced the performance [1].

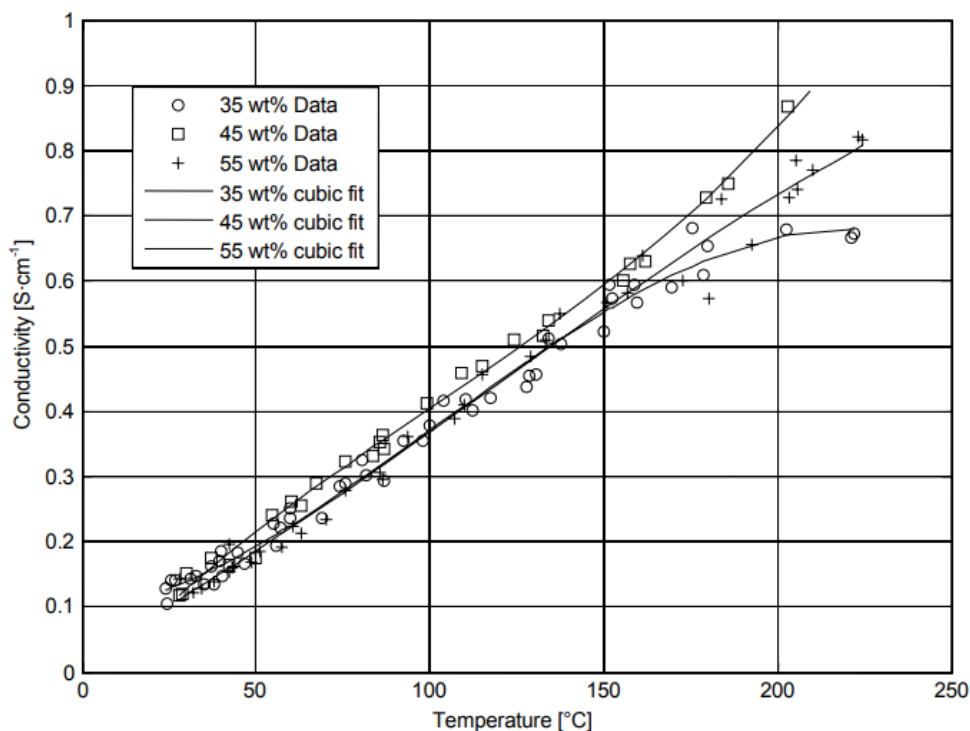


Figure 13: Measured conductivity data and cubic regression analysis for 35,45 and 55 wt% immobilized KOH versus temperature

[2]

$$L = A \times \frac{R}{\rho}$$

$$R = \frac{L \times \rho}{A} = \frac{L}{A \times K}$$

$$\text{When } K = \frac{1}{\rho}$$

$$U = R \times I$$

Current density in alkaline electrolysis = 0,2 - 0,4 A/cm²

2.3. Calculating the current and the voltage for the existing cells

1) The bigger cells in which the distance between the electrodes is 3,6 cm

Cell details :

- The radius of the surface which touches the solution : 14,6 cm .
- The distance between the electrode and the membrane : 3,6 cm .
- We filled only 2/3 of the cell volume .
- Temperature = 25 °C

$$\text{So } R = (3,6 \text{ cm}) / ((446,21 \text{ cm}^2 \times 0,125)) = 0,0645 \Omega .$$

$$I = 178,484 \text{ Amperes}$$

$$U = 11,52 \text{ Volt}$$

2) The smaller cells in which the distance between the electrodes is 1,8 cm

Cell details :

- L = 1,8 cm
- Inner Radius = 14,6 cm

$$\text{So } R = (1,8 \text{ cm}) / ((446,21 \text{ cm}^2 \times 0,125)) = 0,0322 \Omega$$

$$I = 178,484 \text{ Amperes}$$

$$U = 5,747 \text{ volt}$$

2.4. Calculating the current the voltage and the distance between electrodes of the multistage electrolyser cell

$$L = A \times (6) / (A) \times 0,3375 = 2,025 \text{ cm}$$

$$l = 0,4 \times \text{the surface that touches the solution} = 0,4 \times A = 0,4 \times 3,14 \times r^2$$

$$U = 2,4 \text{ Volt}$$

So the distance between the two electrodes shall be 2,025 cm .


And from the text above we seen that it is better to divide this distance into 3 parts
2 parts on the hydrogen production site and one on the oxygen production .

That means 0,675 cm from the anode to the membrane and 1,35 cm from the cathode to the membrane.

2.5. Realization / implementation - Mechanical realization

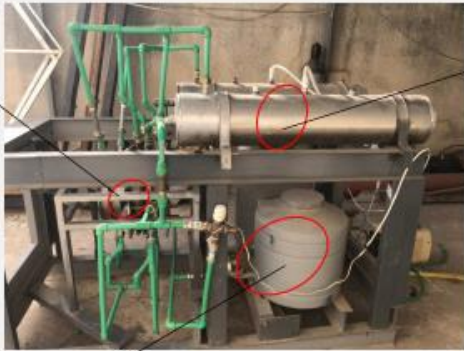
1) System overview


Mechanical



Electrolytic Cells:
An electrolytic cell is a device that split water into its two elements, oxygen and hydrogen, where the oxygen and hydrogen.


خلية التحليل الكهربائي هي عبارة عن جهاز يقوم بتحليل الماء الى عنصريه وهما الاكسجين والهيدروجين حيث يتم تخزين الاوكسجين والهيدروجين.





1: O₂ condenser
2: H₂ condenser
The condenser is mechanical part that serves to condense the excess water vapor that comes with H₂ and O₂ gases to water.

المكثف عبارة عن جزء ميكانيكي يعمل على تكثيف بخار الماء الزائد الذي يأتي مع غازات الهيدروجين و الاكسجين لماء.



1: KOH (electrolyte) tank
2: H₂O (water) tank

ELECTROLYTE:
An electrolyte is a substance that produces an electrically conductive solution when dissolved in a polar solvent, such as water

الإلكترووليت هو مادة تنتج محلول موصل كهربائي عند إذابته في مذيب قطبي ، مثل الماء



2) Pipe installation from O₂ and H₂ condenser to fuel burner with filters and expansion tanks











3) H₂ burning kit

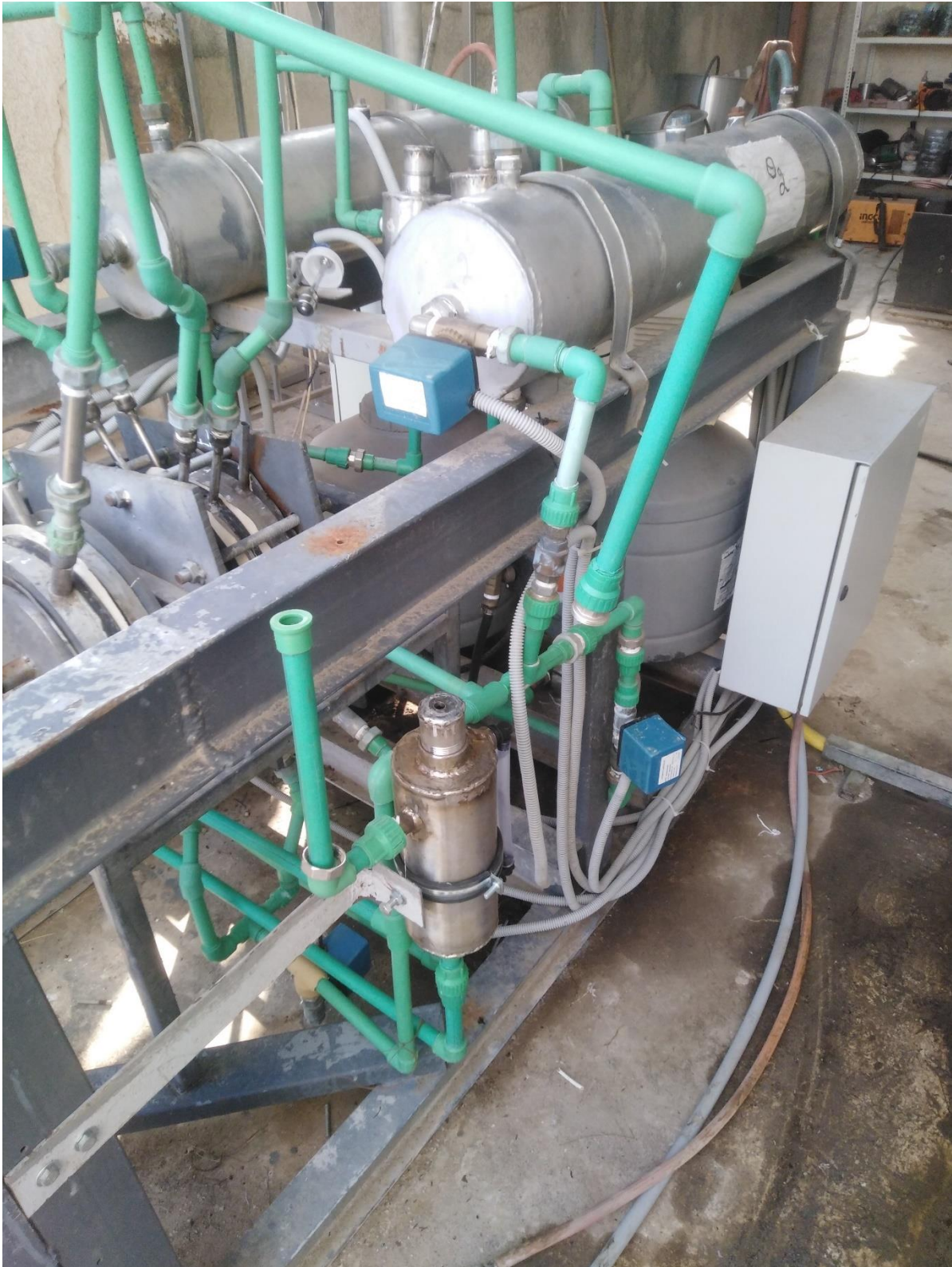


Check Valve

4) Nitrogen can pipe installation



5) Level sensor





2.6. Process control system realization (PLC + GUI)

- PLC Code :



ICPT-Electrolyzer_PC
S_PLC Code_270522.

- Graphical User Interface code (C#) :



ICPT-Electrolyzer_PC
S_GUI_070722.rar

- ICPT Electrolyser PCS - PLC Modbus address :



ICPT-Electrolyzer
PCS (MODBUS-address)

1) Process control system for the Electrolyzer system

Graphical user interface



Modbus RS 485 Network

Control Panel

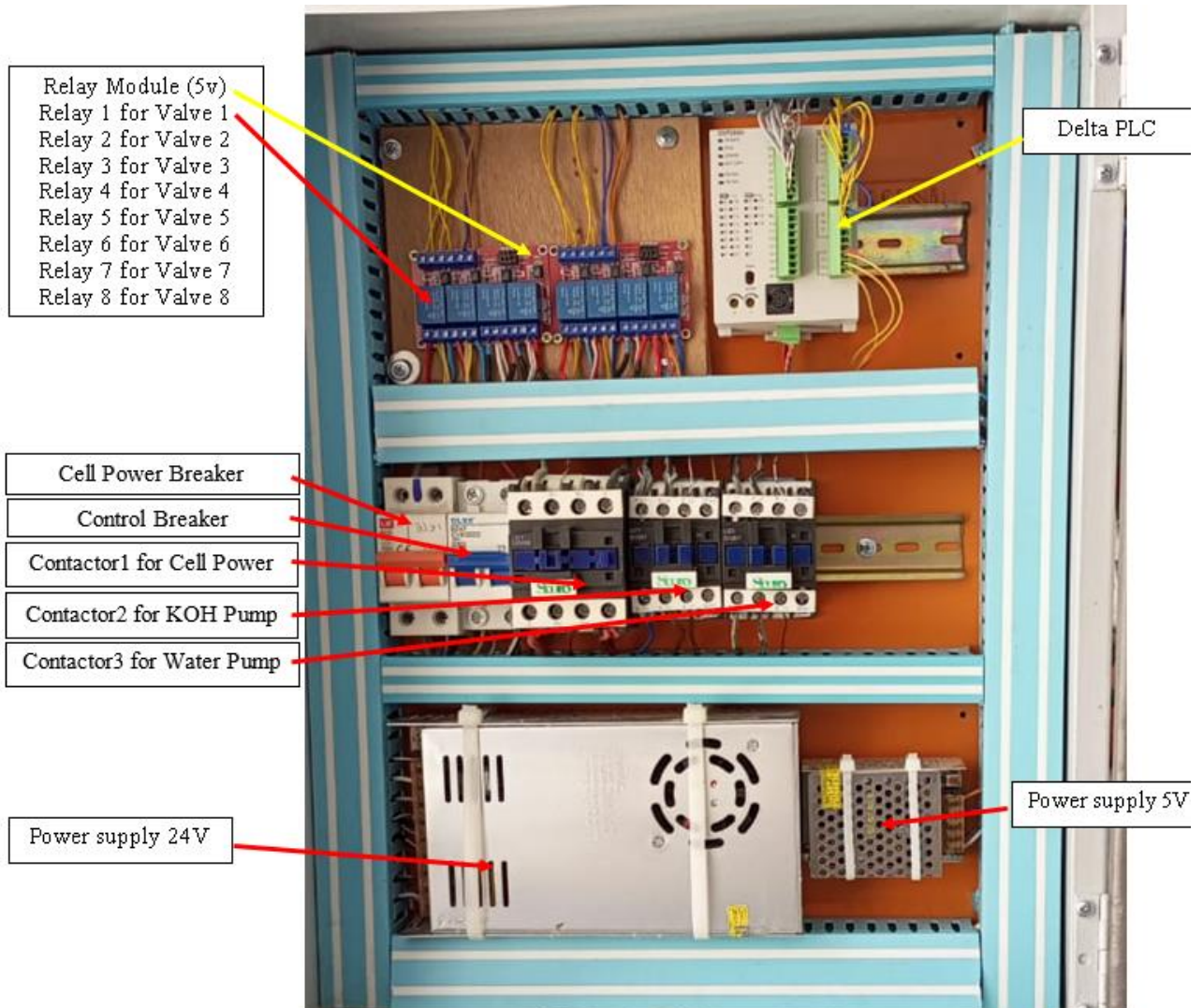


Electrical Cables

Sensor &
Actuator



2) PLC panel



- PLC Point Wiring

Input:

X0 connect to the Level sensor 1
X1 connect to the Level sensor 2
X0 connect to the Level sensor 3
X1 connect to the Level sensor 4

Output:

Y0 Connect to the Relay 1 for Valve 1
Y1 Connect to the Relay 2 for Valve 2
Y2 Connect to the Relay 3 for Valve 3
Y3 Connect to the Relay 4 for Valve 4
Y4 Connect to the Relay 5 for Valve 5
Y5 Connect to the Relay 6 for Valve 6
Y6 Connect to the Relay 7 for Valve 7
Y7 Connect to the Relay 8 for Valve 8
Y4 Connect to the Relay 5 for Valve 5
Y5 Connect to the Relay 6 for Valve 6
Y6 Connect to the Relay 7 for Valve 7
Y7 Connect to the Relay 8 for Valve 8
Y11 Connect to the Contactor 1 for Cell power
Y12 Connect to the Contactor 2 for KOH pump
Y13 Connect to the Contactor 3 for Water pump

V1: Water valve of half cells set of O₂

V2: Water valve of half cells set of H₂

V3: Water emptying valve of H₂ Condenser

V4: Water emptying valve of O₂ Condenser

V5: Electrolyte valve of half cells set of O₂ |

V6: Electrolyte valve of half cells set of H₂

V7: emptying valve of O₂ half cells set

V8: emptying valve of H₂ half cells set

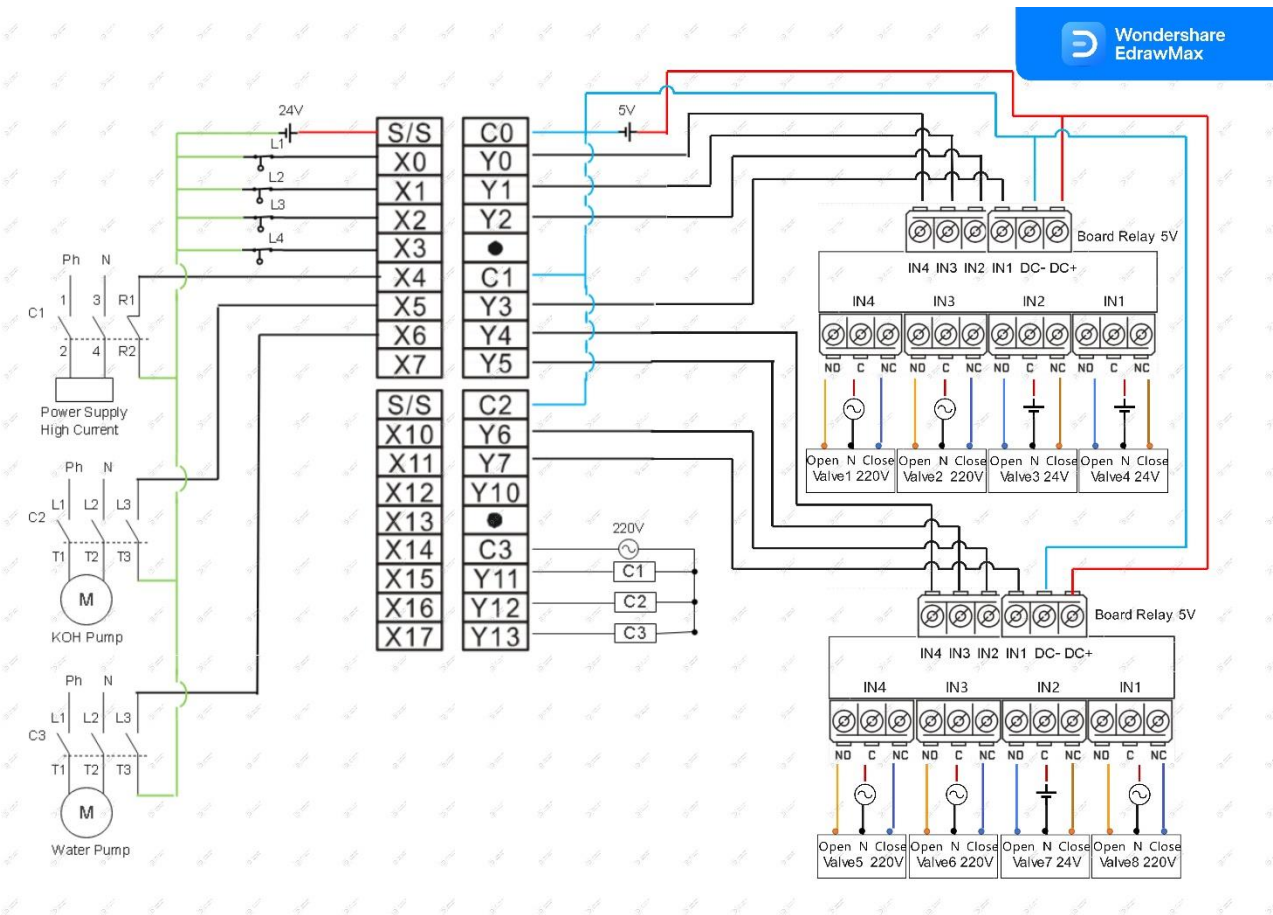
L1: H₂ Condenser level

L2: O₂ Condenser Level

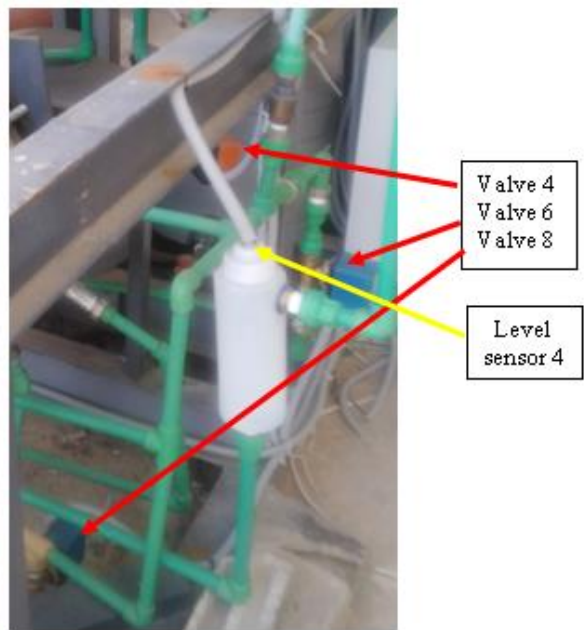
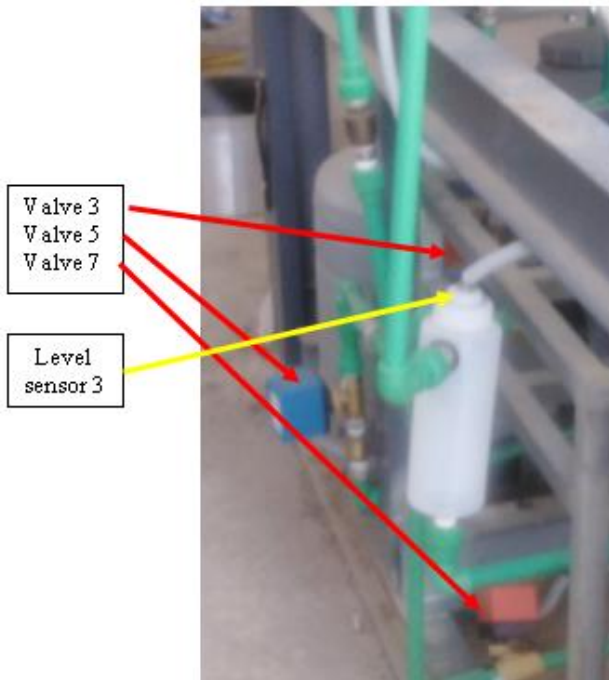
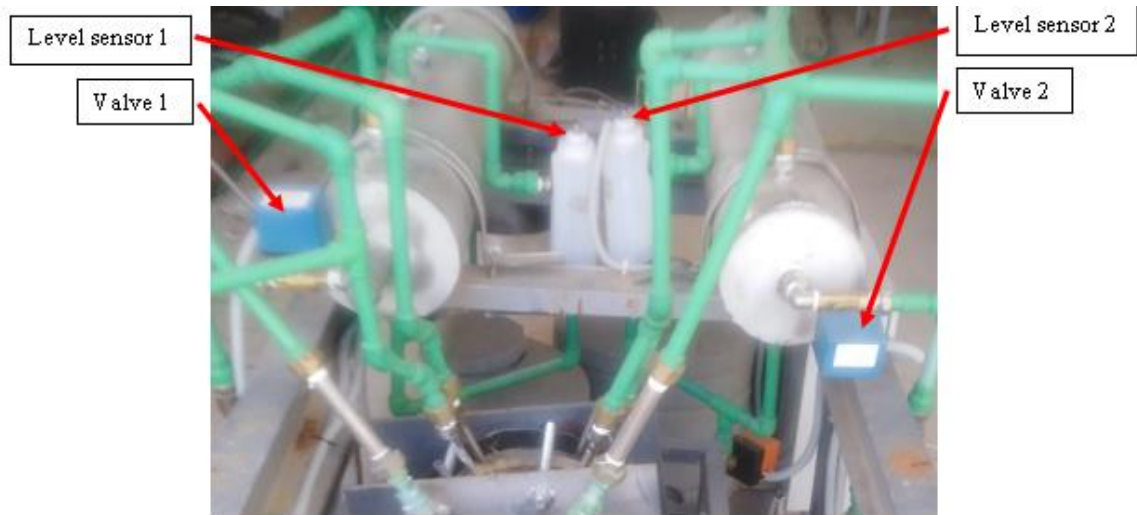
L3: H₂ half cells set level

L4: O₂ half cells set level

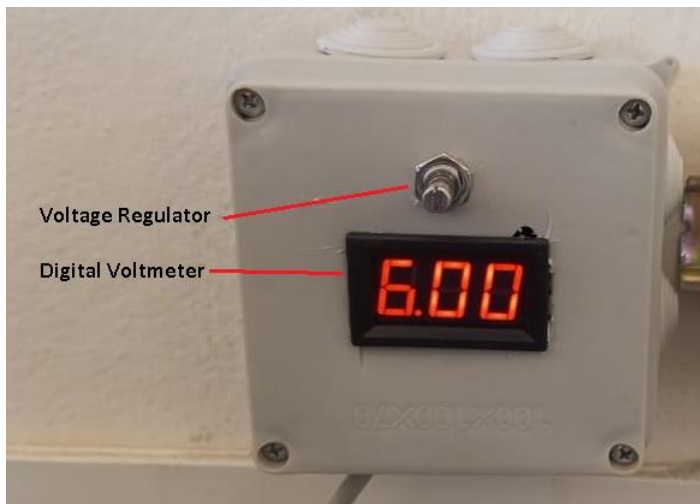
3) PLC Control Panel - Wiring Diagram



4) Instruments (Valves, Level Control Sensors)

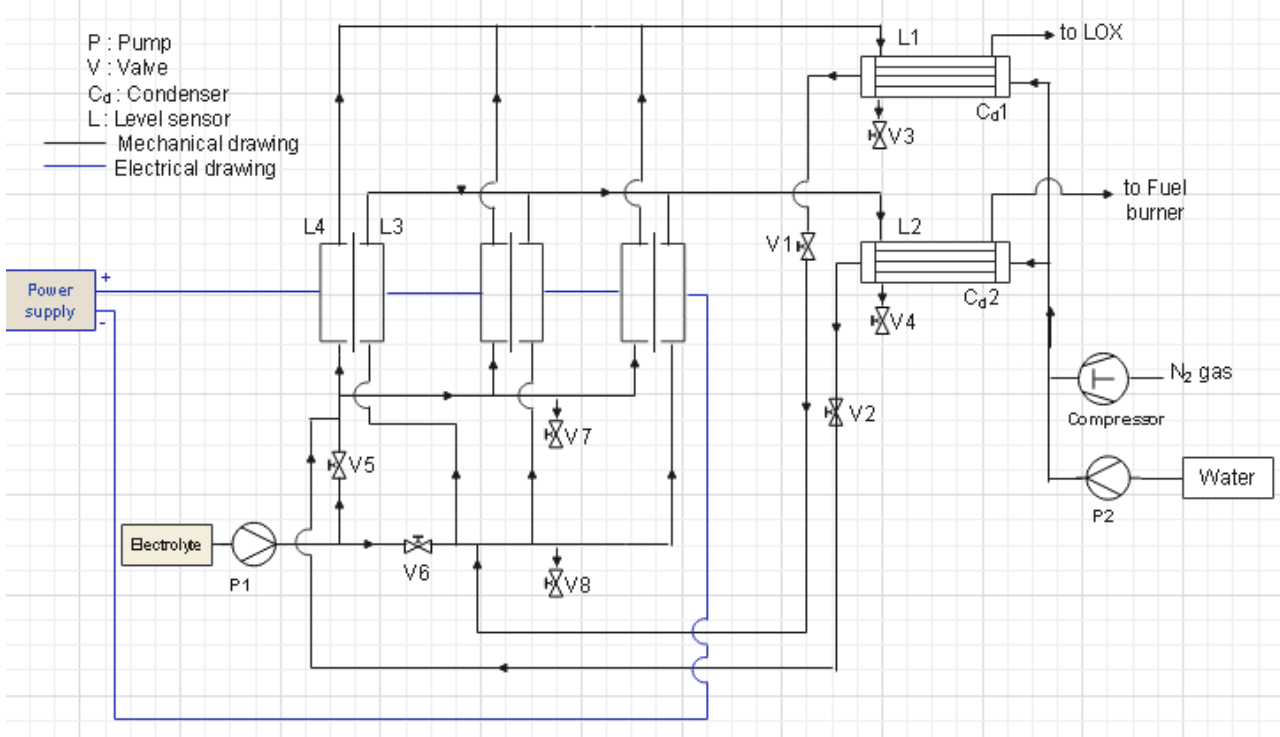


- **Power Supply High Current - Panel & Cable**

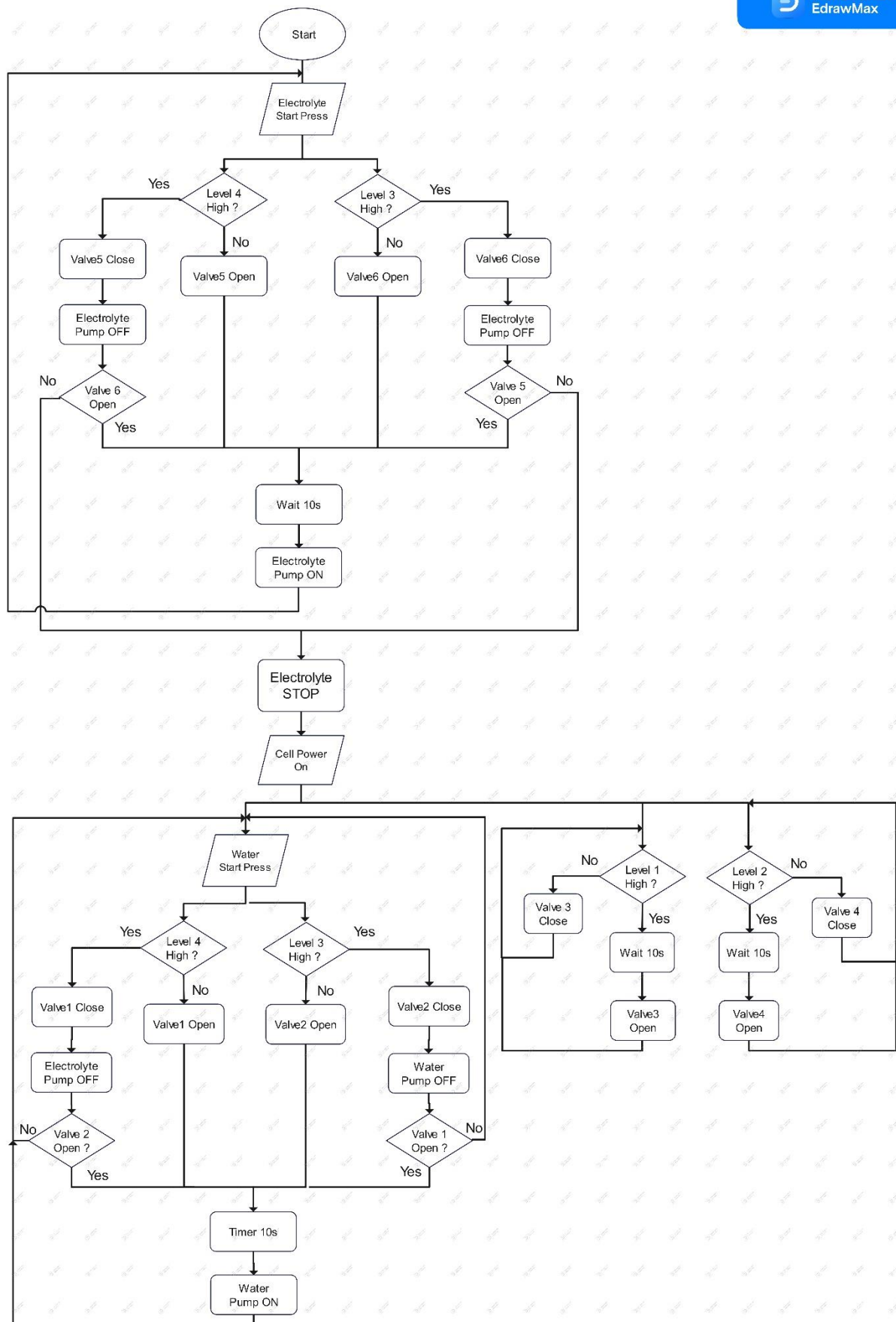




5) GUI- Electrolyzer Design



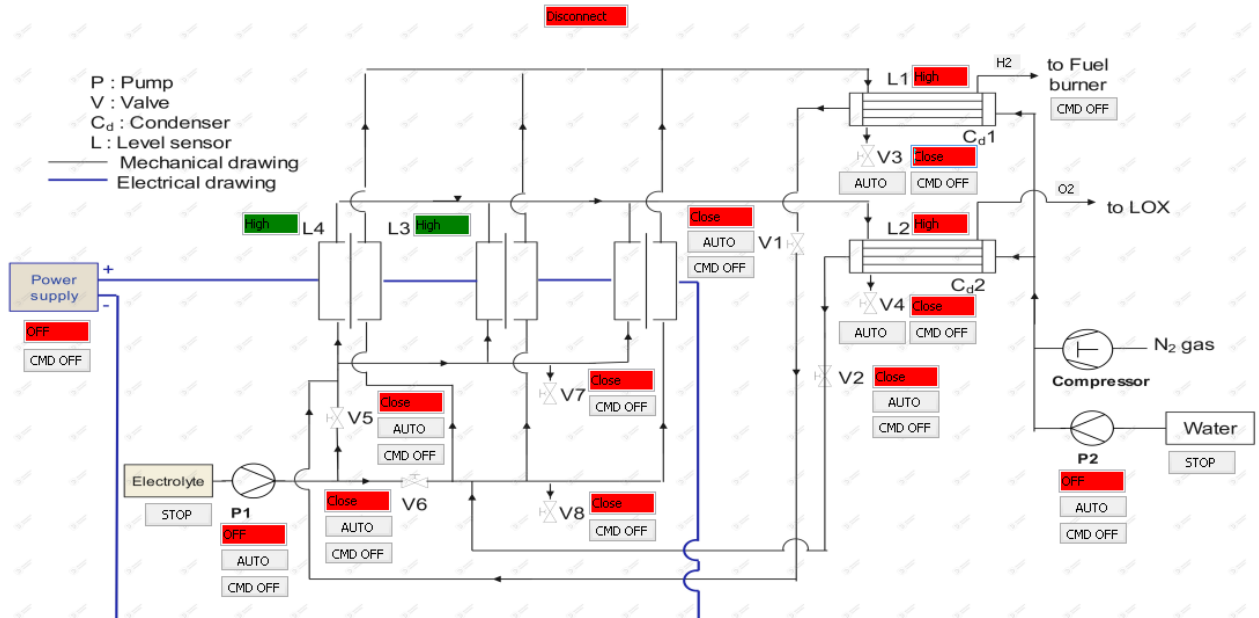
• **Algorithme electrolyser 16.6.2022**



- **GUI 13.7.22**



WhatsApp Video
2021-08-20 at 13.07.



2.7. Electrolysis system test specifications

1) Pre-Starting

Please read these instructions thoroughly. This will make sure you obtain full safe use, Keep this instruction manual in a handy place for future reference.

a) Nitrogen purging

1. Make sure the circuit is closed (all valves are closed)
2. Make sure the power is turned off
3. Connect the Nitrogen tank to the system
4. Open Nitrogen tank valve

The amount of nitrogen needed for this process is based on how many times pressurized purges are needed to reduce the unwanted contaminant to the desired level.

5. Disconnect the nitrogen.

b) Tank

1. Make sure that the water tank has 60 liters of water
2. Make sure that the KOH tank has 60 liters of KOH

c) Safety precaution

Storage of H₂ is dangerous, for this reason, it should be burned using a fuel burner.

2) Electrolysis operation method

1- Ensure all sanitary connections

2- Fill the first tank with distilled water

3- Fill the second tank with KOH mixture with pH = 13.47

4- Ensure that all electrical connections are made, with no electricity connected to the device

5- Filling the device completely with nitrogen gas, starting with the entry of nitrogen gas at the electrodes and its exit from the hydrogen and oxygen vents, passing through the condensate

6- Operation of the distilled water pump

7- Operation of the KOH mixture pump

8- Connect electricity (continuous power) to the device

9- Wait a while and then start collecting the hydrogen and oxygen gases produced separately by connecting the outlets to specific tanks or connecting them directly to the burner.

2.8. Electrolyser system test**1) Test 22.06.2022 – Hydraulic test of pipes**

Hydraulic test to detect Pipe Leakage using a 1.5 HP air compressor at a 2-3 Bar Pressure.

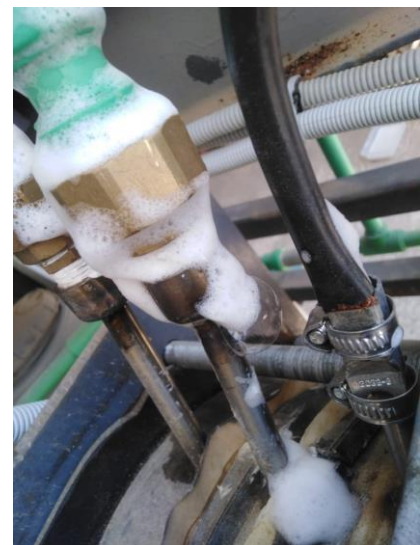
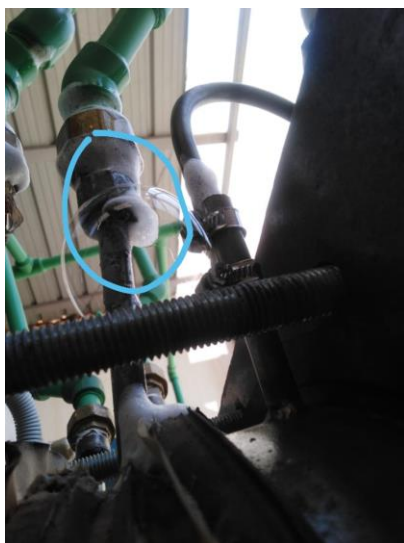
00001: The leak shall be detected when it exists

Step	Step Description	Expected Result	Result
Precondition	System is off		

Switch on the system	Turn on the air compressor	Air enters to the whole system
Lack is detected	Air exit from the pie system	Lack position shall be detected with a marker
Switch off the system.	Turn off the air compressor	The air stops enter to the pipe system
Postcondition	System is off	



a) Place of leakage of stainless steel



b) Place of leakage of PPR pipes

2) Test 04.07.2022 – Electrolysis

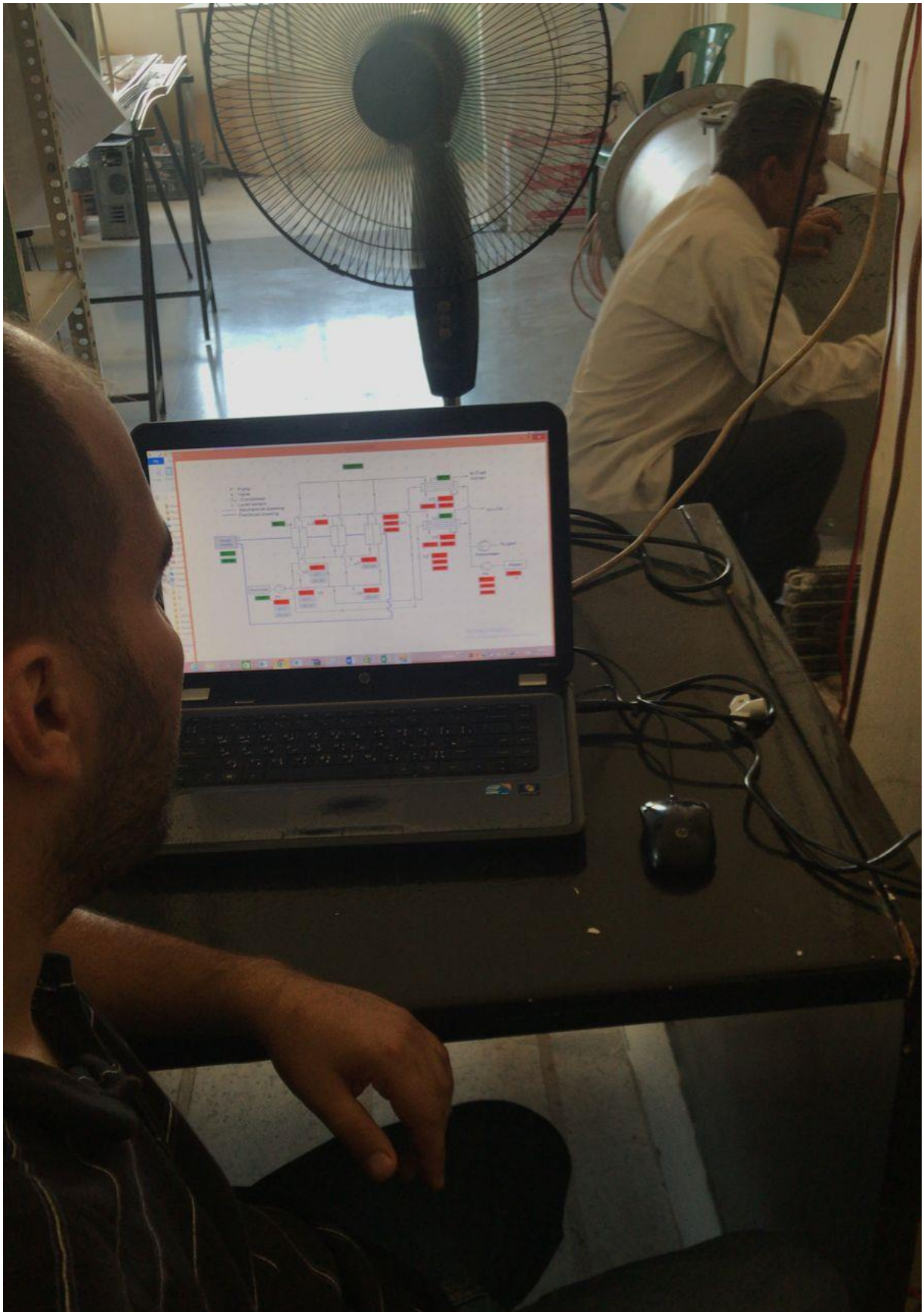
00001: The leak shall be detected when it exists

Step	Step Description	Expected Result	Result
Precondition	System is off		
Switch on the system	Turn on the air compressor	Air enters to the whole system	
Lack is detected	Air exit from the pie system	Lack position shall be detected with a marker	
Switch off the system.	Turn off the air compressor	The air stops enter to the pipe system	
Postcondition	System is off		

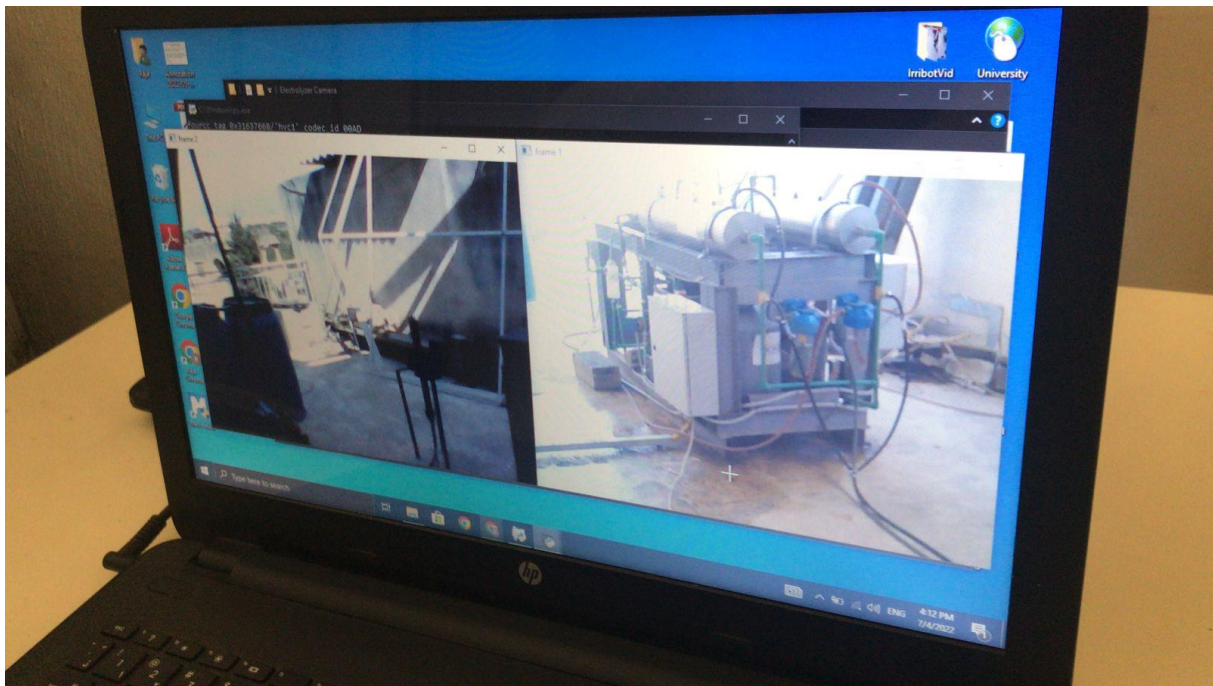
3) Test 04.07.2022 – Electrolysis whole system test

00002: WHOLE SYSTEM TEST

Step	Step Description	Expected Result	Result
Precondition	System is off		
Open the valves V₁ and V₂	Open the valves V₁ and V₂ from the GUI	The valve V ₁ and V ₂ are open and enable to let the nitrogen gas pass	Positive result
WASH THE SYSTEM WITH NITROGENE	Wash the system with Nitrogen for few minutes BY TURNING ON THE VALVE on the nitrogen tank	One can see that there is nitrogen exit from the gas outlets	Positive
Switch on the system	Turn off the nitrogen Turn on the system from the GUI	THE SYSTEM IS GENERATING hydrogen and oxygen	We turned on the system but no hydrogen or oxygen generation
Burn the hydrogen	Turn on the transformator	The Hydrogen is burning	Negative since no hydrogen generated
Switch off the system.	Switch off the system from the GUI Switch off the transformator	The system goes down.	Positive
WASH THE SYSTEM WITH NITROGENE	Wash the system with Nitrogen for few minutes BY TURNING ON THE VALVE on the nitrogen tank	All the hydrogen existing in the pipe system exit	Positive
Postcondition	System is off		



Turning on the system through the GUI after nitrogen purging for more than 10 minutes



We watched everything through 2 cameras and found that nothing had happened.

This could be seen by the fact that no current was withdrawn from the power supply and that no bubbles formed in the 2 containers.

- Analysis of the test results:

The reason why no hydrogen was generated is that the KOH concentration was not high enough.

The desired concentration is 5 to 7 molar = 280,528 g/L

We had entered far too little KOH, which left the conductivity of the solution close to zero.

- What we have to do:

Increase the concentration of the KOH.

4) 05.07.2022 – Electrolysis whole system test

00002: WHOLE SYSTEM TEST

Step	Step Description	Expected Result	Result
Precondition	System is off		
Open the valves V₁ and V₂	Open the valves V₁ and V₂ from the GUI	The valve V ₁ and V ₂ are open and enable to let the nitrogen gas pass	Positive
WASH THE SYSTEM WITH NITROGENE	Wash the system with Nitrogen for few minutes BY TURNING ON THE VALVE on the nitrogen tank	One can see that there is nitrogen exit from the gas outlets	Positive
Switch on the system	Turn off the nitrogen Turn on the system from the GUI	THE SYSTEM IS GENERATING hydrogen and oxygen	Positive
Burn the hydrogen	Turn on the transformator	The Hydrogen is burning	Negative
Switch off the system.	Switch off the system from the GUI Switch off the transformator	The system goes down	Positive
WASH THE SYSTEM WITH NITROGEN	Wash the system with nitrogen for few minutes BY TURNING ON THE VALVE on the nitrogen tank	All the hydrogen existing in the pipe system exit	Positive
Postcondition	System is off		

After correcting the KOH concentration, we started the test and successfully generated hydrogen. However, the quantity was very low, so ignition did not occur.

- Test analysis:

It can be 2 Reason for the low generated quantity:

- 1- Either the concentration is yet too low knowing that we rise it.
 - 2- Or the current passing through the cells is too low.
- or the two reasons together.

- What we have to do:

Do a test with the maximum possible concentration of the KOH. If this is not successful, we have to define which power supply should be used instead. this is done by installing measuring instruments to detect the voltage and the current passing through the cells.

5) Test #2: 05.07.2022 – Electrolysis whole system

00002: WHOLE SYSTEM TEST

Step	Step Description	Expected Result	Result
Precondition	System is off		
Open the valves V₁ and V₂	Open the valves V₁ and V₂ from the GUI	the valve V ₁ and V ₂ are open and enable to let the nitrogen gas pass	
WASH THE SYSTEM WITH NITROGENE	Wash the system with Nitrogen for few minutes BY TURNING ON THE VALVE on the nitrogen tank	One can see that there is nitrogen exit from the gas outlets	
Switch on the system	Turn off the nitrogen Turn on the system from the GUI	THE SYSTEM IS GENERATING hydrogen and oxygen	
Burn the hydrogen	Turn on the transformator	The hydrogen is burning	
Switch off the system.	Switch off the system from the GUI Switch off the transformator	The system goes down.	
WASH THE SYSTEM WITH NITROGENE	Wash the system with Nitrogen for few minutes BY TURNING ON THE VALVE on the nitrogen tank	All the hydrogen existing in the pipe system exit	
Postcondition	System is off		

6) 19.07.2022 – Whole system test with another power supply

Tested according to test specification

00004: WHOLE SYSTEME TEST WITH ANOTHER POWER SUPPLY

WHOLE SYSTEME TEST WITH ANOTHER POWER SUPPLY 15.07.2022

Step	Step Description	Expected Result	RESULTS
Precondition	System is off		
THE CHANGING OF THE POWER SUPPLY WITH A POWER SUPPLY OF HIGHER VOLTAGE	Replacing the power supply with the welding machine	More hydrogen is generated	Positive
Open the valves V₁ and V₂	open the valves V₁ and V₂ from the GUI	The valve V ₁ and V ₂ are open and enable to let the nitrogen gas pass	Positive
WASH THE SYSTEM WITH NITROGEN	Wash the system with Nitrogen for few minutes BY TURNING ON THE VALVE on the nitrogen tank	One can see that there is nitrogen exit from the gas outlets	Positive
Switch on the system	Turn off the nitrogen Turn on the system from the GUI	THE SYSTEM IS GENERATING hydrogen and oxygen	The system is generating hydrogen but not oxygen
Burn the hydrogen	Turn on the transformator	The hydrogen is burning	Positive
Switch off the system.	Switch off the system from the GUI Switch off the transformator	The system goes down.	Positive
WASH THE SYSTEM WITH NITROGENE	Wash the system with nitrogen for few minutes BY TURNING ON THE	All the hydrogen existing in the pipe system exit	Not done yet

VALVE on the nitrogen tank

Postcondition

System is off

system is off

After replacing the power supply with the welding machine, we were able to generate enough hydrogen to burn it. see the pictures below.

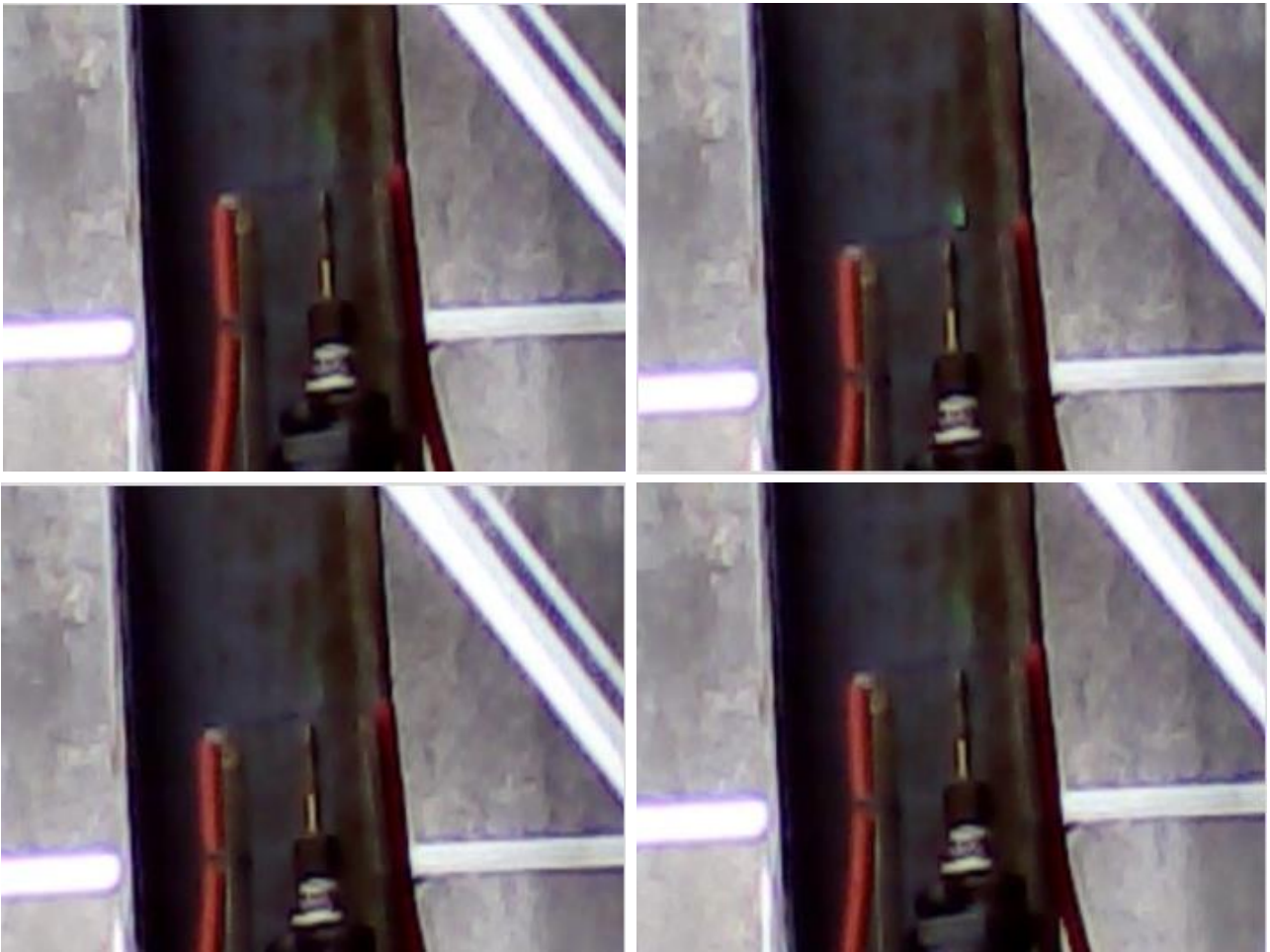


Fig. 1: The Hydrogen flame



Fig. 2: How it looks without flame

But what we noticed is that the current going to the welding machine was only high at the beginning of the start-up (about 13 A at 230 V) and then it kept decreasing until it went down to 1,4 A at 230 V. see the pictures below:



Fig. 3: Just after starting the machine (1A is going to the transformer)



Fig. 4: After a while. One can see how much the current has decreased.

- Test analysis:

The welding machine is not good enough since it cannot withstand for long time.

At the highest power of the welding machine, hydrogen was generated and burned, but even then too little.

- It can be 2 Reason for the low generated quantity :

1- Either the concentration is yet too low knowing that we rise it .

2- Or the current passing through the cells is too low .

or the two reasons together .

- What we have to do :

1- Test whether the membranes are ruptured.

2 - Doing a test with the maximum possible concentration of the KOH. If this is not successful we have to define which power supply should be used instead . This is done by installing measuring instruments to detect the voltage and the current passing through the cells.

7) 05.07.2022 – All system test with only one cell connected

Tested according test specification

00005: WHOLE SYSTEME TEST WITH WITH ONLY ONE CELL CONNECTED

Step	Step Description	Expected Result	RESULTS
Precondition	System is off		
CONNECTING THE COMPLETE VOLTAGE TO ONLY ONE CELL	DISCONNECT THE POWER SUPPLY FROM TWO CELLS AND CONNECT IT TO ONLY ONE CELL.	MORE CURRENT WILL DRIVE THROUGH THE CELL	Instead of 0.5 A, the power source has drawn up to 5 A from the 230 V socket.
Open the valves V₁ and V₂	Open the valves V₁ and V₂ from the GUI	the valve V ₁ and V ₂ are open and enable to let the nitrogen gas pass	Positive
WASH THE SYSTEM WITH NITROGENE	Wash the system with Nitrogen for few minutes BY TURNING ON THE VALVE on the nitrogen tank	One can see that there is nitrogen exit from the gas outlets	Positive
Switch on the system	Turn off the nitrogen Turn on the system from the GUI	THE SYSTEM IS GENERATING hydrogen and oxygen	There is seen that only hydrogen is generated but this is so also in all previous tests we done
Burn the hydrogen	Turn on the transformator	The hydrogen is burning	Negative
Switch off the system.	Switch off the system from the GUI Switch off the transformator	The system goes down.	Positive
WASH THE SYSTEM WITH NITROGENE	Wash the system with Nitrogen for few minutes BY TURNING ON THE VALVE on the nitrogen tank	All the hydrogen existing in the pipe system exit	Positive
Postcondition	System is off	System is off	

We have assumed that the voltage we give to one cell is too low, so we have connected all the voltage that was intended for all three cells to only one cell.

We expected more current to go through the one cell. And that is what happened and more hydrogen was generated. But the amount of hydrogen was not enough to burn it.

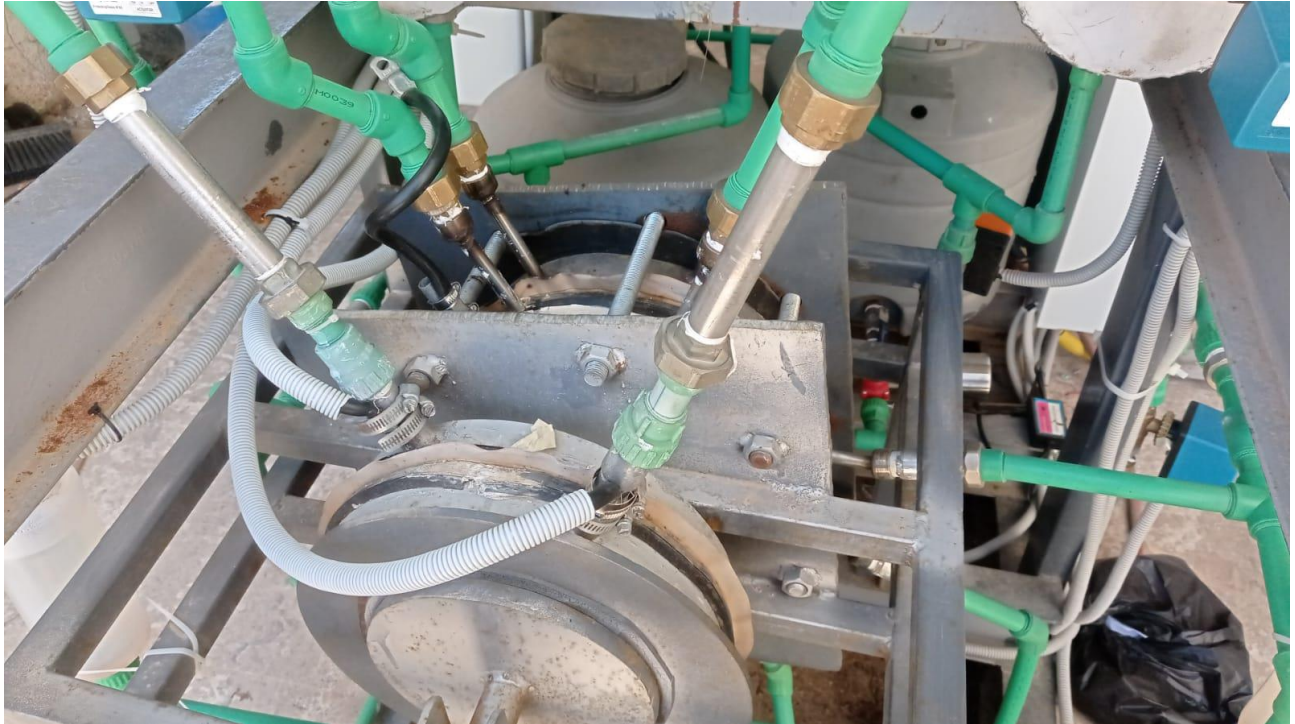


Fig 1: In this figure, it can be seen that only one cell is connected

- Test Analysis:

One can see that the resistance of the 3 cells is too high .

- What to do:

- 1- Test whether the membranes are ruptured.
- 2- Rise the KOH concentration to the maximum.

8) 29.07.2022 – Test whether the membrane is ruptured

Testing according the test 00007: Test whether the membrane is ruptured.

If there are air bubbles from the hydrogen half cells set the membrane have to be changed.

Step	Step Description	Expected Result	Results
Precondition	System is off		
Emptying the cells	Placing a container under the two emptying valves and open the two emptying valves so that the containers are filled with the solution of the cells.	The solution flows into the containers.	Not done
Closing of the emptying valves.	Closing the emptying valves after the whole solution flowed from the cells into the containers.	The emptying valves are closed	Not done
Let the air enter to the half-cell set of oxygen.	Connect the air compressor to one set of the half-cell sets and tur on the compressor.	Air bubbles are seen only in the one set on which the air bubbles are connected	Not done
Stop the air	Turn off the compressor	The compressor is off	Not done
Postcondition	System is off	System is off	

Before we could start with the actual test, we first had to purge the electrolyser with nitrogen.

When we did this, water flowed out of one or more cells.

And the level of the water in the filters and in the containers for the level controllers has changed.

As one can see in the figures below:



Fig. 1: water sprays out of the cells



Fig. 2: the level change in the filters



fig 3 : the level changes in the level controlling containers

- Test Analysis:

Test analysis to be discussed further but we think that the membrane is ruptured and the pressure of the cells on each other has become weaker .

- What we have to do:

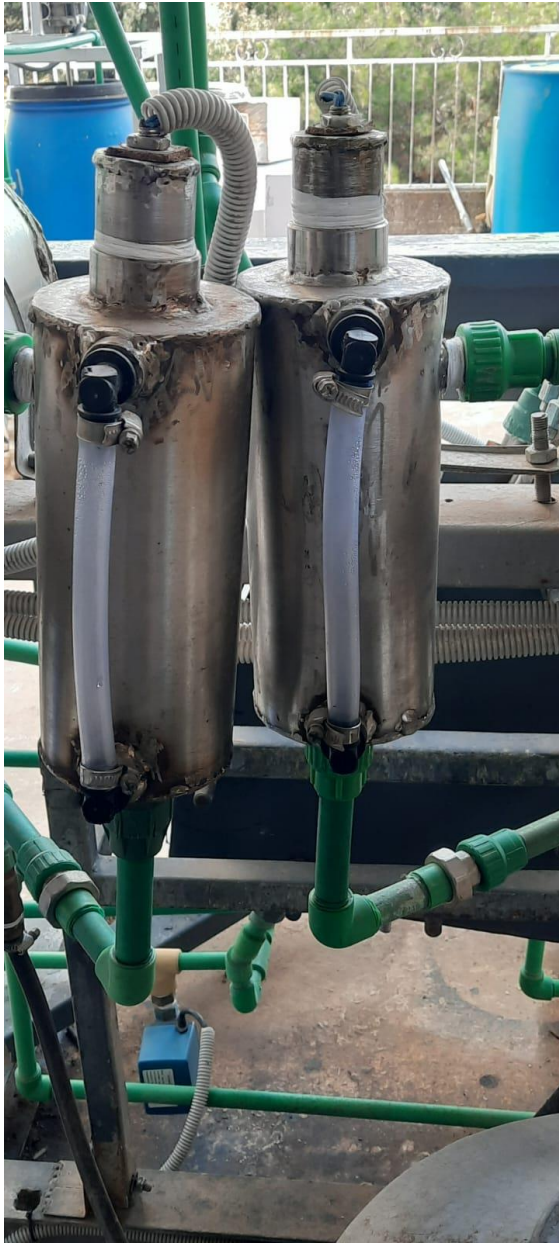
open the cells and change the membranes and refix the cells

9) 14.11.2022 – Electrolysis test

15/12/2022 System test

Leakage places:

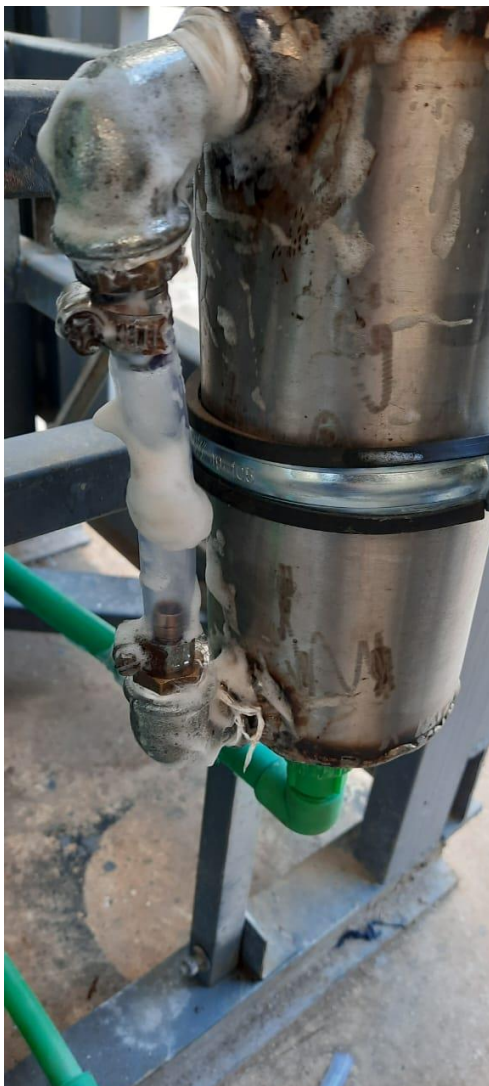




Also, we couldn't see air bubbles in the oxygen water receiver, but we saw them a little in the hydrogen water receiver.



After changing the 4 tanks, we made Nitrogen purging to test the new ones. The results were also negative and the new ones didn't work well. we have leakages.





10) 15/12/2022 - System test

a) Leakage places:



Also, we couldn't see air bubbles in the oxygen water receiver, but we saw them a little in the hydrogen water receiver.



After changing the 4 tanks, we made Nitrogen purging to test the new ones. The results were also negative and the new ones didn't work well. we have leakages.





b) Electrolyser Test 14 December 2022 _ Results

No leakages observed
Greater flame



Both H₂ and O₂ gases water tanks showed air bubbles (for the first time).
Hydrogen took little time to appear, maybe because it's the time needed for the nitrogen gas to leave the system.

We noticed that the tanks 3 & 4 showed different levels of water after the test. The oxygen tank showed lower water level than the Hydrogen tank.



- Video 1 for the test:



WhatsApp Video
2022-12-16 at 11.06.

- Video 2:



WhatsApp Video
2022-12-16 at 11.06.

- Video 3:



WhatsApp Video
2022-12-16 at 11.05.

2.9. What's new

To complete the applied part of the electrolysis project, we only have to do a long-term experiment, showing us the endurance of the model and the amount of hydrogen and oxygen produced with respect to time. After completing this step, we will have successfully completed this project.

Project 3: Ammonia production (ICPT - AP)

3.1. Position of AP project

This project starts in September 19, 2022 in an aim to store Hydrogen gas as a fuel. It is based on the reaction between Hydrogen gas and Nitrogen gas to produce Ammonia gas in specific reaction conditions.

3.2. Introduction

1) General Introduction

Nitrogen and hydrogen combine to generate the inorganic substance ammonia, which has the formula NH_3 . Ammonia is an odorless, colorless gas with a characteristic unpleasant odor. It is a stable binary hydride and the simplest pnictogen hydride. It contributes considerably to the nutritional demands of terrestrial creatures by serving as a precursor to 45 percent of the world's food and fertilizers. Biologically, it is a common nitrogenous waste, especially among aquatic animals. About 70% of ammonia is used to create fertilizers, including urea and diammonium phosphate, in a variety of shapes and compositions. Additionally, pure ammonia is sprayed straight onto the ground. About 40% of the nitrogen in people is thought to have originated from the manufacturing of industrial ammonia. Its significance can therefore hardly be emphasized.

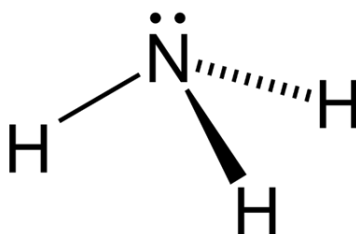


Figure 1 Stereo structural formula of the ammonia molecule.

Ammonia is also a key ingredient in many commercial cleaning solutions and is a building component for the manufacture of numerous medicinal medicines. It is mostly gathered through the displacement of both air and water downward. Although ammonia is widely used and found in nature on Earth and on the outer planets of the Solar System, it is dangerous and caustic when it is concentrated. Facilities that produce, store, or utilize it in sizable amounts are subject to severe reporting requirements in many nations because it is categorized as an exceedingly hazardous material.

A solution of ammonia in water is referred to as ammonia solution, ammonia water, ammonium hydroxide, aqua ammonia, aqueous ammonia, or (inaccurately) ammonia. You can represent it with the symbols NH_3 (aq). It is hard to isolate samples of NH_4OH , despite the term ammonium hydroxide suggesting an alkali with

composition $[\text{NH}_4^+][\text{OH}]$. Except in extremely diluted solutions, the ions NH_4^+ and OH do not contribute significantly to the total quantity of ammonia.

The creation of ammonia from the elements hydrogen and nitrogen is challenging for fundamental reasons, requiring high pressures and high temperatures. At the start of the twentieth century, the Haber process—which made industrial production possible—revolutionized agriculture. NH_3 must be stored under pressure or at a low temperature because it boils at $33.34\text{ }^\circ\text{C}$ (or $28.012\text{ }^\circ\text{F}$) at a pressure of one atmosphere. NH_3 is dissolved in water to form household ammonia, also known as ammonium hydroxide. The density of such solutions is measured in units of the Baumé scale, with 26 degrees Baumé being the usual high-concentration commercial product (about 30% (by weight) ammonia at $15.5\text{ }^\circ\text{C}$ or $59.9\text{ }^\circ\text{F}$).

2) Properties

Ammonia is a colourless gas with a characteristically pungent smell. It is lighter than air, its density being 0.589 times that of air. It is easily liquefied due to the strong hydrogen bonding between molecules; the liquid boils at $-33.1\text{ }^\circ\text{C}$ ($-27.58\text{ }^\circ\text{F}$), and freezes to white crystals^[23] at $-77.7\text{ }^\circ\text{C}$ ($-107.86\text{ }^\circ\text{F}$).

a) Solid

The crystal symmetry is cubic, Pearson symbol cP16, space group P2₁3 No.198, lattice constant 0.5125 nm.

b) Liquid

Liquid ammonia possesses strong ionising powers reflecting its high ϵ of 22. Liquid ammonia has a very high standard enthalpy change of vaporization (23.35 kJ/mol, cf. water 40.65 kJ/mol, methane 8.19 kJ/mol, phosphine 14.6 kJ/mol) and can therefore be used in laboratories in uninsulated vessels without additional refrigeration. See liquid ammonia as a solvent.

c) Solvent properties

Ammonia readily dissolves in water. In an aqueous solution, it can be expelled by boiling. The aqueous solution of ammonia is basic. The maximum concentration of ammonia in water (a saturated solution) has a density of 0.880 g/cm^3 and is often known as '.880 ammonia'.

d) Combustion

Ammonia does not burn readily or sustain combustion, except under narrow fuel-to-air mixtures of 15–25% air. When mixed with oxygen, it burns with a pale yellowish-green flame. Ignition occurs when chlorine is passed into ammonia,

forming nitrogen and hydrogen chloride; if chlorine is present in excess, then the highly explosive nitrogen trichloride (NCl_3) is also formed.

e) Decomposition

At high temperature and in the presence of a suitable catalyst or in a pressurized vessel with constant volume and high temperature (e.g. $1,100\text{ }^\circ\text{C}$ ($2,010\text{ }^\circ\text{F}$)), ammonia is decomposed into its constituent elements. Decomposition of ammonia is a slightly endothermic process requiring 23 kJ/mol (5.5 kcal/mol) of ammonia, and yields hydrogen and nitrogen gas. Ammonia can also be used as a source of hydrogen for acid fuel cells if the unreacted ammonia can be removed. Ruthenium and platinum catalysts were found to be the most active, whereas supported Ni catalysts were less active.

3) Structure

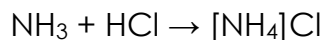
The ammonia molecule has a trigonal pyramidal shape as predicted by the valence shell electron pair repulsion theory (VSEPR theory) with an experimentally determined bond angle of 106.7° . The central nitrogen atom has five outer electrons with an additional electron from each hydrogen atom. This gives a total of eight electrons, or four electron pairs that are arranged tetrahedrally. Three of these electron pairs are used as bond pairs, which leaves one lone pair of electrons. The lone pair repels more strongly than bond pairs, therefore the bond angle is not 109.5° , as expected for a regular tetrahedral arrangement, but 106.8° . This shape gives the molecule a dipole moment and makes it polar. The molecule's polarity, and especially, its ability to form hydrogen bonds, makes ammonia highly miscible with water. The lone pair makes ammonia a base, a proton acceptor. Ammonia is moderately basic; a 1.0 M aqueous solution has a pH of 11.6 , and if a strong acid is added to such a solution until the solution is neutral ($\text{pH} = 7$), 99.4% of the ammonia molecules are protonated. Temperature and salinity also affect the proportion of NH_4^+ . The latter has the shape of a regular tetrahedron and is isoelectronic with methane.

The ammonia molecule readily undergoes nitrogen inversion at room temperature; a useful analogy is an umbrella turning itself inside out in a strong wind. The energy barrier to this inversion is 24.7 kJ/mol , and the resonance frequency is 23.79 GHz , corresponding to microwave radiation of a wavelength of 1.260 cm . The absorption at this frequency was the first microwave spectrum to be observed ^[30] and was used in the first maser.

4) Amphotericity

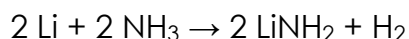
One of the most characteristic properties of ammonia is its basicity. Ammonia is considered to be a weak base. It combines with acids to form salts; thus with hydrochloric acid it forms ammonium chloride (sal ammoniac); with nitric acid, ammonium nitrate, etc. Perfectly dry ammonia gas will not combine with perfectly dry hydrogen chloride gas; moisture is necessary to bring about the reaction.

As a demonstration experiment under air with ambient moisture, opened bottles of concentrated ammonia and hydrochloric acid solutions produce a cloud of ammonium chloride, which seems to appear "out of nothing" as the salt aerosol forms where the two diffusing clouds of reagents meet between the two bottles.



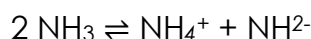
The salts produced by the action of ammonia on acids are known as the ammonium salts and all contain the ammonium ion (NH_4^+).

Although ammonia is well known as a weak base, it can also act as an extremely weak acid. It is a protic substance and is capable of formation of amides (which contain the NH_2^- ion). For example, lithium dissolves in liquid ammonia to give a blue solution (solvated electron) of lithium amide:



5) Self-dissociation

Like water, liquid ammonia undergoes molecular auto-ionisation to form its acid and base conjugates:



Ammonia often functions as a weak base, so it has some buffering ability. Shifts in pH will cause more or fewer ammonium cations (NH_4^+) and amide anions (NH_2^-) to be present in solution. At standard pressure and temperature,

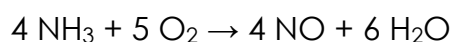
$$K = [\text{NH}_4^+] \times [\text{NH}_2^-] = 10^{-30}.$$

6) Combustion

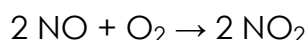
The combustion of ammonia to form nitrogen and water is exothermic:

$4 \text{NH}_3 + 3 \text{O}_2 \rightarrow 2 \text{N}_2 + 6 \text{H}_2\text{O}(\text{g})$, $\Delta H^\circ_r = -1267.20 \text{ kJ}$ (or -316.8 kJ/mol if expressed per mol of NH_3)

The standard enthalpy change of combustion, ΔH°_c , expressed per mole of ammonia and with condensation of the water formed, is -382.81 kJ/mol . Dinitrogen is the thermodynamic product of combustion: all nitrogen oxides are unstable with respect to N_2 and O_2 , which is the principle behind the catalytic converter. Nitrogen oxides can be formed as kinetic products in the presence of appropriate catalysts, a reaction of great industrial importance in the production of nitric acid:



A subsequent reaction leads to NO_2 :



The combustion of ammonia in air is very difficult in the absence of a catalyst (such as platinum gauze or warm chromium(III) oxide), due to the

relatively low heat of combustion, a lower laminar burning velocity, high auto-ignition temperature, high heat of vaporization, and a narrow flammability range. However, recent studies have shown that efficient and stable combustion of ammonia can be achieved using swirl combustors, thereby rekindling research interest in ammonia as a fuel for thermal power production. The flammable range of ammonia in dry air is 15.15–27.35% and in 100% relative humidity air is 15.95–26.55%. For studying the kinetics of ammonia combustion, knowledge of a detailed reliable reaction mechanism is required, but this has been challenging to obtain.

7) Formation of other compounds

Ammonia is a direct or indirect precursor to most manufactured nitrogen-containing compounds.

In organic chemistry, ammonia can act as a nucleophile in substitution reactions. Amines can be formed by the reaction of ammonia with alkyl halides or with alcohols. The resulting $-NH_2$ group is also nucleophilic so secondary and tertiary amines are often formed. When such multiple substitution is not desired, an excess of ammonia helps minimise it. For example, methylamine is prepared by the reaction of ammonia with chloromethane or with methanol. In both cases, dimethylamine and trimethylamine are co-produced. Ethanolamine is prepared by a ring-opening reaction with ethylene oxide, and when the reaction is allowed to go further it produces diethanolamine and triethanolamine. The reaction of ammonia with 2-bromopropanoic acid has been used to prepare racemic alanine in 70% yield.

Amides can be prepared by the reaction of ammonia with carboxylic acid derivatives. For example, ammonia reacts with formic acid ($HCOOH$) to yield formamide ($HCONH_2$) when heated. Acyl chlorides are the most reactive, but the ammonia must be present in at least a twofold excess to neutralise the hydrogen chloride formed. Esters and anhydrides also react with ammonia to form amides. Ammonium salts of carboxylic acids can be dehydrated to amides by heating to 150–200 °C as long as no thermally sensitive groups are present.

The hydrogen in ammonia is susceptible to replacement by a myriad of substituents. When dry ammonia gas is heated with metallic sodium it converts to sodamide, $NaNH_2$.^[31] With chlorine, monochloramine is formed.

Pentavalent ammonia is known as λ^5 -amine or, more commonly, ammonium hydride. This crystalline solid is only stable under high pressure and decomposes back into trivalent ammonia and hydrogen gas at normal conditions. This substance was once investigated as a possible solid rocket fuel in 1966.

8) History

The ancient Greek historian Herodotus mentioned that there were outcrops of salt in an area of Libya that was inhabited by a people called the "Ammonians" (now: the Siwa oasis in northwestern Egypt, where salt lakes still exist). The Greek geographer Strabo also mentioned the salt from this region. However, the ancient authors Dioscorides, Apicius, Arrian, Synesius, and Aëtius of Amida described this

salt as forming clear crystals that could be used for cooking and that were essentially rock salt.^[44] *Hammoniacus sal* appears in the writings of Pliny, although it is not known whether the term is identical with the more modern sal ammoniac (ammonium chloride).

The fermentation of urine by bacteria produces a solution of ammonia; hence fermented urine was used in Classical Antiquity to wash cloth and clothing, to remove hair from hides in preparation for tanning, to serve as a mordant in dyeing cloth, and to remove rust from iron. It was also used by ancient dentists to wash teeth.

In the form of sal ammoniac (نشادر *nushadir*), ammonia was important to the Muslim alchemists. It was mentioned in the *Book of Stones*, likely written in the 9th century and attributed to Jābir ibn Hayyān. It was also important to the European alchemists of the 13th century, being mentioned by Albertus Magnus. It was also used by dyers in the Middle Ages in the form of fermented urine to alter the colour of vegetable dyes. In the 15th century, Basilius Valentinus showed that ammonia could be obtained by the action of alkalis on sal ammoniac. At a later period, when sal ammoniac was obtained by distilling the hooves and horns of oxen and neutralizing the resulting carbonate with hydrochloric acid, the name "spirit of hartshorn" was applied to ammonia.

Gaseous ammonia was first isolated by Joseph Black in 1756 by reacting *sal ammoniac* (ammonium chloride) with *calcined magnesia* (magnesium oxide). It was isolated again by Peter Woulfe in 1767, by Carl Wilhelm Scheele in 1770 and by Joseph Priestley in 1773 and was termed by him "alkaline air". Eleven years later in 1785, Claude Louis Berthollet ascertained its composition.

The Haber–Bosch process to produce ammonia from the nitrogen in the air was developed by Fritz Haber and Carl Bosch in 1909 and patented in 1910. It was first used on an industrial scale in Germany during World War I, following the allied blockade that cut off the supply of nitrates from Chile. The ammonia was used to produce explosives to sustain war efforts.

Before the availability of natural gas, hydrogen as a precursor to ammonia production was produced via the electrolysis of water or using the chloralkali process.

With the advent of the steel industry in the 20th century, ammonia became a byproduct of the production of coking coal.

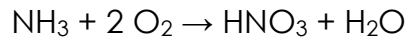
3.3. Applications

1) Fertilizer

In the US as of 2019, approximately 88% of ammonia was used as fertilizers either as its salts, solutions or anhydrously. When applied to soil, it helps provide increased yields of crops such as maize and wheat. 30% of agricultural nitrogen applied in the US is in the form of anhydrous ammonia and worldwide 110 million tonnes are applied each year.

2) Precursor to nitrogenous compounds

Ammonia is directly or indirectly the precursor to most nitrogen-containing compounds. Virtually all synthetic nitrogen compounds are derived from ammonia. An important derivative is nitric acid. This key material is generated via the Ostwald process by oxidation of ammonia with air over a platinum catalyst at 700–850 °C (1,292–1,562 °F), ≈9 atm. Nitric oxide is an intermediate in this conversion:



Nitric acid is used for the production of fertilizers, explosives, and many organonitrogen compounds.

Ammonia is also used to make the following compounds:

- Hydrazine, in the Olin Raschig process and the peroxide process
- Hydrogen cyanide, in the BMA process and the Andrussov process
- Hydroxylamine and ammonium carbonate, in the Raschig process
- Phenol, in the Raschig–Hooker process
- Urea, in the Bosch–Meiser urea process and in Wöhler synthesis
- Amino acids, using Strecker amino-acid synthesis
- Acrylonitrile, in the Sohio process

Ammonia can also be used to make compounds in reactions which are not specifically named. Examples of such compounds include: ammonium perchlorate, ammonium nitrate, formamide, dinitrogen tetroxide, alprazolam, ethanolamine, ethyl carbamate, hexamethylenetetramine, and ammonium bicarbonate.

3) Fuel

The raw energy density of liquid ammonia is 11.5 MJ/L, which is about a third that of diesel. There is the opportunity to convert ammonia back to hydrogen, where it can be used to power hydrogen fuel cells, or it may be used directly within high-temperature solid oxide direct ammonia fuel cells to provide efficient power sources that do not emit greenhouse gases.

The conversion of ammonia to hydrogen via the sodium amide process, either for combustion or as fuel for a proton exchange membrane fuel cell, is possible. Another method is the catalytic decomposition of ammonia using solid catalysts. Conversion to hydrogen would allow the storage of hydrogen at nearly 18 wt% compared to ≈5% for gaseous hydrogen under pressure.

Ammonia engines or ammonia motors, using ammonia as a working fluid, have been proposed and occasionally used. The principle is similar to that used in a fireless locomotive, but with ammonia as the working fluid, instead of steam or compressed air. Ammonia engines were used experimentally in the 19th century by Goldsworthy Gurney in the UK and the St. Charles Avenue Streetcar line in New Orleans in the 1870s and 1880s, and during World War II ammonia was used to power buses in Belgium.



Figure 2 Ammoniacal Gas Engine Streetcar in New Orleans drawn by Alfred Waud in 1871.

Ammonia is sometimes proposed as a practical alternative to fossil fuel for internal combustion engines.

Its high octane rating of 120 and low flame temperature allows the use of high compression ratios without a penalty of high NO_x production. Since ammonia contains no carbon, its combustion cannot produce carbon dioxide, carbon monoxide, hydrocarbons, or soot.

Ammonia production currently creates 1.8% of global CO_2 emissions. "Green ammonia" is ammonia produced by using green hydrogen (hydrogen produced by electrolysis), whereas "blue ammonia" is ammonia produced using blue hydrogen (hydrogen produced by steam methane reforming where the carbon dioxide has been captured and stored).

However, ammonia cannot be easily used in existing Otto cycle engines because of its very narrow flammability range, and there are also other barriers to widespread automobile usage. In terms of raw ammonia supplies, plants would have to be built to increase production levels, requiring significant capital and energy sources. Although it is the second most produced chemical (after sulfuric acid), the scale of ammonia production is a small fraction of world petroleum usage. It could be manufactured from renewable energy sources, as well as coal

or nuclear power. The 60 MW Rjukan dam in Telemark, Norway, produced ammonia for many years from 1913, providing fertilizer for much of Europe.

Despite this, several tests have been run. In 1981, a Canadian company converted a 1981 Chevrolet Impala to operate using ammonia as fuel. In 2007, a University of Michigan pickup powered by ammonia drove from Detroit to San Francisco as part of a demonstration, requiring only one fill-up in Wyoming.

Compared to hydrogen as a fuel, **ammonia is much more energy efficient**, and could be produced, stored, and delivered at a much lower cost than hydrogen, which must be kept compressed or as a cryogenic liquid.

Rocket engines have also been fueled by ammonia. The Reaction Motors XLR99 rocket engine that powered the X-15 hypersonic research aircraft used liquid ammonia. Although not as powerful as other fuels, it left no soot in the reusable rocket engine, and its density approximately matches the density of the oxidizer, liquid oxygen, which simplified the aircraft's design.

In early August 2018, scientists from Australia's Commonwealth Scientific and Industrial Research Organisation (CSIRO) announced the success of developing a process to release hydrogen from ammonia and harvest that at ultra-high purity as a fuel for cars. This uses a special membrane. Two demonstration fuel cell vehicles have the technology, a Hyundai Nexa and Toyota Mirai.

In 2020, Saudi Arabia shipped forty metric tons of liquid "blue ammonia" to Japan for use as a fuel. It was produced as a by-product by petrochemical industries, and can be burned without giving off greenhouse gases. Its energy density by volume is nearly double that of liquid hydrogen. If the process of creating it can be scaled up via purely renewable resources, producing green ammonia, it could make a major difference in avoiding climate change. The company ACWA Power and the city of Neom have announced the construction of a green hydrogen and ammonia plant in 2020.

Green ammonia is considered as a potential fuel for future container ships. In 2020, the companies DSME and MAN Energy Solutions announced the construction of an ammonia-based ship, DSME plans to commercialize it by 2025. The use of ammonia as a potential alternative fuel for aircraft jet engines is also being explored.

Japan is targeting to bring forward a plan to develop ammonia co-firing technology that can increase the use of ammonia in power generation, as part of efforts to assist domestic and other Asian utilities to accelerate their transition to carbon neutrality. In October 2021, the first International Conference on Fuel Ammonia (ICFA2021) was held.

In June 2022, IHI Corporation succeeded in reducing greenhouse gases by over 99% during combustion of liquid ammonia in a 2,000-kilowatt-class gas turbine achieving truly CO₂-free power generation. In July 2022, Quad nations of Japan, the U.S., Australia and India agreed to promote technological development for clean-burning hydrogen and ammonia as fuels at the security grouping's first energy meeting.

4) Solvent

Liquid ammonia is the best-known and most widely studied nonaqueous ionising solvent. Its most conspicuous property is its ability to dissolve alkali metals to form highly coloured, electrically conductive solutions containing solvated electrons. Apart from these remarkable solutions, much of the chemistry in liquid ammonia can be classified by analogy with related reactions in aqueous solutions. Comparison of the physical properties of NH_3 with those of water shows NH_3 has the lower melting point, boiling point, density, viscosity, dielectric constant and electrical conductivity; this is due at least in part to the weaker hydrogen bonding in NH_3 and because such bonding cannot form cross-linked networks, since each NH_3 molecule has only one lone pair of electrons compared with two for each H_2O molecule. The ionic self-dissociation constant of liquid NH_3 at $-50\text{ }^\circ\text{C}$ is about 10^{-33} .

5) Cleansing agent

Household "ammonia" (or more correctly called ammonium hydroxide) is a solution of NH_3 in water, and is used as a general purpose cleaner for many surfaces. Because ammonia results in a relatively streak-free shine, one of its most common uses is to clean glass, porcelain and stainless steel. It is also frequently used for cleaning ovens and soaking items to loosen baked-on grime. Household ammonia ranges in concentration by weight from 5 to 10% ammonia. United States manufacturers of cleaning products are required to provide the product's material safety data sheet which lists the concentration used.

Solutions of ammonia (5–10% by weight) are used as household cleaners, particularly for glass. These solutions are irritating to the eyes and mucous membranes (respiratory and digestive tracts), and to a lesser extent the skin. Experts advise that caution be used to ensure the substance is not mixed into any liquid containing bleach, due to the danger of toxic gas. Mixing with chlorine-containing products or strong oxidants, such as household bleach, can generate chloramines.

Experts also warn not to use ammonia-based cleaners (such as glass or window cleaners) on car touchscreens, due to the risk of damage to the screen's anti-glare and anti-fingerprint coatings.

6) Fermentation

Solutions of ammonia ranging from 16% to 25% are used in the fermentation industry as a source of nitrogen for microorganisms and to adjust pH during fermentation.

7) Antimicrobial agent for food products

As early as in 1895, it was known that ammonia was "strongly antiseptic ... it requires 1.4 grams per litre to preserve beef tea (broth)." In one study, anhydrous ammonia destroyed 99.999% of zoonotic bacteria in 3 types of animal feed, but not silage. Anhydrous ammonia is currently used commercially to reduce or eliminate microbial contamination of beef. Lean finely textured beef (popularly known as "pink slime") in the beef industry is made from fatty beef trimmings (c. 50–

70% fat) by removing the fat using heat and centrifugation, then treating it with ammonia to kill *E. coli*. The process was deemed effective and safe by the US Department of Agriculture based on a study that found that the treatment reduces *E. coli* to undetectable levels. There have been safety concerns about the process as well as consumer complaints about the taste and smell of ammonia-treated beef.

8) What prospects does green ammonia have?

Additional possibilities for the transition to net-zero carbon dioxide emissions may be provided by the manufacture of green ammonia. These consist of:

Ammonia is easily kept in large quantities as a liquid at low pressures (10–15 bar) or chilled to $-33\text{ }^{\circ}\text{C}$. It is therefore the perfect chemical storage system for renewable energy. Ammonia is currently distributed around the world via a network of pipes, road tankers, and ships to transfer it from massive chilled tanks.

Ammonia is a zero-carbon fuel that may be burned in an engine or converted into power in a fuel cell. The only by-products of ammonia use are water and nitrogen. The maritime sector is most likely to replace the use of fuel oil in marine engines as an early adopter.

Hydrogen carrier - although hydrogen gas is employed in some applications (such as PEM fuel cells), it is difficult and expensive to store in large quantities (needing cryogenic tanks or high-pressure cylinders). Ammonia is simpler to store, transport, and purify, and it can easily be "cracked" when needed to produce hydrogen gas.

3.4. Electrochemical Synthesis of Ammonia

1) Electrochemical Production (Electrolysis)



The fact that protons and electrons were required for the reaction to be completed suggested that ammonia may be generated electrochemically. To do this, numerous research teams evaluated the performance of aqueous electrochemical cells that generated NH_3 from H_2O and N_2 . However, the fact that these cells required to function at low temperatures where reaction kinetics were slow presented a challenge.

Solid state materials with significantly high proton (H^+) conductivity at high temperatures (500–1000 $^{\circ}\text{C}$) were found in 1981 by Iwahara and colleagues. Experimental evidence of the electrochemical synthesis of ammonia from its constituent parts was presented in 1998 using a high-temperature solid electrolyte cell of this type (Fig. 1).

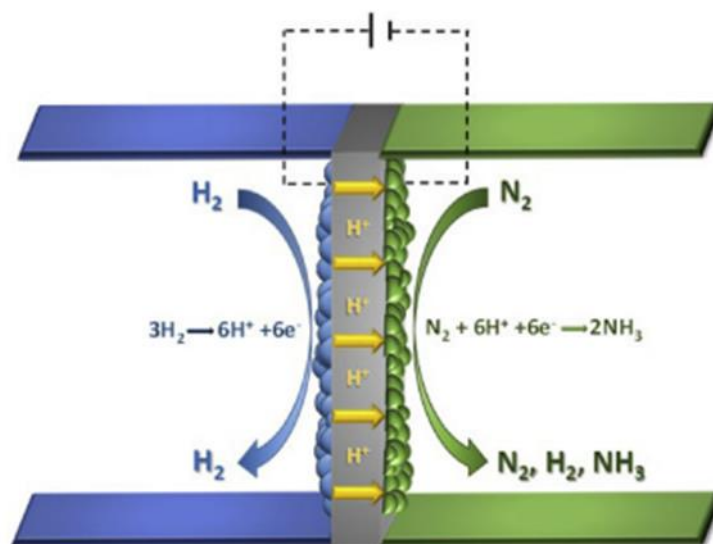


Fig. 1. Schematic diagram of the solid state ammonia synthesis (SSAS) process in a double chamber proton conducting reactor cell.

The procedure was easy. H^+ was created as gaseous hydrogen passed over the proton conducting cell's anodic electrode. The generated protons were electrochemically carried to the cathode by applying the correct voltage, where they interacted with gaseous nitrogen to make ammonia. Because the high-pressure need was balanced by the expenditure of electrical energy, the cell operated at atmospheric pressure.

In an effort to increase reaction rates and reduce electric energy consumption, various research teams have researched the Solid-State Ammonia Synthesis (SSAS) over the past 20 years. Amar et al., Giddey et al., and Garagounis et al. recently examined the key findings from research published prior to 2013.

The current review provides an update on the development of liquid and solid electrolyte cells used in the electrochemical production of ammonia. The experimental studies are separated into three groups based on the operational temperature range: high temperature ($T > 500\text{ }^\circ\text{C}$), intermediate temperature ($500\text{ }^\circ\text{C} > T > 100\text{ }^\circ\text{C}$), and low temperature ($T < 100\text{ }^\circ\text{C}$).

2) Electrochemical Synthesis at High Temperatures

The reported data on the electrochemical synthesis of ammonia at high temperatures ($T > 500^\circ\text{C}$) up until the end of 2015 are listed in Table 1.

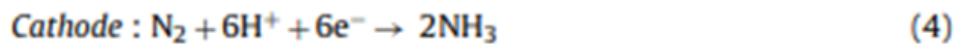
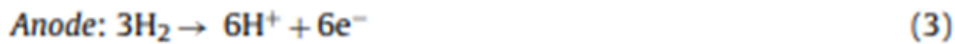
Table 1
Experimental studies and results achieved for electrochemical ammonia synthesis at high temperatures (T > 500 °C).

T, °C	Cathode	Electrolyte	Anode	Reactants Cathode/Anode	r_{NH_3} , mol s ⁻¹ cm ⁻² (I, mA cm ⁻²)	FE, %
570	Pd	ScCe _{0.95} Yb _{0.05} O _{3-δ} (SCY)	Pd	N ₂ /H ₂	4.50 × 10 ⁻⁹ (1.15 [*])	78
550-680 (620)	Ag-Pd	Ba ₂ (Ca _{1.18} Nb _{0.82})O _{6-δ} (BCN18)	Ag-Pd	N ₂ /H ₂	1.42 × 10 ⁻⁹	-
550-680 (620)	Ag-Pd	Ba ₂ CaZr _{0.5} Nb _{1.5} O _{6-δ} (BCZN)	Ag-Pd	N ₂ /H ₂	1.82 × 10 ⁻⁹	-
550-680 (620)	Ag-Pd	Ba ₂ Ca _{0.8} Nd _{0.28} Nb _{1.82} O _{6-δ} (BCNN)	Ag-Pd	N ₂ /H ₂	2.16 × 10 ⁻⁹	-
550-680 (620)	Ag-Pd	BaCe _{0.9} Sm _{0.1} O _{3-δ} (BCS)	Ag-Pd	N ₂ /H ₂	5.23 × 10 ⁻⁹	-
550-680 (620)	Ag-Pd	BaCe _{0.8} Gd _{0.1} Sm _{0.1} O _{3-δ} (BCGS)	Ag-Pd	N ₂ /H ₂	5.82 × 10 ⁻⁹	-
550-650 (550)	Ni-BZCY72	BaZr _{0.9} Ce _{0.1} Y _{0.1} O _{3-δ} (BZCY72)	Rh	N ₂ - H ₂	2.86 × 10 ⁻⁹ (13)	6.2
550	Ag-Pd	La _{0.9} Sr _{0.1} Ga _{0.8} Mg _{0.2} O _{3-δ} (LSGM)	Ag-Pd	N ₂ /H ₂	2.37 × 10 ⁻⁹ (2.1)	≈70
520	Ag-Pd	La _{1.05} Ca _{0.05} Zr ₂ O _{7-δ} (LCZO)	Ag-Pd	N ₂ /H ₂	2.00 × 10 ⁻⁹	-
520	Ag-Pd	La _{1.05} Ca _{0.05} Ce ₂ O _{7-δ} (LCC)	Ag-Pd	N ₂ /H ₂	1.30 × 10 ⁻⁹	-
500-700 (650)	Pd-Ru/MgO	8% Y ₂ O ₃ /ZrO ₂ (YSZ)	Ag	H ₂ O - N ₂ /He	1.50 × 10 ⁻¹³ (8.5)	<1 [*]
500-650 (650)	Ru-Ag/MgO	ScCe _{0.95} Yb _{0.05} O _{3-δ} (SCY)	Pd	N ₂ /H ₂ O	3.00 × 10 ⁻¹³ (10)	<1 [*]
500-600 (550)	Ag	BaZr _{0.8} Y _{0.2} O _{3-δ} (BZY)	Ag	N ₂ /H ₂ O	4.90 × 10 ⁻¹¹ (4.5)	0.46
500-600 (550)	Pt	BaZr _{0.8} Y _{0.2} O _{3-δ} (BZY)	Pt	N ₂ /H ₂ O	<1.00 × 10 ⁻¹² (4.8)	<1 [*]
500-600 (550)	La _{0.8} Sr _{0.4} Co _{0.2} Fe _{0.8} O _{3-δ} (LSCF)	BaZr _{0.8} Y _{0.2} O _{3-δ} (BZY)	La _{0.8} Sr _{0.4} Co _{0.2} Fe _{0.8} O _{3-δ} (LSCF)	N ₂ /H ₂ O	8.50 × 10 ⁻¹¹ (5.5)	0.33
500	La _{0.8} Sr _{0.5} Ti _{0.6} Ru _{0.4} O ₃ (LSTR40)	BaCe _{0.9} Y _{0.1} O _{3-δ} (BCY10)	Pt	N ₂ /H ₂	5.00 × 10 ⁻¹² (0.45)	2
500	Ag-Pd	BaCe _{0.9} Y _{0.1} O _{3-δ} (BCY10)	Pt	N ₂ /H ₂	3.00 × 10 ⁻¹¹ (0.8)	<1 [*]
460-560 (520)	Ag-Pd	La _{1.9} Ca _{0.1} Zr ₂ O _{7-δ} (LCZO)	Ag-Pd	N ₂ /H ₂	1.76 × 10 ⁻⁹ (0.6 [*])	≈80
460-560 (480)	Ag-Pd	BaCe _{0.8} Gd _{0.2} O _{3-δ} (BCGO)	Ag-Pd	N ₂ /H ₂	3.09 × 10 ⁻⁹	-
450-600 (450)	Fe	SrZr _{0.9} Y _{0.1} O _{3-δ} (SZY)	Ag	N ₂ /H ₂	6.50 × 10 ⁻¹² (1.5 [*])	<1 [*]
440-580 (500)	Ag-Pd	BaCe _{0.85} Y _{0.15} O _{3-δ} (BCY)	Ag-Pd	N ₂ /H ₂	2.10 × 10 ⁻⁹	≈60
420-660 (620)	Ni-BZCY72	BaZr _{0.7} Ce _{0.2} Y _{0.1} O _{3-δ} (BZCY72)	Cu	N ₂ /H ₂	1.70 × 10 ⁻⁹ (23)	2.7
420-660 (620)	Ni-BZCY72	BaZr _{0.7} Ce _{0.2} Y _{0.1} O _{3-δ} (BZCY72)	Cu	H ₂ - N ₂ /H ₂	4.10 × 10 ⁻⁹ (18.5)	≈10
420-540 (500)	Ag-Pd	Ba _{0.98} Ce _{0.8} Y _{0.2} O _{3-δ} + 0.04ZnO (BCYZ)	Ag-Pd	N ₂ /H ₂	2.6 × 10 ⁻⁹ (3 [*])	45
410-600 (530)	Ba _{0.3} Sr _{0.5} Co _{0.8} Fe _{0.2} O _{3-δ} (BSCF)	BaCe _{0.85} Y _{0.15} O _{3-δ} (BCY)	Ni-BCY	N ₂ /H ₂	4.10 × 10 ⁻⁹ (2 [*])	60
400-800 (650)	Ag-Pd	Ce _{0.8} Y _{0.2} O _{1.9} (YDC) - Ca ₃ (PO ₄) ₂ -K ₃ PO ₄	Ag-Pd	N ₂ /H ₂	9.50 × 10 ⁻⁹	-
400-800 (650)	Ag-Pd	Ce _{0.8} Y _{0.2} O _{1.9} (YDC) - Ca ₃ (PO ₄) ₂ , K ₃ PO ₄	Ag-Pd	N ₂ /Natural Gas	6.95 × 10 ⁻⁹	-
400-800 (650)	Ag-Pd	Ce _{0.8} La _{0.2} O _{2-δ} (LDC)	Ag-Pd	N ₂ /H ₂	7.20 × 10 ⁻⁹	-
400-800 (650)	Ag-Pd	(Ce _{0.8} La _{0.2}) _{0.975} Ca _{0.025} O _{2-δ} (CLC)	Ag-Pd	N ₂ /H ₂	7.50 × 10 ⁻⁹	-
400-800 (650)	Ag-Pd	Ce _{0.8} Sm _{0.2} O _{1.9} (SDC)	Ag-Pd	N ₂ /H ₂	7.20 × 10 ⁻⁹	-
400-800 (650)	Ag-Pd	Ce _{0.8} Gd _{0.2} O _{1.9} (GDC)	Ag-Pd	N ₂ /H ₂	7.50 × 10 ⁻⁹	-
400-800 (650)	Ag-Pd	Ce _{0.8} Y _{0.2} O _{1.9} (YDC)	Ag-Pd	N ₂ /H ₂	7.70 × 10 ⁻⁹	-
400-800 (650)	Ag-Pd	Ce _{0.8} La _{0.2} O _{1.9} (LDC)	Ag-Pd	N ₂ /H ₂	8.20 × 10 ⁻⁹	-
400-620 (520)	Ag-Pd	La _{0.9} Ca _{0.1} Ga _{0.8} Mg _{0.2} O _{3-δ} (LCCGM)	Ag-Pd	N ₂ /H ₂	1.63 × 10 ⁻⁹ (1)	47
400-620 (520)	Ag-Pd	La _{0.9} Sr _{0.1} Ga _{0.8} Mg _{0.2} O _{3-δ} (LSGM)	Ag-Pd	N ₂ /H ₂	2.53 × 10 ⁻⁹ (1)	73
400-620 (520)	Ag-Pd	La _{0.9} Ba _{0.1} Ga _{0.8} Mg _{0.2} O _{3-δ} (LBGM)	Ag-Pd	N ₂ /H ₂	2.04 × 10 ⁻⁹ (1)	60
400-600 (600)	Pt	Ce _{0.9} Gd _{0.1} O _{2-δ} (GDC)	Pt	H ₂ O - N ₂ /-	3.67 × 10 ⁻¹¹ (6)	4.53
400-600 (520)	Ag-Pd	La _{0.9} Ba _{0.1} Ga _{0.8} Mg _{0.2} O _{3-δ} (LBGM)	Ag-Pd	N ₂ /H ₂	1.89 × 10 ⁻⁹ (0.88 [*])	60
400-560 (480)	Ag-Pd	BaCe _{0.85} Gd _{0.15} O _{3-δ} (BCGO)	Ni-BCGO	N ₂ /H ₂	5.00 × 10 ⁻⁹ (3.75 [*])	70
400-550 (500)	Ag-Pd	BaCe _{0.7} Zr _{0.2} Sm _{0.1} O _{3-δ} (BCZS)	Ag-Pd	N ₂ /H ₂	2.67 × 10 ⁻⁹ (1.6 [*])	50
400-520 (480)	Ag-Pd	BaCe _{0.9} Ca _{0.1} O _{3-δ} (BCC)	Ag-Pd	N ₂ /H ₂	2.69 × 10 ⁻⁹ (1.6 [*])	50
380-580 (530)	Ag-Pd	BaCe _{0.85} Dy _{0.15} O _{3-δ} (BCD)	Ag-Pd	N ₂ /H ₂	3.50 × 10 ⁻⁹ (1.9 [*])	52 [*]

* Calculated based on reference data.

The maximal ammonia synthesis (and current density at which it was reached) and Faradaic Efficiency (FE) values attained while employing these materials are shown in this table together with the electrolytes and electrodes employed by various research organizations. Asterisks are used to indicate certain current density or FE values. These numbers were derived using the data provided in the specified reference even though they were not reported there. Additionally, in other instances no exact value is supplied because these works lacked the necessary details to enable its calculation. Similar tables have been created for research carried out at low and moderate temperatures (Tables 2 and 3, respectively)

In a reactor-cell architecture similar to that shown in Fig. 1, solid electrolytes were used in the majority of the research described in Table 1. The electrolyte substance used in the majority of these instances was perovskite. There have also been reports of materials with fluorite or pyrochlore structures being used as electrolytes. One group observed surprisingly high ammonia rates using a composite electrolyte made of calcium-potassium phosphate and YDC. The electrochemical processes at the two electrodes can be expressed as follows when, as in Fig. 1, the electrolyte is a proton conductor:



Together, reactions (3) and (4) provide an overall reaction that is identical to reaction (1). The most frequent reactants at the anode and cathode, as shown in Table 1, were gaseous H₂ and N₂, respectively.

The highest rates have been noted over catalysts containing Pd. The cathodic electrode (catalyst) used in the initial SSAS experiments was Pd, and the greatest reaction rate recorded there was 4.5×10^{-9} mol s⁻¹ cm⁻², while the highest FE was 78%.

Numerous researchers have examined Ag-activities Pd's over the last ten years. Li et al. observed reaction rates as high as 5.82×10^{-9} mol s⁻¹ cm⁻² using barium cerates (BCS, BCGS) as electrolytes.

Liu et al. achieved a reaction rate of 8.2×10^{-9} mol s⁻¹ cm⁻² using a lanthanum-doped cerium oxide electrolyte (LDC). The highest Faradaic Efficiencies have been produced using Ag-Pd electrodes in addition to having high reaction speeds. The FEs obtained by Zhang et al., Chen et al., and Xie et al. when utilizing lanthanum gallate and lanthanum zirconate electrolytes were 70%, 73%, and 80%, respectively.

The protonic conductivity of perovskite electrolytes has been shown to increase in the presence of water vapor (steam). In order to do this, the introduction of humidified hydrogen as opposed to dry hydrogen has also been tested on a variety of materials. Table 1 shows that greater reaction rates and FEs are produced with wet hydrogen over the anode when using barium cerate-based electrolytes.

The industrial process's preparation of the hydrogen input gas, more specifically its purification, accounts for a sizeable portion of the entire cost. Natural gas is the main source of hydrogen production. The latter contains substances that can contaminate the industrial catalyst even in minute concentrations. H₂ must therefore undergo substantial purification.

This prerequisite is not met by the electrochemical synthesis (Fig. 1) because only protons (H⁺) are transported through the solid electrolyte. Furthermore, using gaseous H₂ is not required. Evidently, any substance containing hydrogen might be utilized.

Thus, the viability of SSAS from steam and nitrogen was demonstrated in 2009 utilizing the solid electrolyte cell of Fig. 2 and an Ag-Ru/MgO catalyst (cathode).

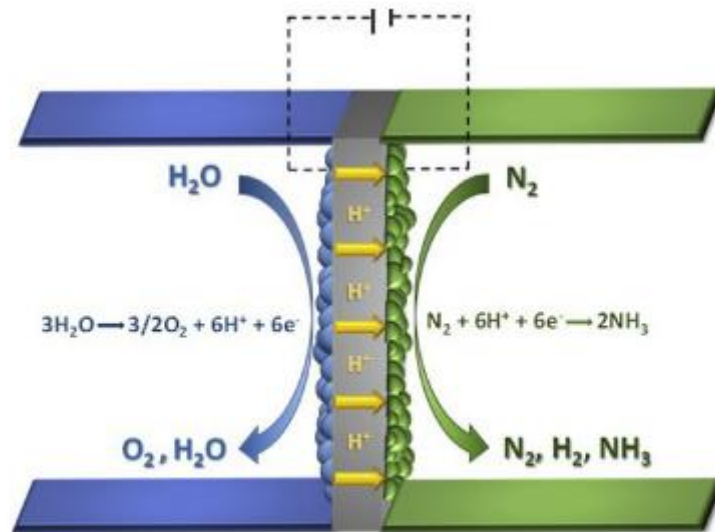


Fig. 2. A schematic of the SSAS process in a double chamber proton conducting cell with steam instead of molecular hydrogen as the source of protons.

Similar investigations using Pt and Ag electrodes came after. Using natural gas (CH_4) as the hydrogen source, Wang et al. examined the reaction at 650°C on an Ag-Pd cathode with a composite electrolyte made of $\text{YDC-Ca}_3(\text{PO}_4)_2, \text{K}_3\text{PO}_4$. One of the highest ammonia rates at these temperatures was $6.95 \cdot 10^{-9} \text{ mol s}^{-1} \text{ cm}^{-2}$ that they could measure.

The usage of an oxygen-ion (O^{2-}) conductor for SSAS is schematically depicted in Fig. 3. The following processes result in ammonia when gaseous nitrogen and steam are combined:

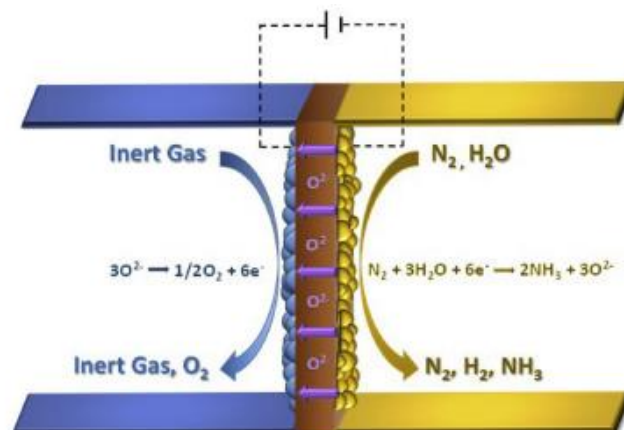
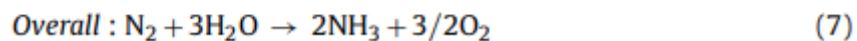
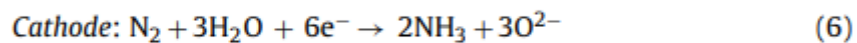


Fig. 3. A schematic of the SSAS process where an oxygen ion (O^{2-}) conductor is employed as the electrolyte.

In this instance, the cathode serves as the site for both steam electrolysis and ammonia production. Table 1 demonstrates that compared to the cells in Figure 1, the response rates in these O₂ cells were one to three orders of magnitude lower. This is explained by the oxygen-containing molecules (H₂O) that are present near the cathode. Such a setup allows for the supply of gaseous fuel rather than inert gas to the anode. The oxygen pumped away from the cathode could oxidize this fuel, which could lower the energy needed for the in-situ synthesis of hydrogen (steam electrolysis). The entire process might even become spontaneous, fully negating the requirement for an electrical energy source, depending on the fuel and the operating temperature.

3) Electrochemical Synthesis at Intermediate Temperatures

The findings from tests carried out at intermediate temperatures, or between 100°C and 500°C, are presented in Table 2. Molten salts and composite materials were the two types of electrolytes used in these investigations.

Table 2
Results with various electrochemical systems for ammonia formation at intermediate temperatures (100 °C < T < 500 °C).

T, °C	Cathode	Electrolyte	Anode	Reactants Cathode/Anode	Γ_{NH_3} , mol s ⁻¹ cm ⁻² (l, mA cm ⁻²)	FE, %
500	Porous Ni Plate	LiCl, KCl, CsCl (0.5% Li ₃ N)	Porous Al Plate	N ₂ /CH ₄	–	10
400–475(450)	La _{0.6} Sr _{0.4} Fe _{0.8} Cu _{0.2} O _{3–δ} (LSFCu) – SDC	(Li,Na,K) ₂ CO ₃ – Ce _{0.8} Sm _{0.2} O _{2–δ} (SDC)	Ni-SDC	N ₂ /H ₂	5.39 × 10 ⁻⁹ (55)	7.5 ^a
400–450(425)	Fe ₃ Mo ₃ N-Ag (catalyst)	LiAlO ₂ – ((Li/Na/K) ₂ CO ₃)	Ag-Pd	N ₂ /H ₂	1.88 × 10 ⁻¹⁰ (3)	6.5
400–450(450)	Co ₃ Mo ₃ N-Ag	LiAlO ₂ – (Li/Na/K) ₂ CO ₃	Ag-Pd	N ₂ /H ₂	3.27 × 10 ⁻¹⁰ (3.21)	3.83
400–450(400)	CoFe ₂ O ₄ -Ag	LiAlO ₂ – (Li/Na/K) ₂ CO ₃	Ag-Pd	N ₂ /H ₂	2.32 × 10 ⁻¹⁰ (3)	2.3 ^a
400–450(400)	La _{0.8} Cs _{0.2} Fe _{0.8} Ni _{0.2} O _{3–δ} (LCFN) – CGO	Ce _{0.8} Gd _{0.2} O _{2–δ} (CGO) – (Li/Na/K) ₂ CO ₃	La _{0.8} Cs _{0.2} Fe _{0.8} Ni _{0.2} O _{3–δ} (LCFN) – CGO	H ₂ O – N ₂	1.23 × 10 ⁻¹⁰ (8.7)	0.55
400–450(400)	La _{0.8} Cs _{0.2} Fe _{0.8} Ni _{0.2} O _{3–δ} (LCFN) – CGO	Ce _{0.8} Gd _{0.2} O _{2–δ} (CGO) – (Li/Na/K) ₂ CO ₃	La _{0.8} Cs _{0.2} Fe _{0.8} Ni _{0.2} O _{3–δ} (LCFN) – CGO	H ₂ O – Air	9.21 × 10 ⁻¹¹ (60)	0.06
375–450(400)	CoFe ₂ O ₄ (CFO) – CGDC	(Li,Na,K) ₂ CO ₃ – Ce _{0.8} Gd _{0.18} Ca _{0.02} O _{2–δ} (CGDC)	Sm _{0.5} Sr _{0.5} CoO _{3–δ} (SSCo) – CGDC	H ₂ O – N ₂ /Air	6.50 × 10 ⁻¹¹ (11.28)	0.17
375–450(400)	La _{0.6} Sr _{0.4} Fe _{0.8} Cu _{0.2} O _{3–δ} (LSFCu) – CGDC	Ce _{0.8} Gd _{0.18} Ca _{0.02} O _{2–δ} (CGDC) – (Li/Na/K) ₂ CO ₃	Sm _{0.5} Sr _{0.5} CoO _{3–δ} (SSCo) – CGDC	H ₂ O – N ₂ /Air	5.00 × 10 ⁻¹¹ (14.5)	0.39
375–450(400)	La _{0.6} Sr _{0.4} Fe _{0.8} Cu _{0.2} O _{3–δ} (LSF) – CGDC	Ce _{0.8} Gd _{0.18} Ca _{0.02} O _{2–δ} (CGDC) – (Li/Na/K) ₂ CO ₃	Sm _{0.5} Sr _{0.5} CoO _{3–δ} (SSCo) – CGDC	H ₂ O – N ₂ /Air	7.00 × 10 ⁻¹¹ (12.5)	0.22
375–425(375)	La _{0.75} Sr _{0.25} Cr _{0.5} Fe _{0.5} O _{3–δ} (LSCrF) – CGDC	Ce _{0.8} Gd _{0.18} Ca _{0.02} O _{2–δ} (CGDC) – (Li/Na/K) ₂ CO ₃	Sm _{0.5} Sr _{0.5} CoO _{3–δ} (SSCo) – CGDC	H ₂ O – N ₂ /Air	4.00 × 10 ⁻¹⁰ (3)	3.87
400	Pr _{0.6} Ba _{0.4} Fe _{0.8} Cu _{0.2} O _{3–δ} (PBFCu) – CGO	Ce _{0.8} Gd _{0.2} O _{2–δ} (CGO) – (Li/Na/K) ₂ CO ₃	Pr _{0.6} Ba _{0.4} Fe _{0.8} Cu _{0.2} O _{3–δ} (PBFCu) – CGO	H ₂ O – N ₂	1.83 × 10 ⁻¹⁰ (1)	5.4
400	Pr _{0.6} Ba _{0.4} Fe _{0.8} Cu _{0.2} O _{3–δ} (PBFCu) – CGO	Ce _{0.8} Gd _{0.2} O _{2–δ} (CGO) – (Li/Na/K) ₂ CO ₃	Pr _{0.6} Ba _{0.4} Fe _{0.8} Cu _{0.2} O _{3–δ} (PBFCu) – CGO	H ₂ O – Air	1.07 × 10 ⁻¹⁰ (4)	0.75
400	Sm _{0.6} Ba _{0.4} Fe _{0.8} Cu _{0.2} O _{3–δ} (SBFCu) – CGO	Ce _{0.8} Gd _{0.2} O _{2–δ} (CGO) – (Li/Na/K) ₂ CO ₃	Sm _{0.6} Ba _{0.4} Fe _{0.8} Cu _{0.2} O _{3–δ} (SBFCu) – CGO	H ₂ O – N ₂	1.53 × 10 ⁻¹⁰ (2.6)	1.19
400	Sm _{0.6} Ba _{0.4} Fe _{0.8} Cu _{0.2} O _{3–δ} (SBFCu) – CGO	Ce _{0.8} Gd _{0.2} O _{2–δ} (CGO) – (Li/Na/K) ₂ CO ₃	Sm _{0.6} Ba _{0.4} Fe _{0.8} Cu _{0.2} O _{3–δ} (SBFCu) – CGO	H ₂ O – Air	9.19 × 10 ⁻¹¹ (2.2)	0.74
400	Porous Ni Plate	LiCl, KCl, CsCl (0.5% Li ₃ N)	Porous Ni Plate	N ₂ /H ₂	3.33 × 10 ⁻⁹ (1.34 ^a)	72
400	Al	LiCl, KCl, CsCl (Li ₃ N)	Porous Ni Plate	N ₂ /H ₂	3.33 × 10 ⁻⁸ (16)	72
300	Porous Ni Plate	LiCl, KCl, CsCl (0.5% Li ₃ N)	BDD (baron-doped diamond)	N ₂ /H ₂ O	5.80 × 10 ^{-9a} (25)	80
300	Porous Ni Plate	LiCl, KCl, CsCl (0.5% Li ₃ N)	Glassy carbon rod	N ₂ /H ₂ O	2.00 × 10 ⁻⁸ (23)	23
300	Porous Ni Plate	LiCl, KCl, CsCl (0.5% Li ₃ N)	Glassy carbon rob/Porous Ni	H ₂ S/N ₂	–	70
300	Porous Ni Plate	LiCl, KCl, CsCl (0.5% Li ₃ N)	Glassy carbon rob	HCl/N ₂	–	–
200	Ni	NaOH/KOH Nano-Fe ₂ O ₃	Ni	H ₂ O/N ₂	1.00 × 10 ⁻⁸ (200)	35
105,200 (200)	Monel (nickel-copper alloy)	Na _{0.5} K _{0.5} OH Nano-Fe ₂ O ₃	Ni	H ₂ O/N ₂	1.62 × 10 ⁻⁸ (20)	76

^a Calculated based on reference data.

Temperatures between 200 and 500 °C have been used to operate the cells with molten salt electrolytes. Murakami et al. first investigated ammonia synthesis in the schematically depicted cell in Fig. 4. The electrodes were porous nickel, and the electrolyte was a eutectic mixture of LiCl, KCl, and CsCl. The electrolyte included 0.5 mol% Li₃N, which was the source of the nitride ions (N³⁻). The cathode-supplied nitrogen was converted to N³⁻, which moved through the electrolyte and interacted with hydrogen at the anode to make ammonia:

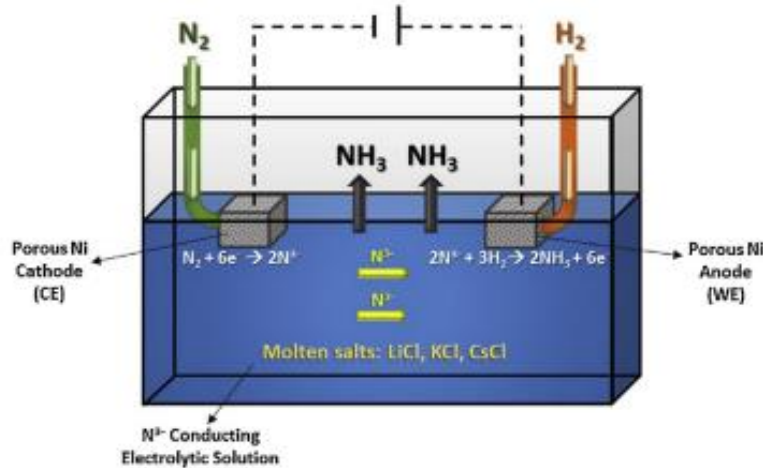


Fig. 4. Apparatus used by Murakami et al. [55]. The electrolyte was a N³⁻ conducting molten salt mixture (57.5LiCl, 13.3KCl, 29.2CsCl mol%) and nitrogen was reduced on a porous Ni cathode.

A certain combination of at least two solid components called a eutectic mixture causes a shift in phase from solid to liquid at a particular temperature. The minimum melting point of the various potential compositions is at this temperature, which is also known as the eutectic point temperature.

The greatest rate they recorded had a FE of 72% and was 3.33*10⁻⁹ mol s⁻¹ cm⁻² at 400 °C and 0.7 volts vs the Li⁺/Li electrode. The same cell also briefly functioned with methane, hydrogen sulfide, and hydrogen chloride as sources of hydrogen. Similar research looked at how substituting hydrogen with steam affected the rate of ammonia production. A glassy carbon rod that functioned as the anode was fed steam into the reactor. In this instance, the anode reaction was:



The FE was much lower (23%), but the reaction rate was higher when H₂O was employed in place of H₂ (2*10⁻⁸ mol s⁻¹ cm⁻² at 2.9V vs. the Li⁺/Li electrode). The carbon electrode and the oxygen ions produced by reaction (9) combined to form carbon dioxide. The glassy carbon anode was swapped out for boron-doped diamond to improve cell stability. As a result, O₂ rather than CO₂ was created at the anode. With the inert anode, the reaction yield was substantially reduced, perhaps as a result of the NH₃ and O₂ reaction. Murphy et al. elaborated on the aforementioned and proposed additional ways to enhance the system. Suggested improvements include, changing the electrolyte (e.g. with bromides in place of chlorides, or organic salts) or the electrodes and the use of multiple

cathodes. But these suggestions have not been implemented by any researchers to date.

More recently, a similar setup was presented by Licht et al., however this time the molten electrolyte also contained a nano-particle catalyst. The catalyst was a nano powder of Fe_2O_3 , and the electrolyte was a molten combination of NaOH and KOH (1:1 molar ratio). The maximal ammonia generation rate was $1 \cdot 10^{-8} \text{ mol s}^{-1} \text{ cm}^{-2}$ at a 1.45% FE with the application of 2.4V vs. the counter electrode. The gas supplies were nitrogen and steam at the cathode and anode, respectively (CE). The authors reported FEs up to 76% and indicated that the performance of the cell might be enhanced by passing a high current for 15–30 minutes prior to applying the operational current. The catalyst's particle size was important because anything larger than 40 microns was completely inert.

Composite electrolytes have been tested during the past ten years in hydrogen fuel cells that operate between 400 and 800 °C. These electrolytes are composed of a solid oxide and a second phase that modifies the material's overall electrical, thermal, or mechanical properties. This extra phase is often a eutectic mixture of alkali metal salts such as carbonates, halides, sulphates or hydroxides. The electrolyte's working temperature is lowered and the ionic conductivity is improved when the molten phase is present.

Similar to those shown in Figs. 1 and 2, Amar et al. investigated these composite electrolytes for SSAS in cell topologies. LiAlO_2 was mixed with $(\text{Li}/\text{Na}/\text{K})_2\text{CO}_3$ at a mass ratio of 1:1 to create a eutectic salt solution. $\text{Fe}_3\text{MO}_3\text{N}$, $\text{Co}_3\text{MO}_3\text{N}$, and CoFe_2O_4 were three distinct catalysts/cathodes that were evaluated under pure nitrogen with wet hydrogen on the anode side (Table 2). The best of these materials, $\text{Co}_3\text{MO}_3\text{N}$, was discovered to have a maximum rate of $3.27 \cdot 10^{-10} \text{ mol s}^{-1} \text{ cm}^{-2}$ at 450 °C and 0.8V applied versus the CE. At 0.4V versus CE, the maximum faradaic efficiency (3.83%) was found, however at a slightly lower production rate ($0.75 \cdot 10^{-10} \text{ mol s}^{-1} \text{ cm}^{-2}$). It was determined that the quick hydrogen evolution process at this temperature was to blame for the low efficiency in all situations. When the electrolyte was changed to $(\text{Li}, \text{Na}, \text{K})_2\text{CO}_3$ -SDC (30:70%wt), the same research team observed a reaction rate 10 times faster than the above ($5.39 \cdot 10^{-9} \text{ mol s}^{-1} \text{ cm}^{-2}$ at 0.8V vs the CE), using a cathodic electrode made up of a 70:30 mixture (by weight) of LSF_{Cu} and SDC.

Furthermore, Amar et al. have also tested ammonia synthesis in an oxygen-ion conducting composite electrolyte (see Fig. 3). Using $(\text{Li}, \text{Na}, \text{K})_2\text{CO}_3$ -CGdC (30:70 wt%) as the electrolyte they studied three different cathodes: CoFe_2O_4 , LSF [51] and LSCrF. The most efficient of them was the LSCrF electrode mixed, with CGdC at a 70:30% wt ratio. The anode was SSCo -CGdC (30:70%wt) and was exposed to the atmosphere, while wet air was fed to the cathode. With this configuration, the researchers observed an ammonia rate equal to $4 \times 10^{-10} \text{ mol s}^{-1} \text{ cm}^{-2}$ with a FE of 3.87% at 375 °C at an applied voltage of 1.4V vs CE. The higher voltage used in

these studies compared to those of the same group with proton conductors, is dictated by the need to electrolyze steam which was the hydrogen source.

The same group have also studied the ammonia synthesis in a symmetrical single chamber reactor configuration, using $(\text{Li,Na,K})_2\text{CO}_3\text{-(CGO)}$ (70:30 wt%) as the electrolyte. This setup is similar to that shown in Fig. 3, but with both electrodes exposed to the same atmosphere. This means that, not only the ammonia synthesis electrode is exposed to steam which is a potential poison, but also the produced ammonia can react with gaseous oxygen generated by the electrolysis. Nevertheless, they tested three different perovskite type catalysts achieving a maximum ammonia rate of $1.83 \times 10^{-10} \text{ mol s}^{-1} \text{ cm}^{-2}$ with a FE of 4.8% at 400 °C and 1.4V vs the CE with PBFCu.

An interesting approach, though not strictly electrochemical, was investigated by Itoh et al. The apparatus is shown in Fig. 5. An Ag-Pd membrane was used to separate hydrogen, generated in situ by water electrolysis.

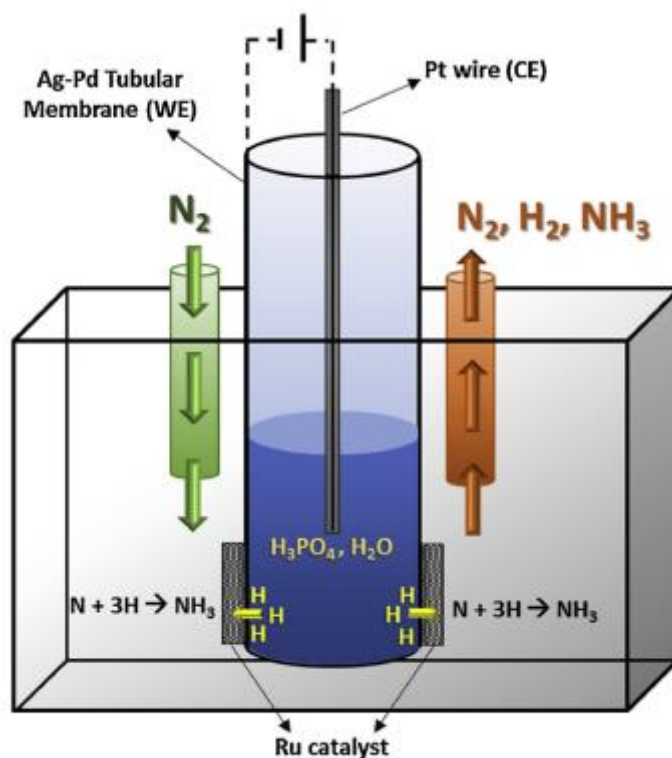


Fig. 5. Schematic representation of the apparatus used by Itoh et al. [64]. Hydrogen is produced in situ from the electrolysis of water.

The membrane was shaped like a closed-ended tube and contained a phosphoric acid solution which served as electrolyte and water source. A Pt-wire was used as the anode, while the membrane also functioned as the cathode. The produced hydrogen, permeated through the membrane in atomic form, to react on a Ru catalyst deposited on its outer surface, over which gaseous nitrogen was flowing. Thus, hydrogen was produced electrochemically, while ammonia was produced catalytically. The highest ammonia synthesis rate measured in this study

was $2.22 \times 10^{-6} \text{ mol s}^{-1} \text{ cm}^{-2}$ at $150 \text{ }^\circ\text{C}$ but it was not stable. To improve stability, the authors introduced a porous Al_2O_3 layer on the ruthenium side of the membrane by a surface coating method. In this way they achieved much better stability but at the cost of catalytic activity ($2.7 \times 10^{-8} \text{ mol s}^{-1} \text{ g}_{\text{cat}}^{-1}$ at $100 \text{ }^\circ\text{C}$).

4) Electrochemical Synthesis at Low Temperatures

Table 3 contains the results from studies conducted at low temperatures, i.e. $T < 100 \text{ }^\circ\text{C}$.

Table 3
Experimental studies on electrochemical ammonia synthesis at low temperatures ($T < 100 \text{ }^\circ\text{C}$).

T, °C	Cathode	Electrolyte	Anode	Reactants Cathode/Anode	$r_{\text{NH}_3}, \text{ mol s}^{-1} \text{ cm}^{-2} (\text{I, mA cm}^{-2})$	FE, %
80–110 (105)	13.2% Ru – Fe	Nafion	–	N_2/H_2	1.10×10^{-10} (1200)	<1 ^a
80	Fe_2O_3	AEM	Pt	$\text{H}_2\text{O} - \text{N}_2/-$	2.50×10^{-10} (1500)	<1 ^a
50	Fe	AEM	–	$\text{H}_2\text{O} - \text{N}_2/-$	3.80×10^{-12}	41
25–95 (80)	$\text{SmBaCuFeO}_{5+\delta}$ (SBCF)	Nafion	$\text{Ni-Ce}_{0.8}\text{Sm}_{0.2}\text{O}_{2-\delta}$ (SDC)	N_2/H_2	6.90×10^{-9}	–
25–95 (80)	$\text{SmBaCuCoO}_{5+\delta}$ (SBCC)	Nafion	$\text{Ni-Ce}_{0.8}\text{Sm}_{0.2}\text{O}_{2-\delta}$ (SDC)	N_2/H_2	7.20×10^{-9}	–
25–95 (80)	$\text{SmBaCuNiO}_{5+\delta}$ (SBCN)	Nafion	$\text{Ni-Ce}_{0.8}\text{Sm}_{0.2}\text{O}_{2-\delta}$ (SDC)	N_2/H_2	8.70×10^{-9}	–
25	Pt	Nafion	Pt	N_2/H_2	3.13×10^{-9} (40)	2.2
25	Pt	Nafion	Pt	Air/ H_2	3.50×10^{-9} (150)	0.7
25	Pt	Nafion	Pt	Air/ H_2O	1.14×10^{-9} (72)	0.55
20–100 (90)	Ru	Nafion	Pt	$\text{H}_2\text{O} - \text{N}_2$	2.12×10^{-11} (2.6 ^a)	0.92
20–100 (80)	$\text{Sm}_{0.5}\text{Sr}_{0.5}\text{CoO}_{3-\delta}$ (SSC)	SPSF	$\text{Ni-Ce}_{0.8}\text{Sm}_{0.2}\text{O}_{2-\delta}$ (SDC)	N_2/H_2	6.50×10^{-9}	–
20–100 (80)	$\text{NiO} - \text{Ce}_{0.8}\text{Sm}_{0.2}\text{O}_{2-\delta}$ (SDC)	SPSF	$\text{Ni-Ce}_{0.8}\text{Sm}_{0.2}\text{O}_{2-\delta}$ (SDC)	N_2/H_2	2.40×10^{-9}	–
20–100 (80)	$\text{Sm}_{1.5}\text{Sr}_{0.5}\text{NiO}_4$	Nafion	$\text{Ni-Ce}_{0.8}\text{Sm}_{0.2}\text{O}_{2-\delta}$ (SDC)	N_2/H_2	1.05×10^{-8}	–
20–100 (80)	$\text{Sm}_{1.5}\text{Sr}_{0.5}\text{NiO}_4$	SPSF	$\text{Ni-Ce}_{0.8}\text{Sm}_{0.2}\text{O}_{2-\delta}$ (SDC)	N_2/H_2	1.03×10^{-8}	–
20–100 (25)	$\text{SmFe}_{0.7}\text{Cu}_{0.1}\text{Ni}_{0.2}\text{O}_3$ (SFCN)	Nafion	$\text{Ni-Ce}_{0.8}\text{Sm}_{0.2}\text{O}_{2-\delta}$ (SDC)	N_2/H_2	1.13×10^{-8} (3.5)	90.4
20–80 (80)	Pt	Nafion	Pt	$\text{H}_2\text{O} - \text{Air}$	9.37×10^{-10} (10)	0.83

^a Calculated based on reference data.

The proton conducting electrolytes used in these studies were Nafion and sulfonated polysulfone (SPSF). Operation at low temperatures provides two advantages.

- Firstly, reaction (1) is spontaneous
- secondly, the proton conductivity of low-temperature electrolytes, such as Nafion, is much higher than of those which operate at intermediate and high temperatures.

On the other hand, reaction kinetics are quite slow at low temperatures.

In 2000, the first low temperature ammonia synthesis was reported. Kordali et al. using a Nafion electrolyte combined with an alkaline solution and produced ammonia from water and nitrogen at temperatures up to $100 \text{ }^\circ\text{C}$. **Fig. 6** is a schematic diagram of their cell.

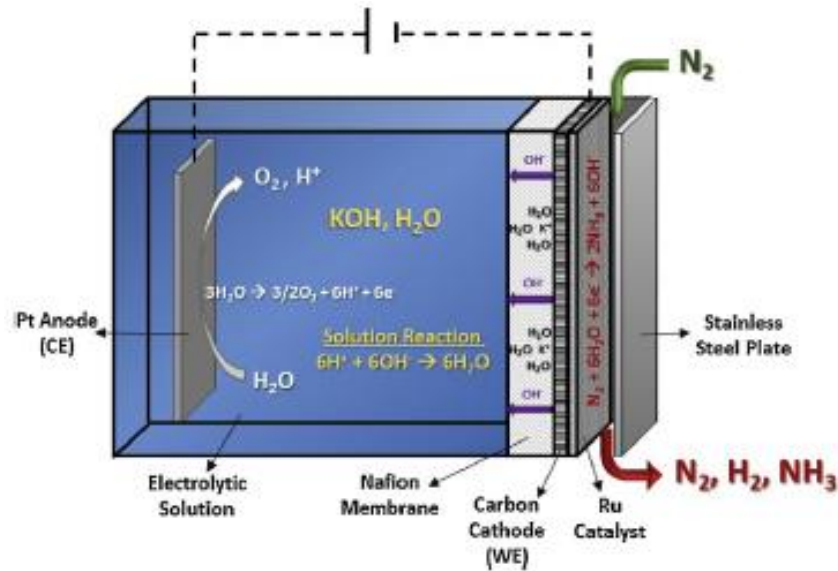
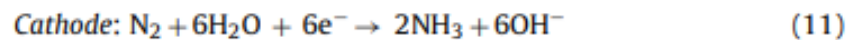


Fig. 6. Illustration of the electrochemical synthesis of ammonia from nitrogen and water at low temperatures as implemented by Kordali et al. [69].

The anodic electrode was Pt, immersed in a KOH solution. The latter was in contact with a Nafion membrane. The cathode was a carbon cloth, on which the Ru catalyst was deposited. Gaseous N_2 was introduced at the cathode side. The reactions at the two electrodes and in the KOH solution can be written as:



The above reactions combine to produce the overall reaction (7):



The hydrogen source for ammonia synthesis in the low temperature experiments was either gaseous H_2 or H_2O . The reactor cell configuration in these two cases were similar to those of Fig. 1 and Fig. 2, respectively. Using a SFCN electrode, Xu et al. reported the highest rate of $1.13 \times 10^{-8} \text{ mol s}^{-1} \text{ cm}^{-2}$ and the highest FE of 90.4%. In general, high reaction rates of the order of $10^{-8} \text{ mol s}^{-1} \text{ cm}^{-2}$ were observed on mixed oxide (e.g. SSN) and perovskite (e.g. SBCN) cathodes. Lan et al. used Pt electrodes and operated their cell at 25 °C. The reaction rate and FE achieved were not among the highest ($1.14 \times 10^{-9} \text{ mol s}^{-1} \text{ cm}^{-2}$ and 0.55, respectively) but this work is a significant contribution to the promotion of the electrochemical synthesis of ammonia because the most abundant substances were used as reactants (water and air) and the reaction was carried out at ambient conditions (25 °C and atmospheric pressure).

5) Factors that affect the production

Today, the Haber-Bosch process is a mature technology. Due to its tremendous industrial importance, the catalytic reaction of ammonia synthesis from its elements has been studied in detail in the past hundred years. The reaction is equilibrium limited and the catalyst accelerates both the forward and the reverse reaction. The composition of the effluent mixture of NH_3 , H_2 and N_2 is very close to that predicted by the equilibrium of reaction (1).

The yield to ammonia is a function of:

- the reactant feed flowrate
- the reactant composition
- the reaction temperature
- the pressure of operation
- and (primarily) the catalyst used.

The effect of the operating temperature on X_{NH_3} , the equilibrium-predicted molar fraction of ammonia, for stoichiometric reactant mixture ($P_{\text{H}_2}/P_{\text{N}_2} = 3/1$) and for various operating pressures, is depicted in Fig. 7a.

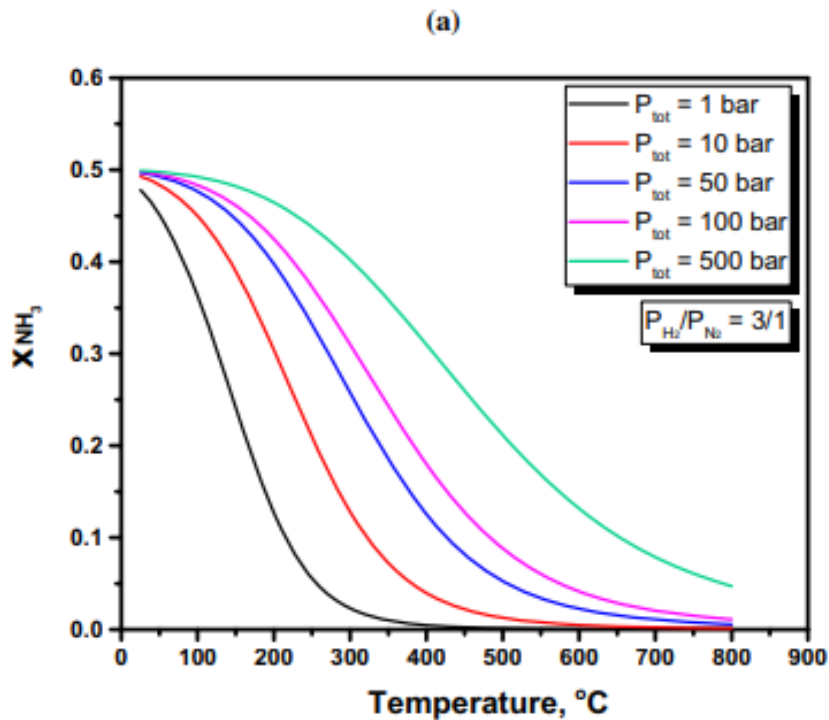


Fig. 7a. Equilibrium mole fraction of ammonia versus temperature (a) under various (total) pressures for the stoichiometric feed ratio

It can be seen that for temperatures between 400 °C and 500 °C, an industrially acceptable conversion (15-20%) is attainable at pressures between 50 and 100 bar.

In Fig. 7b, X_{NH_3} is plotted vs temperature for atmospheric pressure and for various $P_{\text{H}_2}/P_{\text{N}_2}$ ratios.

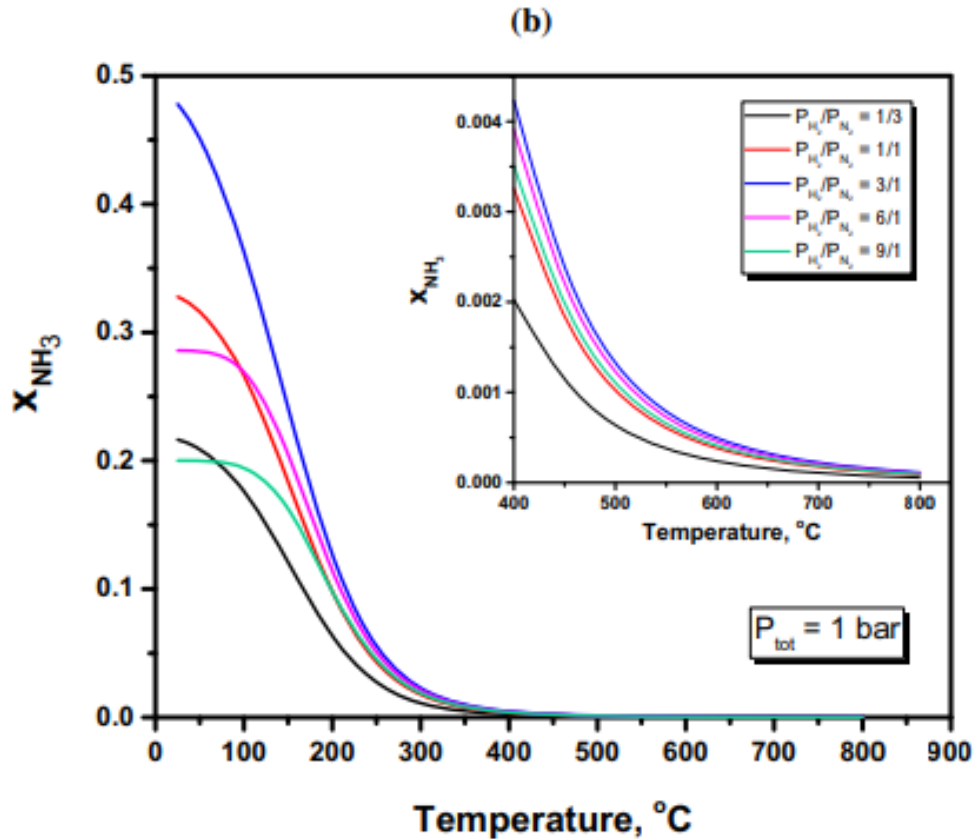


Fig. 7b. Equilibrium mole fraction of ammonia versus temperature (b) for various feed ratios under atmospheric pressure (inset showing temperature effect between 400 and 800 °C).

As expected, the stoichiometric P_{H_2}/P_{N_2} ratio gives the highest conversion to ammonia. It should be pointed out that these are maximum theoretical concentrations and that reaction kinetics, as well as reactor design and operating conditions (e.g. flow rate) play an important role in achieving them.

The electrochemical synthesis of ammonia has been studied only in the laboratory and for less than twenty years. Moreover, it is a more complicated system because there are additional factors that affect the reaction rate. The reactants are fed in separately and thus, the inlet flowrate of N_2 and H_2 can be controlled independently of each other. Furthermore, in addition to the effect of temperature and pressure, the rate of the electrochemical synthesis depends on the applied voltage and the generated current. Although the role of these electrochemical parameters has been addressed in previous reviews, a brief summary is presented below in order to include recent experimental findings.

a) Effect of applied potential

Ammonia is not produced unless the voltage becomes more negative (cathodic polarization) than a certain value. This onset value can be calculated from ΔG_R° , the free energy change of reaction (1):

$$E^\circ = -\Delta G_R^\circ / nF \quad (19)$$

- where F is Faraday's constant.
- n is the number of electrons (or protons) per molecule of reacting N_2 .

Similarly, if ammonia is produced from water and nitrogen, this onset value for E° can be calculated from the above equation using the free energy change of reaction (7).

Fig. 8 shows the dependence of the onset potential, V , on the operating temperature.

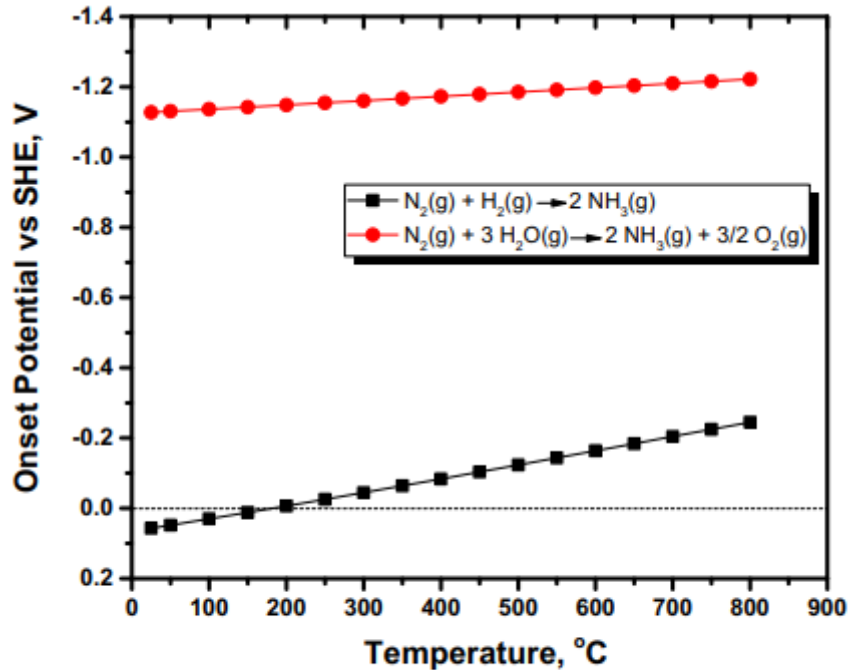


Fig. 8. Dependence of the equilibrium potential (calculated from equation (19)) on the operating temperature for the electrochemical production of ammonia from hydrogen (squares) and steam (circles).

If ammonia is produced from reaction (1), the threshold values of E° are 0.057V and -0.123V vs SHE at 25 °C and 500 °C, respectively. When the hydrogen source is H_2O (equation (7)), the corresponding E° values are -1.13V vs SHE at 25 °C and -1.21V vs SHE at 500 °C.

According to most of the experimental studies, the effect of applied voltage on the rate of NH_3 synthesis follows the behavior shown schematically in Fig. 9.

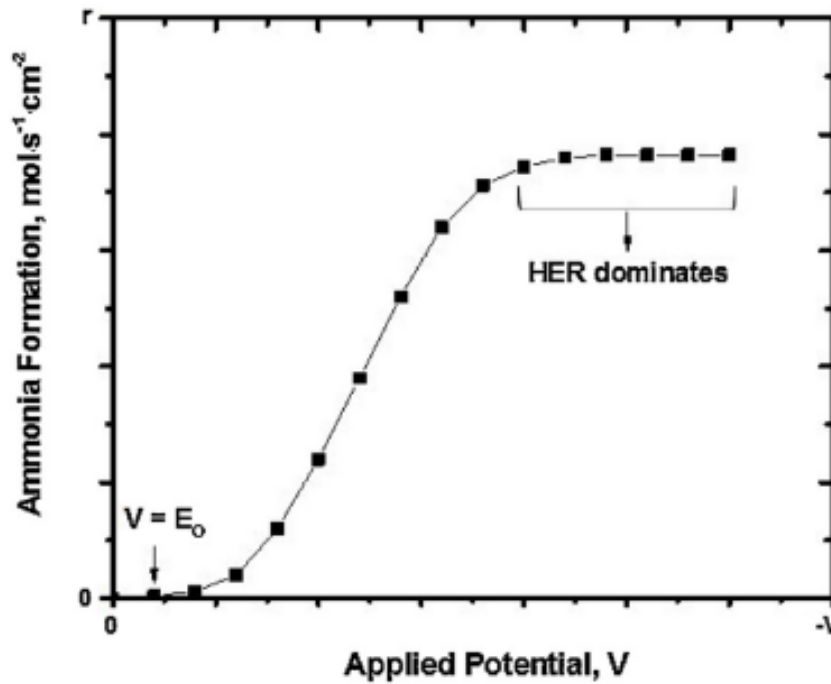


Fig. 9. Dependence of electrocatalytic rate of ammonia synthesis on the applied potential. E_0 denotes the onset potential calculated from equation (19).

The production rate, r_{NH_3} , increases with cell potential, $-V$, up to a certain value, above which the rate levels off. At higher applied potential values, HER is completely dominant.

The above reaction rate-voltage behavior stimulated the search for electrochemical promotion, a phenomenon observed in studies in which the catalyst is the working electrode of a solid electrolyte cell. For SSAS, this phenomenon could be studied in the H^+ cell of Fig. 1. If, instead of pure N_2 , a gaseous mixture of N_2 and H_2 is introduced over the cathode, ammonia will be formed under both, open- and closed-circuit conditions. If the reaction rate at open circuit is r_0 and a constant current I is imposed, the reaction rate will increase from r_0 to r . The rate increase can be correlated with I by means of the dimensionless parameter Λ :

$$\Lambda = (r - r_0)/(I/3F) \quad (20)$$

If $\Lambda = 1$, i.e. the rate increase is equal to the rate of H^+ "pumping", the effect is Faradaic. Since 1981, the phenomenon of Non-Faradaic ($\Lambda > 1$) Electrochemical Modification of Catalytic Activity (NEMCA), also called Electrochemical Promotion of Catalysis (EPOC) has been observed in numerous catalytic reaction systems.

Values of Λ as high as 3×10^5 have been reported.

In the case of SSAS, however the measured values were very low. On a Pd electrode, the values measured Λ by Marnellos et al. were as high as 2.0.

Yiokari et al. used an industrial Fe catalyst and were able to increase the open-circuit rate by up to 13 times but only when operating under low conversions, i.e. far from equilibrium.

In a thermodynamic analysis for reactions with limited conversion, Garagounis et al. provided an explanation for the weak NEMCA effect observed in SSAS. Specifically, the thermodynamic analysis indicated that for temperatures between 500 and 600 °C, λ cannot exceed the value of 10. This is because the role of protons in equilibrium limited reaction is both, electrochemical and catalytic. The promotional effect of the H^+ flux is weak because the pumped protons are used not only to modify the catalytic properties of the cathode, but also to carry the electrical power required for ammonia synthesis.

Nevertheless, introducing a H_2 - N_2 mixture, rather than N_2 alone, over the cathode, was found to have a positive effect on the electrochemical synthesis rate. Recently, SSAS was studied over a Ni-BZCY72 cathodic electrode, with and without H_2 in the gas phase. Without H_2 , the highest rate was $1.7 \times 10^{-9} \text{ mol s}^{-1} \text{ cm}^{-2}$. When H_2 was present ($P_{H_2}/P_{N_2} = 1$), an electrochemical reaction rate of $4.1 \times 10^{-9} \text{ mol s}^{-1} \text{ cm}^{-2}$ was obtained, corresponding to a 140% enhancement of the open-circuit rate.

b) Effect of applied current

The effects of current and voltage are not independent of each other. At a given temperature and gas composition, the overall resistance of the cell remains constant. Therefore, the effect of applied current is expected to be similar to that of the potential (Fig. 9).

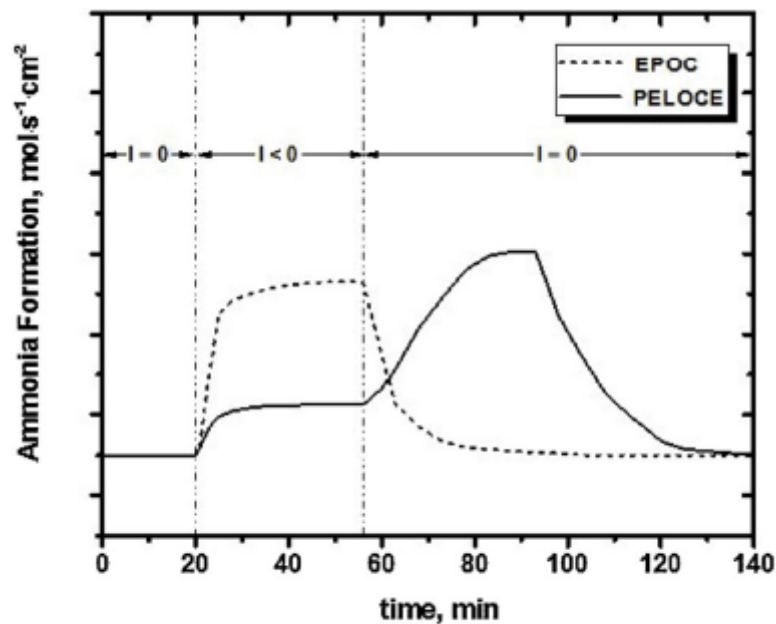


Fig. 10. Ammonia formation rate transients during typical EPOC (dotted line) and PELOCE (continuous line) experiments [89].

In general, the reaction rate will increase up to a certain level above which, it will become current independent. Wang et al. however, observed a negative order dependence of the reaction rate on the imposed current. At low current density values, the rate increased with current. At $I = 1$ mA, the rate reached a maximum and attained lower values at higher currents. A physical explanation of this behavior is that, at high currents, the catalyst surface is “poisoned” by protons, which combine with electrons and each other, thus forming H_2 rather than NH_3 .

Fig. 10 describes the characteristics of a peculiar phenomenon observed in a recent SSAS study. The dotted line, is a typical plot of the electrochemical rate of NH_3 synthesis vs. time in an EPOC experiment. The initial rate ($I = 0$) is enhanced upon closing the circuit. When the circuit is opened again, the rate quickly returns to its original value. The continuous line shows the variation of the reaction rate with time when a $BaZr_{0.7}Ce_{0.2}Y_{0.1}O_{2.9}$ (BZCY72) proton conducting ceramic was used as the electrolyte and a Ni-BZCY72 cermet was used as cathode. At $T > 600$ °C, after establishing a steady state open-circuit operation, the circuit was closed and a new steady state, which corresponded to a moderate increase in the reaction rate, was reached. Upon current interruption, instead of decreasing, the reaction rate increased and reached a maximum. After a period of time, during which it remained essentially unchanged, the rate decreases slowly to reach its open-circuit value. This phenomenon (Post-Electrochemical Open-Circuit Enhancement-PELOCE) was explained assuming that, under closed circuit, a fraction of protons transported to the cathode, is “stored” in the Ni-BZCY72 electrode in the form of a nickel hydride (Fig. 10). Upon current interruption, this hydride reacts with adsorbed N species to form ammonia.

One important difference between catalytic and electrocatalytic ammonia synthesis is that in the latter, one of the reactants (hydrogen) is supplied electrochemically. Hence, the electrolyte conductivity and specifically, the protonic conductivity, is crucial in determining the maximum reaction rate that can be achieved.

The protonic conductivity of low temperature electrolytes, such as Nafion and SPSF, is much higher than that of ceramic high temperature conductors. Thus, there is no need to search for more effective low temperature conductors because the reaction rate is limited by the slow reaction kinetics rather than the supply of protons. This is not the case for high temperature SSAS. The conductivity of a solid electrolyte increases with temperature and is inversely proportional to the thickness of the membrane. With a thin solid electrolyte, significantly higher proton fluxes will be obtained at a given temperature. Alternatively, the thin electrolyte can provide the same proton flux at a lower temperature. Recently, Coors et al. succeeded in fabricating anode supported tubular proton conducting

cells with an electrolyte (BZCY72) thickness of only 30 micrometers. This is a considerable step forward in scaling up SSAS at elevated temperatures.

c) The appropriate electro-catalyst

An ideal electro-catalyst should exhibit high catalytic activity and electronic conductivity and at the same time it should suppress HER. Unfortunately, the best Haber-Bosch catalysts often contain large proportions of oxides, which significantly decreases their conductivity. This has led many researchers to explore materials used in typical hydrogenation reactions.

Tables 1–3 show that many materials have been tested as working electrodes (catalysts) in the past fifteen years, including Ru, Fe, Pt, Pd, Ag-Pd, Ni, Ni-Cu as well as conductive oxides and composite materials such as SSN, SBCN, BSCF, SSCO, Ni-BZCY72, etc. The Ag-Pd cathode was used in almost half of the studies and it was the electrode on which the most promising results were obtained.

This is an unexpected result. The Haber-Bosch catalysts are Fe- and Ru-based materials. Ag and Pd are among the worst catalysts for nitrogen dissociative adsorption. Furthermore, under cathodic polarization conditions the surfaces of these two metals are expected to be “flooded” with protons making the side-on nitrogen adsorption difficult.

Table 1, however, shows that on Ag-Pd electrodes, both high reaction rates ($> 10^{-9} \text{ mol s}^{-1} \text{ cm}^{-2}$) and FE (up to 80%), were observed. The work of Skúlason et al. [9], may provide an indirect explanation for the high catalytic activity of the Ag-Pd electrode. This study suggested that early transition metals such as Sc, Y, Ti and Zr could effectively catalyze ammonia synthesis upon imposing a negative voltage, i.e., when used as electrodes. In the studies presented in Table 1, the solid electrolytes contained early transition metals such as Y and Zr. Hence, it is possible that the observed activity of Ag-Pd is due to the presence of these early transition metals at the electrode-electrolyte interphase.

Unfortunately, the experimental studies to date show that cathodic electrodes based on the best known catalysts (Ru and Fe) facilitate HER at the expense of nitrogen hydrogenation. Another important category of ammonia synthesis catalysts which have recently attracted much interest is the transition metal nitrides. Interestingly, only Amar and co-workers tested nitrides in an electrochemical configuration. In particular, $\text{Fe}_3\text{Mo}_3\text{N-Ag}$ and $\text{Co}_3\text{Mo}_3\text{N-Ag}$ were studied at operation temperatures of 400–450 °C. The formation rate and FE observed were rather low and reached $3.27 \times 10^{-10} \text{ mol s}^{-1} \text{ cm}^{-2}$ and 6.5%, respectively. This could possibly be attributed to the lack of adequate electronic conductivity of these particular nitrides. On the other hand, theoretical studies based on DFT calculations identified certain nitrides as promising electro-catalysts

at ambient conditions. The theoretical analysis of Abghoui et al. predicted stable operation and FEs higher than 75% for V, Cr, Nb and Zr mononitrides at applied bias between 0.5 and 0.76V vs SHE. These results are very promising and further research in this direction could move the electrochemical approach one step forward.

d) Techno-economic considerations

The electrochemical synthesis of ammonia exhibits several advantageous characteristics compared to the catalytic (Haber Bosch) process. The first is that the solid electrolyte is a selective ionic membrane, i.e. protons (H^+) are the only species that can be transported to the cathode. Today, a significant fraction of the overall cost for NH_3 production is due to the extensive purification of hydrogen. This is necessary because hydrogen, which is produced from steam reforming of natural gas, contains carbon monoxide, water vapor, oxygen and sulfur compounds, which, even in trace amounts, may cause poisoning of the catalyst. In SSAS, hydrogen is supplied in the form of protons and therefore the cost of purification is completely eliminated.

Another advantage of the electrochemical method is that the use of gaseous hydrogen can be bypassed. In the Haber-Bosch process, NH_3 is produced exclusively via reaction (1). In the electrochemical synthesis, depending on the temperature of operation, either steam or an aqueous solution can be the hydrogen source. Ammonia can be thus produced via either reaction (1) or (7). In the latter case, the electrical energy consumption will be higher because of the more negative voltage required for water electrolysis. Consequently, the economic feasibility of the electrochemical process will depend strongly on the electrical energy cost. If solar or wind energy is the electricity source, the economics may be favourable, especially when taking into account the environmental effect (use of renewable energy, no CO_2 emissions).

Regardless of the electricity source, scaling up of an electrochemical process requires high FE's to be achieved. Giddey et al. suggested that the industrial promotion of SSAS will require the combination of reaction rates of the order of $10^{-7} \text{ mol s}^{-1} \text{ cm}^{-2}$ with FE's exceeding 50%. Table 3 shows that, with the exception of ref., the FEs at low temperatures are very low (typically <1%) because of the slow reaction kinetics. At high temperatures (Table 1), the FE's are acceptably high, but a large fraction of the produced ammonia is inevitably lost because of the reverse reaction (ammonia decomposition), the rate of which increases with temperature. It is unfortunate that there are no solid state materials exhibiting both, mechanical and chemical strength and high protonic conductivity at temperatures between 250 °C and 450 °C.

Over the past two decades, a large number of studies worldwide have contributed to the promotion of the electrochemical synthesis of ammonia. New proton conducting materials have been employed and numerous materials have been used as working electrodes. The search for efficient electro-catalysts has been supported by theoretical studies, primarily based on DFT calculations. Reaction rates and Faradaic Efficiencies as high as a $3.3 \times 10^{-8} \text{ mol s}^{-1} \text{ cm}^{-2}$ and 90.4%, respectively, have been reported. Also, ceramic proton conductors with a $30 \mu\text{m}$ thickness, capable of producing NH_3 at rates of the order of $10^{-6} \text{ mol H}_2 \text{ s}^{-1} \text{ cm}^{-2}$, have been fabricated and tested [89,90]. Hence, considerable progress has been achieved. Intense collaboration, however, among researchers in the fields of materials science, solid state ionics and heterogeneous catalysis, will be required in order to promote the electrochemical synthesis to the industrial level.

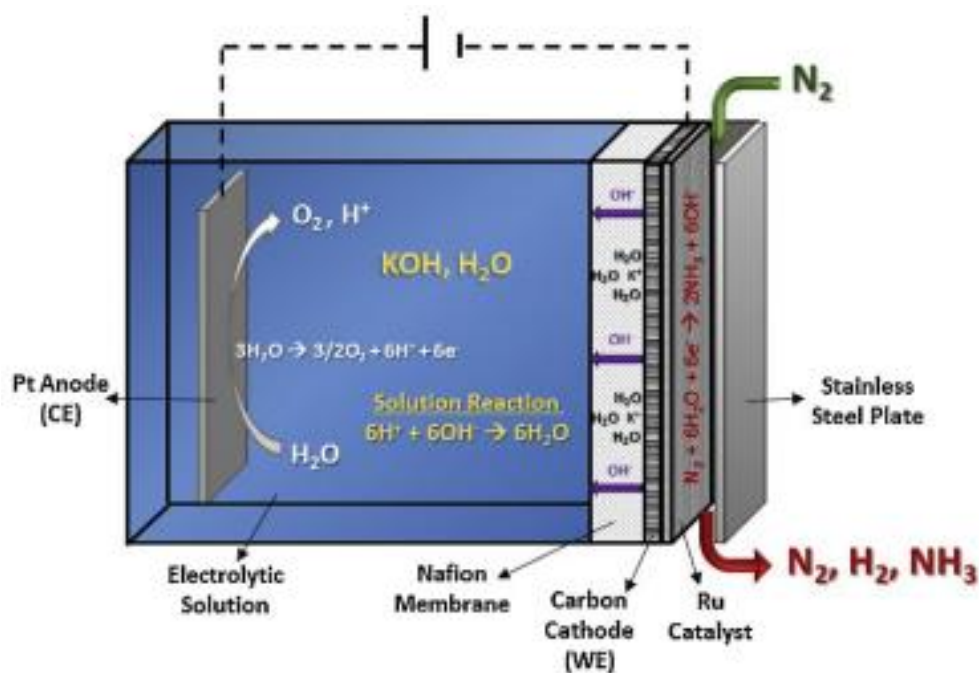
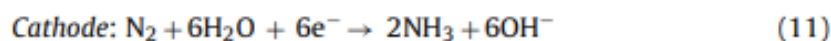
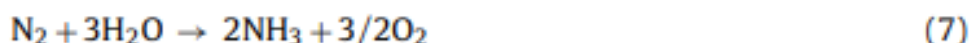


Fig. 6. Illustration of the electrochemical synthesis of ammonia from nitrogen and water at low temperatures as implemented by Kordali et al. [69].

The anodic electrode was Pt, immersed in a KOH solution. The latter was in contact with a Nafion membrane. The cathode was a carbon cloth, on which the Ru catalyst was deposited. Gaseous N_2 was introduced at the cathode side. The reactions at the two electrodes and in the KOH solution can be written as:



The above reactions combine to produce the overall reaction (7):

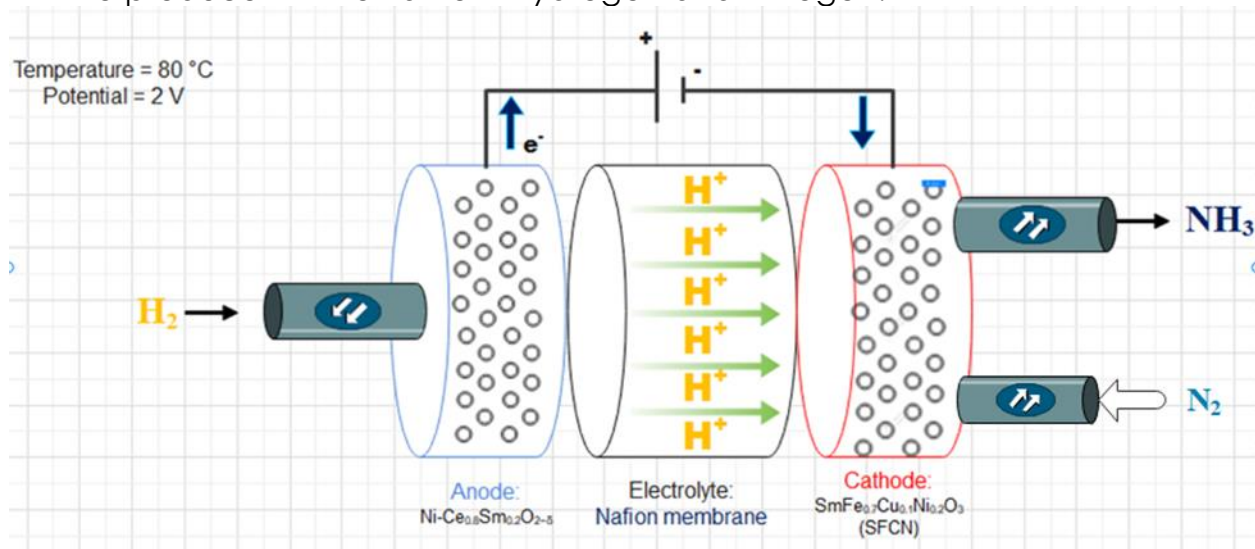


The hydrogen source for ammonia synthesis in the low temperature experiments was either gaseous H₂ or H₂O. The reactor cell configuration in these two cases were similar to those of Fig. 1 and Fig. 2, respectively. Using a SFCN electrode, Xu et al. reported the highest rate of $1.13 \times 10^{-8} \text{ mol s}^{-1} \text{ cm}^{-2}$ and the highest FE of 90.4%. In general, high reaction rates of the order of $10^{-8} \text{ mol s}^{-1} \text{ cm}^{-2}$ were observed on mixed oxide (e.g. SSN) and perovskite (e.g. SBCN) cathodes. Lan et al. used Pt electrodes and operated their cell at 25 °C. The reaction rate and FE achieved were not among the highest ($1.14 \times 10^{-9} \text{ mol s}^{-1} \text{ cm}^{-2}$ and 0.55, respectively) but this work is a significant contribution to the promotion of the electrochemical synthesis of ammonia because the most abundant substances were used as reactants (water and air) and the reaction was carried out at ambient conditions (25 °C and atmospheric pressure).

3.5. AP system concept

Electrochemical synthesis of ammonia using a cell with a Nafion membrane and SmFe_{0.7}Cu_{0.1}Ni_{0.2} cathode at atmospheric pressure and lower temperature

To produce Ammonia from Hydrogen and Nitrogen.

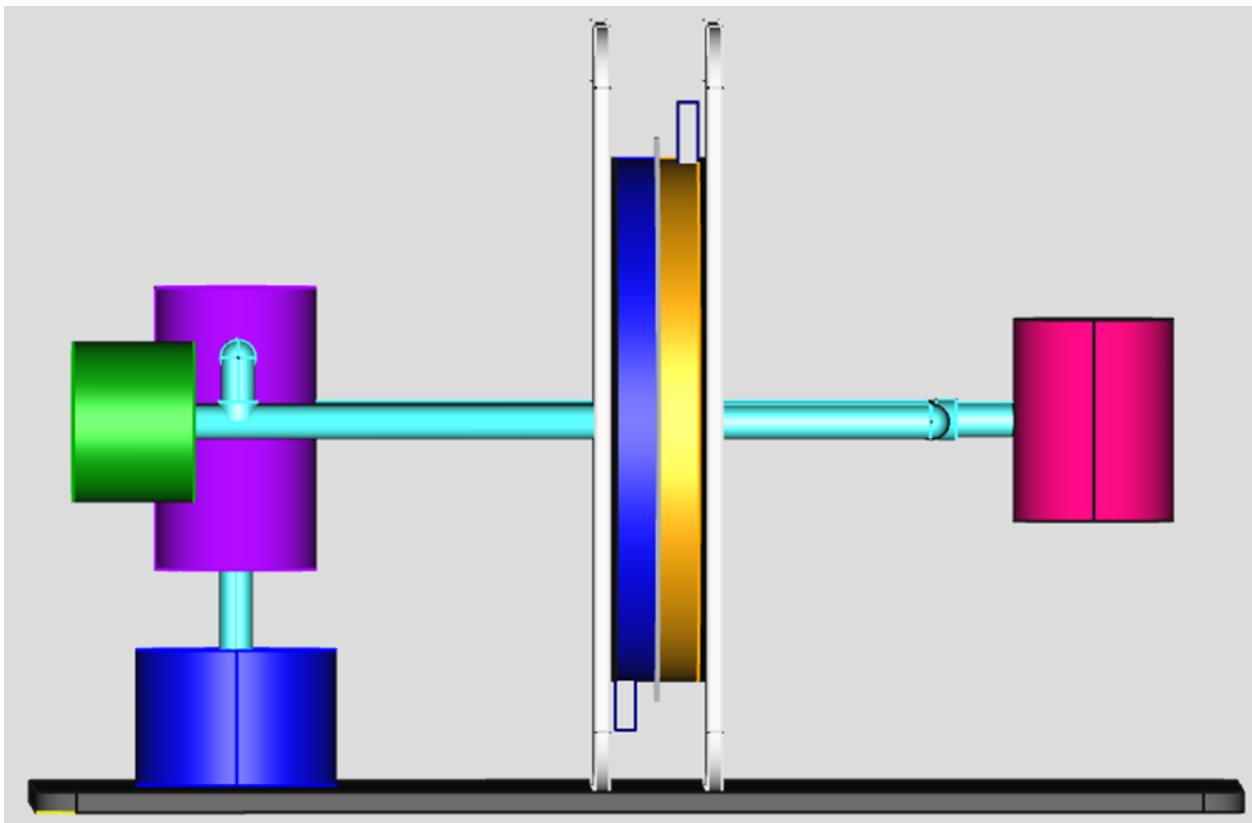
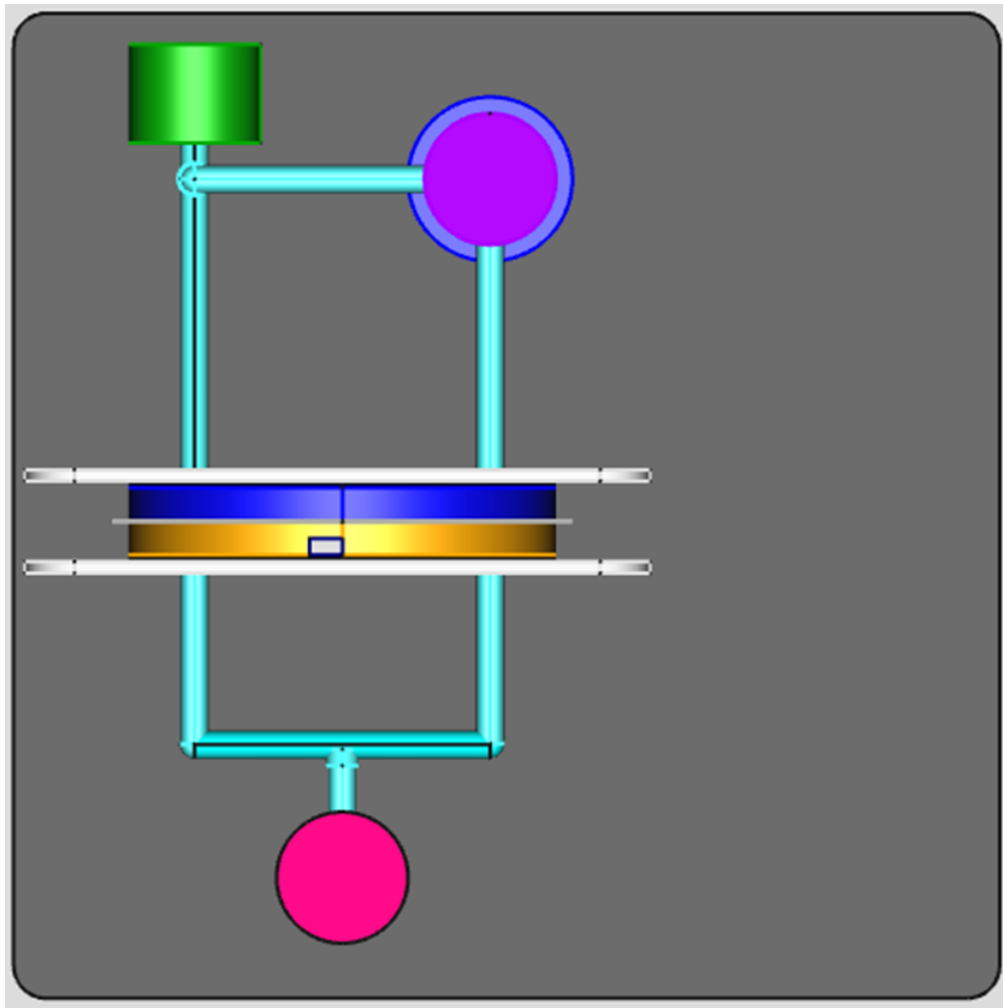


Electrochemical methods of ammonia synthesis have been most widely studied. It is recognized that Nafion is the best polymer proton exchange membrane.

1) FreeCAD design



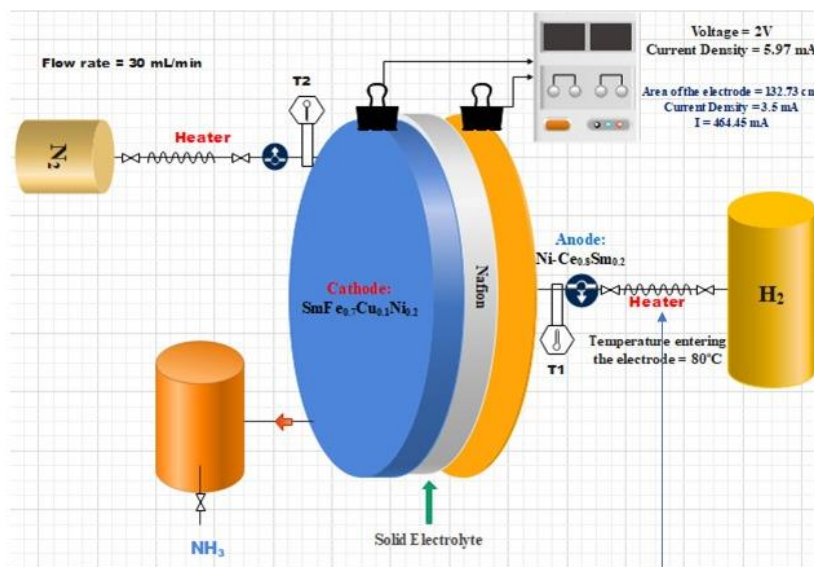
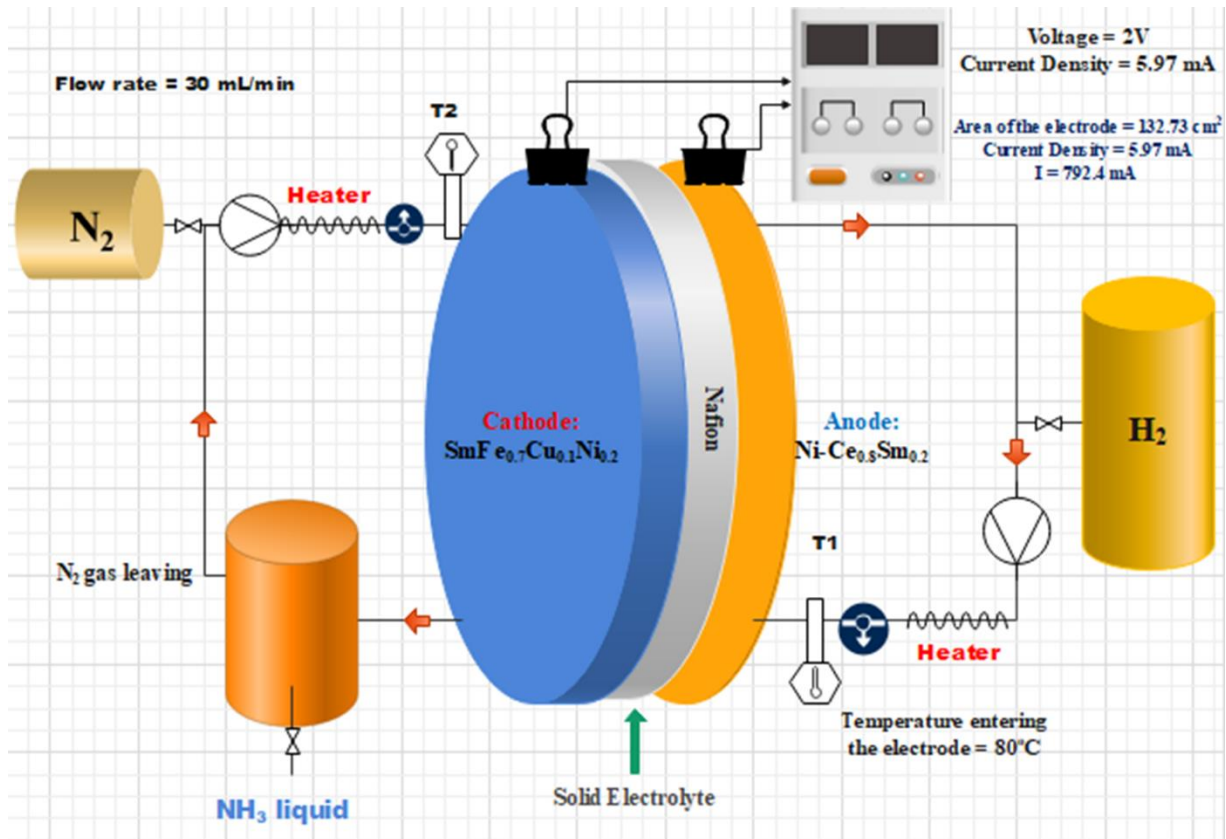
AP 01112022.FCStd



2) Flow chart



Flow chart.eddx



3.6. Characterization: Ammonia synthesis and measurement

Wet H₂ (the gas is bubbled through distilled water at 25°C before entering the reactor, since water vapour may provide some protons[13] and increase the conductance and the rate of evolution of ammonia) was supplied to the anode, while dry N₂ was supplied to the cathode.

The flow velocities of wet H₂ and dry N₂ are 30 mL·min⁻¹. The vent gas from the cathode is absorbed by dilute H₂SO₄ (10 mL, pH 3.85) for 10 min under the closed circuit conditions. When Nessler's reagent was added to the solution, a stable yellow color appeared immediately, which confirmed the presence of NH₄⁺ in the solution. The concentration of NH₄⁺ in the solution is determined by spectrophotometry[14] using a standard curve method in order to calculate the rate of ammonia synthesis.

NH₃ Detection The amounts of NH₃ trapped in the acid solutions are determined by indophenol and Nessler methods.

For the indophenol method, 1 mL of an aqueous 0.64 M C₆H₅OH, 0.38 M NaOH, and 1.3 mM C₅FeN₆Na₂O solution was mixed with 1 mL of 55 mM NaOCl and 0.75 M NaOH prior to NH₃. Then, 1 mL of either a standard NH₃ solution (a known quantity of NH₄Cl in an aqueous 10 mM H₂SO₄ solution) or the NH₃-containing acid trap solution was added to the indophenol solution after dilution with aqueous 0.1 M KOH. The dissolved NH₄⁺ ions were quantified by assessing the absorbance at 633 nm using UV-Vis spectroscopy. The measurements were calibrated by subtracting the background absorbance measured at 875 nm.

In the Nessler method, the acid-trapped-NH₃ solution or the standard NH₄OH solution was diluted in aqueous 90 mM K₂Hgl₄ (Nessler reagent, Sigma Aldrich) and 0.1 M KOH before spectroscopic analysis. The absorbance measured at approximately 375 nm (corrected using the background at 700 nm) was used to determine the NH₄⁺.

For both the indophenol and Nessler NH₃ detection methods, standard calibration curves were obtained using known amounts of NH₄Cl or NH₄OH, respectively.

3.7. AP System Realization

1) Anode Preparation

Chemical Formula: **Ni-Ce_{0.8}Sm_{0.2}**

Metal	Melting point	Density (g.cm ⁻³)
Nickel	1455 °C	8.902
Cerium	795 °C	6.76
Samarium	1072 °C	7.52

Total volume for 100g mass of this alloy = 13.53 cm³

$$\rho = 100/14.2 = 7.391 \text{ g/cm}^3$$

Volume of the anode (disc shape):

Radius = 6.5 cm; Height = 0.1 cm or more

$$V = \pi r^2 h = \pi * 6.5^2 * 0.1 = 13.273 \text{ cm}^3 = 13273 \text{ mm}^3$$

$$\text{If } h = 1 \text{ mm} \rightarrow V = 13273 \text{ mm}^3 = 13.273 \text{ cm}^3$$

$$M_1 = \rho V = 7.391 * 13.273 = 98.100743 \text{ g}$$

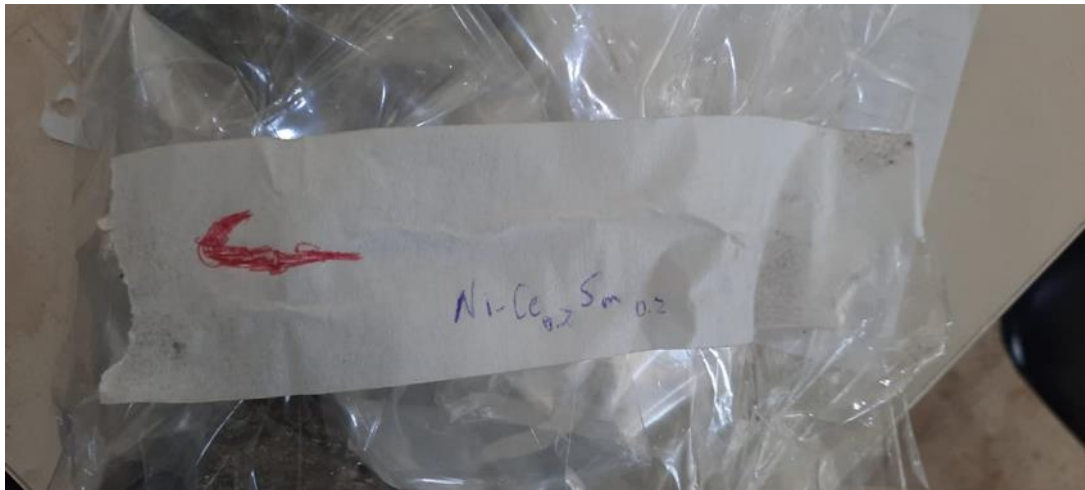
$$M_{Ni} = 286 \text{ g}$$

$$M_{Ce} = 510 \text{ g}$$

$$M_{Sm} = 147 \text{ g}$$

$$M_{Total} = 286 + 510 + 147 = 943 \text{ g}$$

Metal	Mass (g)	%W	No of moles	X _i
Nickel	286	30.33	4.873	0.5134
Cerium	510	54.08	3.640	0.3835
Samarium	147	15.59	0.978	0.1030
Alloy	943	100	9.491	1





2) Cathode preparation

Chemical Formula: $\text{SmFe}_{0.7}\text{Cu}_{0.1}\text{Ni}_{0.2}$

Metal	Melting point °C	Density (g.cm ⁻³)
Samarium	1072	7.52
Iron	1538	7.874
Copper	1085	8.96
Nickel	1455	8.902

Total volume for 100g mass of this alloy = 13.01 cm³

$$\rho = 100/13.01 = 7.69 \text{ g/cm}^3$$

Volume of the cathode (disc shape):

Radius = 6.5 cm; Height = 0.1 cm

$$V = \pi r^2 h = \pi * 6.5 * 0.1 = 13.273 \text{ cm}^3 = 13273 \text{ mm}^3$$

$$\text{If } h = 1 \text{ mm} \rightarrow V = 13273 \text{ mm}^3 = 13.273 \text{ cm}^3$$

$$M_1 = \rho V = 7.69 * 13.273 = 102.06937 \text{ g}$$

$$M_{\text{Sm}} = 740.29 \text{ g}$$

$$M_{\text{Fe}} = 192 \text{ g}$$

$$M_{\text{Cu}} = 31.5 \text{ g}$$

$$M_{\text{Ni}} = 58.5 \text{ g}$$

$$M_{\text{Total}} = 740.29 + 192 + 31.5 + 58.5 = 1022.29 \text{ g}$$

Metal	Mass (g)	%W	No of moles	X _i
Samarium	740.29	72.41	4.9235	0.5
Iron	192	18.78	3.4381	0.35
Copper	31.5	3.08	0.5	0.05
Nickel	58.5	5.72	0.9921	0.1
Alloy	1022.29	100	9.8537	1



3.8. AP Requirements / Experimental

1) Materials and apparatus

1. Solid Electrolyte: Nafion™ NR212
2. 2 Pumps for Hydrogen and Nitrogen. (T=100°C; flow rate= >30mL/min)
3. Sensors
 - 2 Temperature sensors 100°C
 - 2 Flow rate sensors
 - 2 Pressure sensors (1 bar)
4. Hydrogen Peroxide H₂O₂
5. Sulfric acid H₂SO₄
6. Nafion solution **Nafion™ D520CS Alcohol based 1000 EW at 5% weight**

7. Nessler's reagent
8. HDV-7C transistor potentiostat
9. pH meter
10. 7230G visible spectrophotometer
11. The corundum tube reactor and heated reactor with circulating water were made locally.
12. Modified acrylate adhesive
13. Electrodes: We need the following metals for the synthesis of the electrodes: Samarium, Iron, Nickel, Copper, and Cerium.

2) Preparation of cathode and anode and assembly of the single cell

a) Cathode

SmFe_{0.7}Cu_{0.1}Ni_{0.2} (SFCN)

Sm: $m = n \cdot M = 1 \cdot 150.36 = 150.36 \text{ g}$
 Fe: $m = n \cdot M = 0.7 \cdot 55.845 = 39.1 \text{ g}$
 Cu: $m = n \cdot M = 0.1 \cdot 63.546 = 6.3546 \text{ g}$
 Ni: $m = n \cdot M = 0.2 \cdot 58.6934 = 11.73868 \text{ g}$
 Total mass = 207.5 g

Metal	Melting point	%W	Density (g.cm ⁻³)
Samarium	1072 °C	72.45	7.52
Iron	1538 °C	18.84	7.874
Copper	1085 °C	3.1	8.96
Nickel	1455 °C	5.66	8.902

Total volume for 100g mass of this alloy = 13.01 cm³

$\rho = 100/13.01 = 7.69 \text{ g/cm}^3$

Volume of the cathode (disc shape):

Radius = 6.5 cm; Height = 0.1 cm

$V = \pi r^2 h = \pi \cdot 6.5^2 \cdot 0.1 = 13.273 \text{ cm}^3 = 13273 \text{ mm}^3$

If $h = 1 \text{ mm} \rightarrow V = 13273 \text{ mm}^3 = 13.273 \text{ cm}^3$

$M_1 = \rho V = 7.69 \cdot 13.273 = 102.06937 \text{ g}$

$M_{Sm} = 73.95 \text{ g}$

$M_{Fe} = 19.23 \text{ g}$

$M_{Cu} = 3.16 \text{ g}$

$M_{Ni} = 5.78 \text{ g}$

If $h = 2 \text{ mm} \rightarrow V = 26546.46 \text{ mm}^3 = 26.54646 \text{ cm}^3$

$M_2 = \rho V = 7.69 \cdot 26.54646 = 204.1422774 \text{ g}$

$\rightarrow M_3 = M_1 \cdot 3 = 102.06937 \text{ g} \cdot 3 = 306.20811 \text{ g}$

b) Anode

Ni-Ce_{0.8}Sm_{0.2}

Ni: $m = n \cdot M = 1 \cdot 58.6934 = 58.7 \text{ g}$
 Ce: $m = n \cdot M = 0.8 \cdot 140.116 = 112.1 \text{ g}$
 Sm: $m = n \cdot M = 0.2 \cdot 150.36 = 30.1 \text{ g}$
 Total mass = 200.9 g

Metal	Melting point	%W	Density (g.cm ⁻³)
Nickel	1455 °C	29.22	8.902
Cerium	795 °C	55.8	6.76
Samarium	1072 °C	15	7.52

Total volume for 100g mass of this alloy = 13.53 cm³

$\rho = 100/14.2 = 7.391 \text{ g/cm}^3$

Volume of the anode (disc shape):

Radius = 6.5 cm; Height = 0.1 cm

$V = \pi r^2 h = \pi \cdot 6.5^2 \cdot 0.1 = 13.273 \text{ cm}^3 = 13273 \text{ mm}^3$

If $h = 1 \text{ mm} \rightarrow V = 13273 \text{ mm}^3 = 13.273 \text{ cm}^3$

$M_1 = \rho V = 7.391 \cdot 13.273 = 98.100743 \text{ g}$

$M_{Ni} = 28.66482 \text{ g}$

$M_{Ce} = 54.74 \text{ g}$

$M_{Sm} = 14.715 \text{ g}$

If $h = 2 \text{ mm} \rightarrow V = 26546.46 \text{ mm}^3 = 26.54646 \text{ cm}^3$

$\rightarrow M_2 = M_1 \cdot 2 = 98.1 \text{ g} \cdot 2 = 196.2 \text{ g}$

3.9. What's next

After drawing up the initial design of the AP project, the electrodes should be made. After that we will be able to install the whole system. PLC automation should also be worked on.

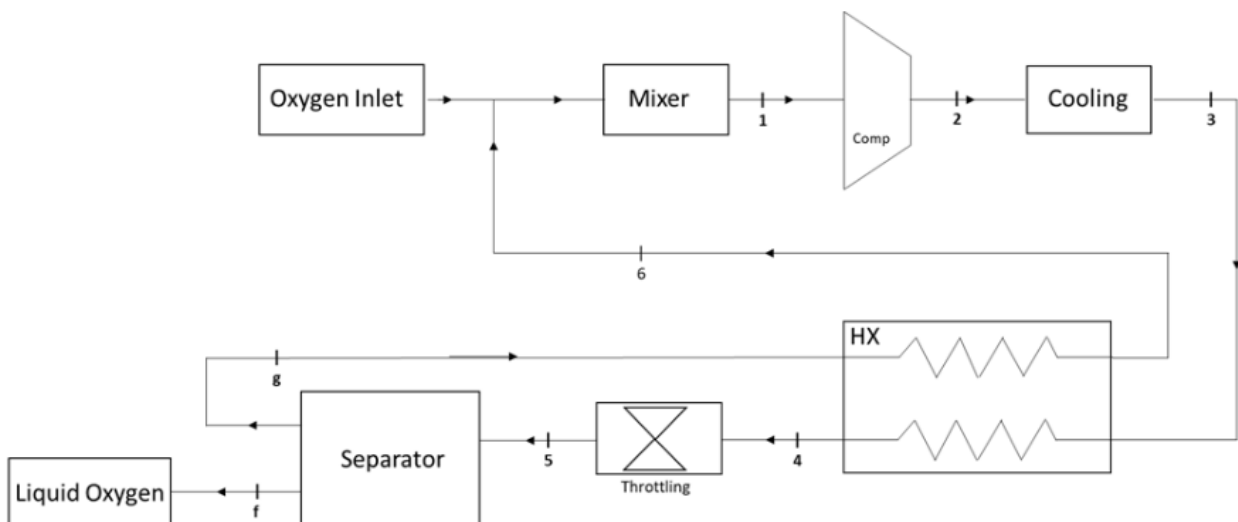
Project 4: Liquefaction of Oxygen (ICPT - LOx)

4.1. Position of LOx project

Work on this project began theoretically in the past years. In this year (2022), the focus was on the practical side, as important amendments were put in place that determined the course of the project, and a large part of the project was implemented.

4.2. LOx introduction

Initially, it was suggested to replace the main cycle (open oxygen cycle for liquefaction of oxygen) with a closed cryogenic cycle running on nitrogen gas for liquefaction of oxygen. This is due to the increased cost of the oil-free oxygen compressor, but it turned out later that nitrogen gas also needs an oil-free compressor, and for this reason we decided to return to the basic suggestion attached below.



In our prototype, we decided to dispense with the heat exchanger in order to avoid expensive materials and manufacturing costs. However, through the theoretical study, it was found that we will face a problem in reaching the required liquefaction temperature, in addition to the compressor failure due to the low gas temperature at the compressor inlet.

Therefore, the following was decided:

- 1) Selection of an oil-free oxygen compressor suitable for previously installed pipes.
- 2) Recalculation of the oxygen liquefaction cycle.
- 3) Heat exchanger
 - a) HX design

- b) Materials of manufacture
- c) Total costs
- 4) Determining the type of insulation suitable for the system
- 5) Manufacture of the HX and its installation in the system
- 6) Resizing of expansion valve
- 7) Design and manufacture of separator and gas mixer
- 8) Completing all required connections and placing the sensors (timer, pressure and temperature sensors) in their appropriate places.
- 9) Connect the oxygen gas bottles needed for the experiment
- 10) Putting the insulation materials in its proper place in the system
- 11) Doing the first experiments.

4.3. Cooling component

In our system, the “Kelvinator” refrigerator has been adopted as a condenser for the compressor outlet. The second refrigeration cycle in the Kelvinator works with refrigerant R-503. This refrigeration cycle needs to be filled with refrigerant R-503. Due to its unavailability in the market, it was replaced with refrigerant R-508b, due to its compatibility with compressor oil.

4.4. Project overview

1) Overview flow chart

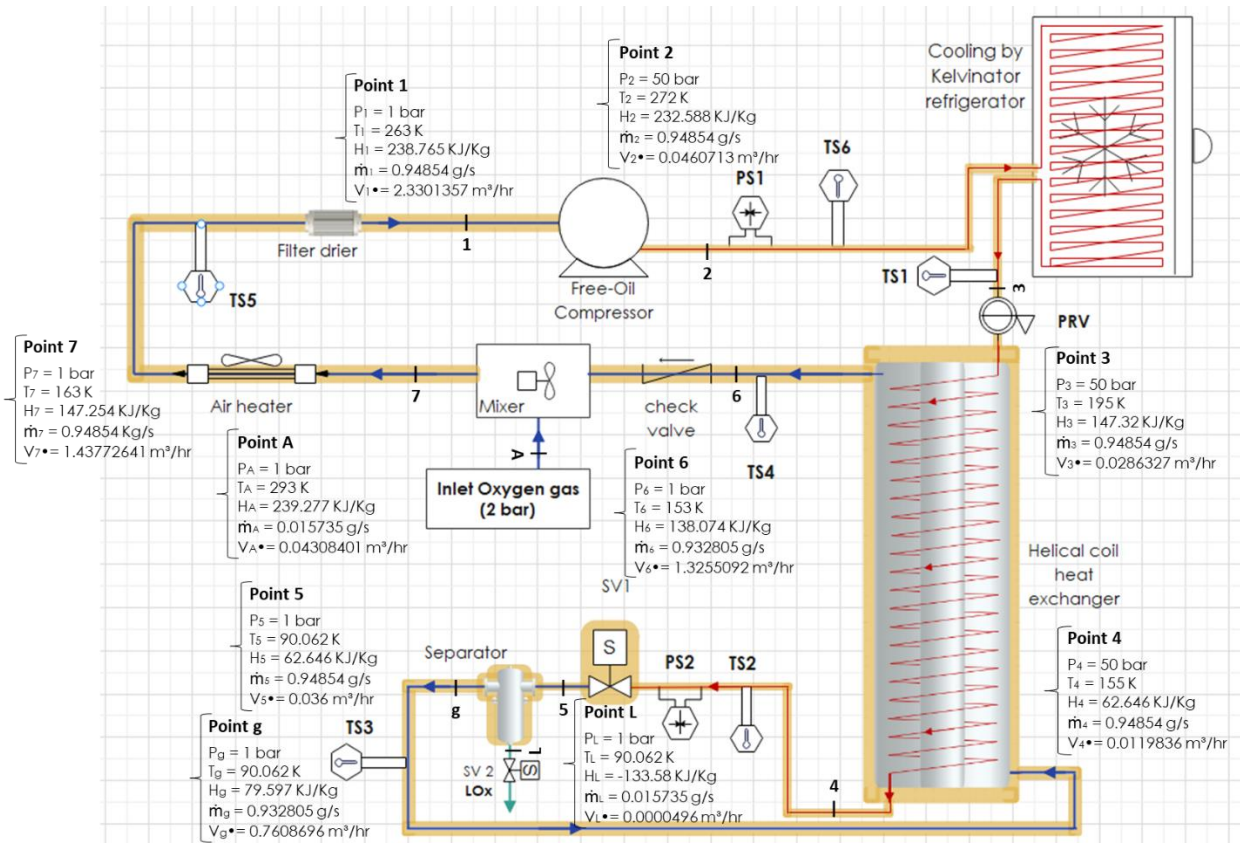
LOX prototype flow chart by EDraw:



29102022_LOX
Prototype Flow char

3) LOx cycle calculation

Calculation of oxygen liquefaction cycle



Points	Pressure	Temperature	Enthalpy	Mass flow			Density	Volumetric flow		
	P [bar]	T [°K / °C]	H [KJ/Kg]	m• [Kg/s]	m• [g/s]	m• [Kg/h]	D [Kg/m³]	V• [L/s]	V• [m³/hr]	V• [L/min]
Pt 1	1	263 / -10	238.765	0.00094854	0.94854	3.414744	1.46547	0.647259923	2.330135724	38.83559541
Pt 2	50	272 / +10	232.588	0.00094854	0.94854	3.414744	74.1186	0.012797597	0.046071351	0.767855842
Pt 3	50	195 / -78	147.32	0.00094854	0.94854	3.414744	119.26	0.007953547	0.028632769	0.477212812
Pt 4	50	155 / -118	62.646	0.00094854	0.94854	3.414744	284.95	0.003328795	0.01198366	0.199727672
Pt 5	1	90.062 / -183	62.646	0.00094854	0.94854	3.414744	94.854	0.01	0.036	0.6
Pt g	1	90.062 / -183	79.597	0.000932805	0.932805	3.358098	4.4135	0.211352668	0.760869605	12.68116008
Pt L	1	90.062 / -183	-133.58	0.000015735	0.015735	0.056646	1141.8	1.37809E-05	4.96111E-05	0.000826852
Pt 6'	1	153 / -120	138.074	0.000932805	0.932805	3.358098	2.53344	0.368196997	1.325509189	22.09181982
Pt 6	1	263 / -10	238.765	0.000932805	0.932805	3.358098	1.22598	0.760864778	2.739113199	45.65188665
Pt A'	1	263 / -10	238.765	0.000015735	0.015735	0.056646	1.22598	0.01283463	0.046204669	0.770077815
Pt A	1	293 / +20	239.277	0.000015735	0.015735	0.056646	1.31478	0.011967782	0.043084014	0.718066901
Pt 7	1	163 / -110	147.254	0.00094854	0.94854	3.414744	2.3751	0.399368448	1.437726412	23.96210686

This table is based on thermodynamic properties tables of oxygen and formula of ideal gas law

4) Yield factor

$$\text{Yield: } Y = m_f \bullet / m \bullet = h_1 - h_2 / h_1 - h_f$$

Where : Point 1: before compressor (inlet)
Point 2: after compressor (outlet)

$$Y = \frac{h_1 - h_2}{h_1 - h_f} = \frac{238.765 - 232.588}{238.765 - (-133.58)} = 0.016589 \approx 1.6589 \%$$

$$Y = m_f \bullet / m \bullet \Rightarrow m_f \bullet = Y * m \bullet = 0.016589 * 0.003 \text{ Kg/s} = 4.9767 \times 10^{-5} \text{ Kg/s}$$

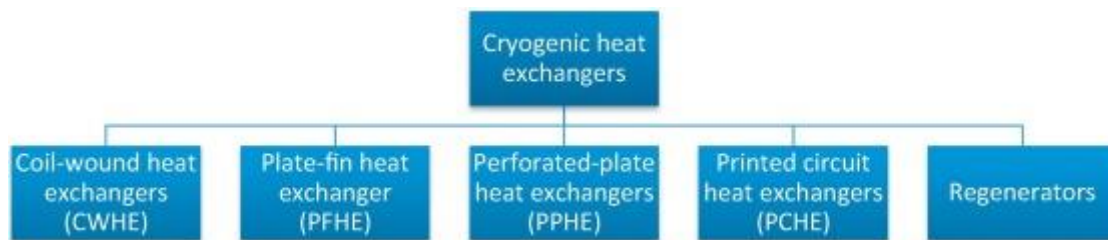
$$m_{f \bullet} = 4.9767 \times 10^{-5} \text{ kg/s} \times 3600 = 0.1792 \text{ Kg/hr}$$

$$\frac{\text{Mass flow}}{\text{Density}} = \frac{m_{f \bullet}}{D} ; \text{ where density } D \text{ of liquid} = 1141.8 \text{ Kg/m}^3$$

$$= \frac{0.1792}{1141.8} = 0.0001569 \text{ m}^3/\text{hr} = 0.1569 \text{ L/hr} = 156.9 \text{ mL/hr} = 2.6152 \text{ mL/min}$$

4.5. Heat exchanger

1) Type of heat exchanger



Types of heat exchanger used in cryogenic systems

We chose helical coil heat exchanger for many features

a) Shape of heat exchanger

The copper pipe used has 9.62 mm outer diameter (O.D.) and 1.2 mm thickness. The coil pitch and the number of turns will be calculated in paragraph 2.c. The schema of the heat exchanger is shown in figure below. The shell inner diameter, outer diameter and height are 80 mm, 160 mm and 1.73 m, respectively.

b) Boundary condition

As can be seen in Fig. 1, hot fluid (Oxygen gas) at the specific temperature of $-80 \text{ }^\circ\text{C}$ with pressure 50 bar and mass flow rate inlet boundary condition enters the helical coil at the top and leaves at the bottom. Cold fluid (Oxygen gas) at a temperature of $-183 \text{ }^\circ\text{C}$ with 1 bar pressure and mass flow rate inlet boundary condition enters the shell at the bottom and leaves at the top.

Equal values of mass flow rate were specified for shell-side and coil-side fluids.

c) Performance analysis of the heat exchanger

Heat transfer enhancement was experimentally investigated by by Jamshidi et al.(2013) [2]. It was observed that the increase in coil diameter, coil pitch and mass flow rate in shell and tube can enhance the heat transfer rate.

It is also seen that the increase in tube diameter and coil diameter enhances the effectiveness because the heat transfer area increases.

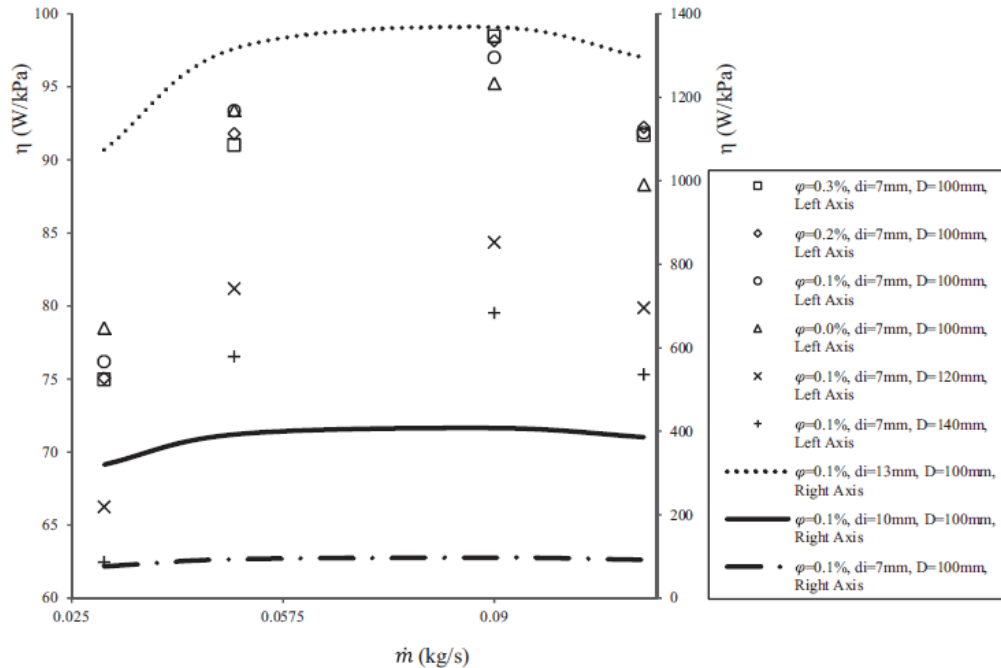


Fig. 2: Variations of performance index vs. mass flow rate based on various parameters [3].

Furthermore, it can be observed from Fig. 2 that with the increase in tube diameter the performance index enhances remarkably. The reason can be attributed to the significant decrease in pressure drop, the increase in heat transfer area and enhanced secondary flow.

The heat transfer rate enhances with coil diameter due to increased heat transfer area and the pressure drop increases with coil diameter because of increased length of the tube.

The effect of coil diameter on pressure drop is more intensive than that of heat transfer rate; consequently, the performance index decreases with an increase in the coil diameter.

For all cases, the optimum value of mass flow rate corresponding to maximum performance index is found to be **0.1 kg/s**.

d) Advantage of Helical Coil Heat Exchanger

Helical coil heat exchanger has many benefits that make it a good choice:

- Highly efficient use of space, especially when it's limited and not enough straight pipe can be laid.
- Under conditions of low flowrates, such that that the typical shell-and-tube exchangers have low heat-transfer coefficients and becoming uneconomical.
 - When there is low pressure in one of the fluids.
 - When one of the fluids has components in multiple phases (solids, liquids, and gases), which tends to create mechanical problems during operations, such as plugging of small-diameter tubes. Cleaning of helical coils for these multiple-phase fluids can prove to be more difficult than its shell and tube counterpart; however, the helical coil unit would require cleaning less often.

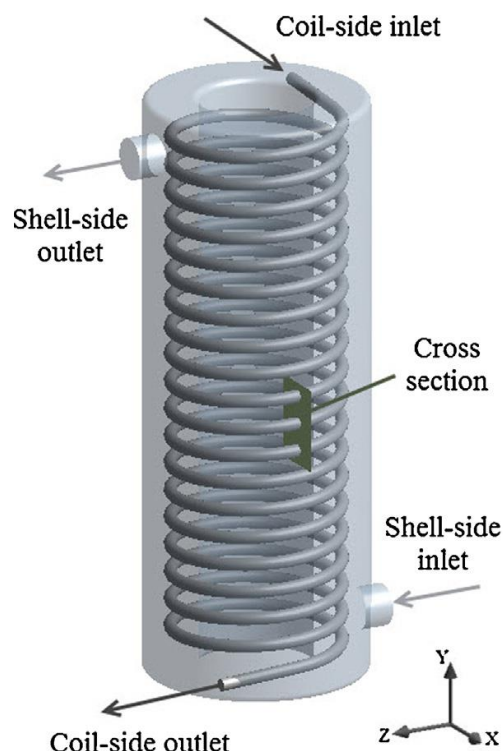


Fig. 1 - Schema of a shell and helical tube heat exchanger

e) Characteristics of helical coil and shell

Helical coil heat exchanger has many benefits that make it a good choice:

- Highly efficient use of space, especially when it's limited and not enough straight pipe can be laid.
- Under conditions of low flowrates, such that that the typical shell-and-tube exchangers have low heat-transfer coefficients and becoming uneconomical.
 - When there is low pressure in one of the fluids.
 - When one of the fluids has components in multiple phases (solids, liquids, and gases), which tends to create mechanical problems during operations, such as plugging of small-diameter tubes. Cleaning of helical coils for these multiple-phase fluids can prove to be more difficult than its shell and

tube counterpart; however, the helical coil unit would require cleaning less often.

2) Material of Helical Coil Heat Exchanger

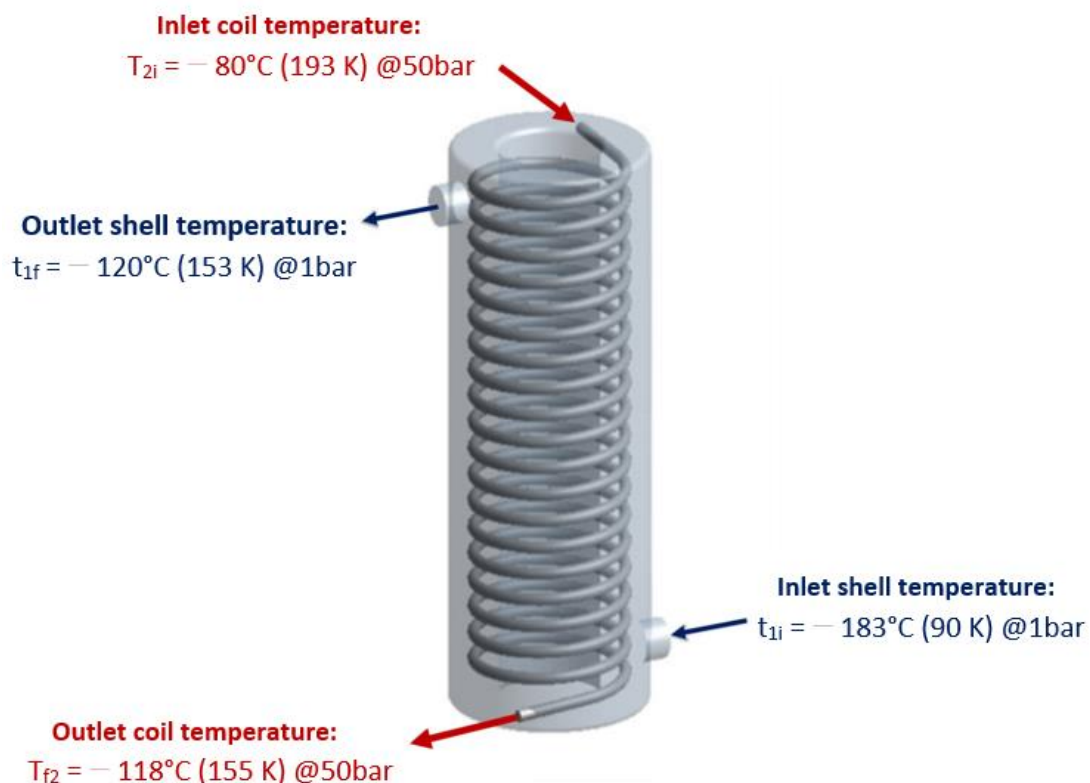
When designing the helical coil heat exchanger, the first thing you need to consider is what material you should use. Copper tube and Stainless-Steel tube are two most common choices. Copper tube have relatively higher heat exchange rate, because copper tube is softer. Stainless steel tube doesn't react with water, which make it last longer, especially when one of the heats transferring fluid is water.

In our case, we will use the copper tube, because stainless steel tubes are not easily available in Lebanon.

Note:

The flow has been adjusted from 0.1 Kg/s to 0.00094854 Kg/s in respect of the accepted flow rate of the solenoid valve ($K_v = 0.6$ L/min). Because the flow is reduced, this will not negatively affect the work of the system, but rather it will give it more time for an ideal heat exchange.

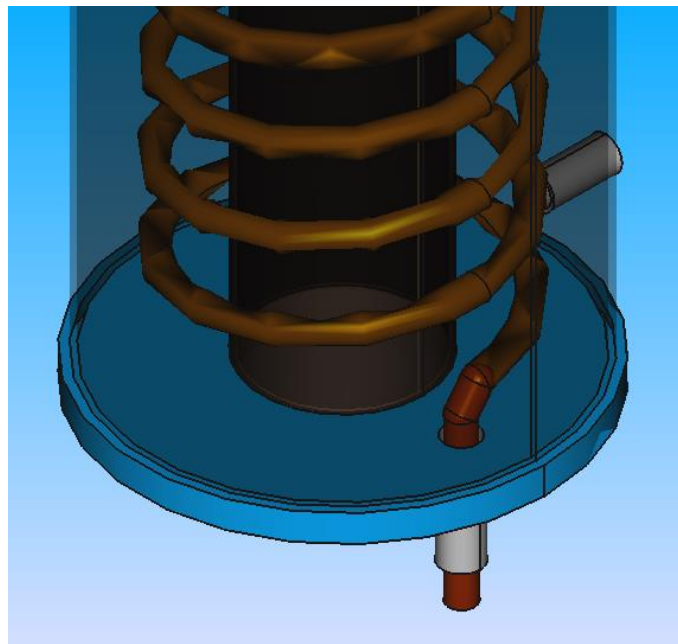
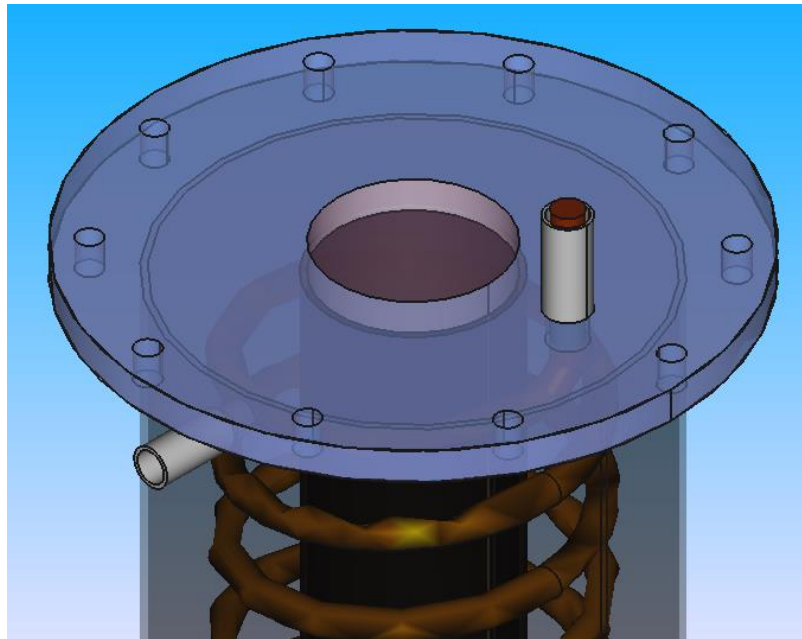
3) Design of heat exchanger



4) HX FreeCAD design and size (v0.17)



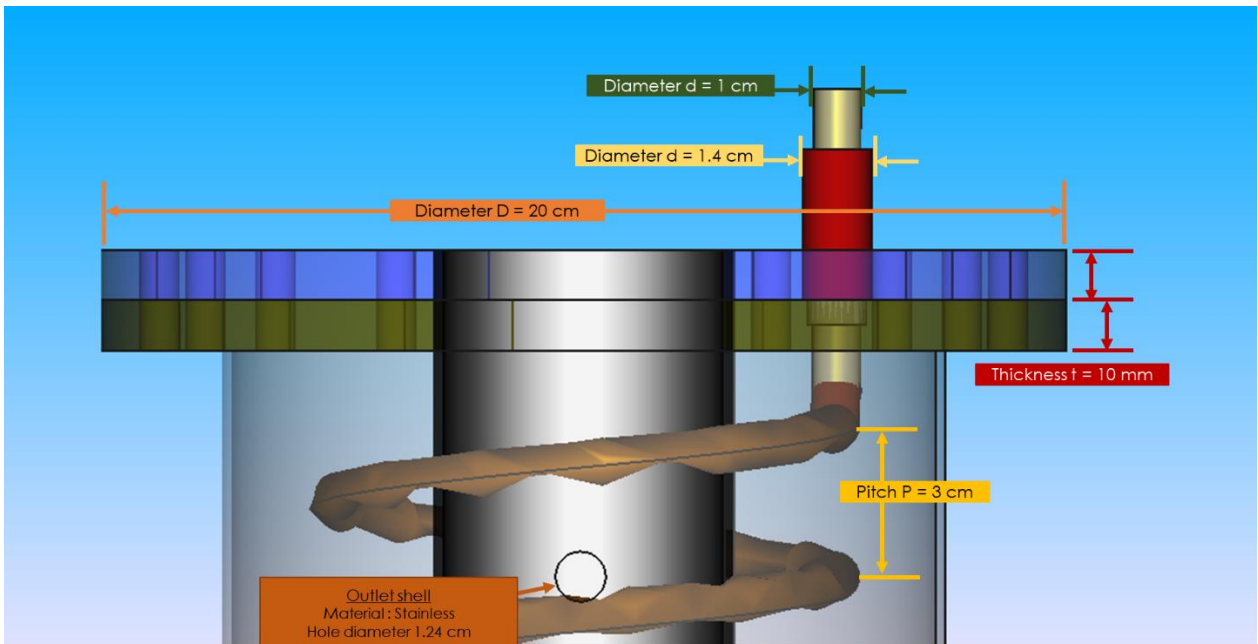
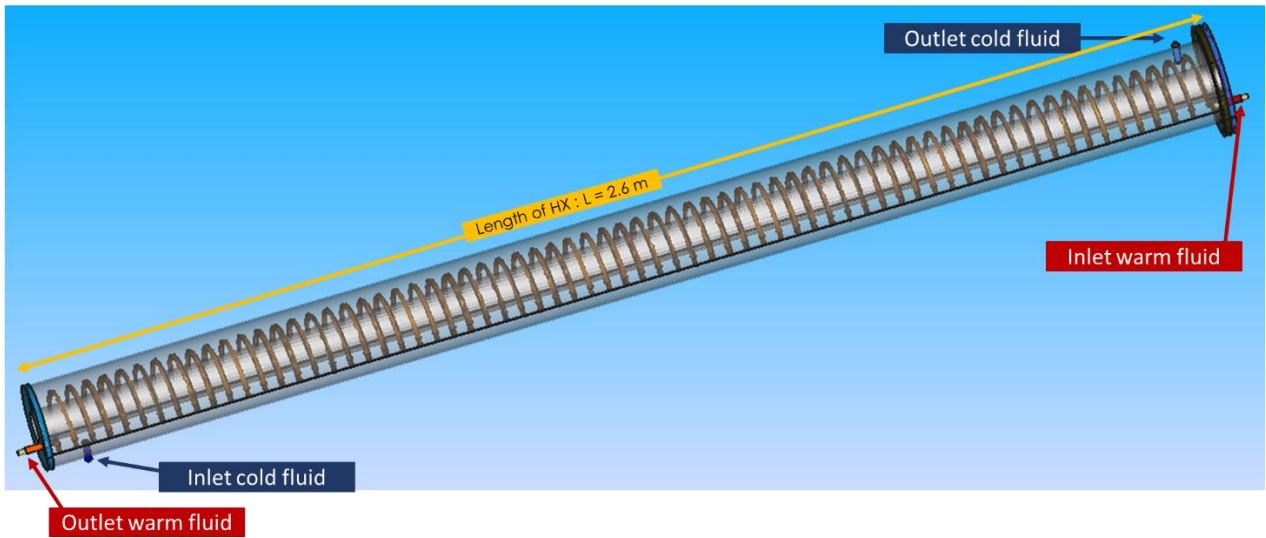
Helical Coil Heat
exchanger.FCStd

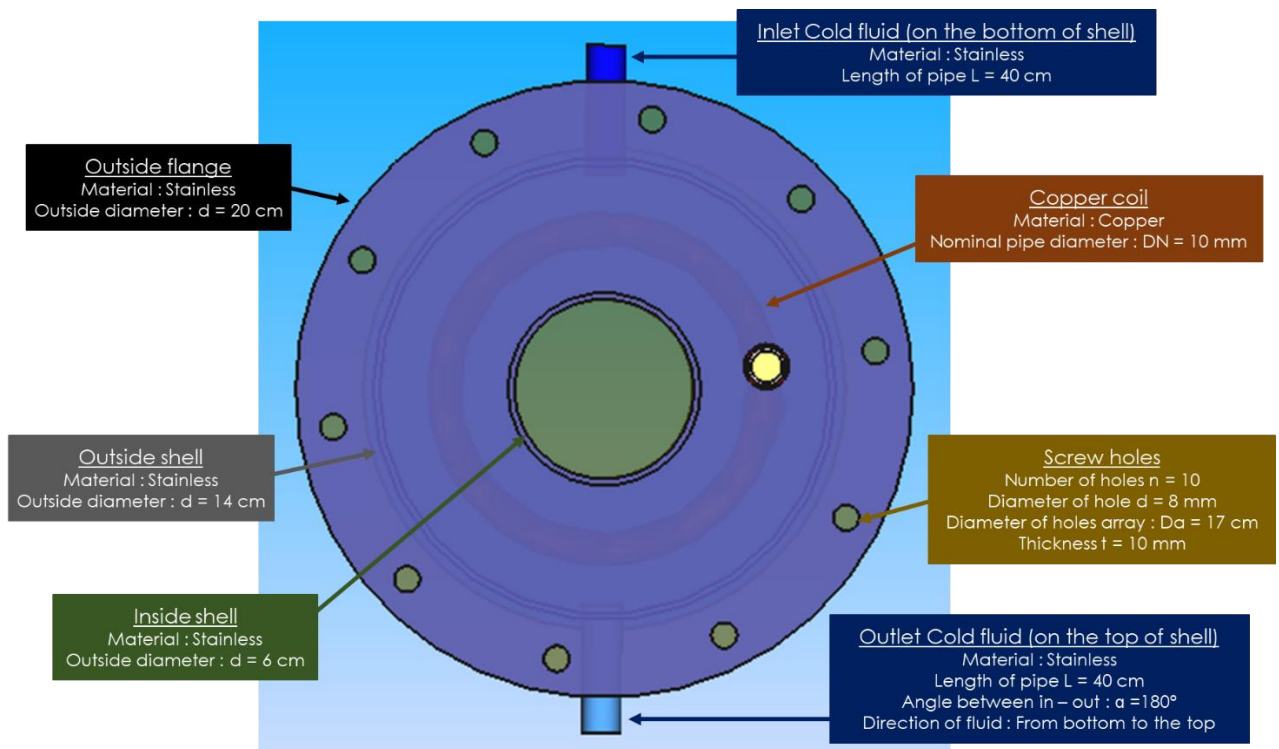
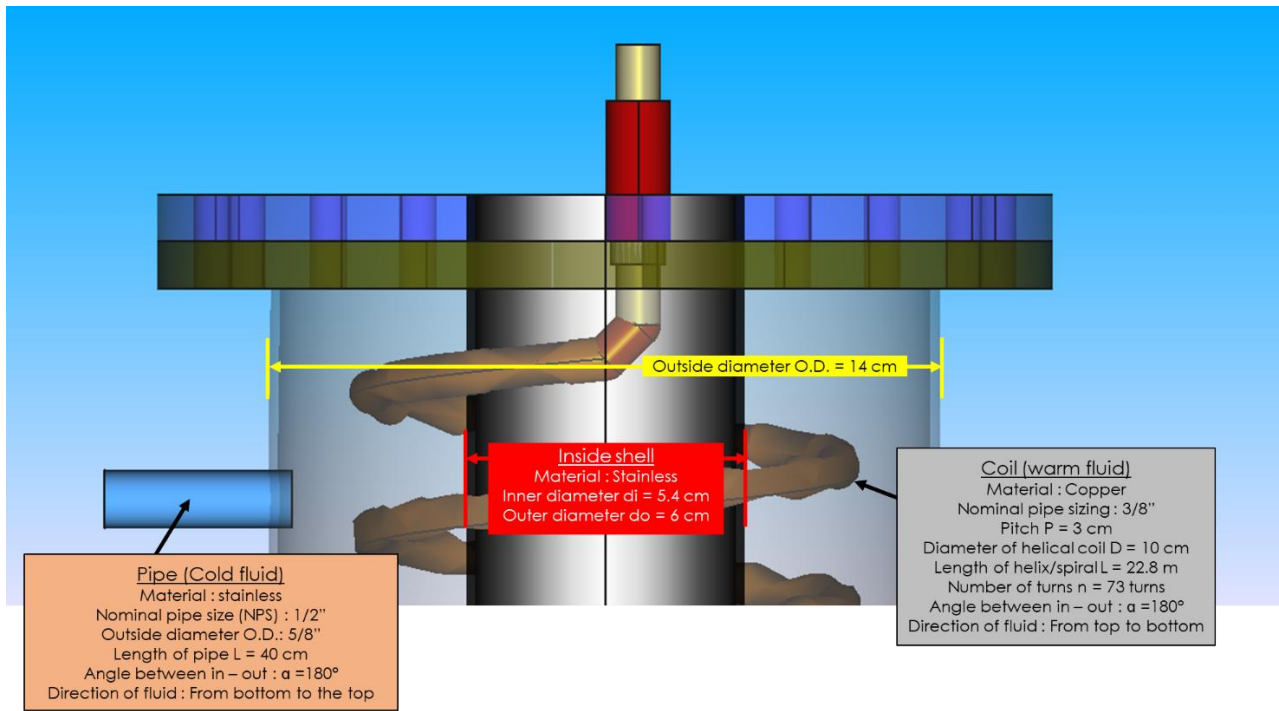


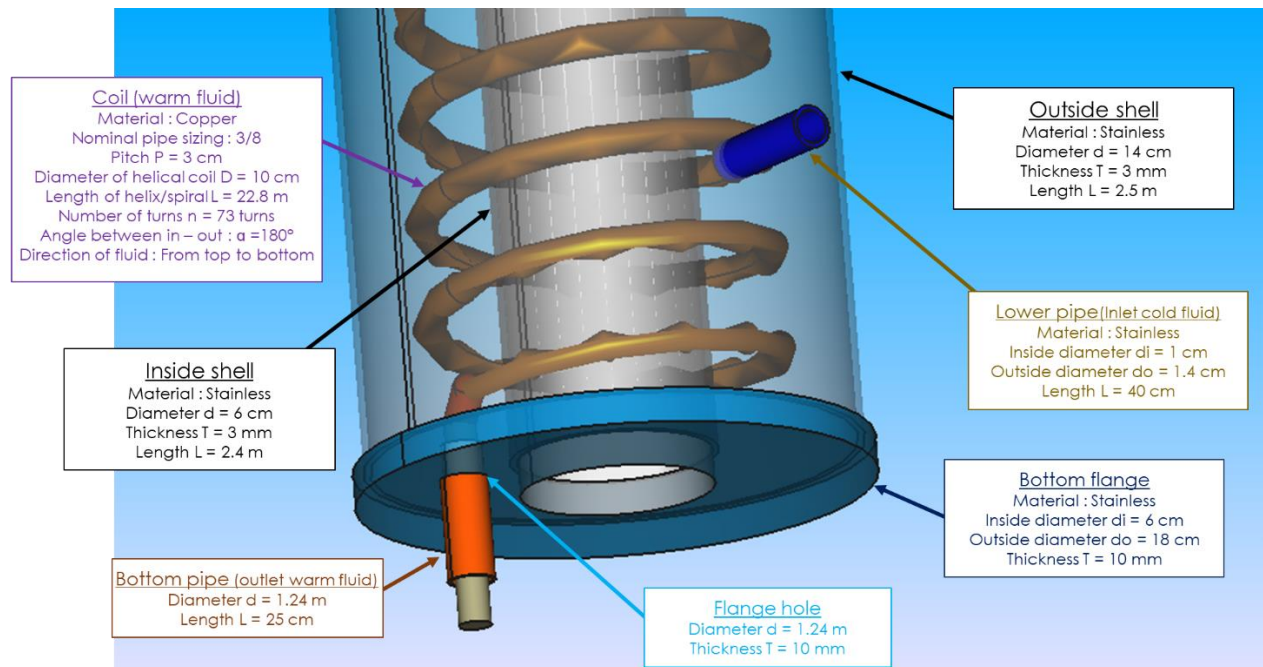
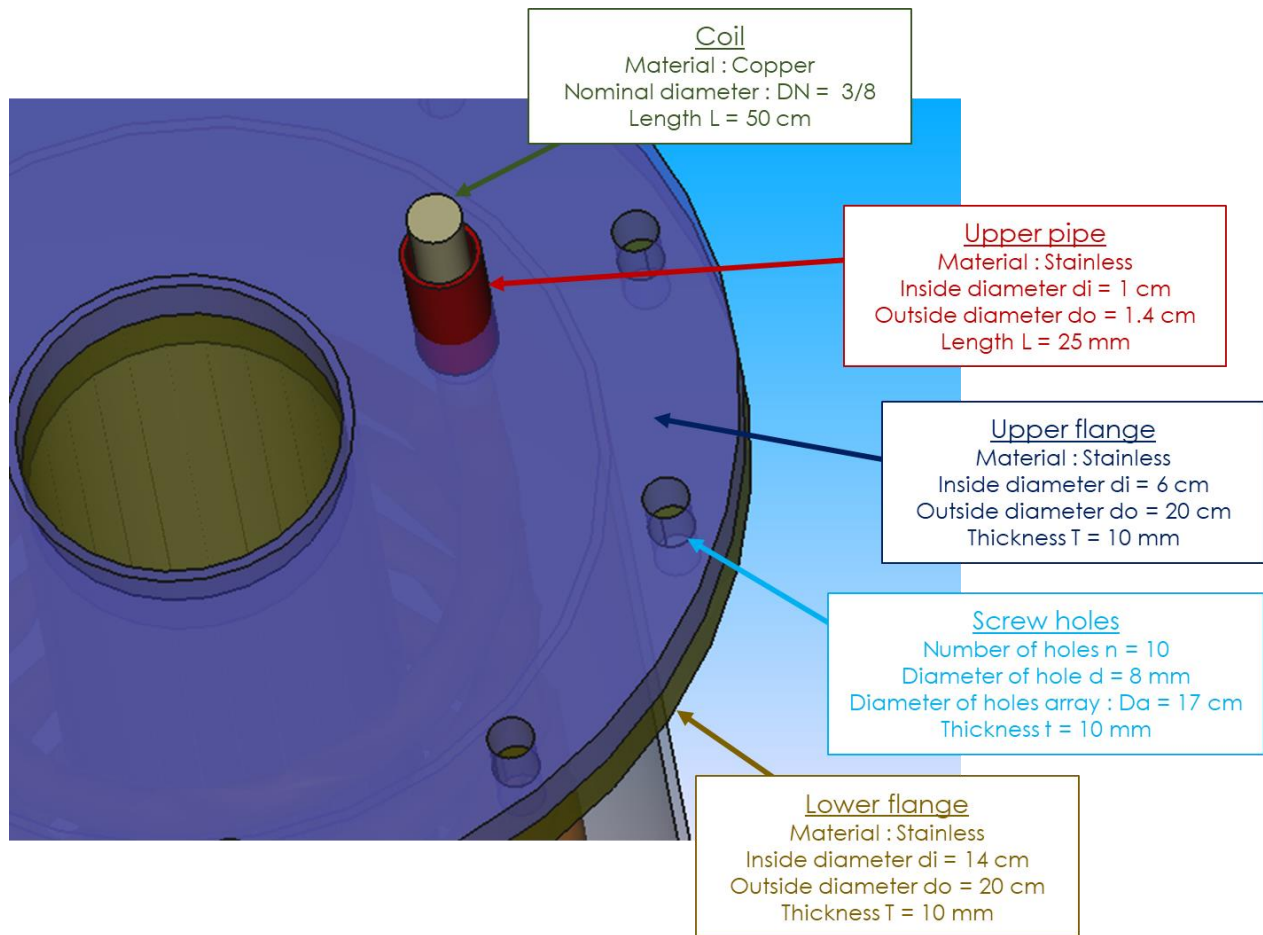
Sizing of helical coil heat exchanger (.pptx)



13092022_ Sizing of
helical coil HX.pptx







5) Heat exchanger - Thermal calculation**a) Average temperature LMTD $\Delta t_m = ?$**

We have:

Warm side: Temperature In = 195 K
 Temperature Out = 155 K

Cold side: Temperature In = 90 K
 Temperature Out = 153 K

$$\text{LMTD} = (\Delta T_1 - \Delta T_2) / \ln (\Delta T_1 / \Delta T_2)$$

For counter current:

$$\Delta T_1 = T_{\text{warm in}} - T_{\text{cold out}} = 195 - 153 = 42$$

$$\Delta T_2 = T_{\text{warm out}} - T_{\text{cold in}} = 155 - 90 = 65$$

$$\text{LMTD} = 52.67$$

- Heat flux Q=?

We estimate $G = 0.1 \text{ Kg/sec}$ with $Q_{\text{hot}} = G.C.(t_{2i} - t_{2f})$

Where:

Q – quantity of heat transferred or received by the heat transfer medium [W],

G – hot and cold heat transfer medium flow rates [kg/sec],

C – heat capacity of hot and cold heat transfer media at (50 bar, 195 K) and (50 bar, 150 K) [kJ/Kg.deg], $C = 1.4 \text{ kJ/Kg.K}$

t_{2f} – final temperature of cold heat transfer media [°C or K],

t_{2i} – initial temperature of cold heat transfer media [°C or K].

$$\Rightarrow Q = 0.1 * 1.4 * (193 - 155) = 5.32 \text{ kW}$$

6) Design calculation**a) Heat exchange surface A=?**

The approximate heat exchange surface is calculated as follows:

$$Q = U \times A \times \text{LMTD}$$

Where:

A: Surface area [m²];

U: the overall heat transfer coefficient [W/m².K], by estimation based on tables below U = 150 W/m².K ;

Types	Application	Overall Heat Transfer Coefficient - U -	
		W/(m ² K)	Btu/(ft ² °F h)
Tubular, heating or cooling	Gas at atmospheric pressure inside and outside tubes	5 - 35	1 - 6
	Gas at high pressure inside and outside tubes	150 - 500	25 - 90
	Liquid outside (inside) and gas at atmospheric pressure inside (outside) tubes	15 - 70	3 - 15
	Gas at high pressure inside and liquid outside tubes	200 - 400	35 - 70
	Liquids inside and outside tubes	150 - 1200	25 - 200
	Steam outside and liquid inside tubes	300 - 1200	50 - 200
Air-cooled heat exchangers	Cooling of water	600 - 750	100 - 130
	Cooling of liquid light hydrocarbons	400 - 550	70 - 95
	Cooling of tar	30 - 60	5 - 10
	Cooling of air or flue gas	60 - 180	10 - 30
	Cooling of hydrocarbon gas	200 - 450	35 - 80
	Condensation of low pressure steam	700 - 850	125 - 150
	Condensation of organic vapors	350 - 500	65 - 90

$$\Rightarrow A = \frac{Q}{U \times LMTD} = \frac{5320 \text{ W}}{150 \left(\frac{\text{W}}{\text{m}^2 \cdot \text{K}} \right) \times 52.67} = 0.6733 \text{ m}^2 \approx 0.68 \text{ m}^2$$

b) Length of tube L=?

During the design calculation of coil heat exchangers, the total length of the coil as well as the number of turns and sections are determined.

$$L = A / \pi d_p$$

With :

L – total length of the coil [m],

A = 0.68 m²,

d_p – design diameter of the coil tube [m]; $d_p = 9.5 \text{ mm} = 0.0095 \text{ m}$

$$\Rightarrow L = \frac{0.68}{\pi \times 0.0095} = 22.78 \text{ m} \approx \mathbf{22.8 \text{ m}}$$

c) Number of turns $n=?$

n – Number of turns

P – Pitch

H – Height

D – Diameter

C – Circumference of spiral

We have $L = 22.8 \text{ m}$

We estimate $D = 10 \text{ cm}$ & $P = 3 \text{ cm}$

Circumference **$C = \pi \times D$**

$$D = 10 \text{ cm} = 0.10 \text{ m} \quad \rightarrow \quad C = 0.3142 \quad \rightarrow \quad C^2 = 0.0987 \text{ m}^2$$

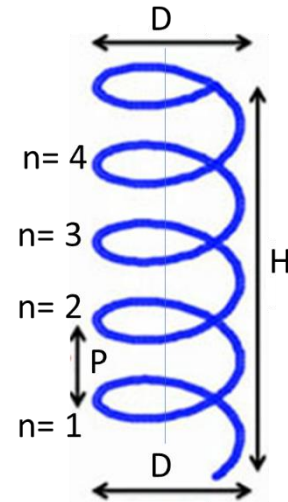
$$P = 3 \text{ cm} = 0.03 \text{ m} \quad \rightarrow \quad P^2 = 0.0009 \text{ m}^2$$

Length of helix: **$L = n\sqrt{C^2 + P^2}$**

$$\Rightarrow n = \frac{L}{\sqrt{C^2 + P^2}} = \frac{22.8}{\sqrt{(0.3142)^2 + (0.03)^2}} = \mathbf{72.243 \text{ turns}}$$

$$\Rightarrow n \approx \mathbf{72.3 \text{ turns}}$$

$$\text{With } n = \frac{H}{P} \Rightarrow H = n \times P = 72.3 \times 0.03 = 2.169 \text{ m} \approx \mathbf{2.2 \text{ m}}$$



7) Measurement summary of the Helical coil heat exchanger

	Parameters	Symbol & Unit	Size
Pipes	Outside diameter of pipe	O.D. [mm]	9.62
	Thickness of pipe	T [mm]	1.2
	Length of helix /spiral bar	L [m]	22.8
	Diameter of helical coil	D [cm]	10
	Pitch	P [cm]	3
	Number of turns	n [Turns]	72.3
	Angle between inlet and outlet	α [°]	180
Shell	Thickness of material	T _m [mm]	2.5 - 3
	Outside diameter of shell	D ₁ [cm]	14
	Inside diameter of shell	D ₂ [cm]	6
	Height	H [m]	2.4
	Angle between inlet and outlet	α [°]	180
	Angle between cold and warm (in/out)	α [°]	90
Holes	Number of shell installation holes	N	10
	Diameter of holes	d [mm]	8
	Diameter of cold fluid holes	D _c [mm]	5
	Diameter of warm fluid holes	D _w [mm]	5

8) List of HX prices

SR. No.	Materials	Specifications	Number of pieces	Available in stores	Average price *
1	Stainless pipe	diameter D = 14 cm	1	1 Kg → 6\$	150 \$ ¹
		Thickness t = 2.5 - 3 mm			
		Height H = 2.4 m			
2	Stainless pipe	diameter D = 6 cm	1	1 Kg → 6\$	68 \$ ²
		Thickness t = 2.5 - 3 mm			
		Height H = 2.5 m			
3	Copper pipe	Nominal pipe size 3/8	1	15 m → 50\$ → 23 m → 100\$	100 \$
		Length L ≈ 23 m			
4	Stainless flanges	In/out radius R _i = 7 cm/R _o = 10 cm	1	1 Kg → 6\$	1.43 \$ ³
		Thickness t = 10 mm			
5	Stainless flanges	In/Out radius R _i = 3 cm/R _o = 10 cm	1	1 Kg → 6\$	7.62 \$ ⁴
		Thickness t = 10 mm			
6	Stainless pipes	Radius R = 0.85 cm	4	1 Kg → 6\$	4 × 0.6 \$ ⁵ = 2.4 \$
		Height H = 5 cm			
7	Caotchouc gasket	In/Out radius R _i = 0.5 cm/R _o = 0.85 cm	4	***	***
8	Cryogenic insulation material **	Will be determined later			
				Total costs ≈ 330 \$	

* These prices is not include the manufacturing costs

** The insulation materials are used to cover most of the LOX equipment

¹ Density of stainless 304 = 7930 Kg/m³, $2\pi R \times H \times t = 2\pi \times 0.07 \times 2.4 \times 0.003 = 0.00317 \text{ m}^3$, $0.00317 \Rightarrow 25.138 \text{ Kg} \Rightarrow \approx 150 \$$

² Density of stainless 304 = 7930 Kg/m³, $2\pi R \times H \times t = 2\pi \times 0.03 \times 2.5 \times 0.003 = 0.00142 \text{ m}^3$, $0.00142 \text{ m}^3 \Rightarrow 11.261 \text{ Kg} \Rightarrow \approx 68 \$$

³ Density of stainless 304 = 7930 Kg/m³, $\pi (R_o - R_i)^2 \times t = \pi \times (0.1 - 0.07)^2 \times 0.010 = 0.00003 \text{ m}^3$, $0.00003 \text{ m}^3 \Rightarrow 0.238 \text{ Kg} \Rightarrow 1.43 \$$

⁴ Density of stainless 304 = 7930 Kg/m³, $\pi (R_o - R_i)^2 \times t = \pi \times (0.1 - 0.03)^2 \times 0.010 = 0.00016 \text{ m}^3$, $0.00016 \text{ m}^3 \Rightarrow 1.27 \text{ Kg} \Rightarrow 7.62 \$$

⁵ Density of stainless 304 = 7930 Kg/m³, $2\pi R \times H \times t = 2\pi \times 0.0085 \times 0.05 \times 0.003 = 0.000008 \text{ m}^3$, $0.000008 \text{ m}^3 \Rightarrow 0.065 \text{ Kg} \Rightarrow \approx 0.6 \$$

4.6. Cooling pipes (Inside kelvinator refrigerator)

After the modifications that occurred in the prototype, the most prominent of which was passing oxygen directly into the tubes. This had to change the pipes in the refrigerator. The tubes in the refrigerator are aluminum tubes previously used in automobile radiators, which are contaminated with oil, which makes them liable to explode with oxygen. They will be replaced with 3/8" copper pipping.

1) Sizing calculation

a) Average temperature LMTD $\Delta T_m = ?$

- Warm side:

$$\text{Temperature In} = 263 \text{ K}$$

$$\text{Temperature Out} = 195 \text{ K}$$

- Cold side :

$$\text{Temperature In} = 193 \text{ K}$$

$$\text{Temperature In} = 193 \text{ K}$$

b) Heat flux $Q = ?$

$$\begin{aligned} Q_{\text{hot}} &= G.C.(t_{2i} - t_{2f}) \quad \text{where } G = 0.00094854 \text{ Kg/s} \\ &= 0.00094854 \text{ kg/s} \times 1.0341 \text{ kJ/Kg.K} \times (263-195) \text{ K} \\ &= 0.667 \text{ KW} \approx 667 \text{ W} \end{aligned}$$

c) Length of tube $L = ?$

$$Q = U \times A \times LMTD$$

$$\Rightarrow A = \frac{Q}{U \times LMTD} = \frac{667 \text{ W}}{50 \left(\frac{\text{W}}{\text{m}^2.\text{K}} \right) \times 19.13} = 0.6974 \text{ m}^2 \approx 0.7 \text{ m}^2$$

$$L = A / \pi d_p \quad \text{where } d_p = 7.9 \text{ mm} = 0.0079 \text{ m}$$

$$\Rightarrow L = \frac{0.7}{\pi \times 0.0079} = 28.205 \text{ m}$$

$$\text{Corrective length: } L_c = L \times \text{safety factor} = 28.205 \times 1.05 = 29.615 \text{ m} \approx 30 \text{ m}$$

Sr no	Size (mm)	Size (Inches)	Temper	SWG	Thick (mm)	Length Feets	Weight per Meter	Internal Radius	Max Working Pressure in Mpa	Bursting Pressure in Mpa
1	6.4	1/4"	1/2 H	21 swg	0.8	10	0.126	2.4	45.6	83.3
2	9.4	3/8"	1/2 H	21 swg	0.8	10	0.196	3.95	27.7	50.6
3	12.7	1/2"	1/2 H	21 swg	0.8	10	0.268	5.55	19.7	36
4	15.9	5/8"	1/2 H	21 swg	0.8	10	0.339	7.15	15.3	28
5	15.9	5/8"	1/2 H	19 swg	1	10	0.419	6.95	19.7	36
6	19.1	3/4"	1/2 H	21 swg	0.8	10	0.411	8.75	12.5	22.9
7	22.2	7/8"	1/2 H	21 swg	0.8	10	0.481	10.3	10.6	19.4
8	25.4	1"	1/2 H	20 swg	0.88	10	0.606	11.82	10.2	18.6

Copper Hard Pipes/Tube Weight and Pressure Details as per ASTM B88 in India [4]

SPECIFIC REQUIREMENT FOR VRF/VRV INSTALLATIONS - SOFT COIL FORM										
Sr no	Size (mm)	Size (Inches)	Temper	Thick (mm)	Length Feets	Aprox Weight per Coil	Internal Radius	Max Working Pressure in Mpa	Bursting Pressure in Mpa	
1	6.4	1/4"	0 (Coil)	0.8	50	1.92	2.4	13.8	68.3	
2	9.5	3/8"	0 (Coil)	0.8	50	2.98	3.95	8.4	41.5	
3	12.7	1/2"	0 (Coil)	0.8	50	4.08	5.55	6.0	29.5	
4	15.9	5/8"	0 (Coil)	1.0	50	6.38	6.95	5.9	29.5	
5	19.1	3/4"	0 (Coil)	1.0	50	7.75	8.55	4.8	24.0	

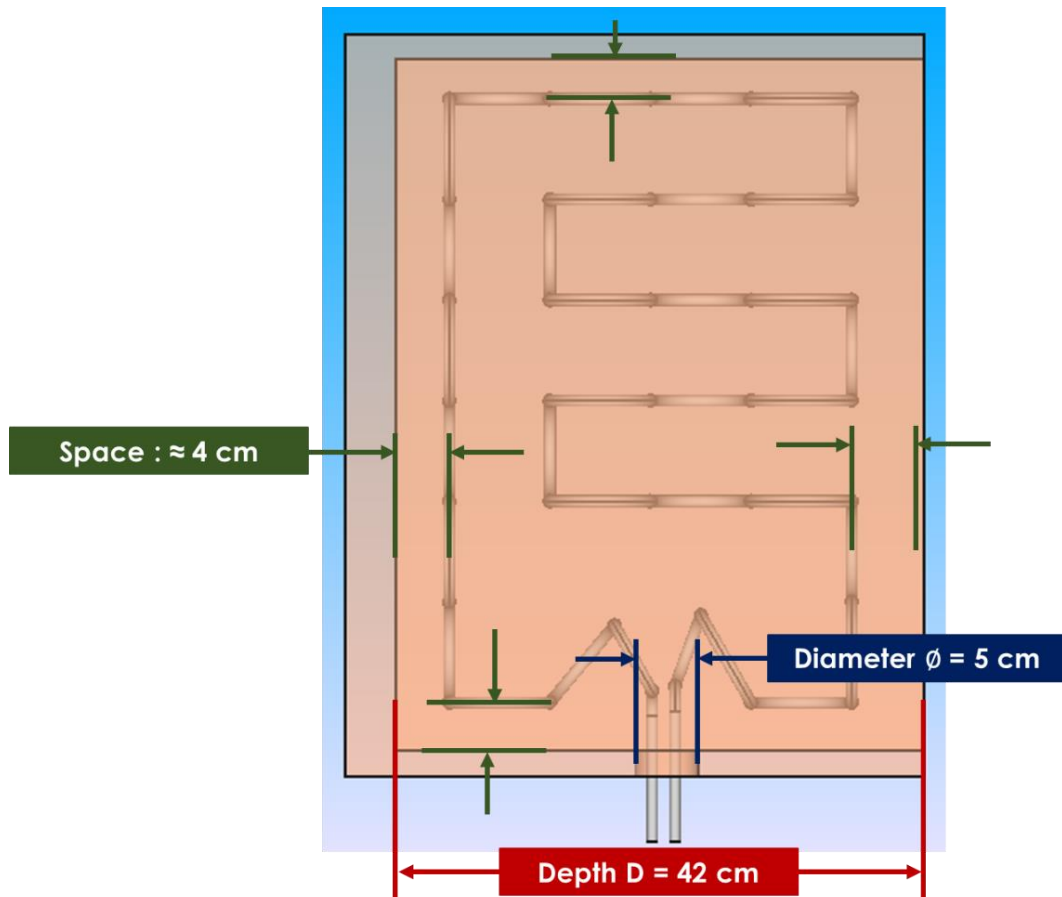
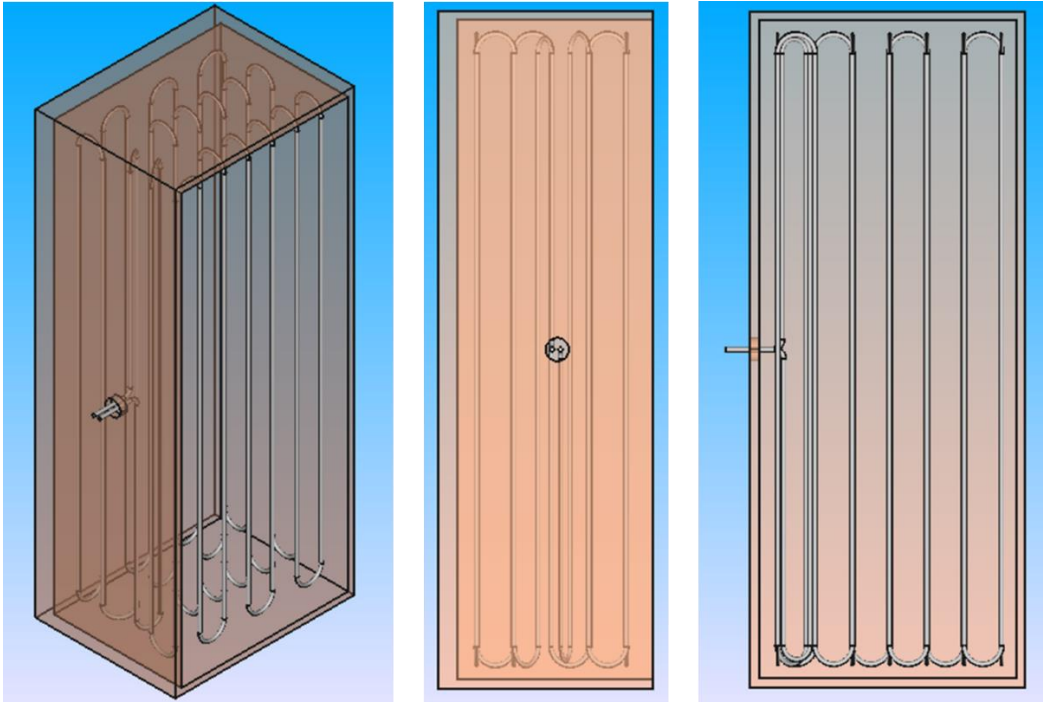
LIGHT WEIGHT NON VRV/VRF INSTALLATIONS - SOFT COIL FORM										
Sr no	Size (mm)	Size (Inches)	SWG	Thick (mm)	Length Feets	Aprox Weight per Coil	Internal Radius	Max Working Pressure in Mpa	Bursting Pressure in Mpa	
1	6.4	1/4"	23G	0.6	50	1.500	2.6	9.5	47.3	
2	9.5	3/8"	23G	0.6	50	2.500	4.15	6	29.6	
3	12.7	1/2"	22G	0.7	50	3.500	5.65	5.1	25.4	
4	15.9	5/8"	22G	0.7	50	4.500	7.25	4	19.8	
5	19.1	3/4"	21G	0.8	50	6.400	8.75	3.8	18.7	

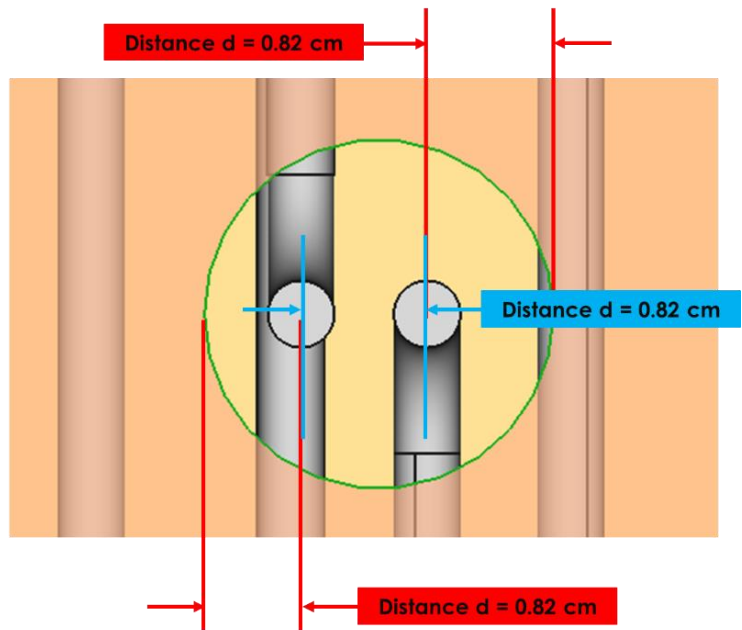
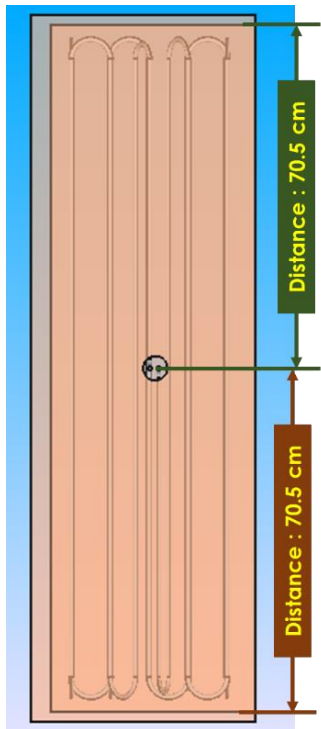
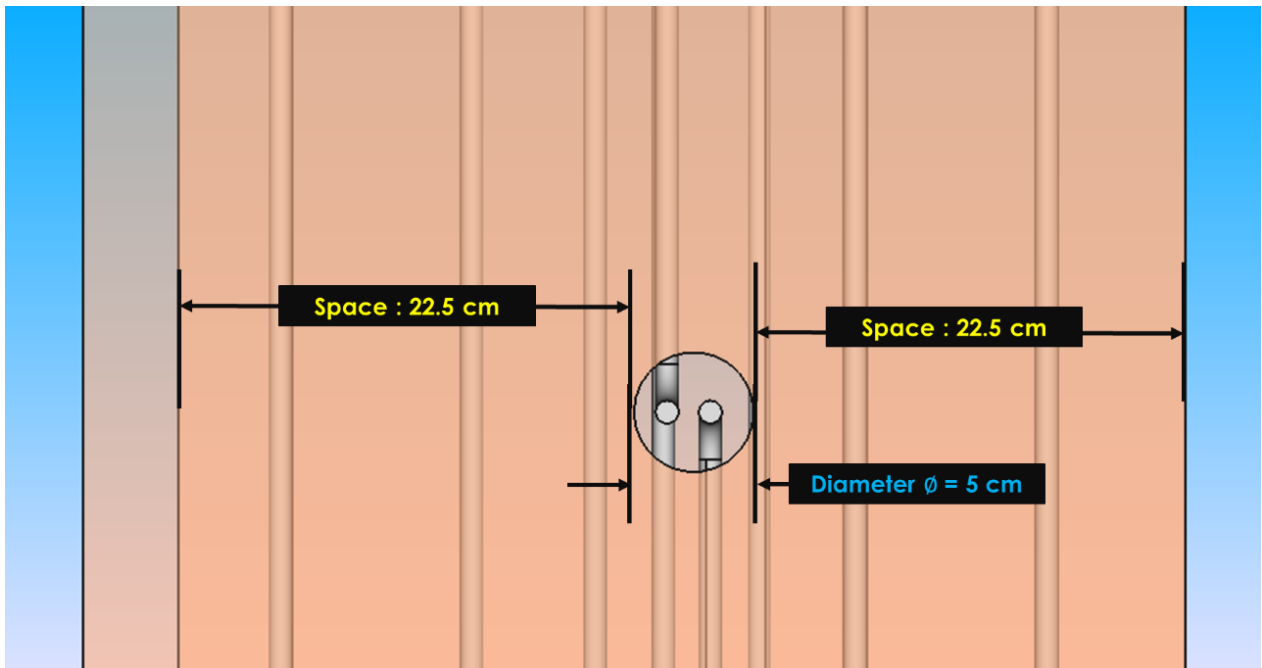
Weight Chart for Copper Non-VRV and VRV/VRF Copper Soft Pipes/ Coils as per Indian Standard [4]

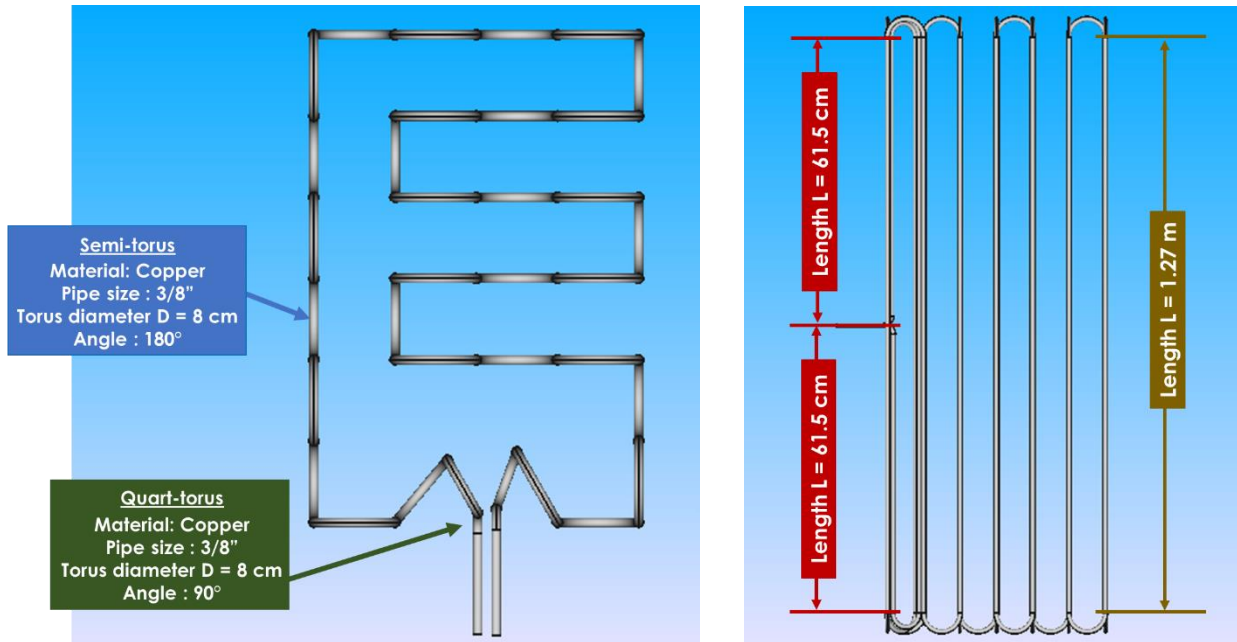
2) FreeCAD Design



14112022_Cooling
pipe design.FCStd







4.7. Compressor

1) Specifications of compressor

Oil free Oxygen compressor	
Working medium	Dry Oxygen Gas
Rated capacity [Nm ³ /h]	3 (@inlet pressure 1 bar)
Rated inlet pressure [MPa(G)]	0.1
Rated outlet pressure [MPa(G)]	5
Inlet temperature [°C]	-10
Outlet temperature [°C]	≈ +5 to +10
Lubricate way shaft and connect rod	Lubricate oil
Lubricate way cylinder	Oil free lubricate
Inlet and Outlet [mm]	DN15/DN15

2) Calculation of rated capacity

$$\text{Volumetric flow} = \frac{\text{Mass flow } m \cdot}{\text{Density}}$$

$$\text{Capacity} = 3.6 \cdot \text{volumetric flow}$$

$$\frac{Kg}{s} \div \frac{Kg}{m^3} = \frac{Kg}{s} \times \frac{m^3}{Kg} = \frac{m^3}{s} = \frac{1000 L}{s} \Rightarrow \frac{m^3}{s} = 3.6 \frac{m^3}{h}$$

4.8. Expansion valve

In this LOx prototype, we need a cryogenic expansion valve, that has the following features:

Specifications of expansion valve	
Media	O2 (Mixture liquid /gas)
Temperature	50°C to -185°C
Pressure	50 bar
Specification	DN10/DN10

A cryogenic expansion valve was not found operating on oxygen gas. therefore, this valve will be replaced by an open-close solenoid valve coupled to a pressure sensor. The solenoid valve, at the request of control, opens when the pressure sensor senses a pressure of 50 bar and closes at 45 bar.

1) Pressure sensor

Detailed will be available in the practical section when it is implemented

2) Solenoid valve

We need a cryogenic solenoid valve that have some specifications:

- Pipe size: 3/8"
- Nominal pressure: 50 bar
- Temperature: 90 K to 320 K

Cryogenic Solenoid Valve S9610 - S9710 Series (G1/8", G1/4", G1/2")

GENERAL FEATURES

- Liquid nitrogen (-320 ° F / -194 ° C), liquid argon (-303 ° F / -184 ° C), and liquid oxygen (-297 ° / -181 ° C)
- Internal Parts : Stainless Steel
- Seals : PTFE
- Fluid Temperature : -196°C to +90°C
- Ambient Temperature : max +50°C

ELECTRICAL CHARACTERISTICS

- Continuous Duty : ED %100
- Coil Insulation Class : H (180°C)(IEC 85)
- Coil Impregnation : Polyester Fiber Glass
- Protection Degree : IP68
- Electrical Safety : IEC 335
- Standard Voltages : AC 12V 15VA, 24V 15VA, 48V 15VA, 110V 15VA, 230V 15VA, 230V 24VA
DC 12V 18W, 24V 18W, 48V 18W, 110V 18W

On request other voltages

- Voltages Tolerance : AC -15%, +10% DC -5%, +10%
 - Frequency : 50 Hz (60 Hz...)
- In order, please specify coil voltage. For details, please look at coil section.



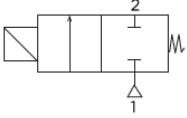
NORMALLY CLOSED
2/2 WAY
DIRECT ACTING
ΔP=0

3/8" size not available. 1/4" or 1/8" is accepted as an alternative pipe size, we can choose between 4 valves found in the S9610 series. Available pressure value up to 100 bar.



S9610 - S9710
Series.pdf

[1]

Solenoid Valve Symbol	Valve Type/ Order No	Connection Size	Orifice Size	Pressure		Kv	Seal	Weight	Tube, Sealing Features
				min/max					
	S9610 - S9710	G	mm	Bar	Bar	l/min	PTFE	kg	
	S9610.00.010T	1/8"	1	0	100	0.6	✓	0,68	Short Tube, Flat Sealing
	S9610.00.018T	1/8"	1.8	0	50	1.6	✓	0,68	Short Tube, Flat Sealing
	S9610.00.030T	1/8"	3	0	16	4.6	✓	0,68	Short Tube, Flat Sealing
	S9610.00.045T	1/8"	4.5	0	8	7.5	✓	0,68	Short Tube, Flat Sealing
	S9610.00.030T - BK	1/8"	3	0	16	4.6	✓	0,68	Short Tube, Flat Sealing
	S9610.00.045T - BK	1/8"	4.5	0	8	7.5	✓	0,68	Short Tube Flat Sealing
	S9610.01.010T	1/4"	1	0	100	0.6	✓	0,67	Short Tube, Flat Sealing
	S9610.01.018T	1/4"	1.8	0	50	1.6	✓	0,67	Short Tube, Flat Sealing
	S9610.01.030T	1/4"	3	0	16	4.6	✓	0,67	Short Tube, Flat Sealing
	S9610.01.045T	1/4"	4.5	0	8	7.5	✓	0,67	Short Tube, Flat Sealing

Model	Description	Unit Price(Euro)
S9610.01.018T	1/4", 1.8 mm orif. 0-50 bar	60,00
S9610.01.010T	1/4", 1 mm orif. 0-100 bar	60,00
S9610.00.010T	1/8", 1 mm orif. 0-100 bar	60,00
S9610.00.018T	1/8", 1.8 mm orif. 0-50 bar	60,00

Selected

The valve is useful for Cryogenic Fluid, Liquid Oxygen, Hydrogen, Helium, Carbon Dioxide, Nitrogen.



www.smstork.com

Yalçın ARAZ
Regional Sales Manager
Electronics & Communications Engineer, MBA

HEAD OFFICE
Y. Dudullu, Bostancı Yolu, Kuru Sok, No 16
Ümraniye 34776 İstanbul TURKEY
P +90 216 364 34 05 - 2134
F +90 216 364 37 57

FACTORY
Çerkeşli OSB Mah. İmes-2 Cad.
No 5 Dilovası Kocaeli TURKEY
P +90 262 290 20 20
F +90 262 290 20 21

yalcin.araz@smstork.com
M +90 530 642 12 42

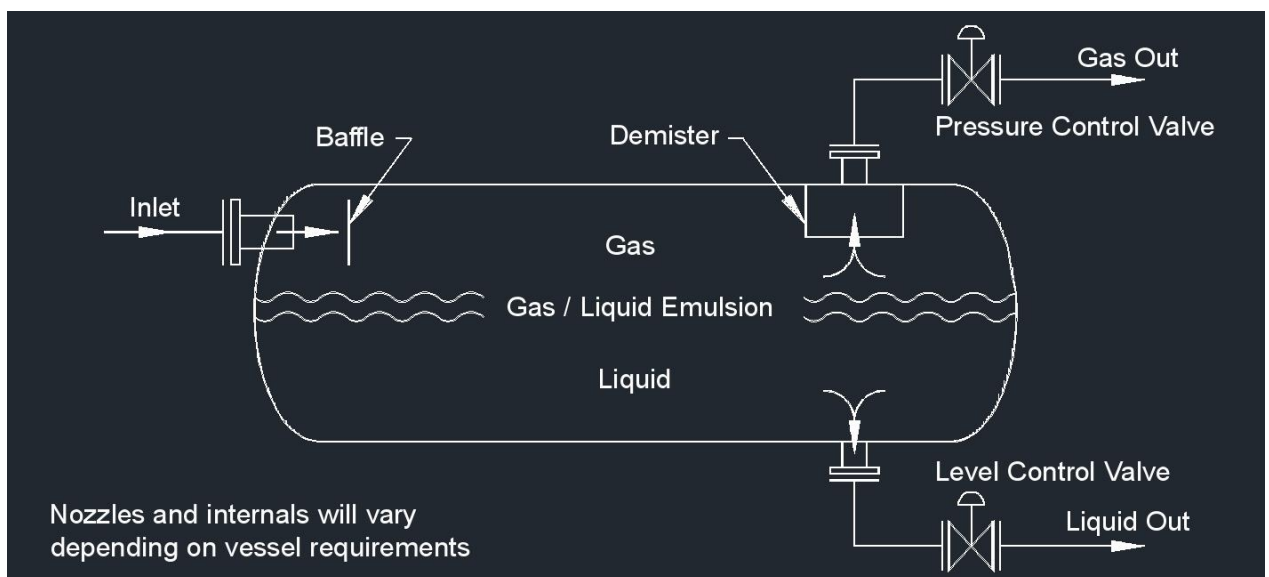
- Causes of leakage of low temperature solenoid operated hydraulic control valve

There are two reasons for the leakage of low temperature solenoid operated hydraulic control valve, firstly the main reasons are the seal deformation in the low temperature state. When the temperature of the medium is decreased, the volume change is caused by the phase change of the material, and the sealing surface with high grinding precision is produced to cause warpage, leading to the bad sealing. Two is the external leakage. It is mainly due to the flange connection

between low temperature solenoid valve and pipe, due to the connection pad, connecting bolts, and the connection between the material at low temperature shrinkage caused by the relaxation of the gap and lead to leakage. Therefore, **the connection mode between the valve body and the pipeline can be changed to the welding structure**, then the low temperature leakage can be avoided. Another is the stem and packing leakage. These are the main reasons for the leakage of low temperature solenoid operated hydraulic control valve.

3) Principle of two phase separator

Separation of the liquid and gas starts when the fluid meets the baffle. At that point, the gas and liquid start to go in different directions. The liquid drops where it is collected at the bottom of the vessel, and the gas rises to the top of the vessel. The gas that is still held in the liquid is in a section called the gas/liquid emulsion, which is in an area at the top of the liquid. In time, the gas is released from the emulsion and rises to the top of the vessel where the rest of the gas resides. Depending on the process, this may contain a mist eliminator or demister. The gas leaves from the top of the vessel, and the liquid leaves from the bottom of the vessel, heading to the next process.




4) Separator calculation

Physically, a decrease in gas pressure corresponds to an expansion in the volume of a gas and a decrease in its temperature. In our case, the purpose of the separator is to provide a place to allow the emergence of a pressure drop difference from 50 bar to 1 bar, which means that oxygen is allowed to expand, which leads to severe coldness of the gas (temperature drop).

- Sizing details depend on volume

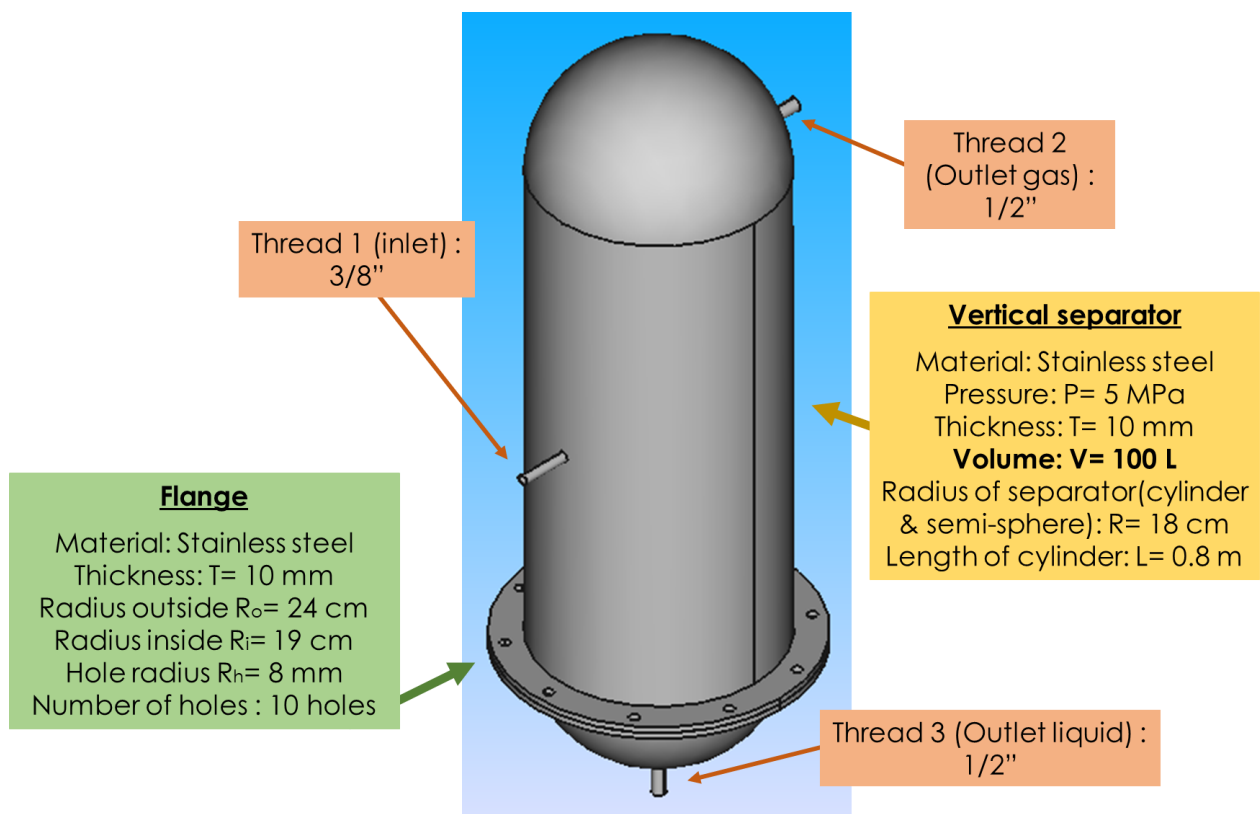
Total volume Vt [m ³]	Radius R [m]	Sphere volume Vs [m ³]	Cylinder volume Vc [m ³]	Length L [m]
0.1	0.18	0.024429024	0.075570976	0.74243792
0.17	0.21	0.038792386	0.131207614	0.947044913
0.35	0.27	0.082447958	0.267552042	1.168236765

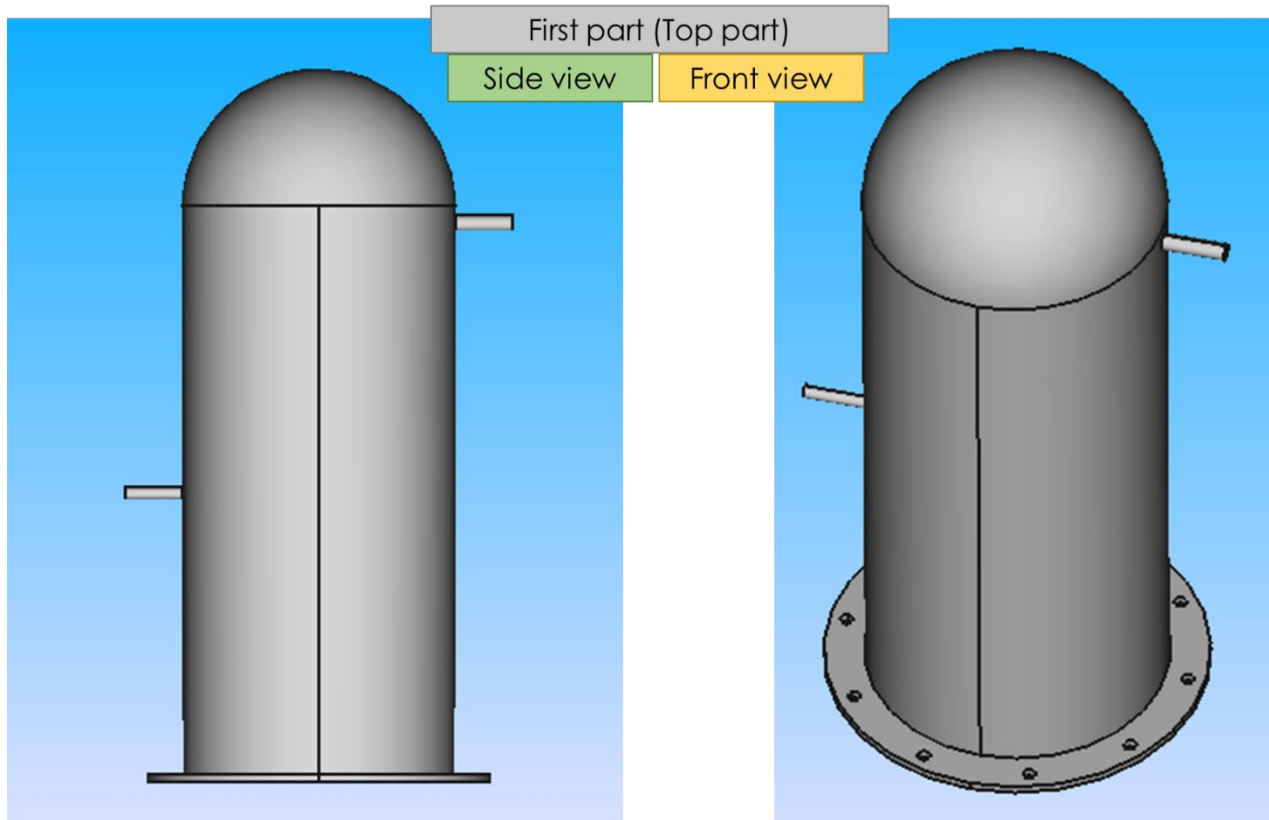
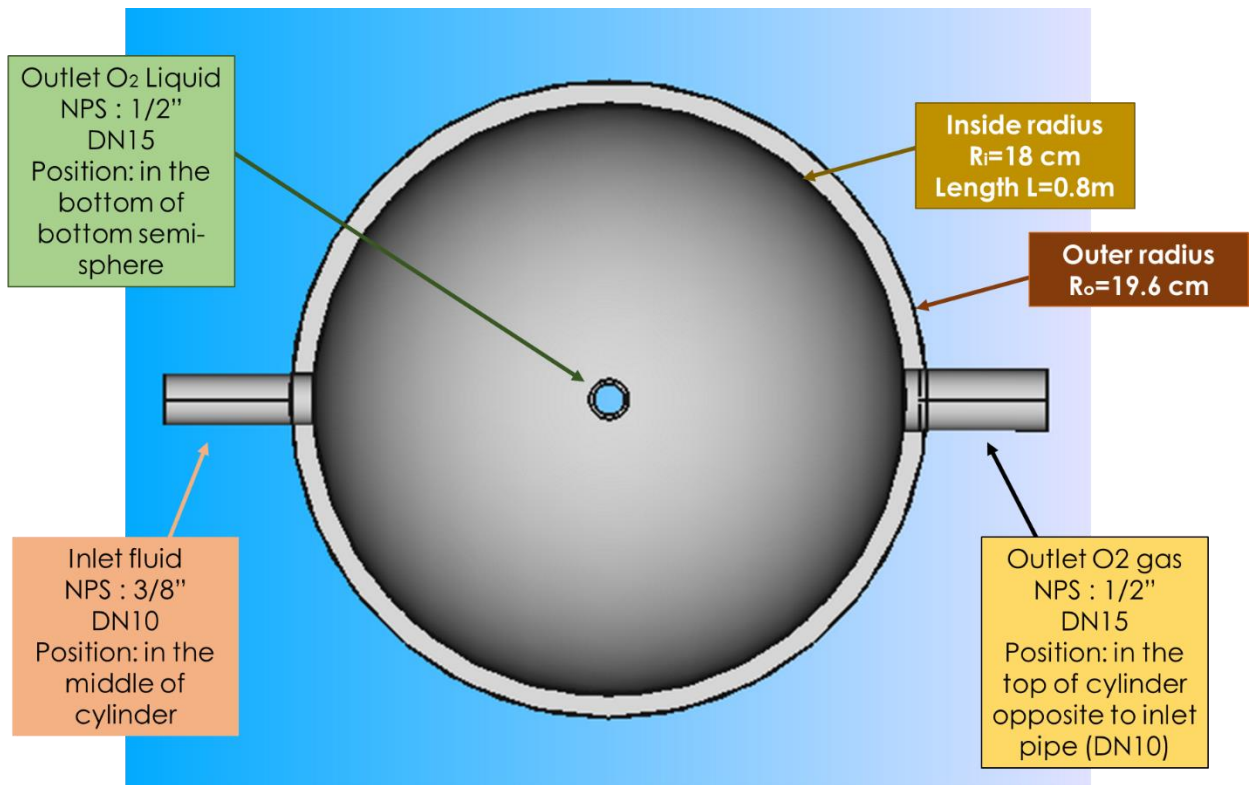
 **N.B.:** Changing the volume of the separator does not affect the size of the pipes (inlet/outlet). In other words, the pipe size will remain constant, and it is not related to the volume of the separator.

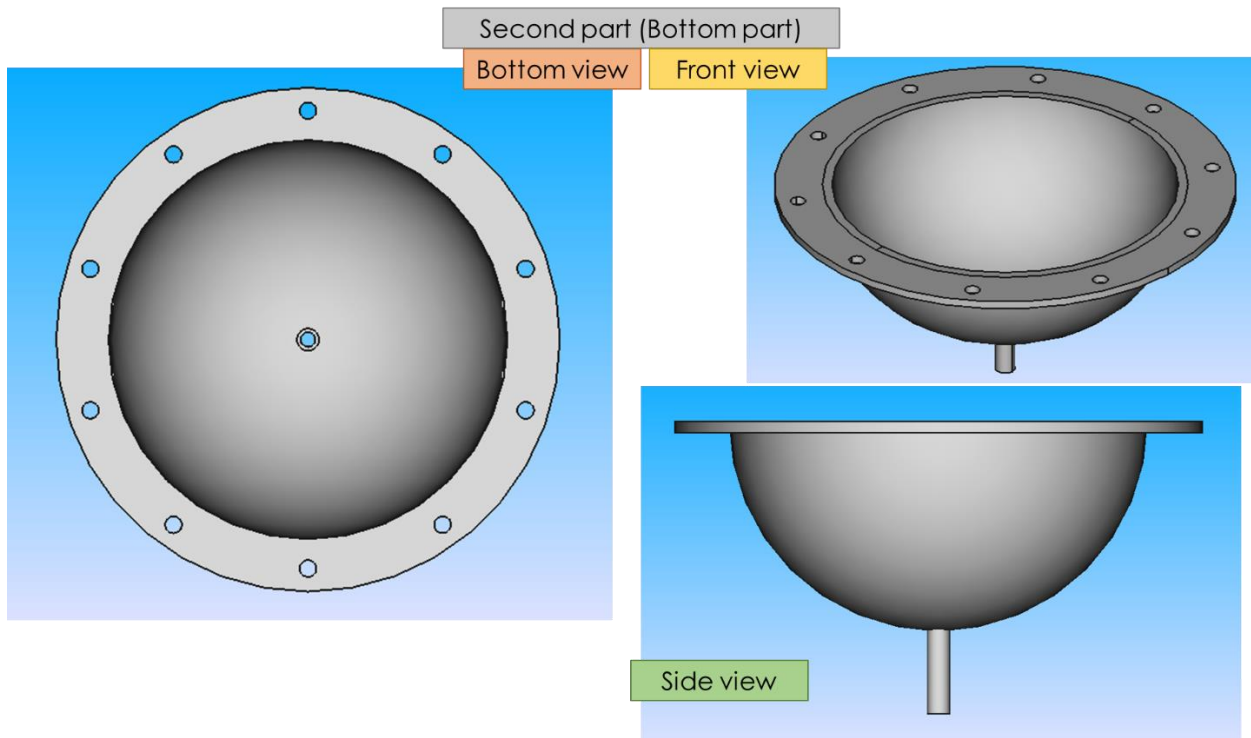
6) Design of separator



19102022_Separator design.FCStd







4.9. Cryogenic insulation material for LOx prototype

1) Flexible EPDM pipe insulation [5][6]

Flexible EPDM Pipe Insulation



EPDM rubber-based elastomeric pipe insulation is flexible, lightweight, UV resistant, and requires no outdoor weather protection. It is noncorrosive to copper and stainless steel, requires no vapor barrier, and is also paintable. It can be used on hot liquid heating systems, cold water plumbing, and chilled water and refrigeration lines to control condensation formation. The insulation can withstand temperatures between -297° to 300°F.

6 ft Insulation Length

↑ Fits Pipe Size	Fits Tube Size	Wall Thickness - Insulation	Insulation Temp. Range	Insulation Approx. R Value	Insulation Approx. K Value	Price
—	3/8 in	3/8 in	-297 °F to 300 °F	1.53	0.25	\$7.28
—	3/8 in	1/2 in	-297 °F to 300 °F	2.04	0.25	\$9.72
—	3/8 in	3/4 in	-297 °F to 300 °F	3.06	0.25	\$14.66
—	3/8 in	1 in	-297 °F to 300 °F	4.08	0.25	\$22.52

Flexible EPDM Pipe Insulation



EPDM rubber-based elastomeric pipe insulation is flexible, lightweight, UV resistant, and requires no outdoor weather protection. It is noncorrosive to copper and stainless steel, requires no vapor barrier, and is also paintable. It can be used on hot liquid heating systems, cold water plumbing, and chilled water and refrigeration lines to control condensation formation. The insulation can withstand temperatures between -297° to 300°F.

6 ft Insulation Length

↑ Fits Pipe Size	Fits Tube Size	Wall Thickness - Insulation	Insulation Temp. Range	Insulation Approx. R Value	Insulation Approx. K Value	Price
1/4 in	1/4 in	3/8 in	-297 °F to 300 °F	1.53	0.25	\$6.15
—	1/4 in	1/2 in	-297 °F to 300 °F	2.04	0.25	\$8.26
—	1/4 in	3/4 in	-297 °F to 300 °F	3.06	0.25	\$13.67
—	1/4 in	1 in	-297 °F to 300 °F	4.08	0.25	\$12.76

2) Cryogenic insulation materials [7][8]

Properties of Common Cryogenic Materials

Cryogenic materials are odorless, tasteless, and colorless when vaporized. Cryogenic liquids need to be carefully handled as they may cause skin burns and frostbite. Table-1 below lists down the liquid temperatures and the liquid to the gas expansion ratio of some of the common cryogenic materials:

Cryogenic Material	Liquid Temperature (°C)	Liquid to gas volume expansion ratio
Oxygen	-183	1: 860

TABLE 1. Thermal performance of cryogenic insulation materials for boundary temperatures of 78 / 293 K.

Insulation Material	Apparent Thermal Conductivity (mW-m/K)	
	High Vacuum	Ambient Pressure
Perlite Powder	0.9	36
Glass Bubbles	0.6	27
Aerogel Beads	1.8	14

4.10. Operating system

1) Preparing the system for operation:

- 1- Ensure that all components of the system are connected
- 2- Ensure that the system is free of leaks
- 3- Ensure that the insulators are placed correctly and in the appropriate places
- 4- Verify that electrical connections are correct
- 5- Make sure the valves are working

- 6- Make sure the oxygen tank is full
- 7- Fill the system tubes with oxygen

2) Operation system

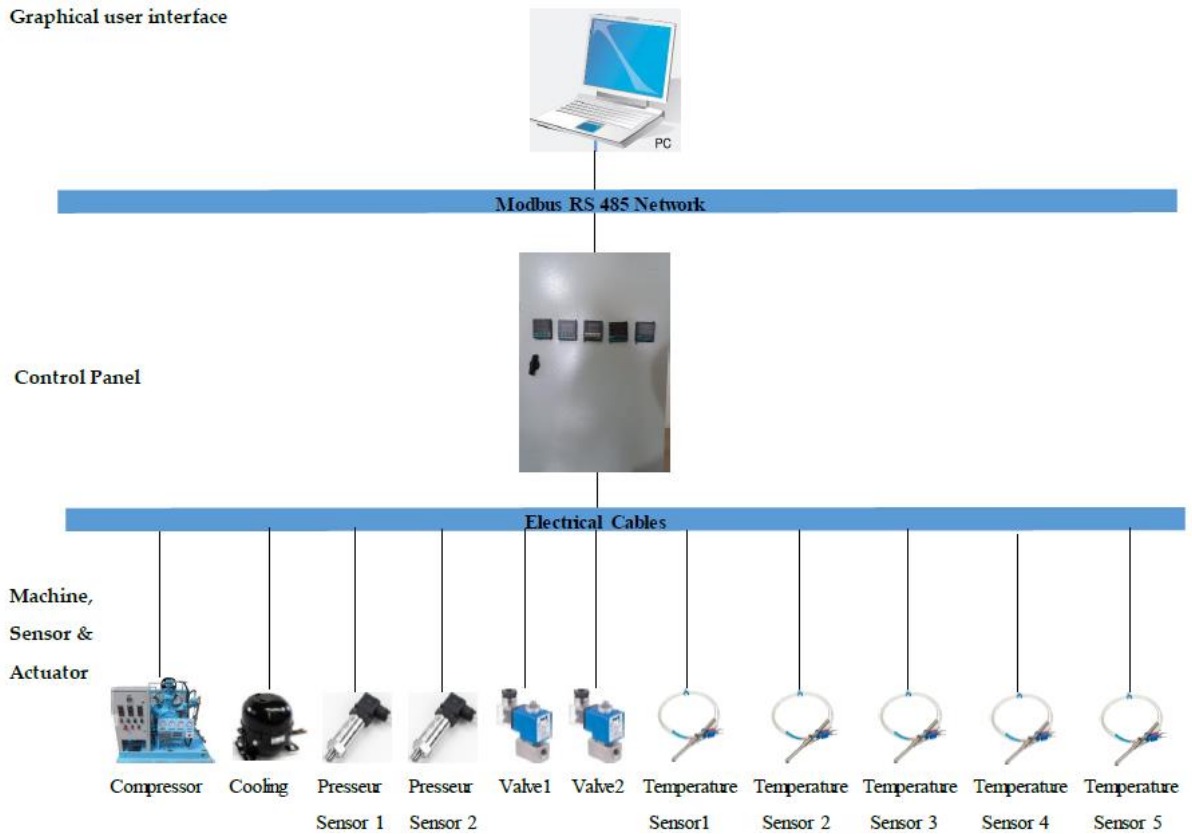
The first step to operate the system begins with operating the compressor, where the oxygen gas is pumped from the tank at ambient temperature (2 bar) to the pipes by the compressor. Oxygen gas passes through the tubes at a pressure of 50 bar. It is inserted into the Kelvinator refrigerator, which plays the role of a cooler, to cool the oxygen passing through the pipes from +10 °C to -78 °C (283 K to 195 K). The compressed oxygen exits from the cooler and enters the heat exchanger. Compressed oxygen exits from the heat exchanger at -118 °C (155 K) and passes into the solenoid valve, which opens at a pressure of 50 bar and closes at 45 bar. When the pressurized oxygen passes through the solenoid valve and the separator, the oxygen expands and its pressure drops from 50 bar to 1 bar. The fluid temperature also drops from -118 °C to -183 °C (from 155 K to 90 K). At a temperature of -183 °C (90 K, 1 bar), part of the fluid turns into liquid oxygen (1.23%) and collects at the base of the separator, while the other part remains in its gaseous state (98.77%), with a temperature close to the liquefaction temperature (-183 °C (90 K)), where it returns to the exchanger to play the role of a cooling medium for compressed oxygen gas passing through a coil. Oxygen gas comes out of the heat exchanger at a temperature of -120 °C (153 K, 1 bar) to reach the mixer, where the cold gas coming out of the heat exchanger is mixed with a certain amount of oxygen gas in the tank. This quantity is equivalent to the amount of liquid produced, taking into account the difference in pressure and temperature, and therefore the volume. The oxygen gas is then transferred to the heater, where it is heated to -10 °C (263 K) to re-enter the compressor again.

N.B.:

- ▶ **1- The required temperatures will not be obtained from the first pass (cycle #1), but this requires several cycles in order to cool the gas itself and the system.**
- ▶ **2- The high pressure and cryogenic temperature may cause fractures (cracks) in the pipes and this may lead to an explosion, so the system must be tested with an upward pressure to reach a high pressure (5 bar, 10 bar, 15 bar, ..., up to 50 bar).**
- ▶ **3- The safety valve (pressure reducing valve) must be placed at the highest point of the pressure tube in the system, to leak excess pressure in the system, especially after stopping the system from working.**

4.11. LOx PCS implementation

1) The process control system for the LOX system



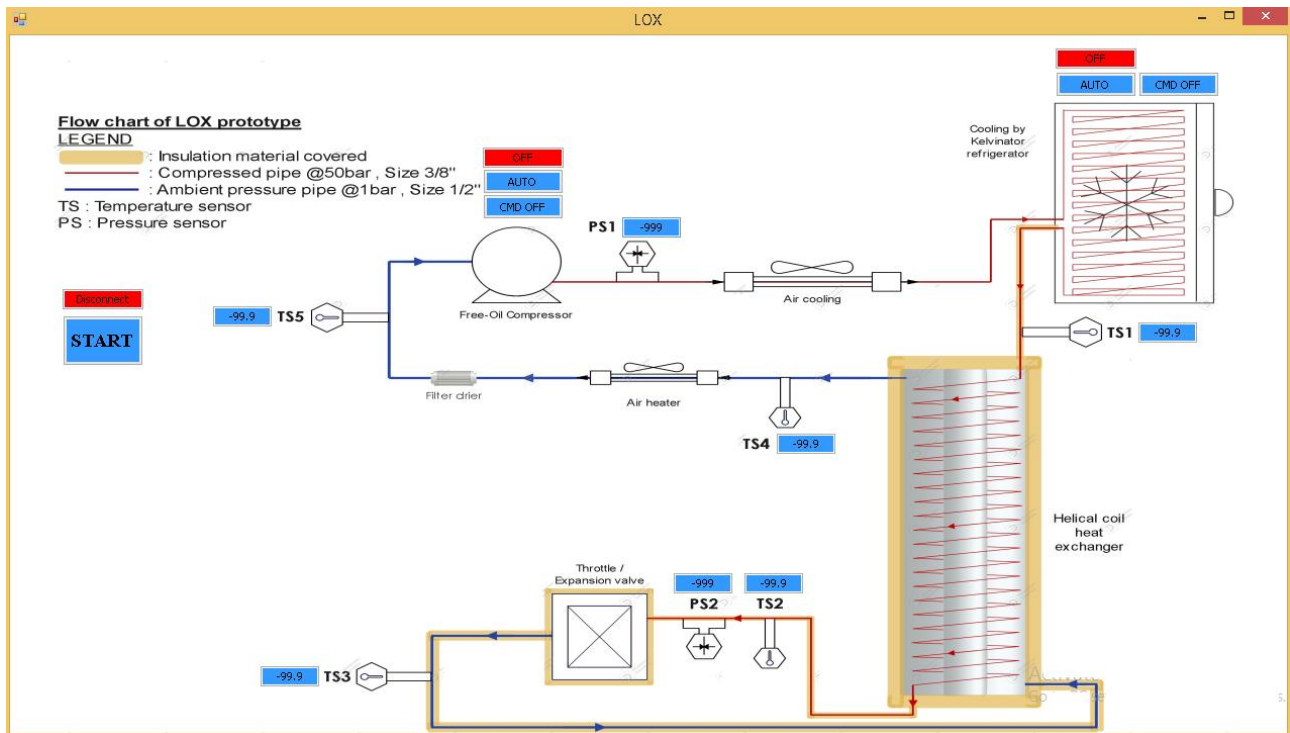
The process control system is the same for the LOX system with/without a heat exchanger (HX) (Version 2021)

LOX system will be controlled via Arduino



Figure 10. Arduino Nano RF

2) Graphical user interface (Version 2022)



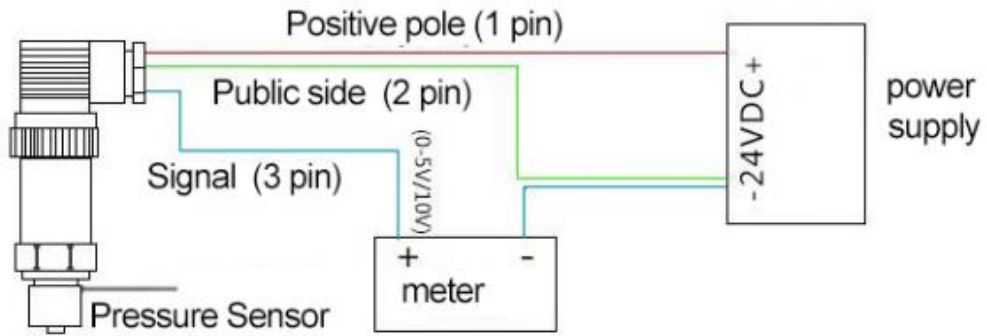
Graphical User Interface code (C#):



230922_ICPT-LOX_P
CS_GUI code.rar

3) The Material Used

- 1-Temperature Controller TE4-DC18W [9]
- 2-Temperature sensor PT100
- 3-Pressure Sensor HDP500 (0-10V Output, 0-10Mpa) [10]



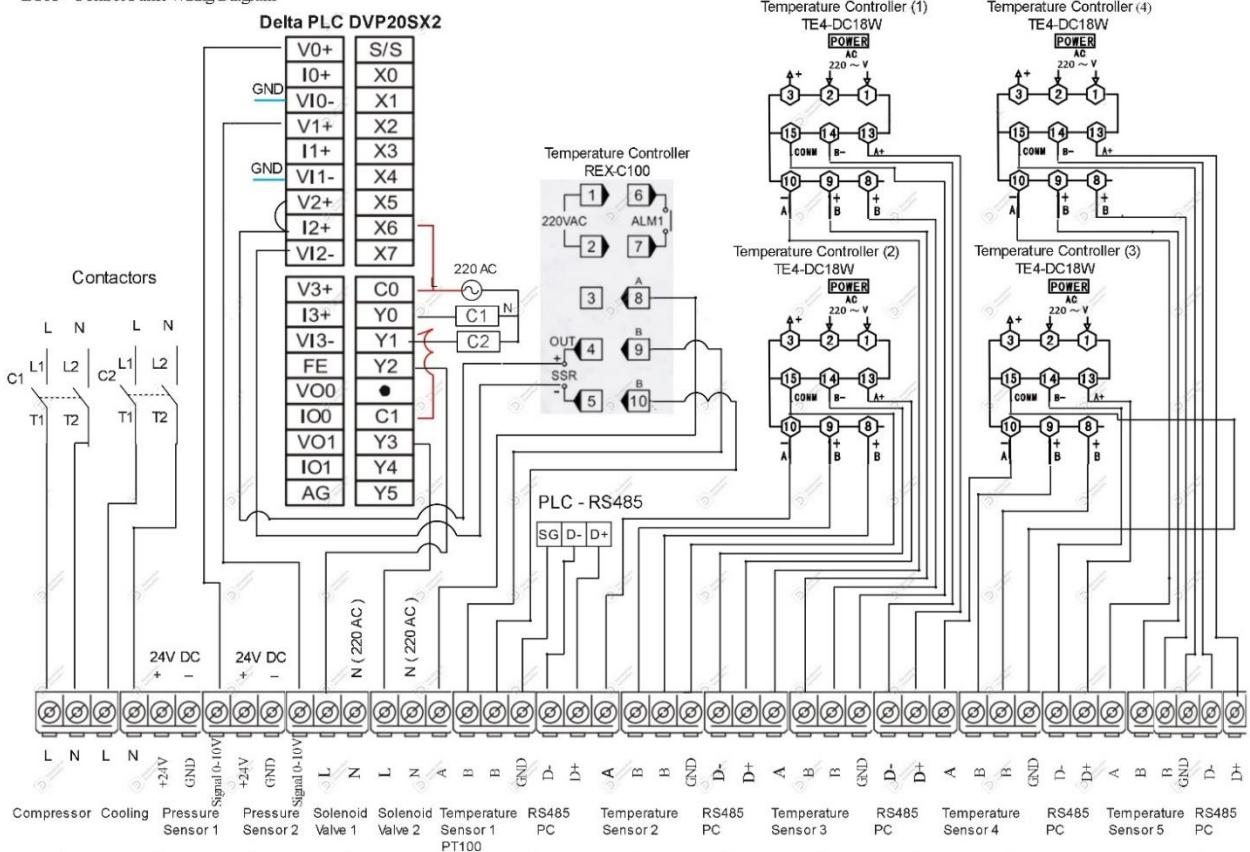
Red line: 24VDC Blue line: voltage output + green line: power supply -

THREE-WIRE VOLTAGE OUTPUT CIRCUIT DIAGRAM

4-Cyrogenic Solenoid Valve [11]

4) Control Panel Wiring Diagram

LOX - Control Panel Wiring Diagram



Control Panel Wiring Diagram:



311022LOX PCS -
Control Panel Wiring

4.12. What's next

To complete the practical part of the LOx project, it is necessary to replace the pipes inside the cooling system and to purchase the oil-free compressor and several other equipment. On the basis of compressor selection, features and design of heater, and mixer will be determined, and remote control will be finalized. After completing these steps, we will be ready to perform the first run.

Project 5: Biogas (ICPT - Biogas)

5.1. Position of biogas project

This project was proposed to produce methane gas for later use in the burner. This project is divided into two parts: a theoretical section and an applied (executive) section. Work on the biogas project started this year. Emphasis was placed on theoretical and applied aspects, as the project was studied, and the proposed design was manufactured without commissioning it.

5.2. Méthanisation: Processes, conditions, étapes, ...

(Anaerobic digestion: process, conditions, steps, ...)

1) Model size

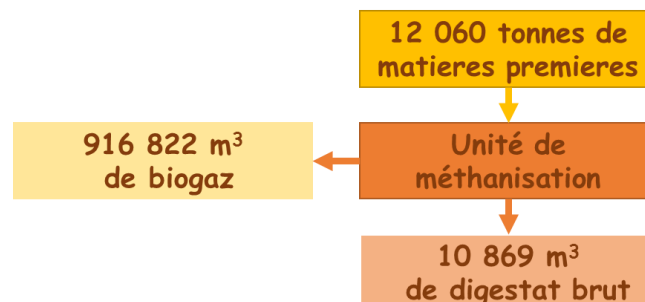
Operation: 91% approximately 8000 hours per year.

Quantity of raw materials: 12,060 tons.

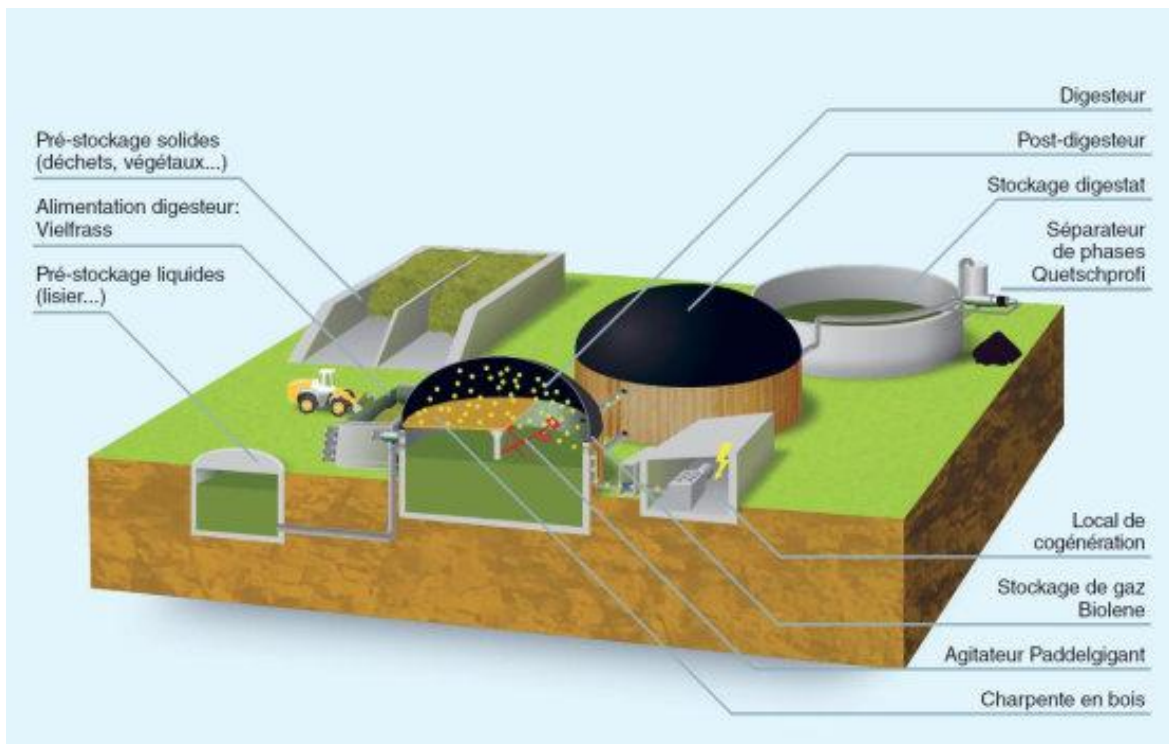
Quantity of biogas produced: 916,822 m³/year (54.3% methane).

Quantity of digestate: 10,869 m³.

2) Bilan des matières



3) Systèmes de production du biogaz



a) Input

Inputs can be of two types:

- EWEB liquid inputs
- Solid inputs (manure, plant matter)

Liquid inputs are pumped to the digester and must be agitated.

Solid substrates are introduced into the digester using a specially designed device.

This device has sufficient capacity to contain the equivalent of one to two days of inputs.

Insulation of the walls reduces the heating needs of the system.

The substrates are finely mixed to avoid the formation of crusts and to favor the expulsion of gas.

b) Digester

Pumping system to introduce liquid materials into the digester. A 160 mm diameter polyethylene pipe will be connected to the pump and the digester to introduce the solid inputs.

c) The stirring system: paddle stirrer

4 blades placed on a rotating axis generate currents in different directions with a high content of dry matter and thus prevent the formation of a surface layer.

The low rotation speed preserves the bacterial population.



Brewing system; 4 blade agitators

d) Membrane

Membrane for biogas storage: 2 mm thick EPDM

In high quality EPDM rubber, elastic, resistant (to UV and Ozone).



Rubber membrane to maintain the biogas

e) Digestion pit heating system

Network of tubes in composite material fixed on the internal wall of the pit.
The passage of hot water keeps the digestate at the right temperature.



Digester heating system

f) Digestion pits (digester)

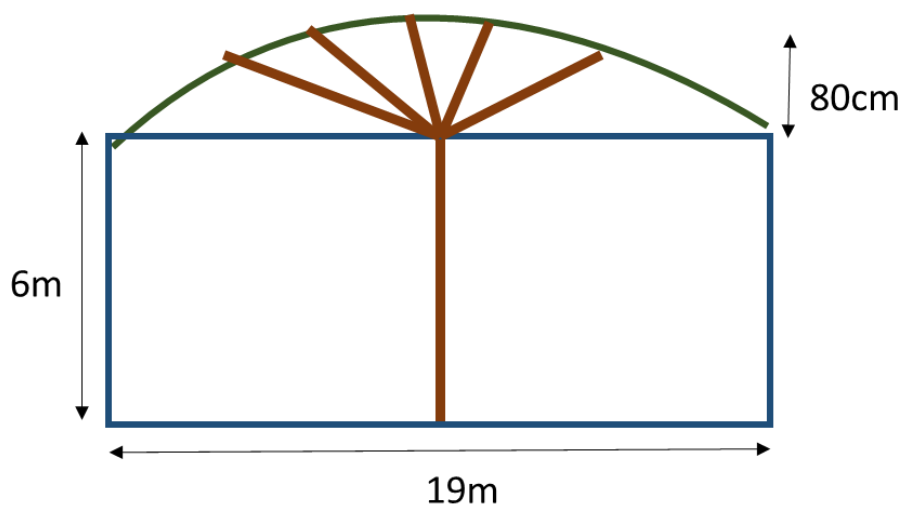
Reinforced concrete pit with a central pillar supporting a wooden frame (supports the EPDM biogas storage membrane, and offers a large colonization

surface for bacteria that transform hydrogen sulphide H_2S into sulfur which is deposited on the wooden frame).



Wood frame

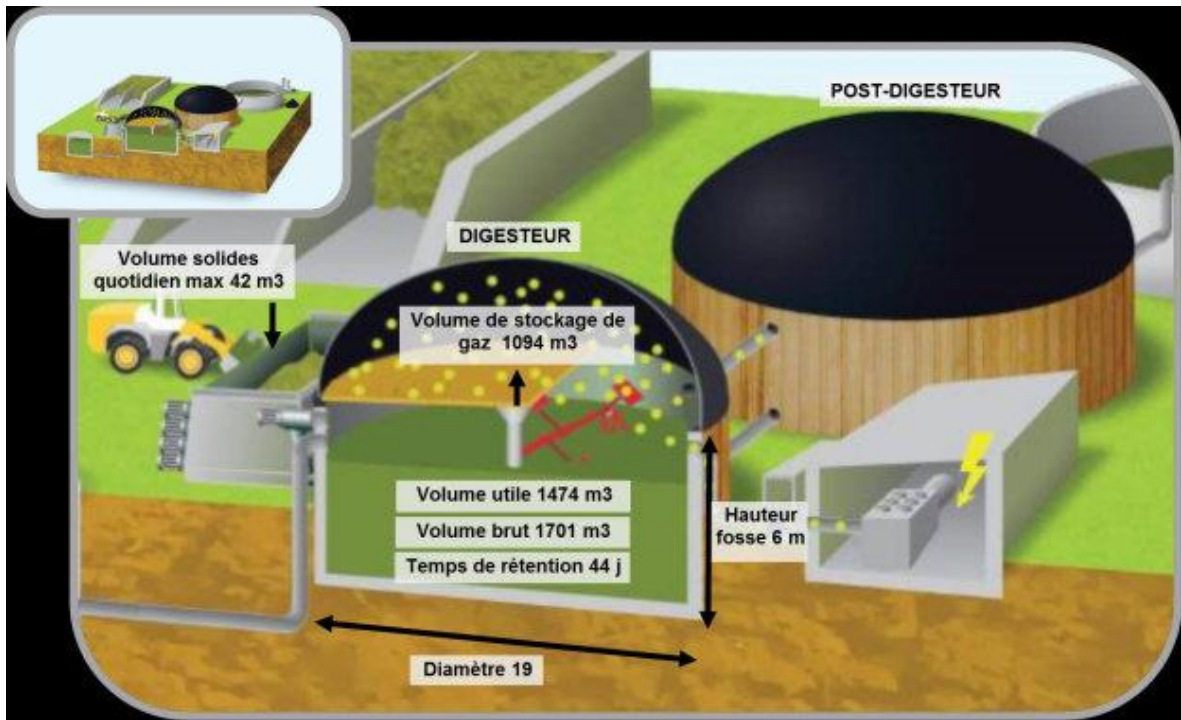
4) Biogaz dimensions



A digester diameter of 19 m allows a hydraulic retention time of 44.1 days

- Duration of methane production: Diameter= 19m => 44.1 days.

- Maximum load = 3.7kg MO/m³/day

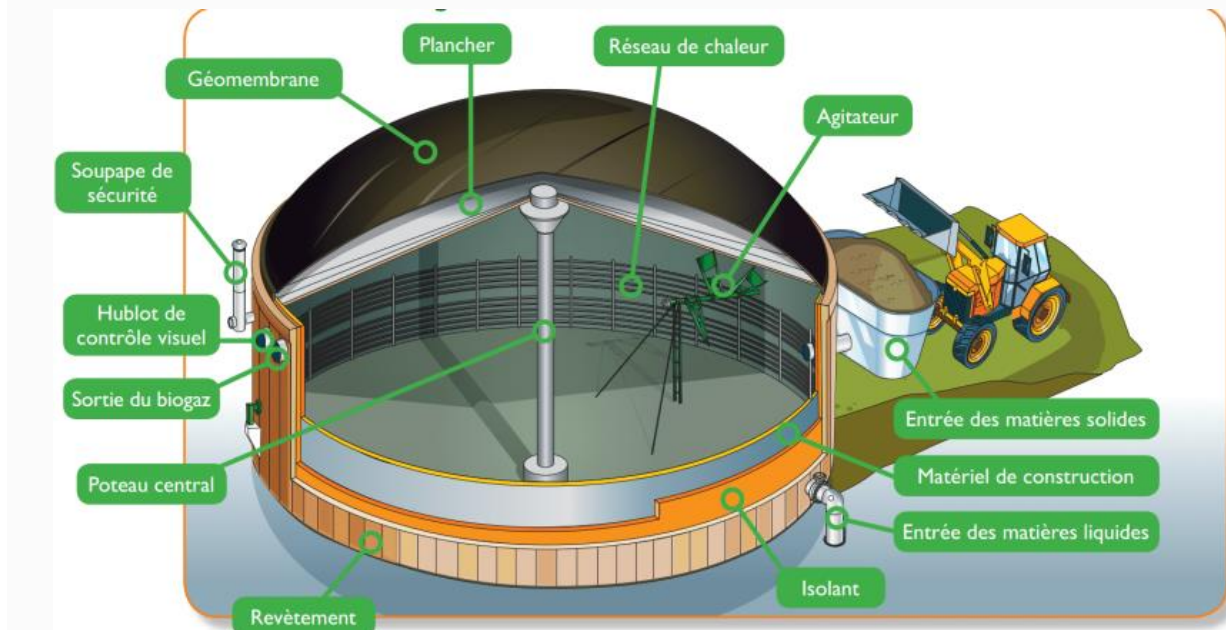


- **Dimensions :**

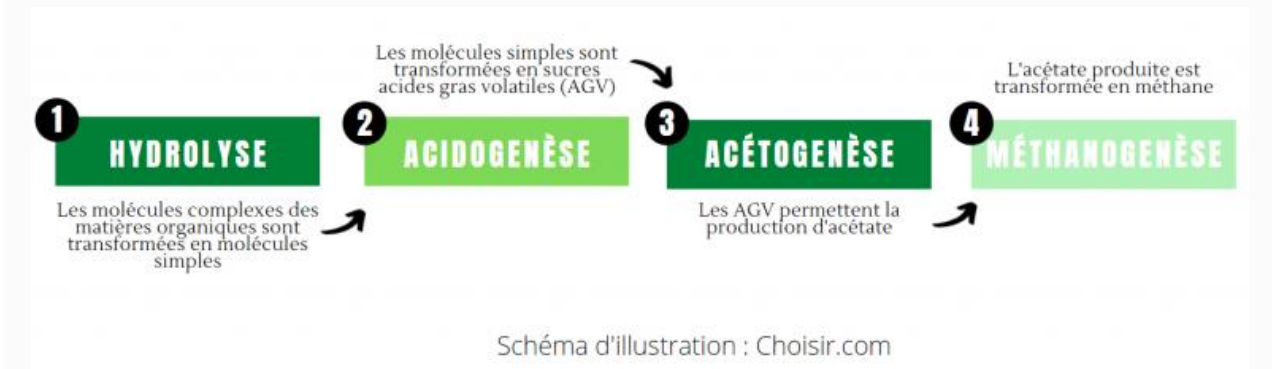
$\Phi=19\text{m}$, $h=6\text{m}$

Gross volume: 1701 m³

Net volume = 1,474 m³



5) Biogas steps



a) Hydrolyze

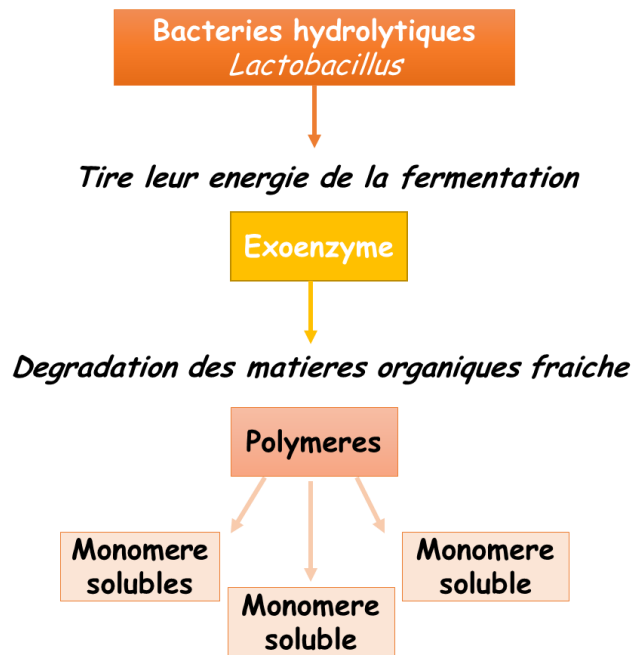


TABLEAU 1 : CARACTERISTIQUES DES BACTERIES HYDROLYTIQUES

Bactéries hydrolytiques	
caractéristiques	bactéries relativement résistantes, tolérantes à O ₂ , production d'exo-enzymes
gamme de pH optimal	[4,5 - 6,3]
temps de division	quelques heures (reproduction rapide)
sensibilité	lignine (pas dégradable, ralenti la réaction)

b) Acidogenesis

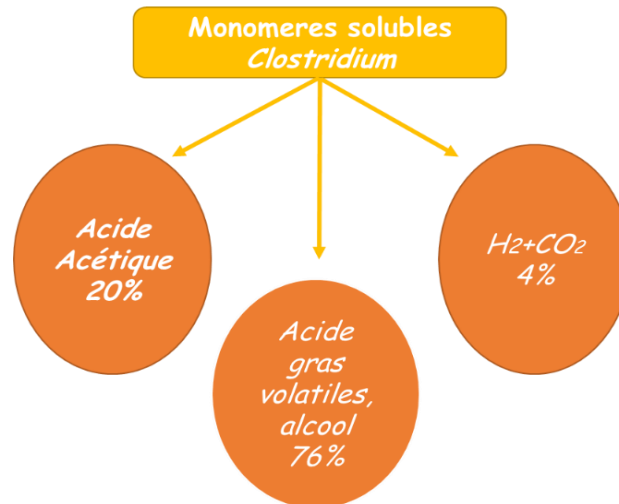


TABLEAU 2 : CARACTERISTIQUES DES BACTERIES ACIDOGENES

Bactéries acidogènes	
caractéristiques	bactéries sensibles à O ₂ , participent en général également à l'hydrolyse
gamme de pH optimal	[4,5 - 6,3]
temps de division	quelques heures (reproduction rapide)
sensibilité	H ₂ S, NH ₃ , sels, antibiotiques

c) Acetogenesis

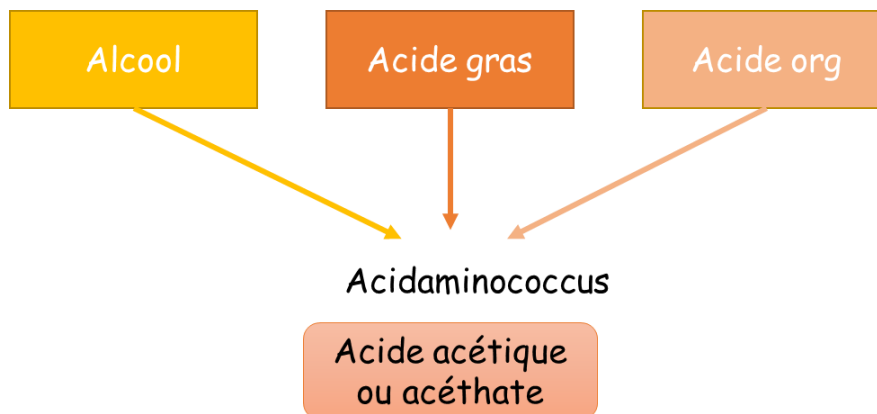


TABLEAU 3 : CARACTERISTIQUES DES BACTERIES ACETOGENES

Bactéries acétogènes	
caractéristiques	bactéries relativement fragiles, sensibles à O ₂ , production de H ₂
gamme de pH optimal	[6,8 - 7,5]
temps de division	quelques jours (1-4 jours ; reproduction lente)
sensibilité	H ₂ en excès, H ₂ S, NH ₃ , sels, antibiotiques, variations de température

d) Methanogenesis

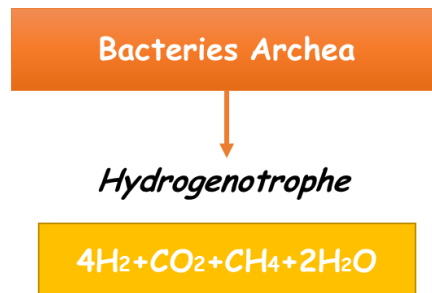


TABLEAU 4 : CARACTERISTIQUES DES BACTERIES METHANOGENES

Bactéries méthanogènes	
caractéristiques	archaebactéries très fragiles, très sensibles à O ₂ , besoin de Ni, plusieurs substrats possibles
gamme de pH optimal	[6,8 - 7,5]
temps de division	quelques jours (5-15 jours ; reproduction lente)
sensibilité	O ₂ , variations de pH et température, Cu, sels

Type de gaz	Proportion
Méthane – CH ₄	55 – 75%
Dioxyde de carbone – CO ₂	25 – 45%
Hydroxyde de soufre – H ₂ S	500 – 8000 ppm
Dioxygène - O ₂	0 – 1%
Vapeur d'eau – H ₂ O	Saturation

It is necessary to heat methane:

- Mesophilic zone: 35°
- Thermophilic zone: 55 to 60°C

 **N.B.:**

Biogas reduces the greenhouse effect. Limits environmental damage

e) The digestate:

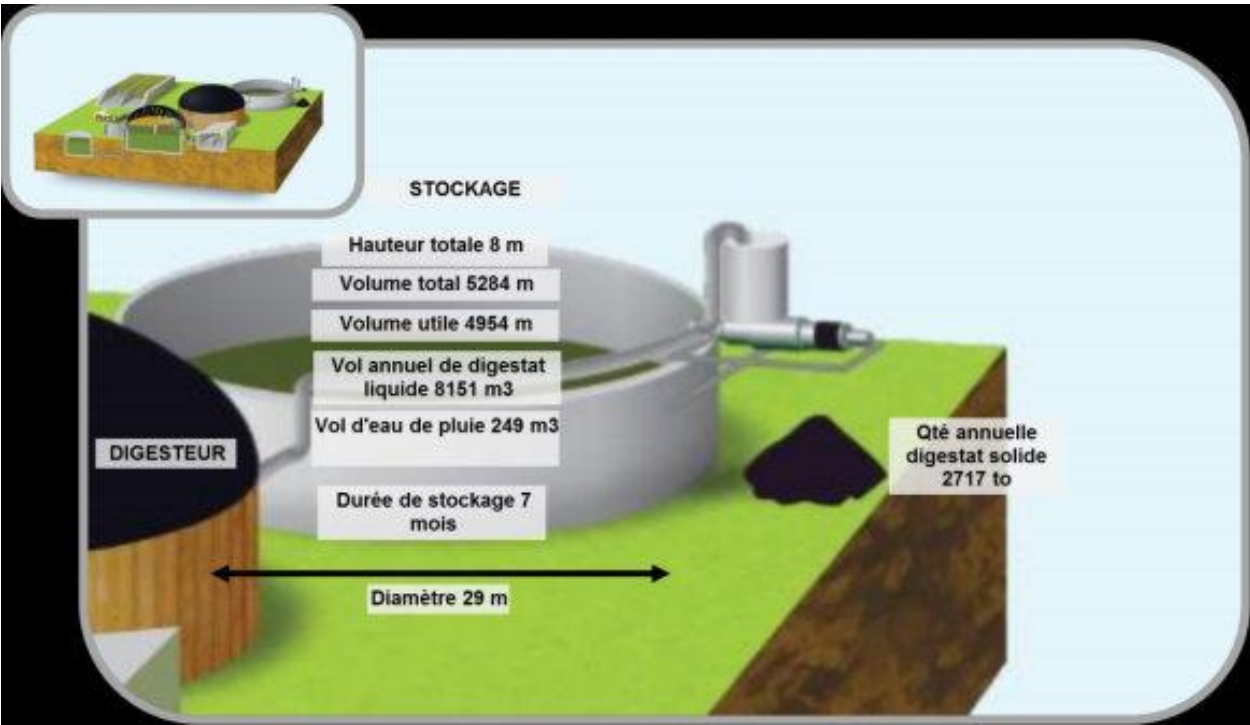
Deodorize, olfactory nuisance is destroyed in the digester.

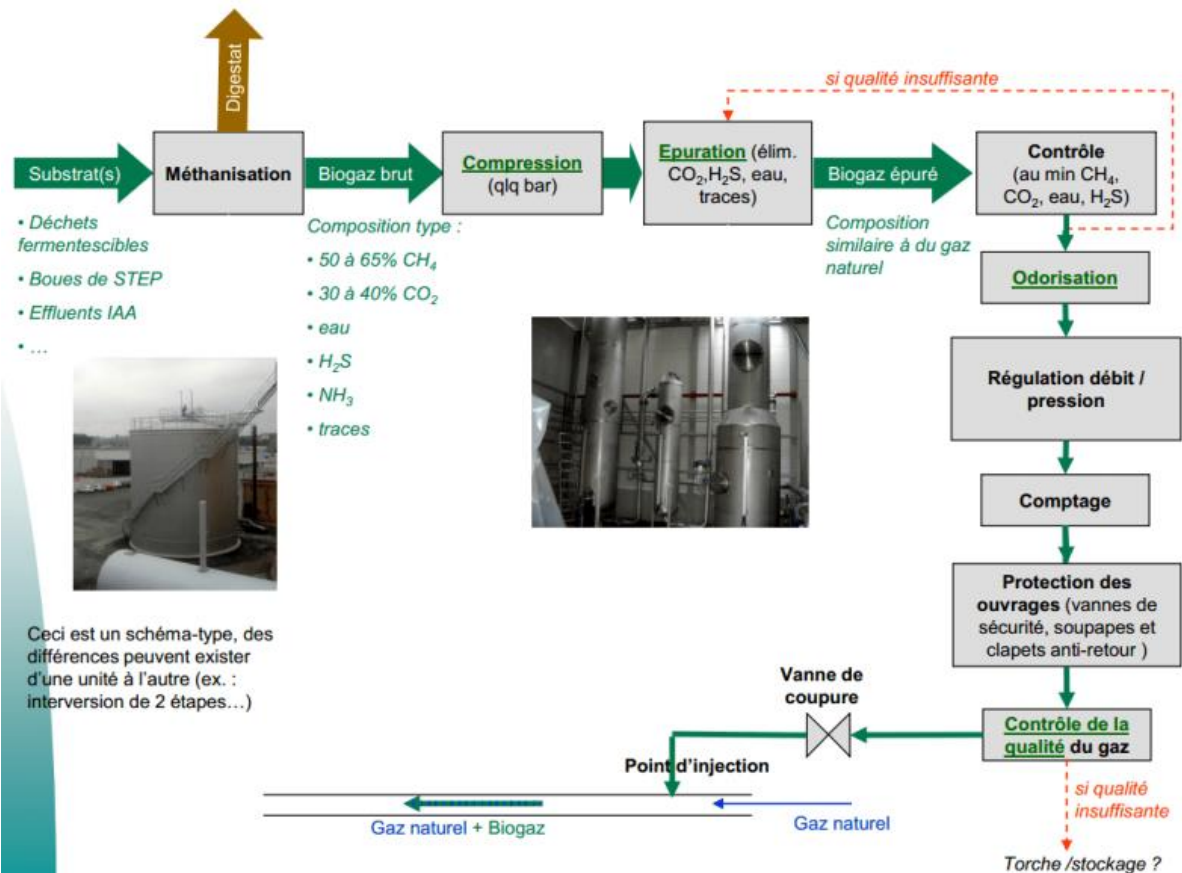
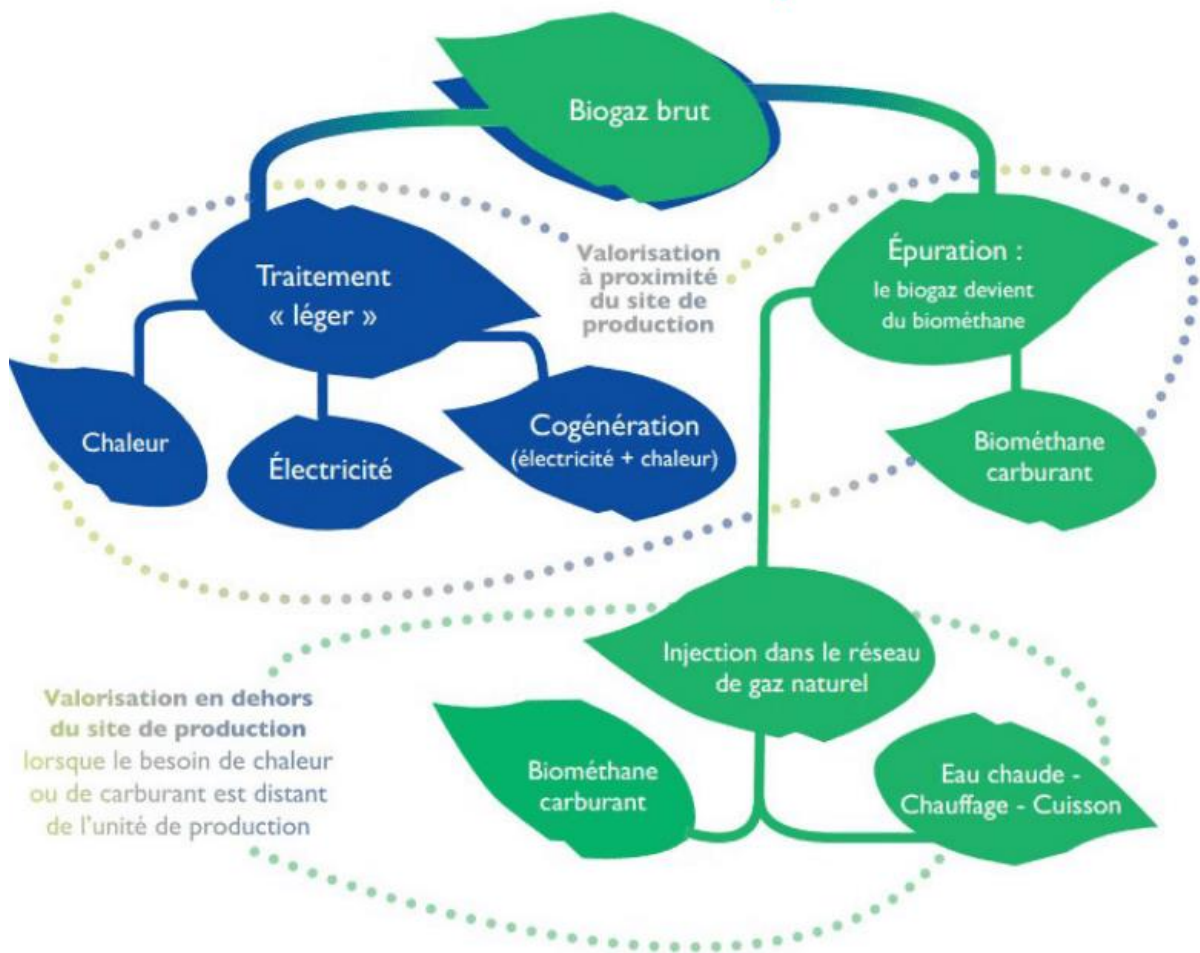
Its fertilizer value is improved, the quantity of nutrients is preserved but the initially organic nitrogen is found in ammoniacal form.

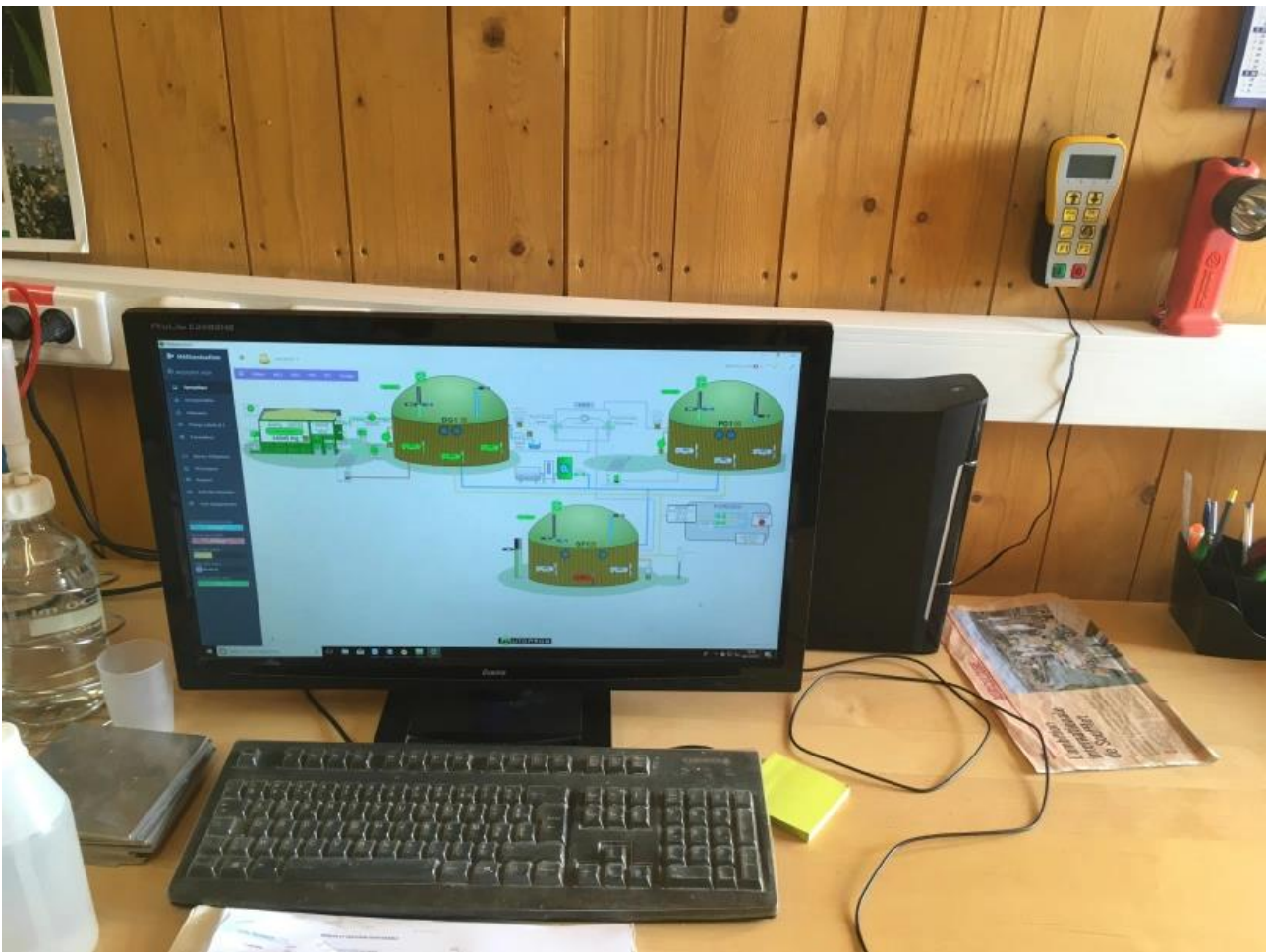
It is therefore assimilable for plants.

This spreading improves microbial activity and soil respiration compared to spreading manure or slurry.

Spreading is carried out using a dropper.







$$1 \text{ m}^3 = 9 \text{ Kwh}$$

$$V_{\text{total}} = \pi \times (r)^2 \times H = \pi \times (1500)^2 \times 2000 = 14.130$$

$$\rho_{\text{eau}} = \frac{m}{V}$$

$$m = \rho \cdot V = 1 \times 7065 = 7.065 \text{ kg}$$

$$\rho_w = \frac{m}{V}$$

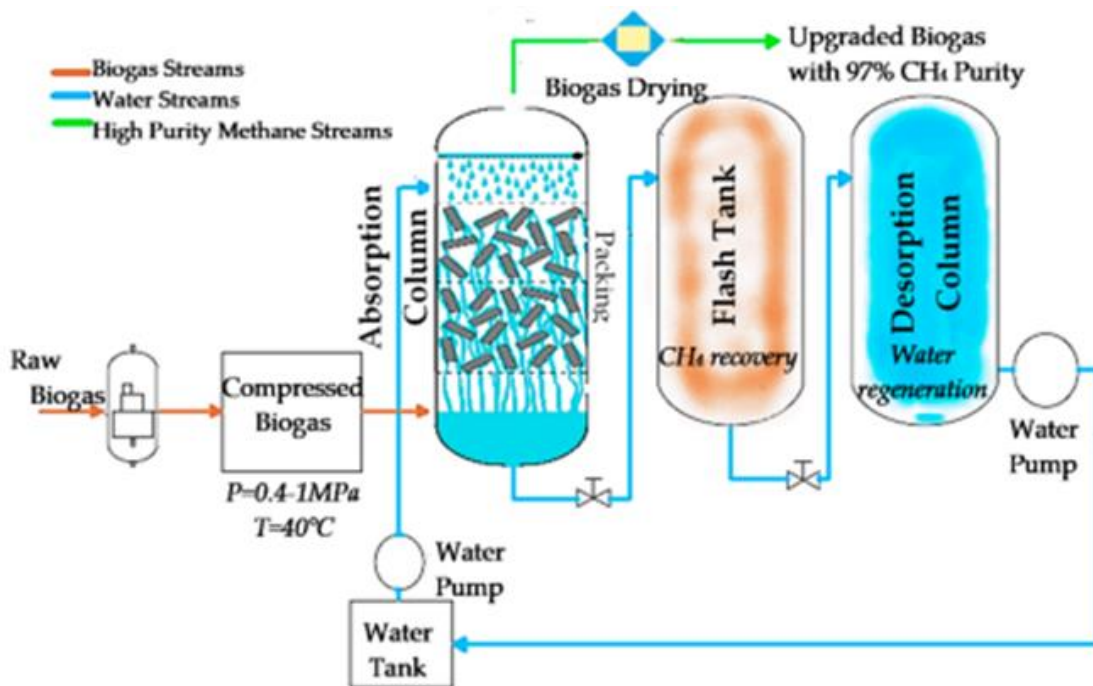
$$m = \rho \times V = 1.5 \times 6065 \text{ kg}$$

$$m_t = m_{\text{water}} = m_{\text{liquid}} = 7065 + 10600 = 17.665 \text{ kg}$$

Flygt 4460	Puissance nominale 50 Hz	Diamètre de l'hélice	Poussée 50 Hz	Installation
Semi rapide	7,5 kW	1,25 m	2860 N	Système de support biogaz (BIS-1)
	12 kW	1,25 m	3650 N	
		1,0 m	2800 N	
Vitesse lente	5,7 kW	2,5 m	3850 N	Tripode

6) Features of the agitator

a) Gas separation



b) Physical Scrubbing

- Working Principle

- CO₂ is more soluble than CH₄ according to Henry's law.
- Raw biogas flow through a counter flow of a liquid in a column.
- Liquid absorb CO₂ leaving biogas with high content of CH₄.

- Type of liquid

- Water for water scrubbing.
- Polyethylene glycol (PEG) / selexol and Genenrob for organic scrubbing.

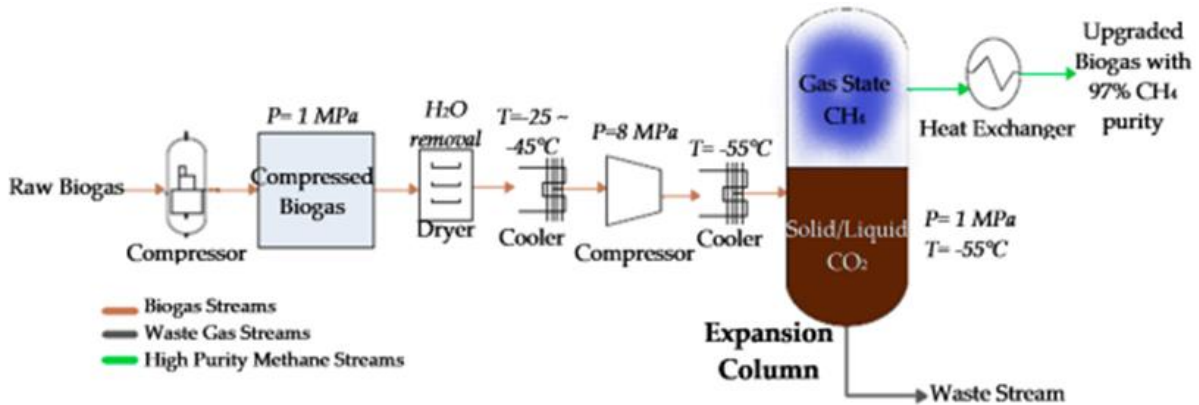
- System upgrading

- Absorption column filled with packing material to increase mass transfer.
- Flash tank installed to recover trace of CH₄.
- Water/PEG regeneration to remove CO₂ for reuse purpose.

- Advantages

- Simple process
- High methane purity
- Less methane loss.

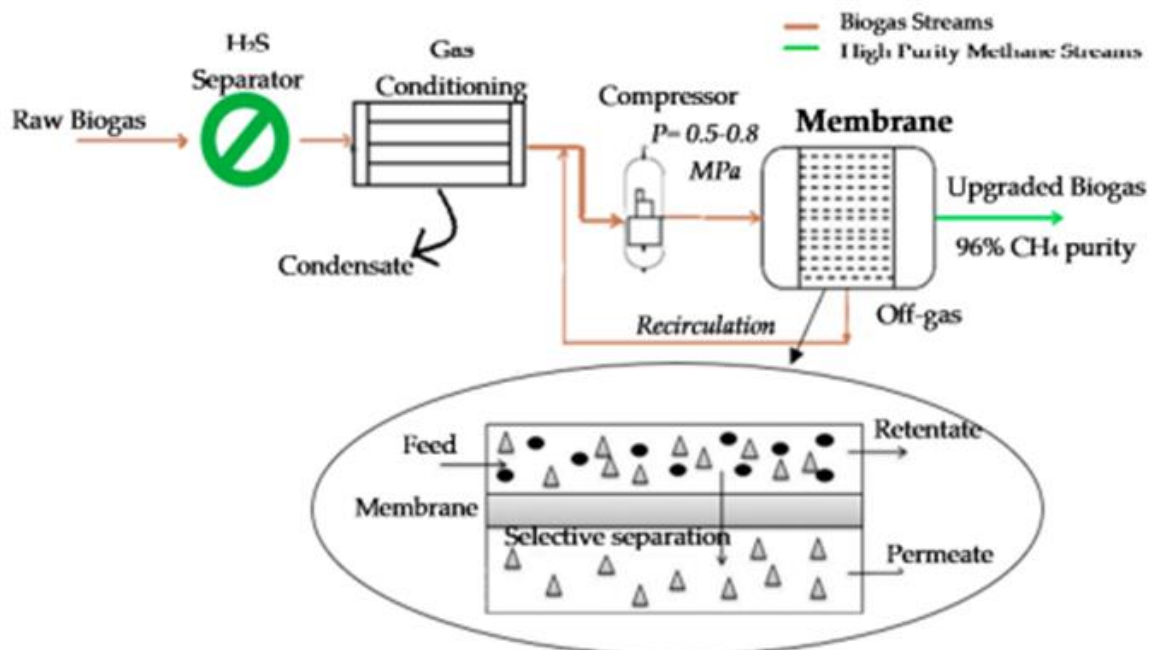
- Low operation and maintenance cost.
 - Disadvantages
- Required huge amount of water.
- High energy needed
- Chances of biological contamination.
- Required external heat.



c) Cryogenic separation:

- Working Principle
 - Different gases condense at different temperature-pressure domains.
 - Boiling point of CO₂ was higher than the CH₄ thus allowing the separation.
 - Biomethane produced by gradual decrease of temperature and compressing the biogas.
 - Equipment: compressor-turbine-heat exchanger and cooler.
- Post treatment
 - Final product is in accordance with the quality standards for liquefied natural Gas (LNG).
 - Further cooling for purification will produce liquid Biomethane (LBM).
- Advantages
 - High gas quality
 - Low methane losses
 - Environmentally friendly
 - Produce LBM with low extra-energy
- Disadvantages
 - High investment operational cost

- Pre-treatment needed
- High energy required for cooling
- Technology is still under development.



d) Membrane separation

- Working Principle

- Separation of biogas components using membrane as permeable material.
- The selection of permeability properties of membrane is crucial.
- Ascending order of permeation rate: CH₄, CO₂, H₂S, N₂ and H₂O.

- Separation techniques

- Gas-gas separation(dry)
 - H₂S and oil vapors were first removed.
 - Biogas is pressurized and injected into membrane.
- Gas-liquid separation (wet)
 - Liquid and gases separated by membrane.
 - Impurity is the gases absorbed by the counter current flows of liquid.

- Increasing efficiency

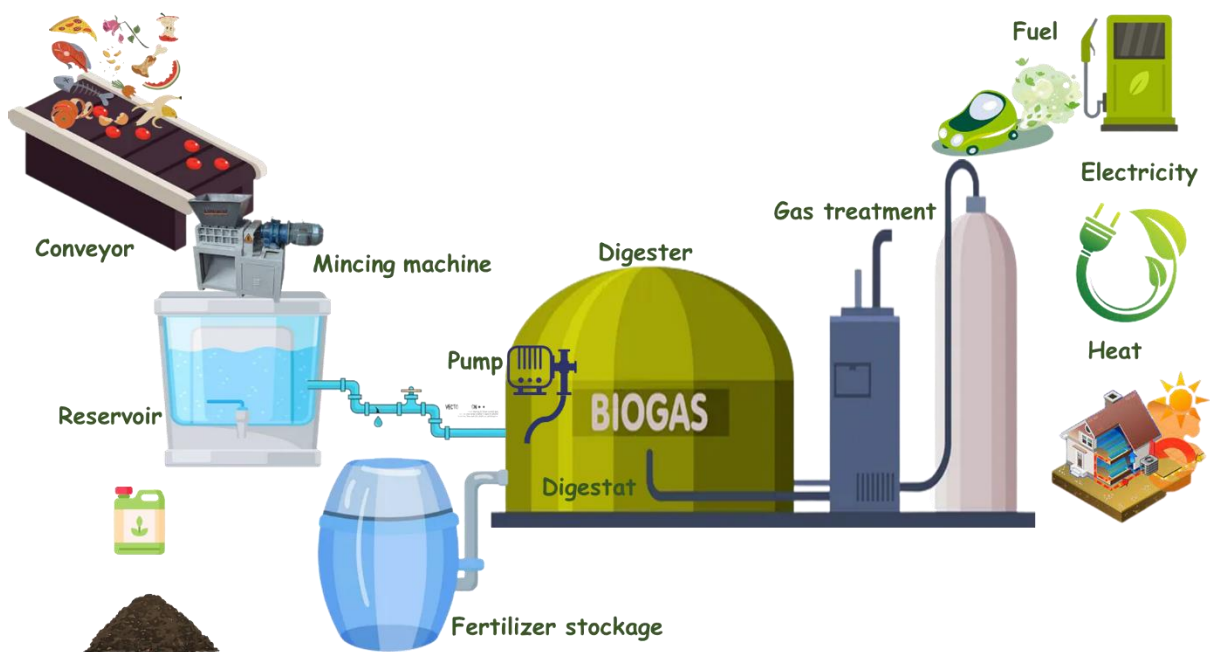
- Enhanced the CH₄ purity by using two or three stage performance.
- Ideal membrane must have high permeability difference between CO₂ and CH₄.

- Advantages

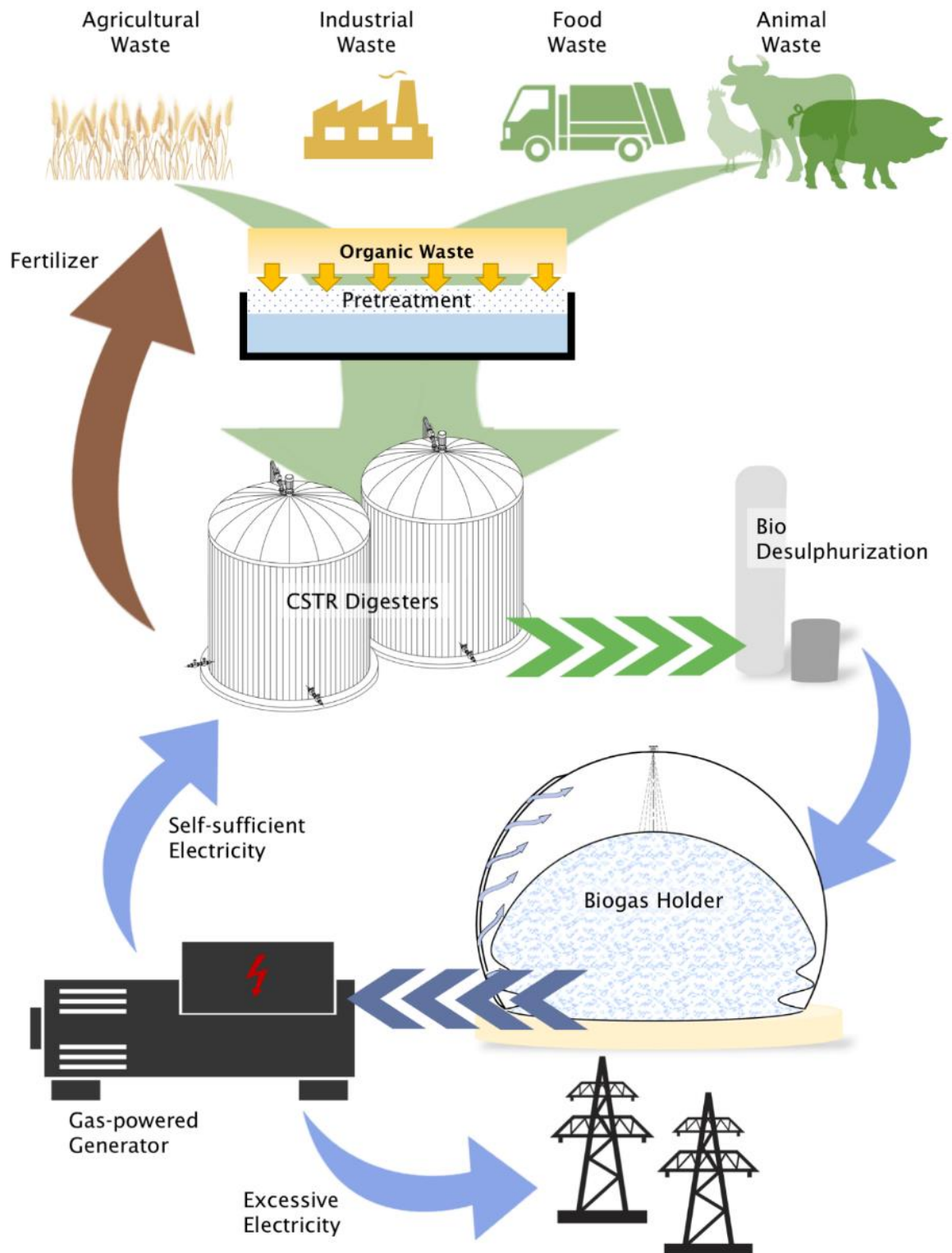
- Environmentally friendly
- Low energy consumption
- Low cost
- Simple process

- Disadvantages

- Low membrane selectivity
- Pre-treatment necessary
- Low CH₄ purity



5.3. Biogas production from municipal waste

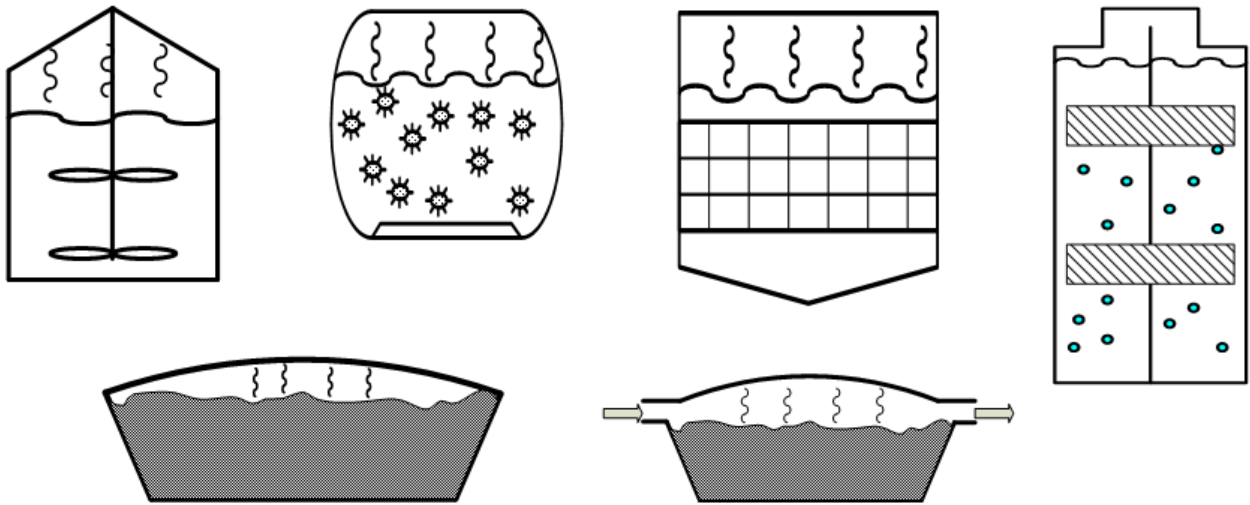


5.4. WET DIGESTION

The process is considered wet digestion when the content of the digester is pumpable. That means that the material inside the digester has a consistency of approximately 10% dry matter or less (90% water).

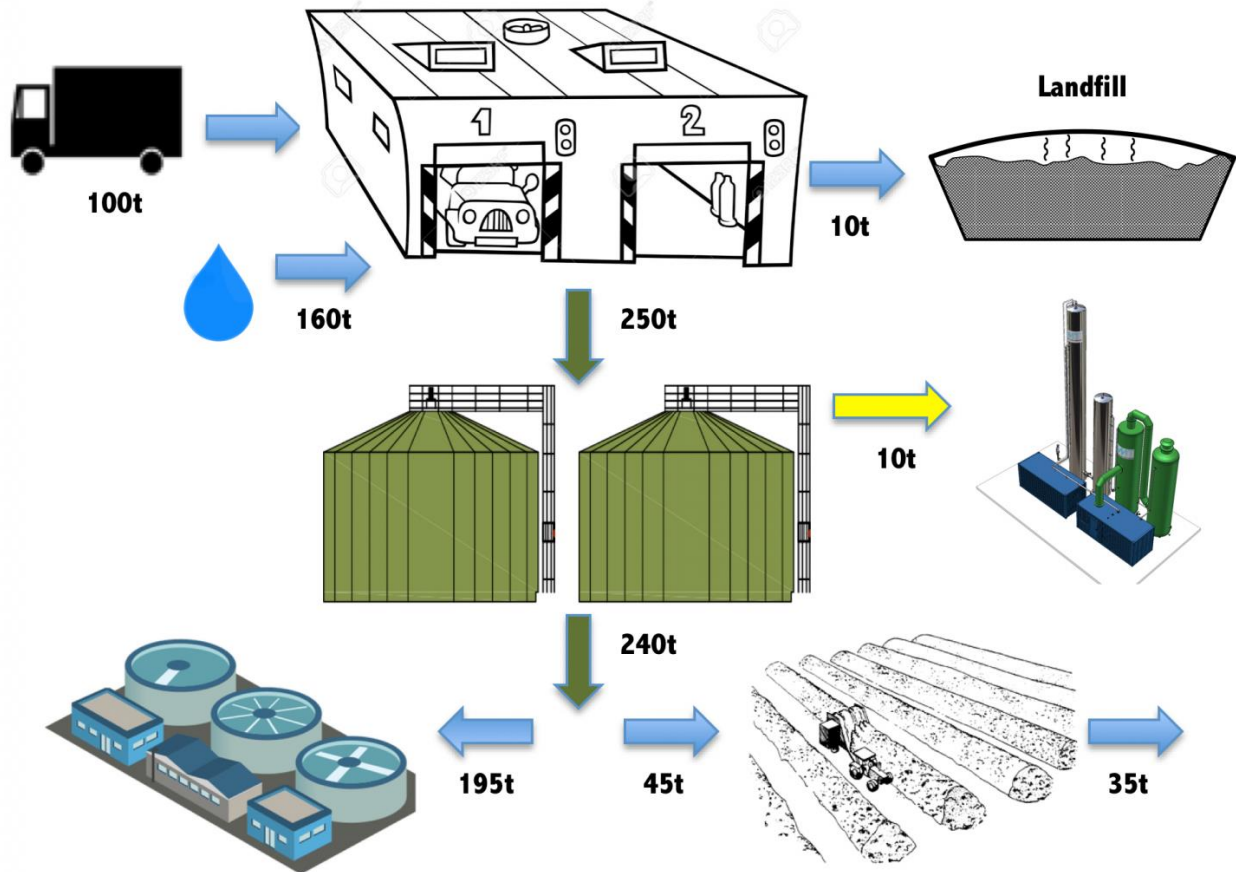
There exist many configurations of **wet digesters**:

- Complete mix or Completely stirred tank reactor (CSTR)
- Plug-flow
- Upflow Anaerobic Sludge Blanket (UASB)
- Fixed film reactor
- Floating films reactors
- Sludge bed reactors
- And more.



These configurations have been designed to optimize the process for various feedstock conditions and market applications.

The mass balance of a typical wet digestion process looks like this:



For example, 100 tons of solid municipal residential source separated organics (SSO) arrives at the biogas plant using wet digestion (complete mix). This feedstock needs to be pretreated to remove potential contaminants (plastics, metal, sands, etc.). Approximately 10 tons will be removed as contaminants and will probably be landfilled.

In order to be pumpable (10% TS), the feedstock will be diluted with water that may come from a fresh source or from a mixed of fresh and recycled water from the wastewater portion of the biogas plant. The liquid feedstock going to the digester will be approximately 250 tons.

In the digesters, the bacteria will consume the majority of the volatile solids in the feedstock and will convert them into biogas. Approximately 10 tons of gas will come out of the digesters. The more liquid digestate will represent approximately 240 tons.

At this point, the digestate may be applied to land directly. Please note that 100 tons of solid material turned into 240 tons of liquid and land applying the digestate in this form will present significant transportation costs.

The digestate may also be separated into a solid fraction (45 tons) to be land applied (or composted down to 35 tons) and a liquid fraction (195 tons) to be returned the sanitary sewage or directly back to nature.

One may be tempted to use the treated wastewater as dilution water for the input feedstock and limit the amount of water consumed and rejected by the process. It is possible only if the wastewater plant removes almost all nutrients (salts and ammonia/ammonium) in the water. Without this removal, there will be a rapid buildup of nutrients in the water and this will inhibit and/or kill the anaerobic digestion process.

The digester must meet the following requirements:

Requirements

No matter which design is chosen, the digester (fermentation tank) must meet the following requirements:

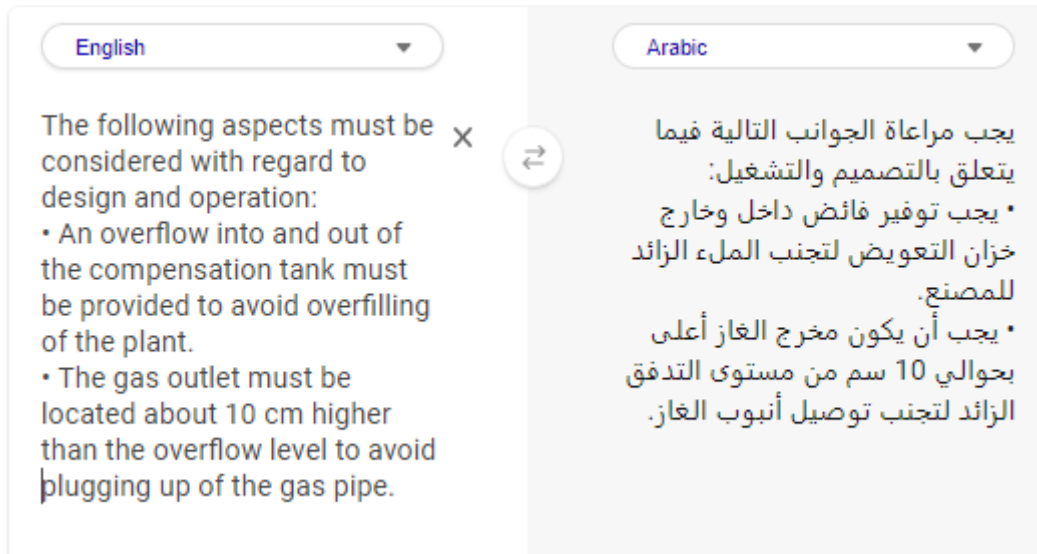
- **Water/gas-tightness** - watertightness in order to prevent seepage and the resultant threat to soil and groundwater quality; gas-tightness in order to ensure proper containment of the entire biogas yield and to prevent air entering into the digester (which could result in the formation of an explosive mixture).
- **Insulation** - if and to which extent depends on the required process temperature, the local climate and the financial means; heat loss should be minimized if outside temperatures are low, warming up of the digester should be facilitated when outside temperatures are high.
- **Minimum surface area** - keeps cost of construction to a minimum and reduces heat losses through the vessel walls. A spherical structure has the best ratio of volume and surface area. For practical construction, a hemispherical construction with a conical floor is close to the optimum.
- **Structural stability** - sufficient to withstand all static and dynamic loads, durable and resistant to corrosion.]

بعض النظر عن التصميم الذي يتم اختياره ، يجب أن يفي الهاضم (خزان التخمر) بالمطلوبات التالية:

- **المياه / التفادية** - مقاومة الماء من أجل منع التسرب وما ينتج عن ذلك من تهديد لنوعية التربة والمياه الجوفية ؛ مقاومة النفاذية من أجل ضمان الاحتواء المناسب لكامل محصول الغاز الحيوي ولمنع دخول الهواء إلى الهاضم (مما قد يؤدي إلى تكوين خليط متفجر).
- **العزل** - إذا كان وإلى أي مدى يعتمد على درجة حرارة العملية المطلوبة ، والمناخ المحلي والوسائل المالية ؛ يجب تقليل فقد الحرارة إلى أدنى حد إذا كانت درجات الحرارة الخارجية منخفضة ، ويجب تسهيل تسخين الهاضم عندما تكون درجات الحرارة الخارجية مرتفعة.
- **الحد الأدنى من مساحة السطح** - يحافظ على تكلفة البناء إلى أدنى حد ويقلل من فقد الحرارة عبر جدران الوعاء. يحتوي الهيكل الكروي على أفضل نسبة من حيث الحجم ومساحة السطح. بالنسبة للبناء العملي ، فإن البناء النصف كروي بأرضية مخروطية يكون قريباً من المستوى الأمثل.
- **الاستقرار الهيكلي** - كافٍ لتحمل جميع الأحمال الساكنة والديناميكية ، ودائم ومقاوم للتآكل.

يجب مراعاة الجوانب التالية فيما يتعلق بالتصميم (والتشغيل)

والتشغيل



5.5. System concept / system design

1) Raw materials for biogas production

Although, cattle dung has been recognized as the chief raw material for biogas plants, other materials like night-soil, poultry litter and agricultural wastes can also be used.

2) Advantages of biogas production

- It is a eco-friendly fuel.
- The required raw materials for biogas production are available abundantly in villages.
- It not only produces biogas, but also gives us nutrient rich slurry that can be used for crop production.
- It prevents the health hazards of smoke in poorly ventilated rural households that use dung cake and fire-wood for cooking.
- It helps to keep the environment clean, as there would be no open heap of dung or other waste materials that attract flies, insects and infections
- Availability of biogas would reduce the use of firewood and hence trees could be saved.

3) Components of biogas plants

- **Mixing tank** - The feed material (dung) is collected in the mixing tank. Sufficient water is added and the material is thoroughly mixed till a homogeneous slurry is formed.
- **Inlet pipe** - The substrate is discharged into the digester through the inlet pipe/tank.
- **Digester** - The slurry is fermented inside the digester and biogas is produced through bacterial action.
- **Gas holder or gas storage dome** - The biogas gets collected in the gas holder, which holds the gas until the time of consumption.
- **Outlet pipe** - The digested slurry is discharged into the outlet tank either through the outlet pipe or the opening provided in the digester.
- **Gas pipeline** - The gas pipeline carries the gas to the point of utilization, such as a stove or lamp.

4) Points to be considered for construction of a biogas plant

a) Site selection

- While selecting a site for a biogas plant, following aspects should be considered
- The land should be levelled and at a higher elevation than the surroundings to avoid water stagnation
- Soil should not be too loose and should have a bearing strength of 2 kg/cm²
- It should be nearer to the intended place of gas use (eg. home or farm).
- It should also be nearer to the cattle shed/ stable for easy handling of raw materials.
- The water table should not be very high.
- Adequate supply of water should be there at the plant site. The plant should get clear sunshine during most part of the day.
- The plant site should be well ventilated.
- A minimum distance of 1.5m should be kept between the plant and any wall or foundation.
- It should be away from any tree to prevent root interference.
- It should be at least 15m away from any well used for drinking water purpose.

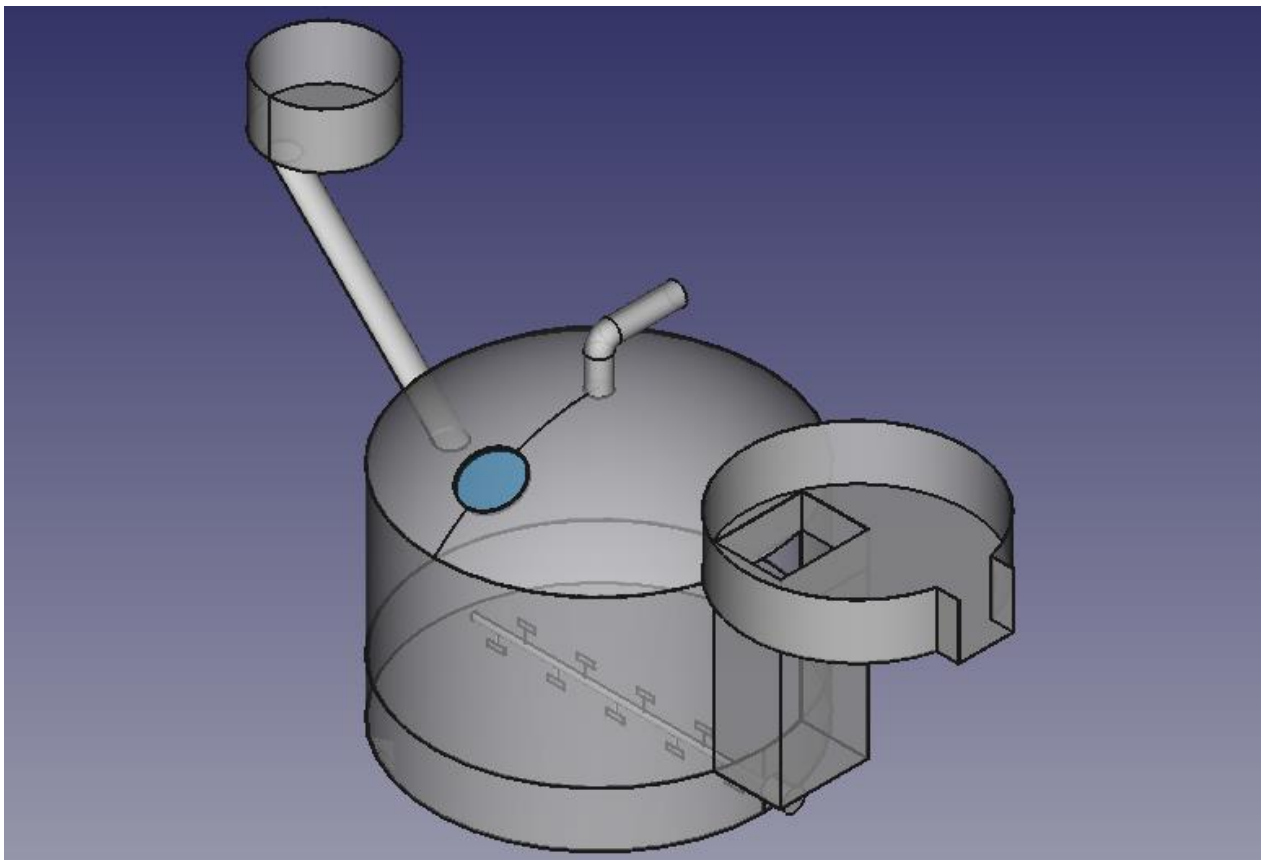
b) Availability of raw materials

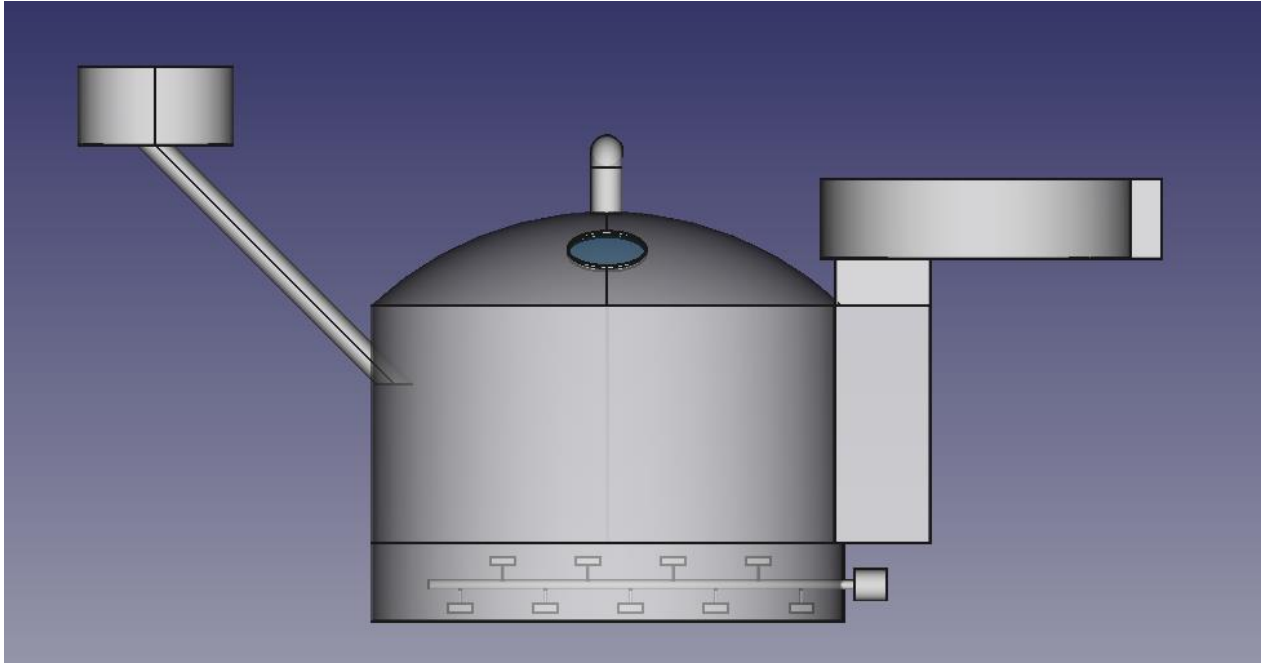
The size of the biogas plant is to be decided based on availability of raw material.

5.6. 18.10.2022 – Proposal FreeCAD design



18102022_Biogas
plant prototype des



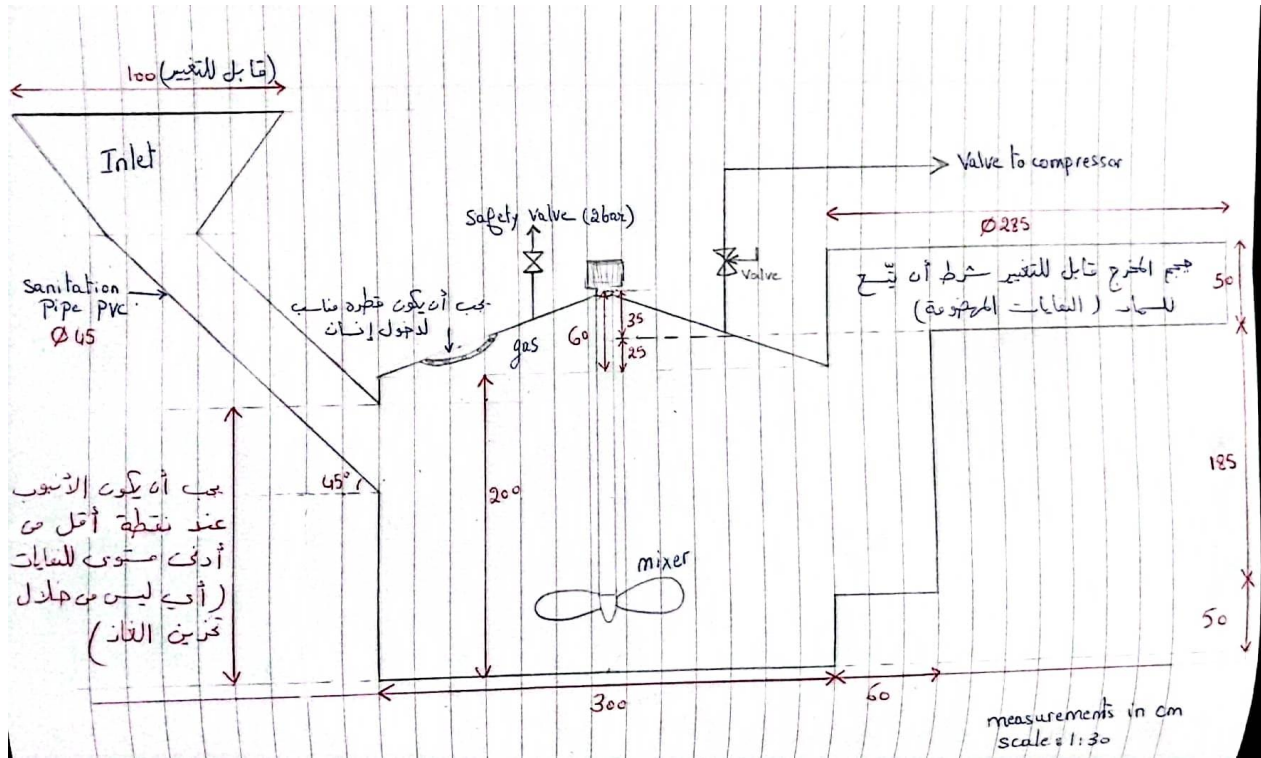


5.7. Design notes

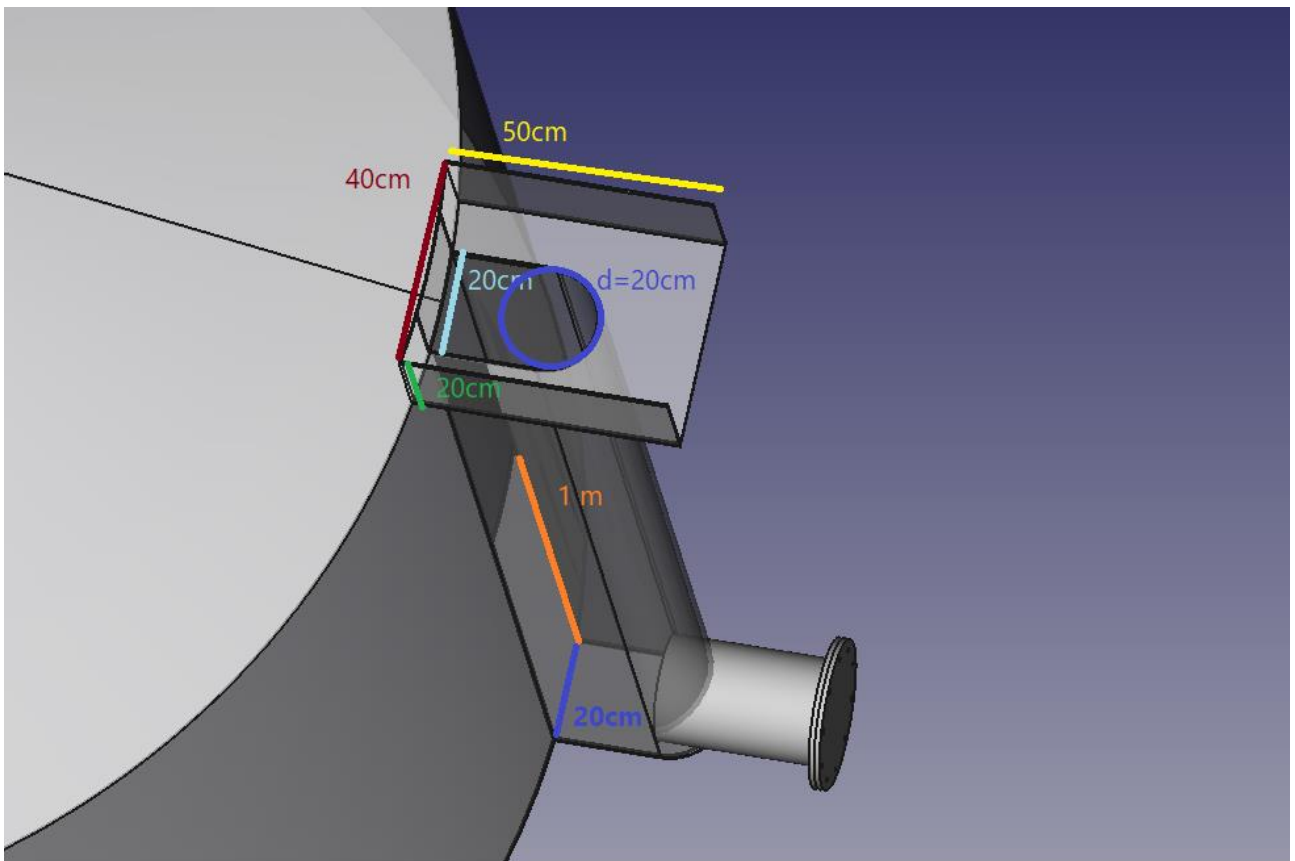
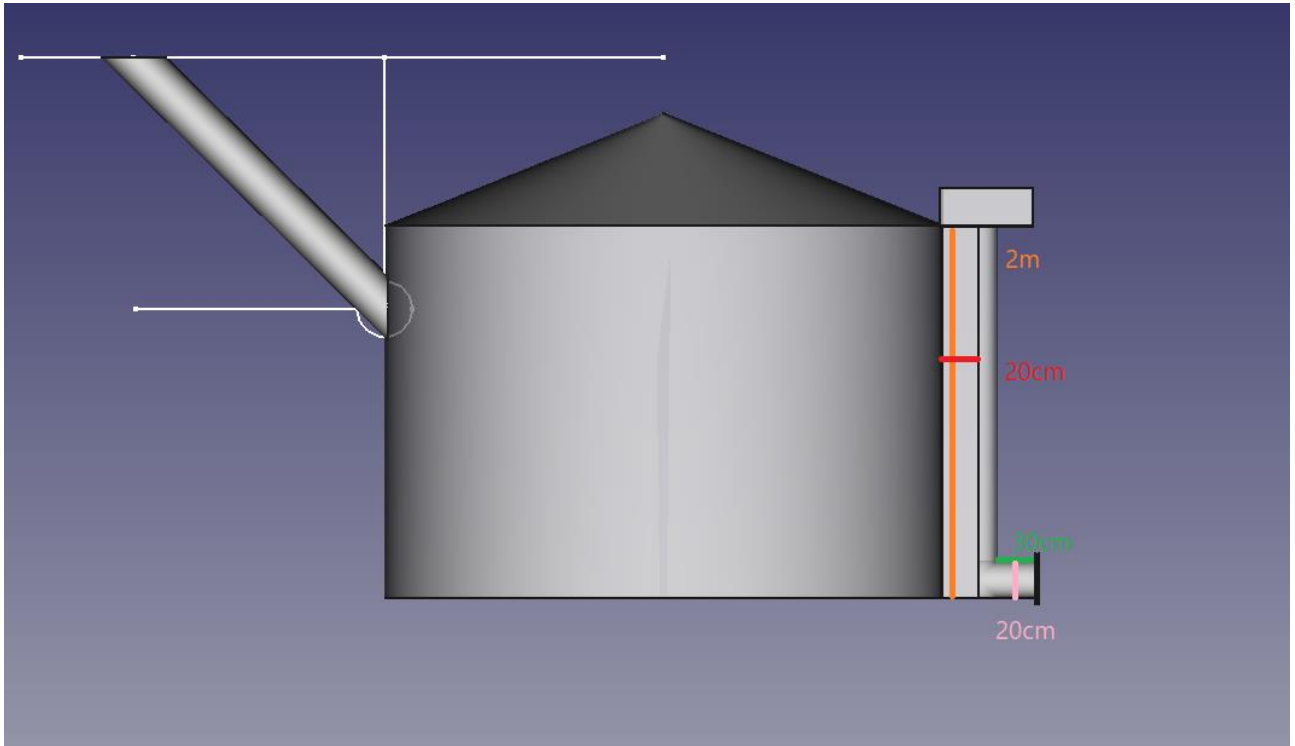
- The inlet pipe lead straight into the digester at a steep angle.
- يجب أن يخترق أنبوب المدخل جدار الهاضم عند نقطة أقل من أدنى مستوى للنفايات (أي ليس من خلال تخزين الغاز).
- يجب إغلاق نقاط الاختراق جيداً منعاً للتسرب.
- ينتهي أنبوب المدخل أعلى في الهاضم من أنبوب المخرج.
- يمكن أن يكون خزان النفايات المهضومة مفتوحاً أو مغلقاً و متصلاً بحامل الغاز لالتقاط إنتاج الغاز المتبقي.
- يمكن تجنب مشاكل التآكل إذا تم استخدام خزان من stainless-steel. سمك اللوح لخزان الغاز الحيوي أقل من 5mm.
- يمكن تشغيل النظام ذاتياً من خلال عملية الهضم الطاردة للحرارة (the exothermic digestion process)، على الرغم من أنه عادة ما يتم توفير حرارة إضافية عن طريق حرق بعض الغاز الحيوي.
- يتم تحسين الهضم عن طريق الحفاظ على درجة الحرارة عند حوالي 40 درجة مئوية، و مستوى PH بين 5.5 و 8.5
- يمكن أن يساعد الموقع المشمس في تدفئة المحتويات قبل إدخالها في الهاضم لتجنب الصدمة الحرارية بسبب مياه الخلط الباردة.
- يؤدي تشغيل أنظمة الهضم اللاهوائي ذات الحالة الصلبة في الظروف المحبة للحرارة (thermophilic conditions) (55-65°C) إلى تسريع عملية الهضم اللاهوائي و توفير فائدة إضافية تتمثل في زيادة قتل مسببات الأمراض خلال مرحلة اللاهوائية.
- the digestion process will stabilize more quickly if the slurry is agitated frequently and intensively. Only if the process shows extreme resistance to stabilisation should lime be added in order to balance the PH value.
- No additional biomass should be put into the biogas plant during the remainder of the starting phase.
- Optimum stirring substantially reduces the retention time. If agitation is excessive, the bacteria have "no time to

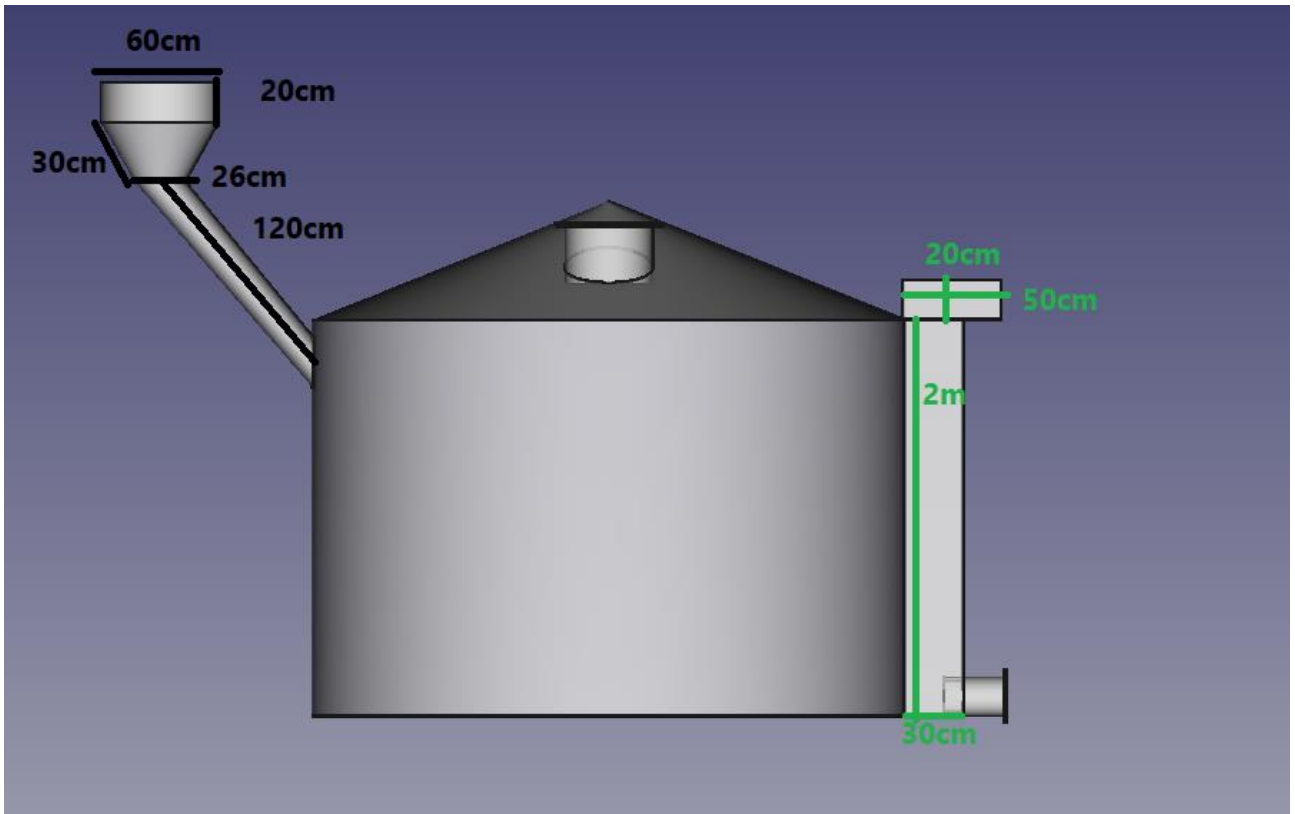
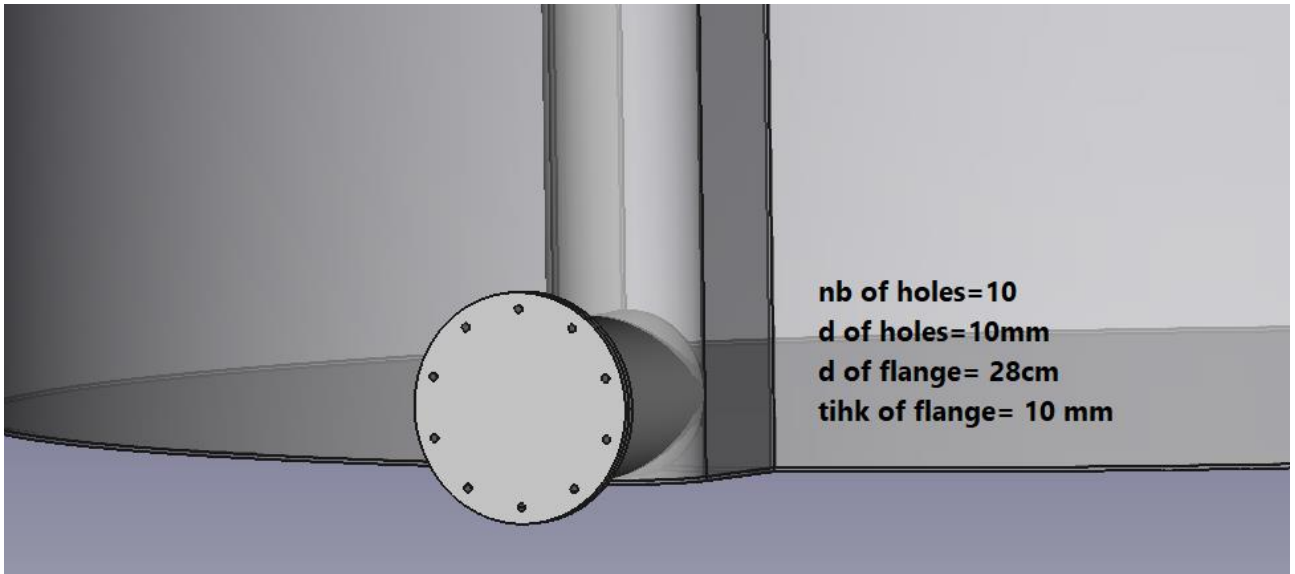
eat". The ideal is gentle but intensive stirring about every four hours.

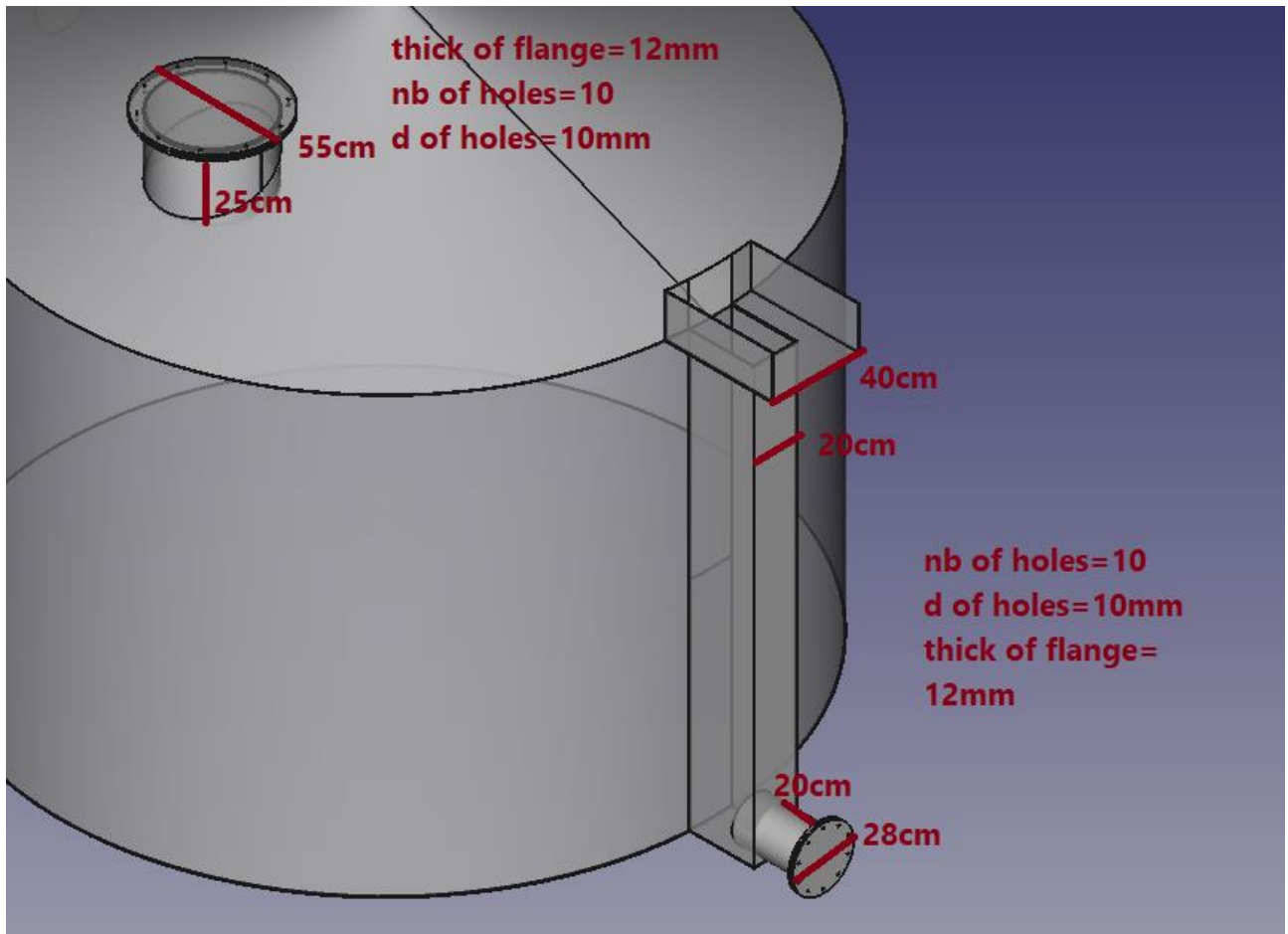
- يجب أن يتكون الملاء الأولي لمصنع جديد للغاز الحيوي، إن أمكن، إما من ملاط مهضوم من مصنع آخر أو روث الماشية.
- عمر و كمية المدخلات لها تأثير كبير على مسار التخمير. من المستحسن البدء في جمع روث الماشية خلال مرحلة البناء من أجل الحصول على ما يكفي بحلول الوقت الذي يتم فيه الانتهاء من المصنع.
- يجب تنفيس أول حشوتين من حامل الغاز دون استخدام لأسباب تتعلق بالسلامة، لأن الأكسجين المتبقي يشكل خطر الانفجار.
- عندما يتم ملء الهاضم لأول مرة، يمكن تخفيف الركيزة بماء أكثر من المعتاد للسماح بملء كامل للهاضم.



5.8. Update design - Version 11-12.11.22







5.9. Mechanical Realization

1) Main Fermenter





2) Outlet

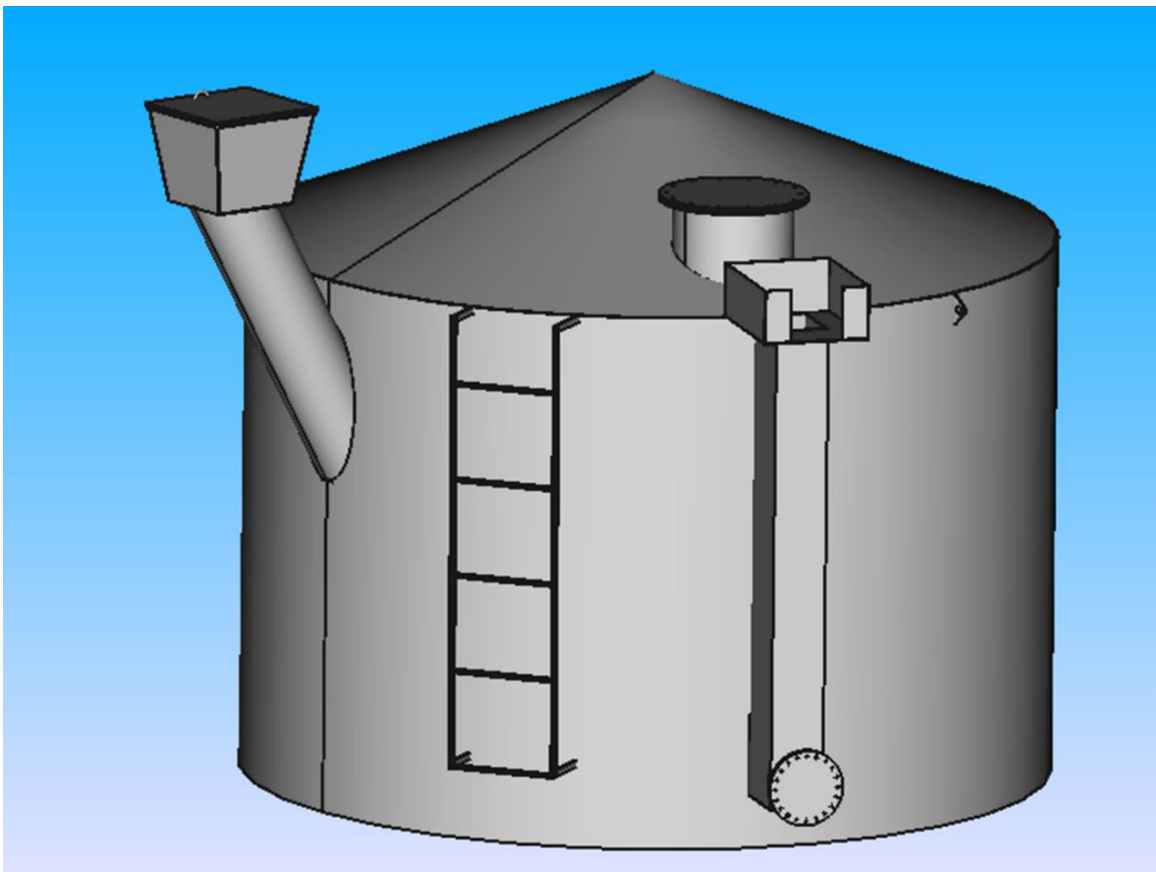
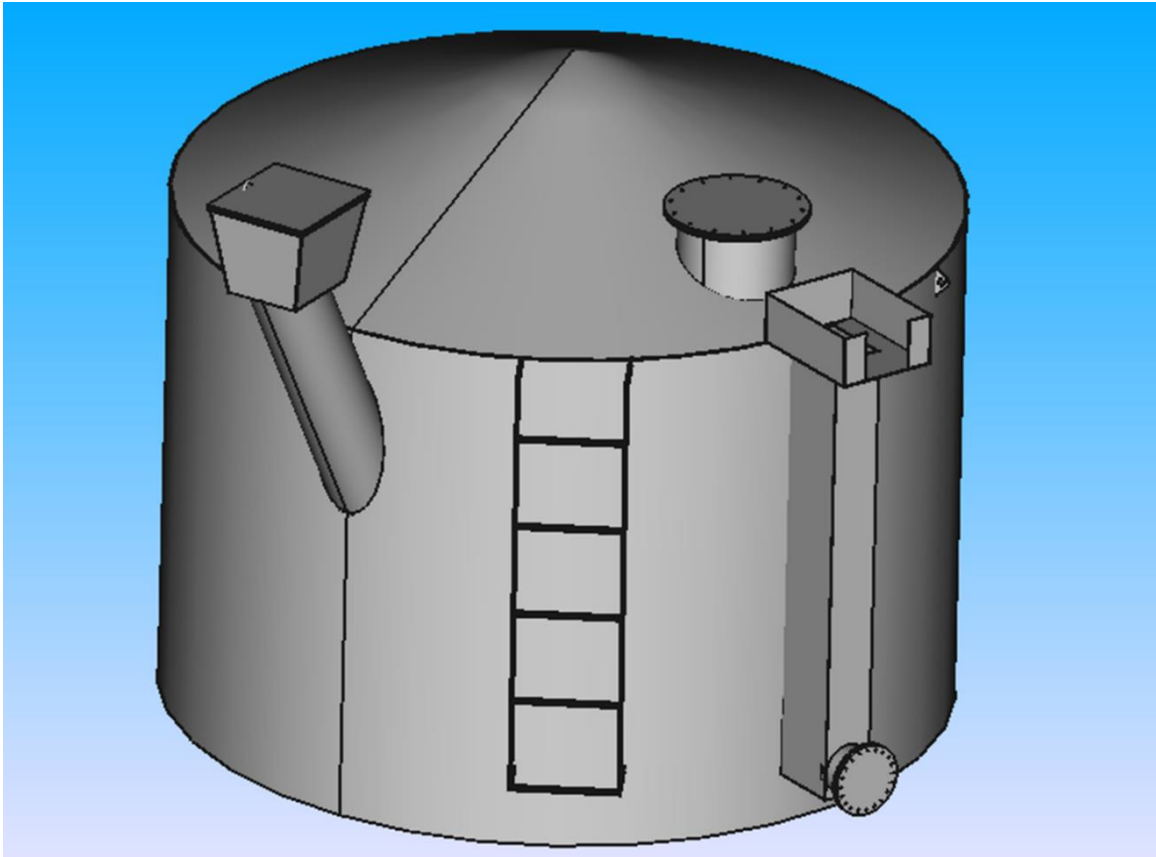


3) Flanges



5.10. Real design

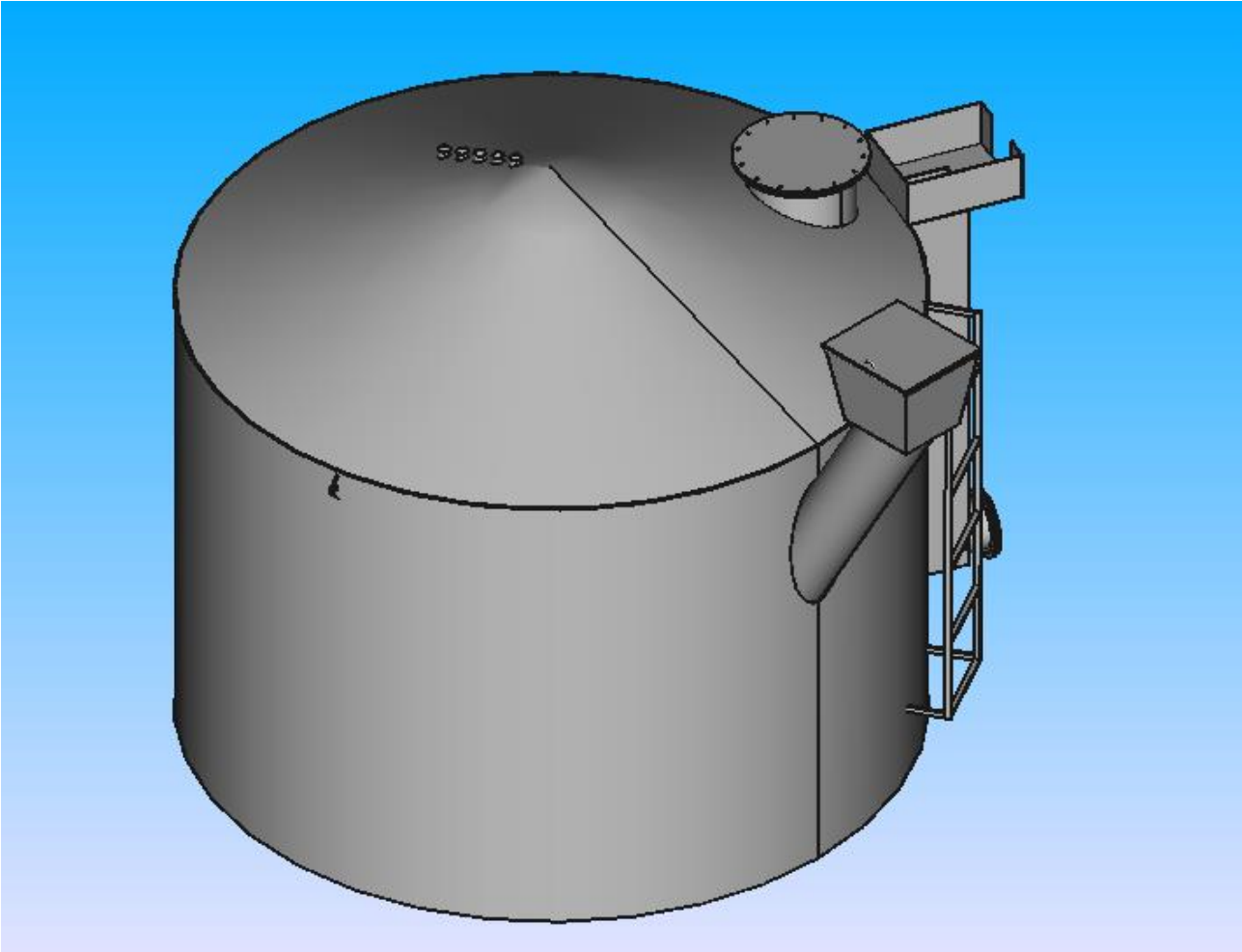
The final design of the biogas prototype

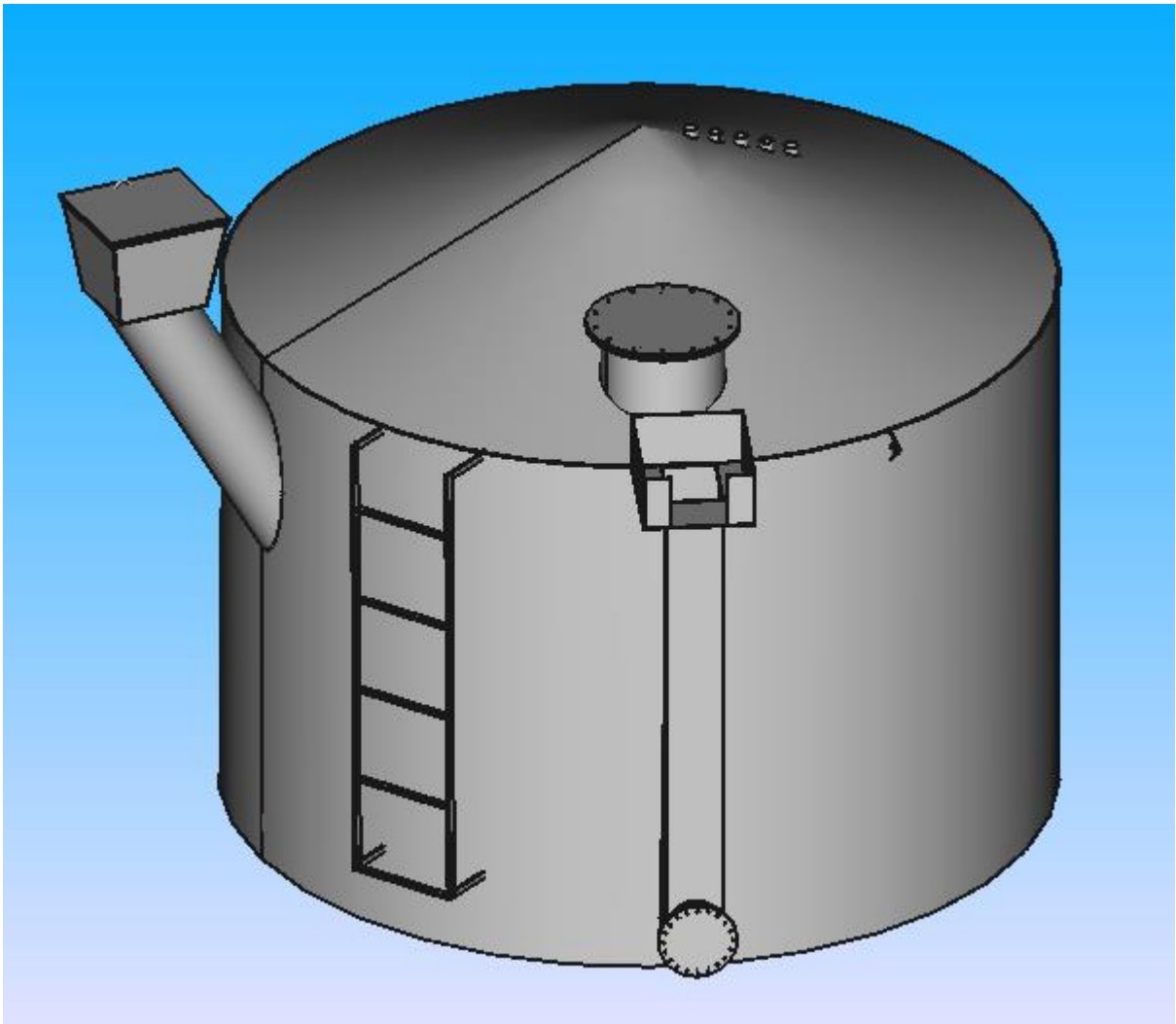


- With sensors holes:



30122022_Bio Gas
FreeCAD design.FCS





5.11. What's next

In this project, after completing the installation of the sensors, we will start with the necessary procedures for operation.

Project 6: Gas Turbine for Methane gas (ICPT – GTM)

6.1. Position of Gas turbine project

This project is divided into two parts: the fuel burner and the gas turbine. Work has been done on the fuel burner section in the past years, this year the stand was manufactured for the burner only. While the focus was on the gas turbine, the project was studied theoretically, and a preliminary design of the gas turbine was developed.

6.2. Relationship between gas turbine and fuel burner

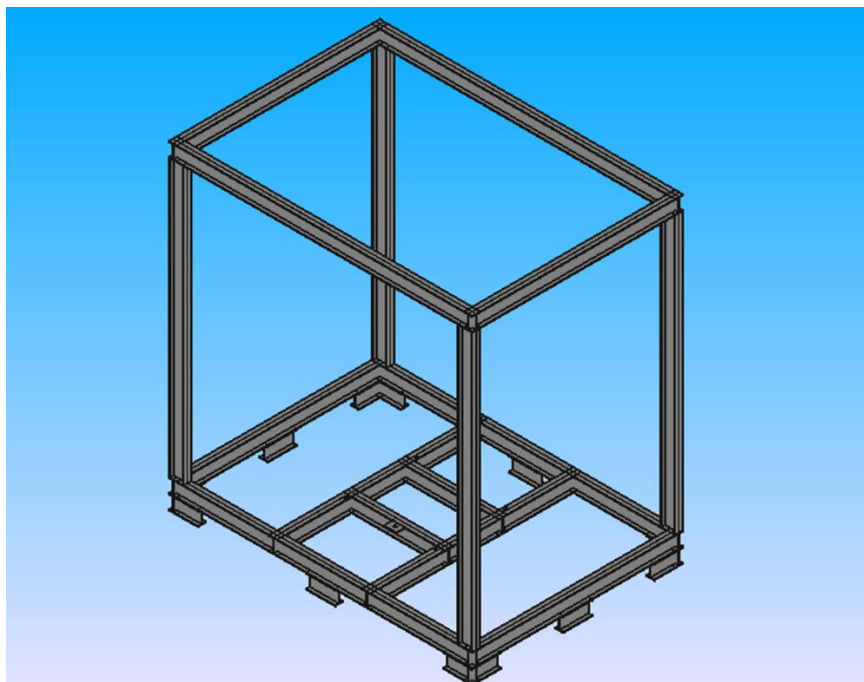
The burner burns gases (hydrogen, natural gas, ...) with oxygen. At the exit of the burner, a gas turbine will be installed in order to adjust the path of the flame formed as a result of combustion. The gas turbine also seeks to regulate combustion and thus regulate the flame.

6.3. Fuel Burner Testrig

1) FreeCAD design of fuel burner stand



21112022_FB -
stand.FCStd

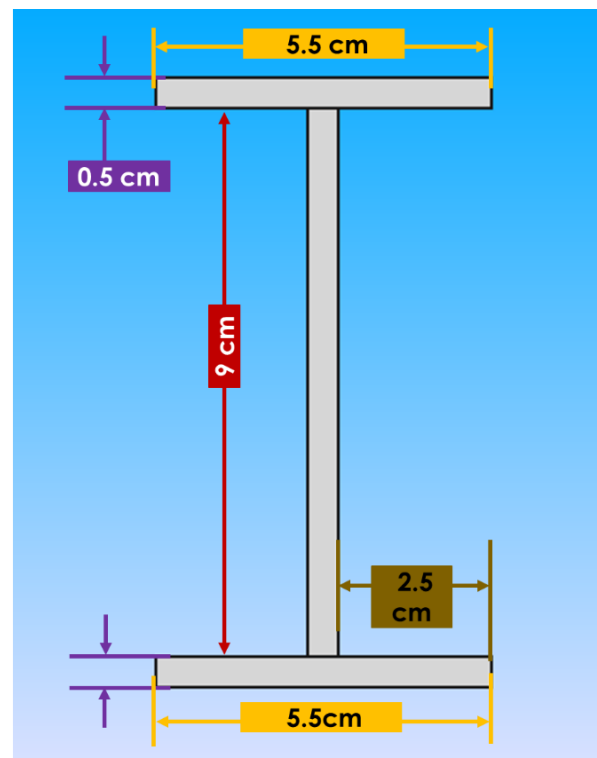
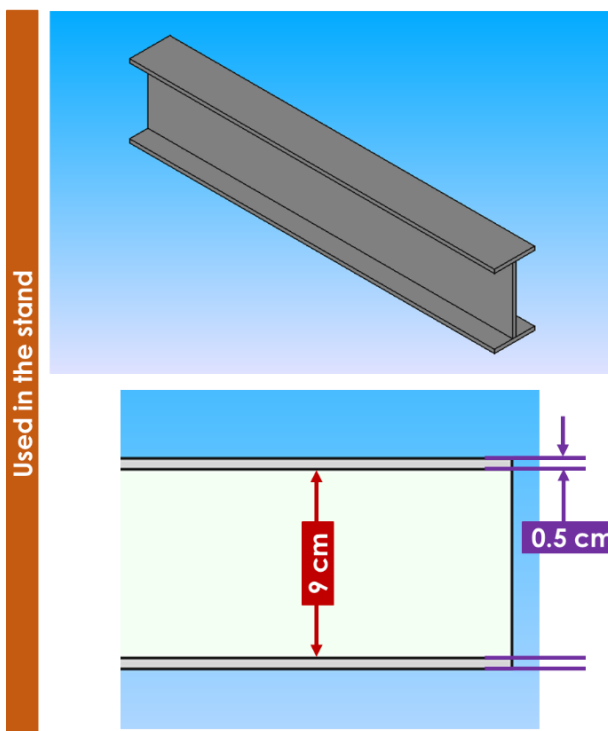
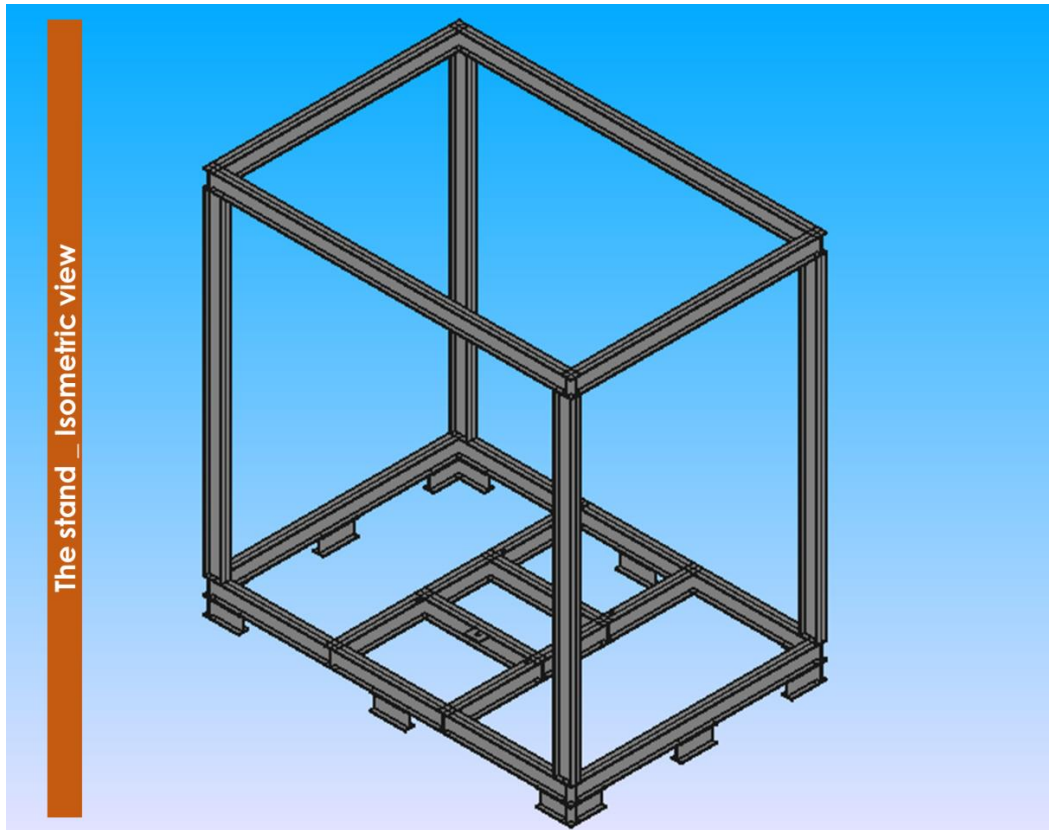


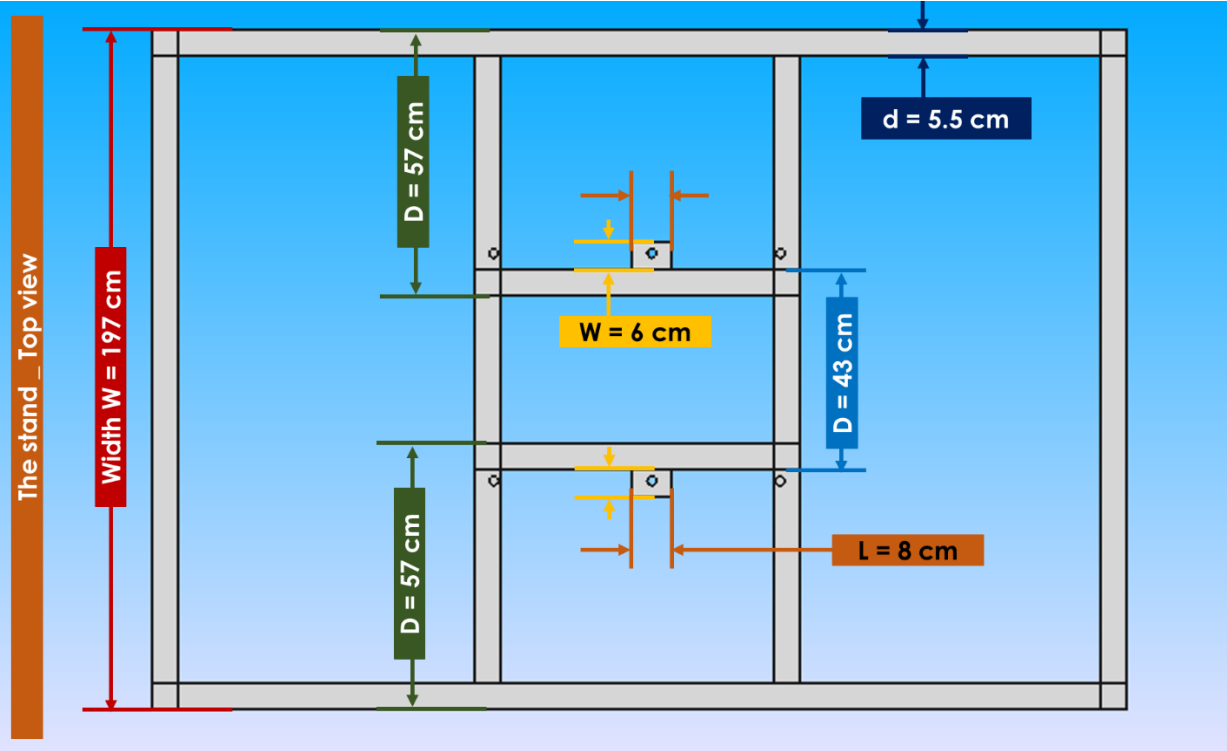
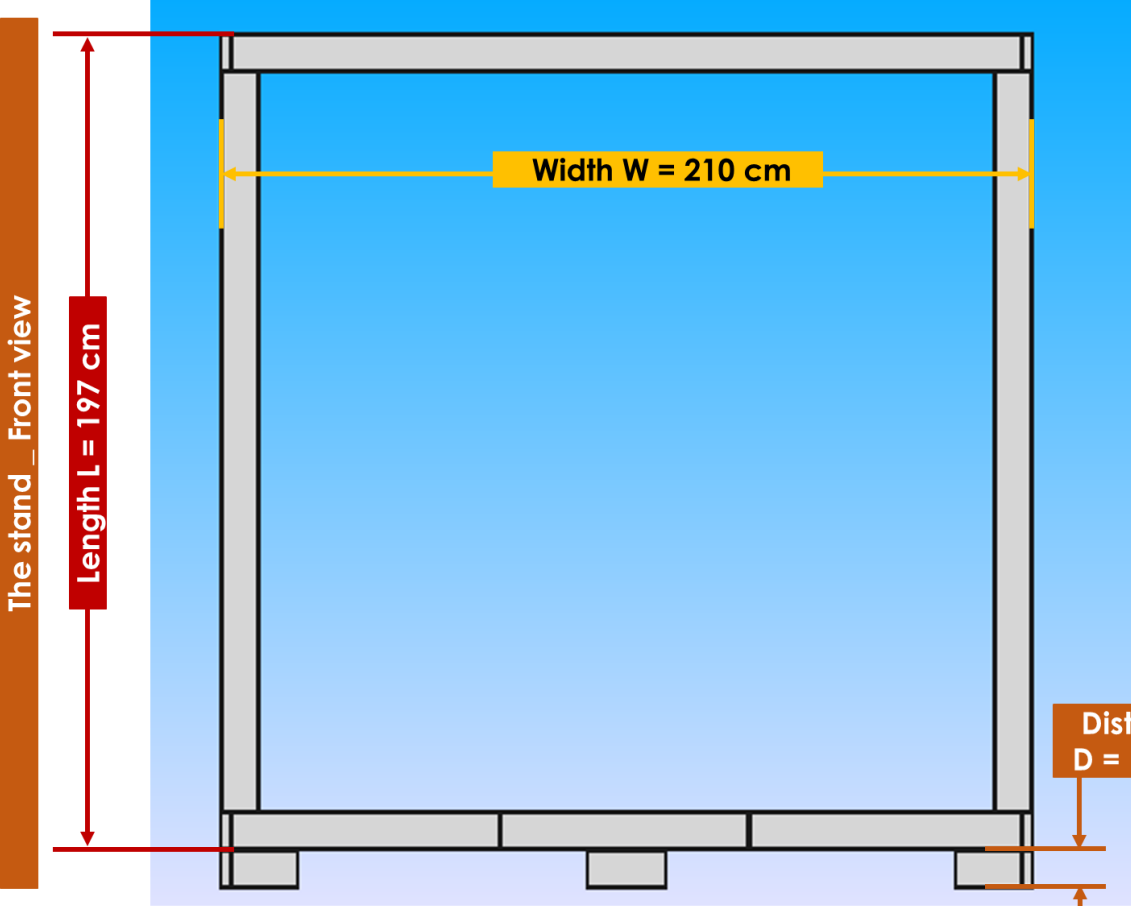
2) Design of fuel burner stand

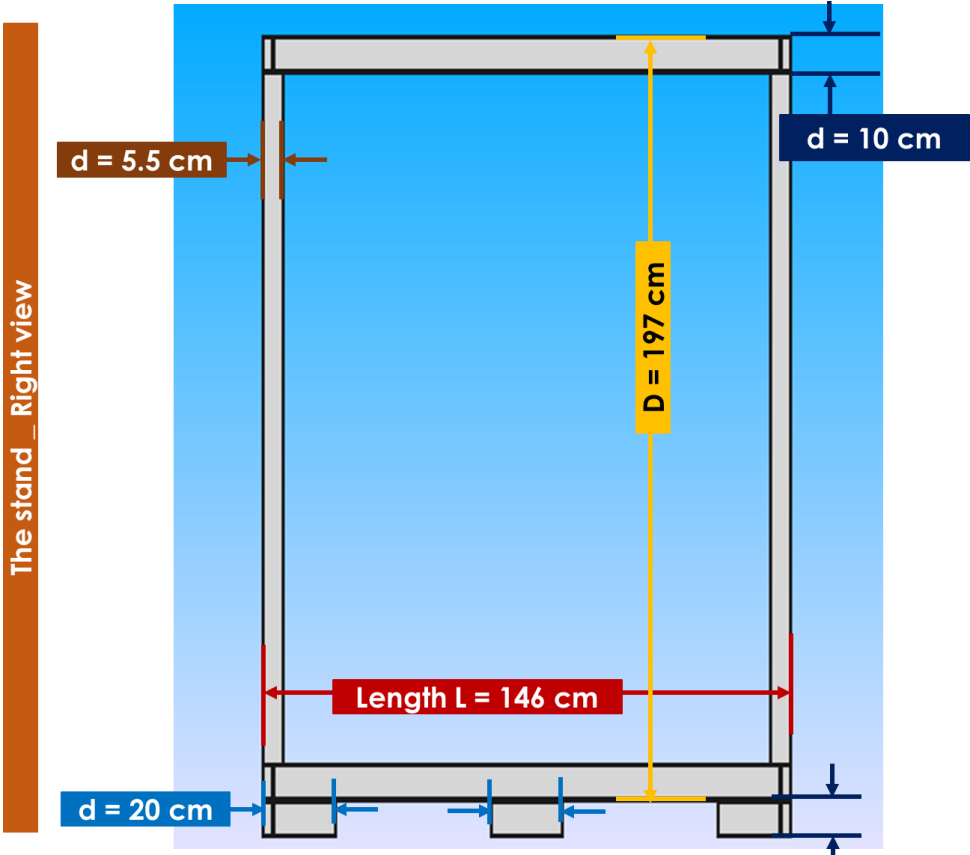
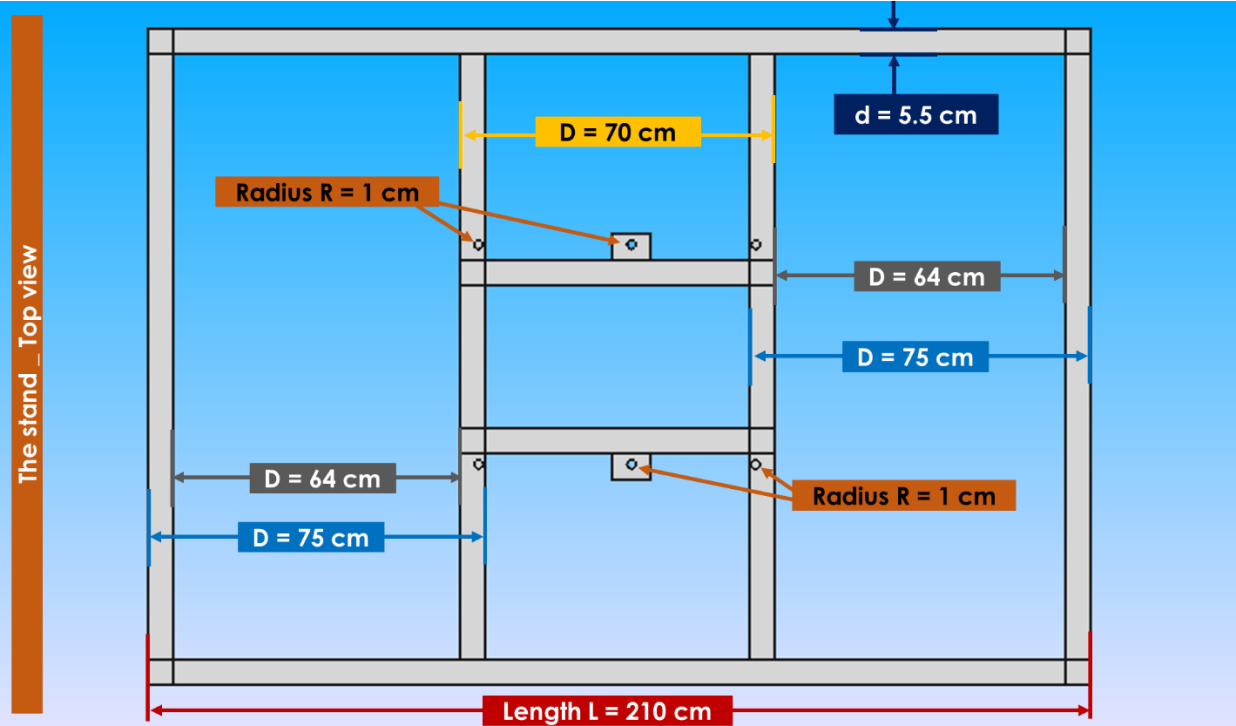
Fuel burner stand – Design and sizing (.pptx)

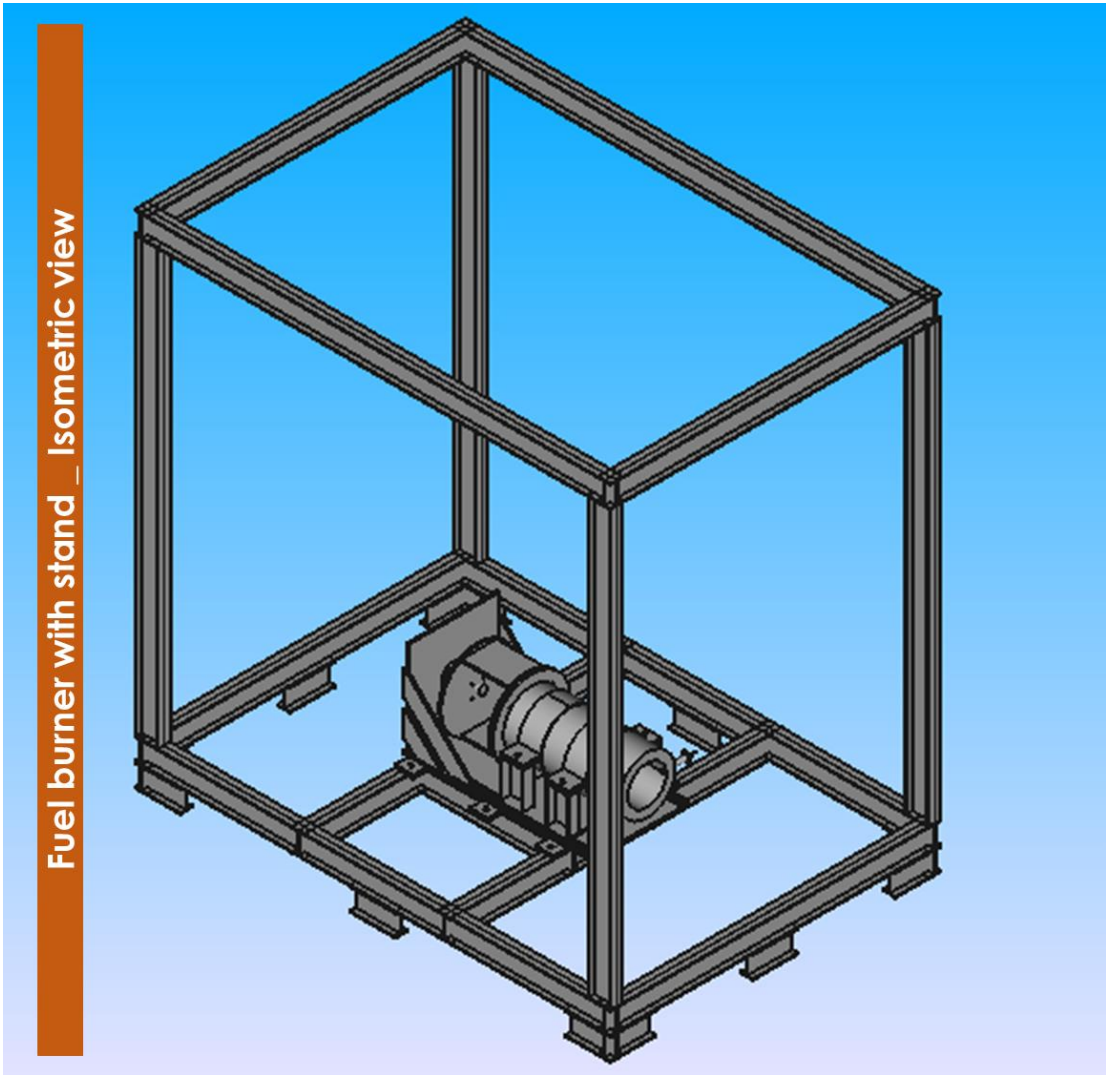
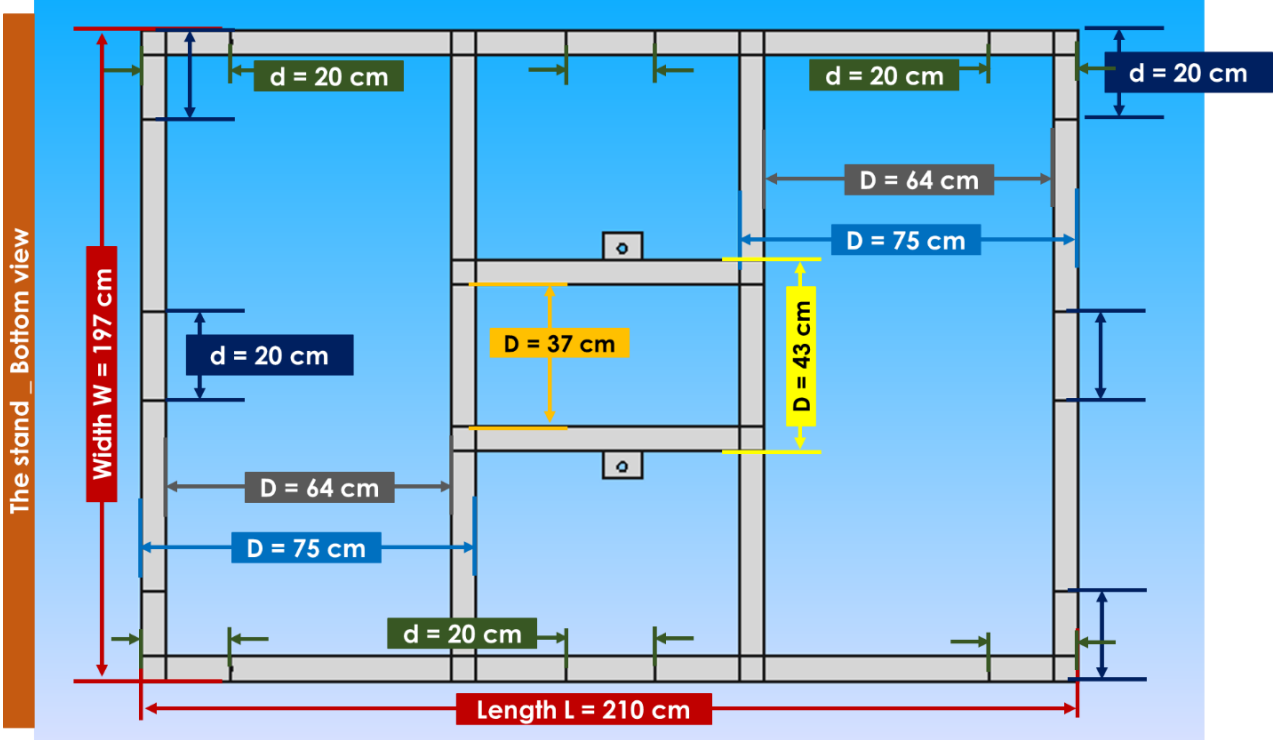


26112022_Sizing -
Fuel Burner with Sta





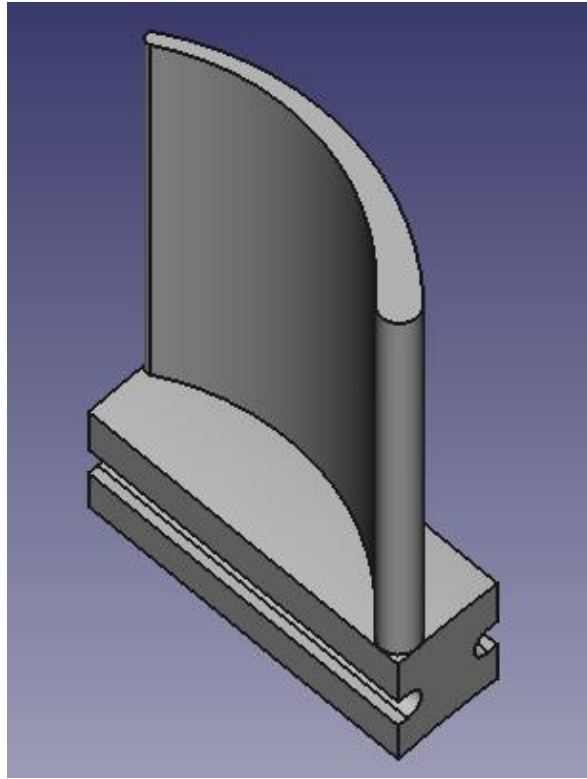




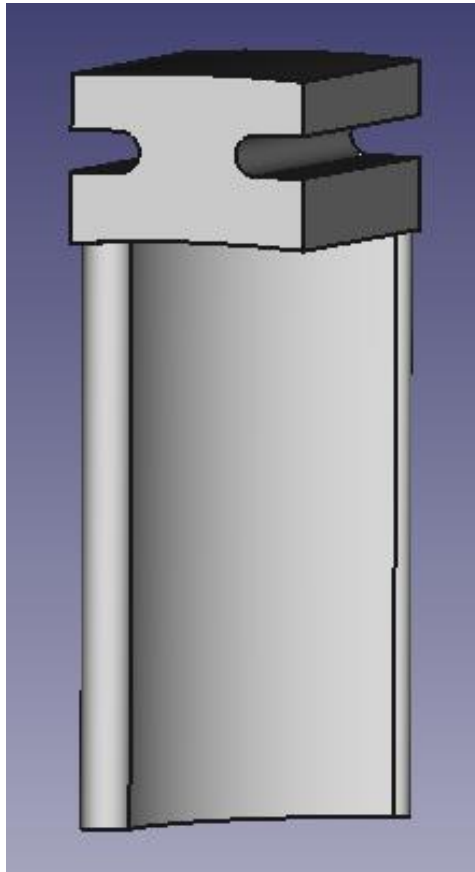


6.4. Gas turbine pieces

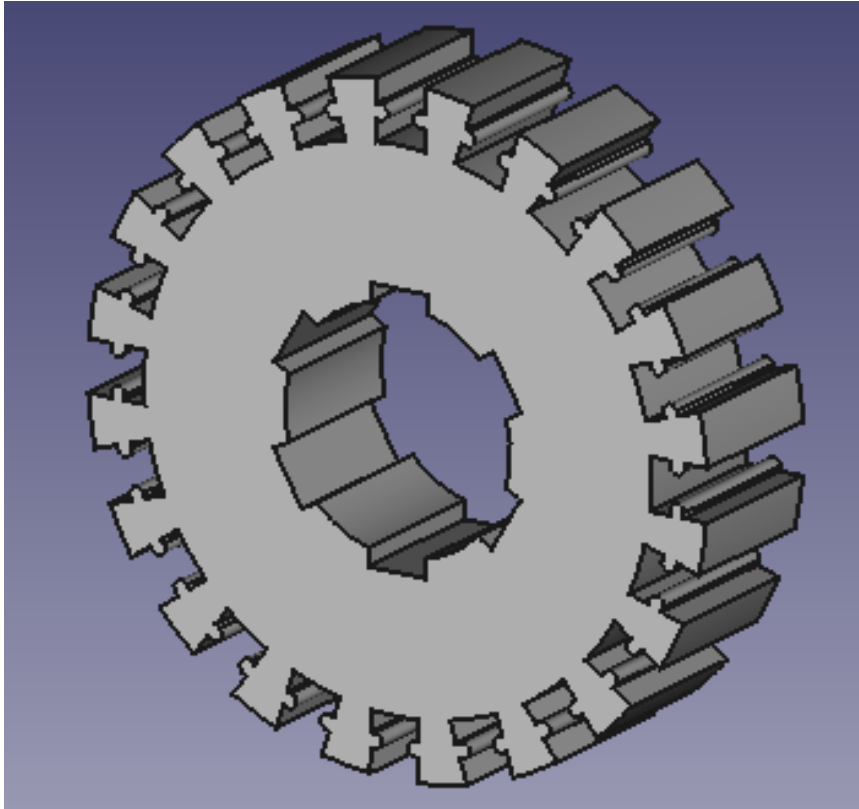
1) Moving blade piece



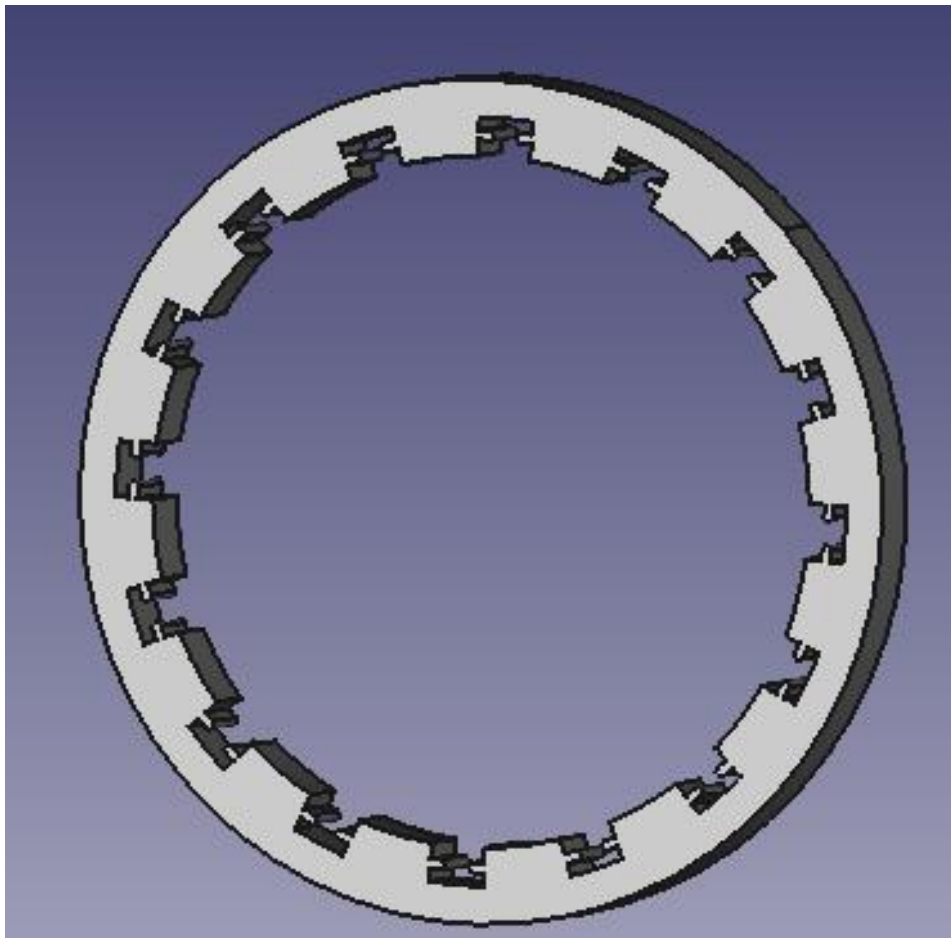
2) Stator blade piece



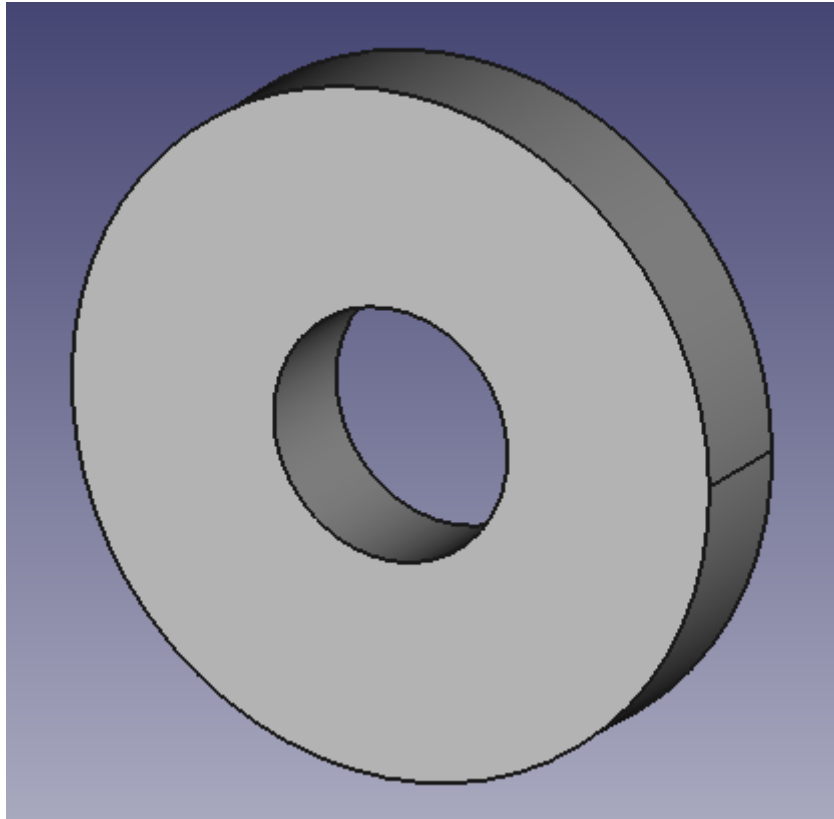
3) Moving blade holder



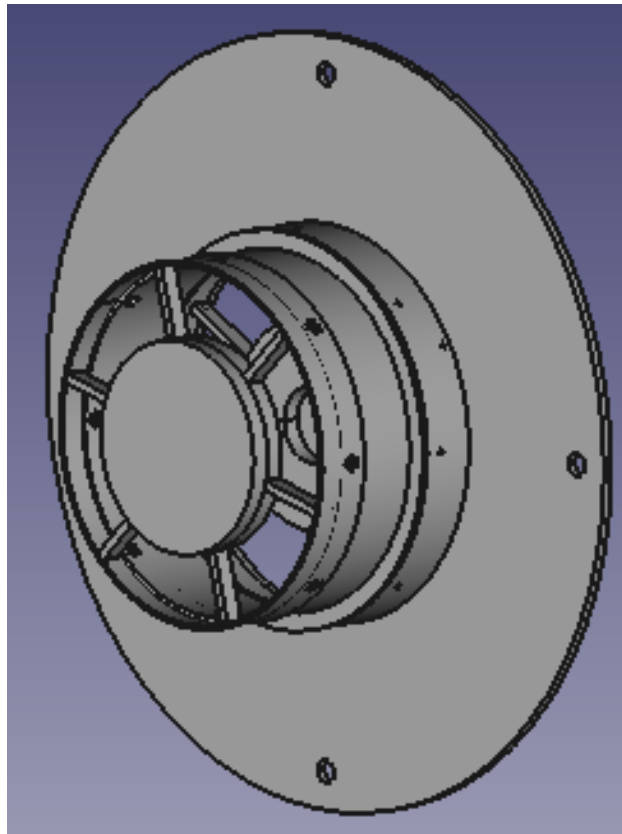
4) Stator blade holder



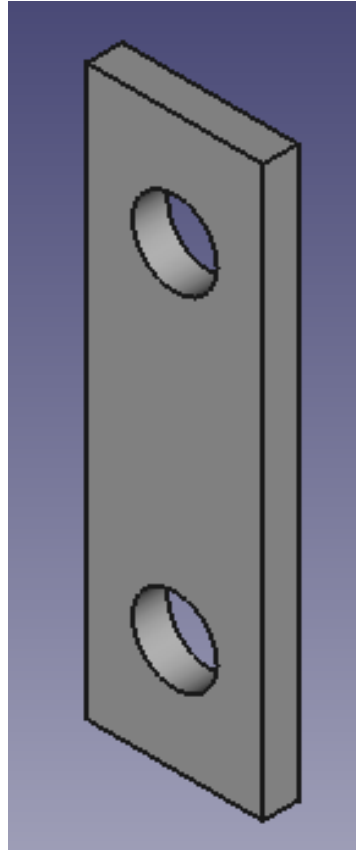
5) Spacer ring



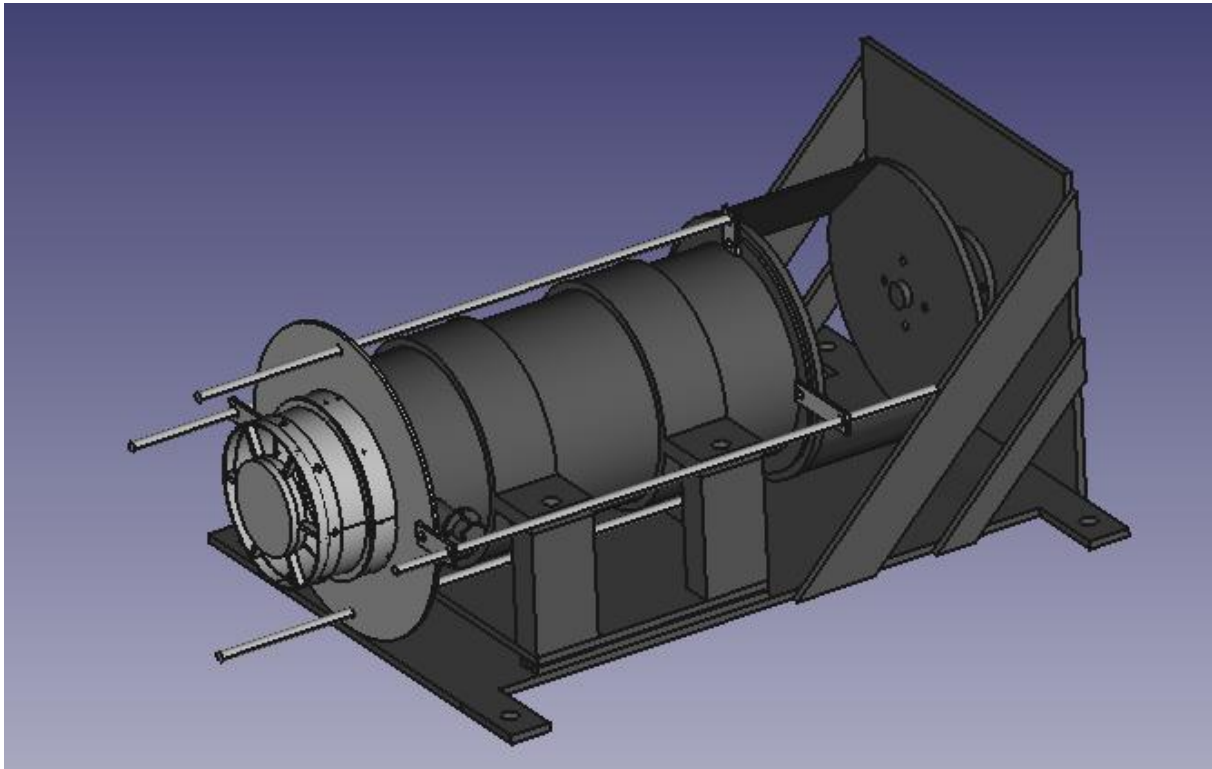
6) Cover



7) Bridge



8) Gas turbine integrated with fuel burner

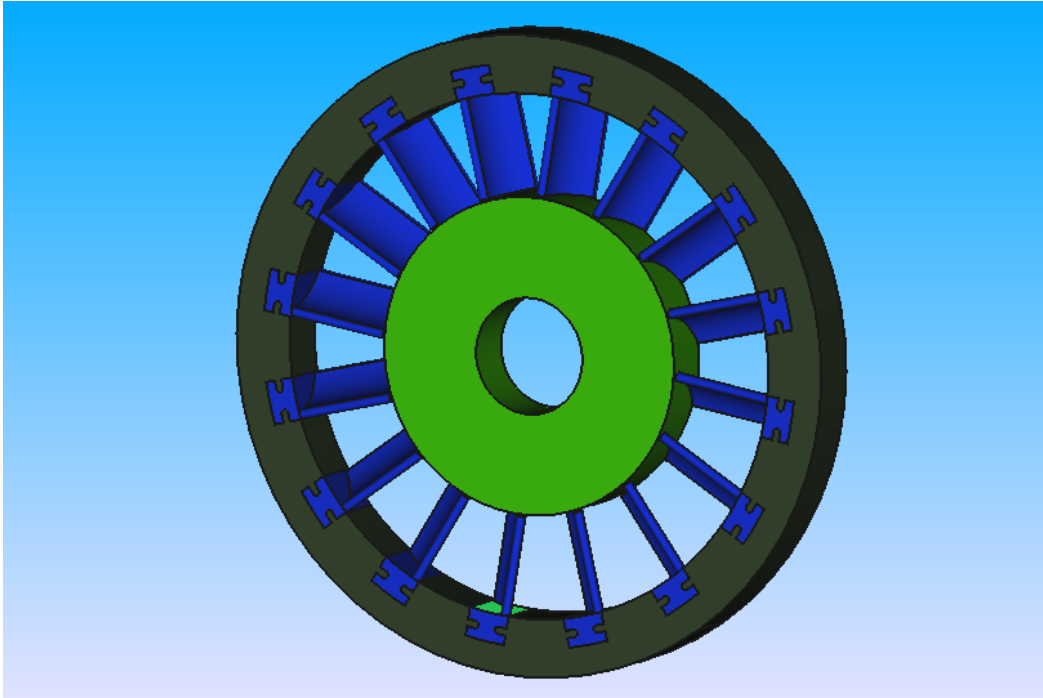


6.5. Gas turbine pieces - FreeCAD design

1) Stator



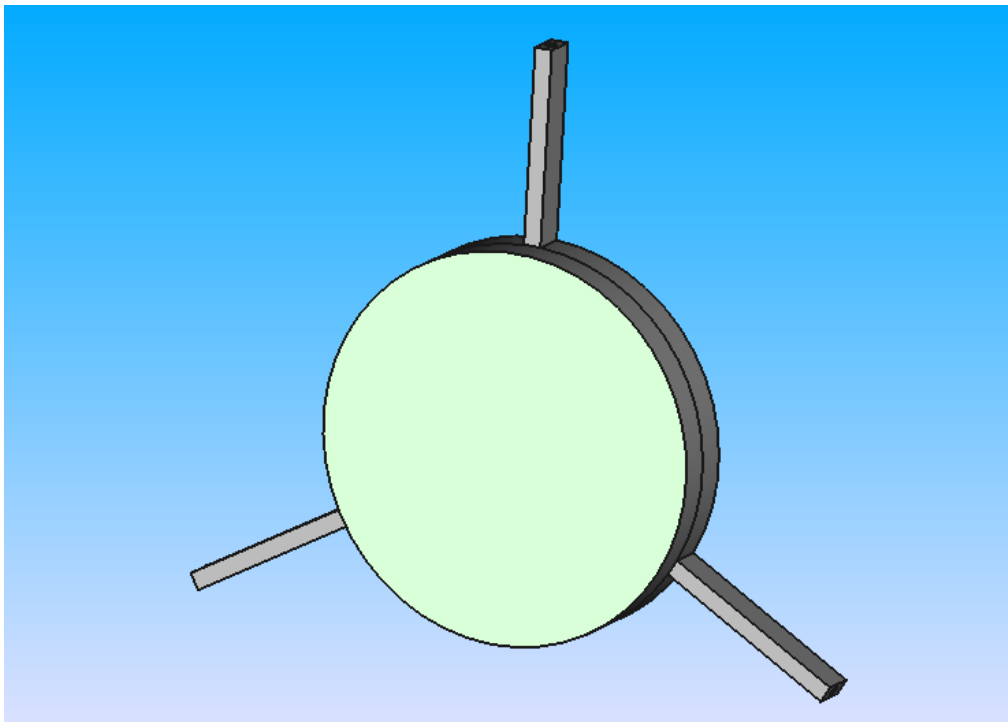
02102022stator.FCS
td

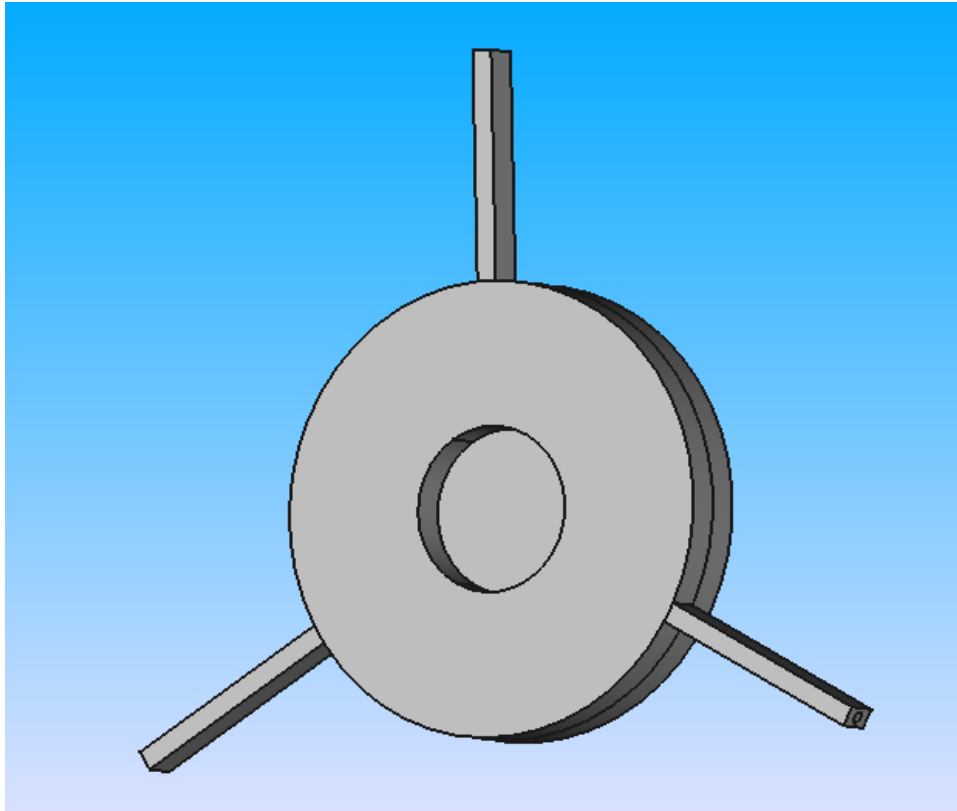


2) Turbine cover A



02102022tb cover
a.FCStd

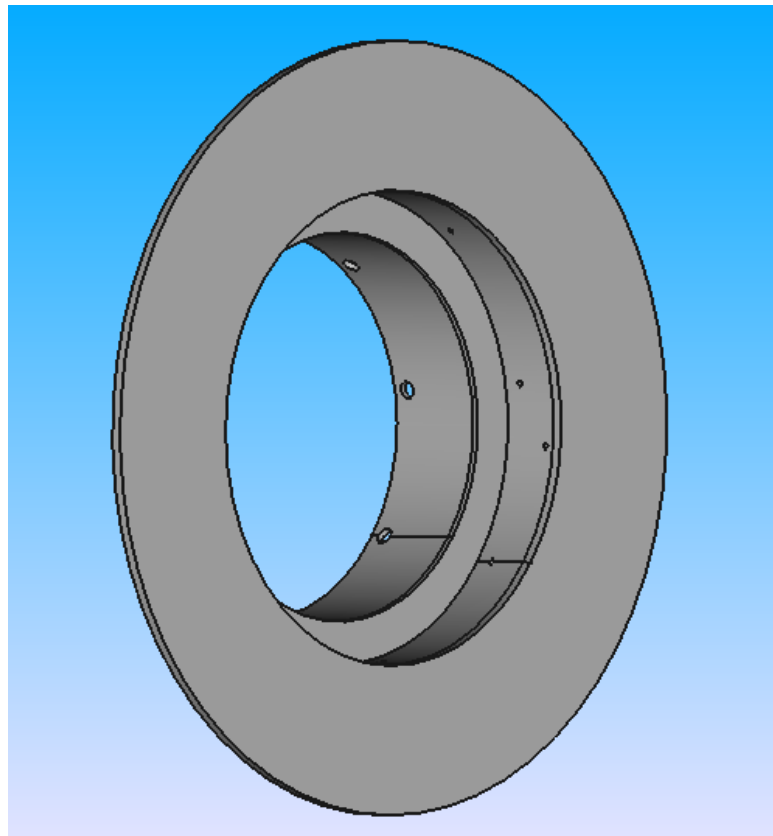




3) Turbine cover B



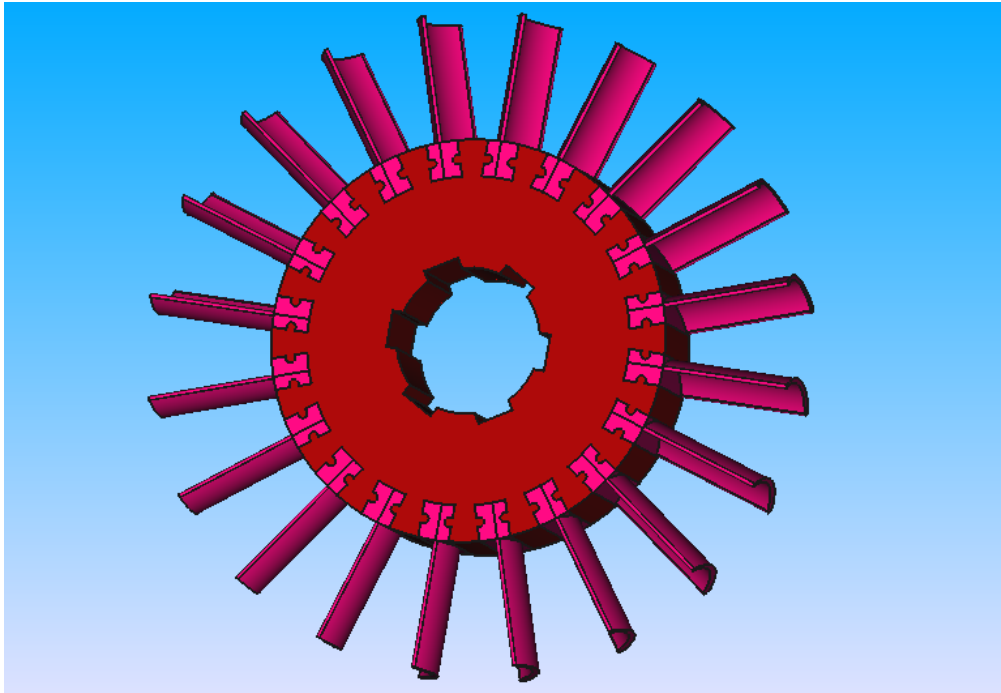
02102022turbine
cover b.FCStd



4) Turbine



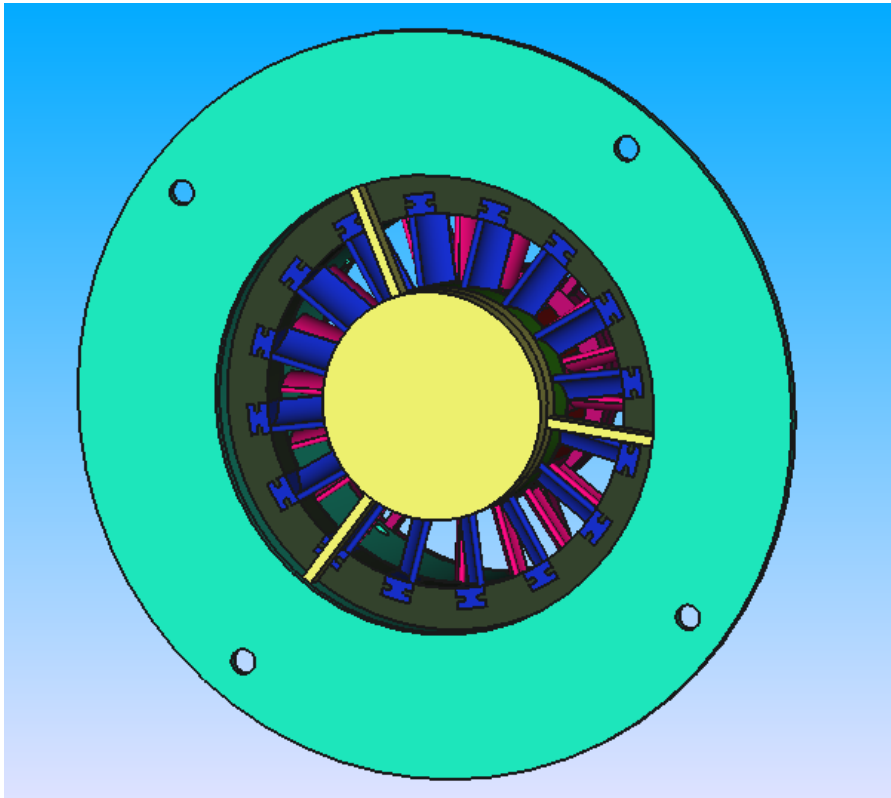
03102022turbine.FC
Std



5) Complete turbine



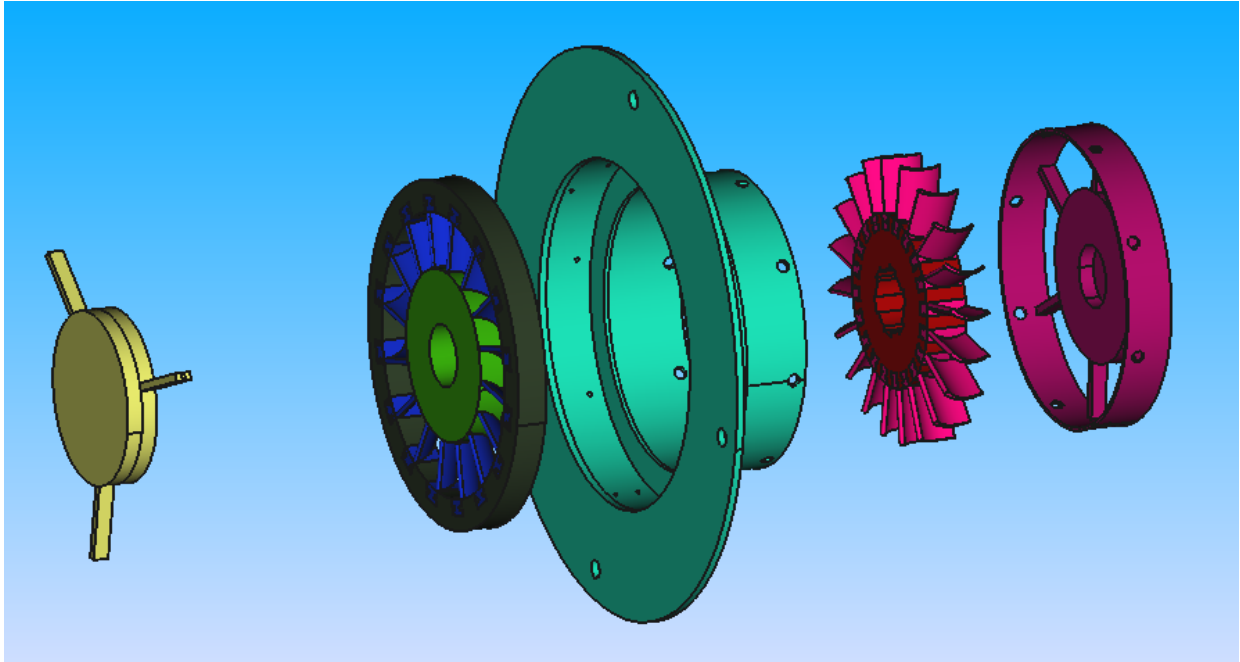
04102022complete-
turbine.FCStd



6) Complete turbine expanded



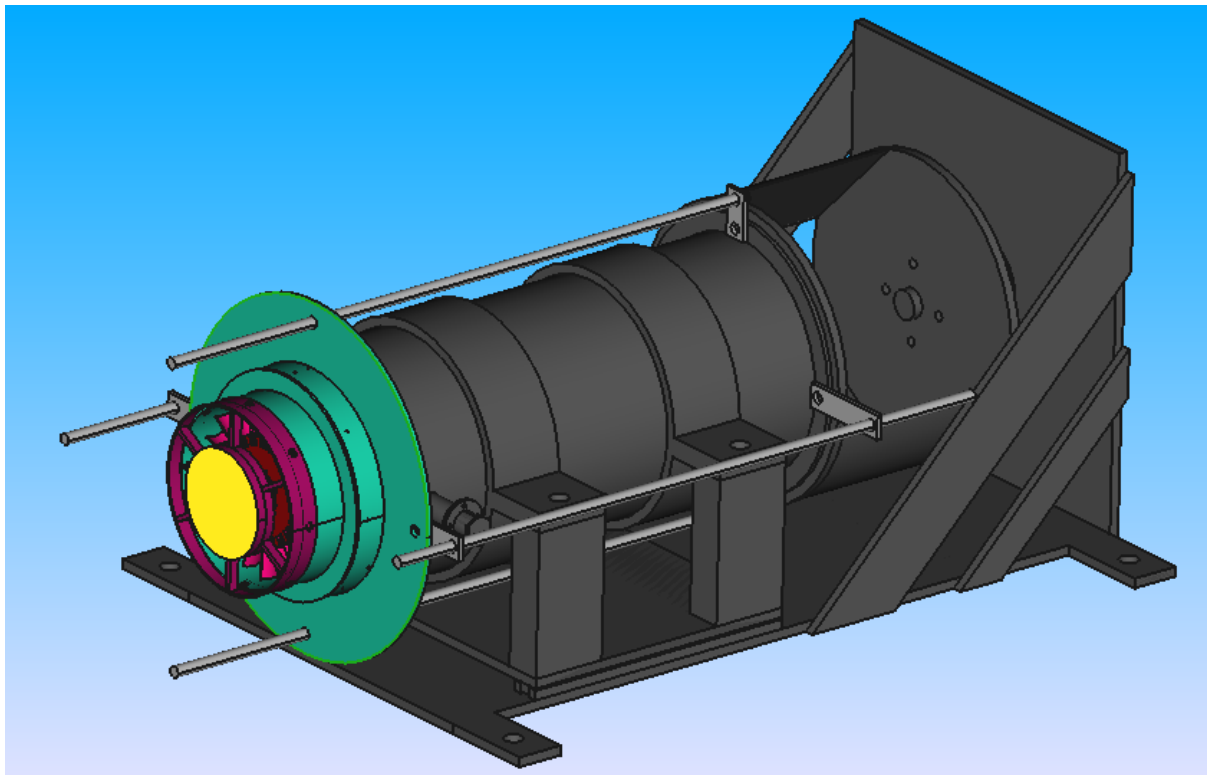
04102022complete-turbine-expanded.F



7) Assembly



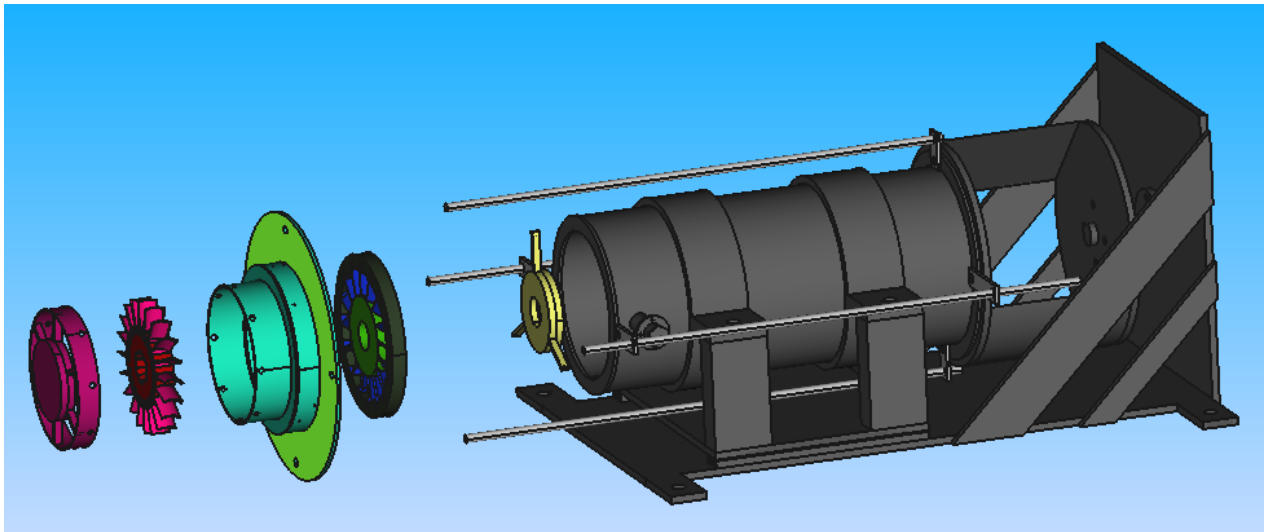
05102022assembly.FCStd



8) Assembly expanded



05102022assembly-
expanded.FCStd

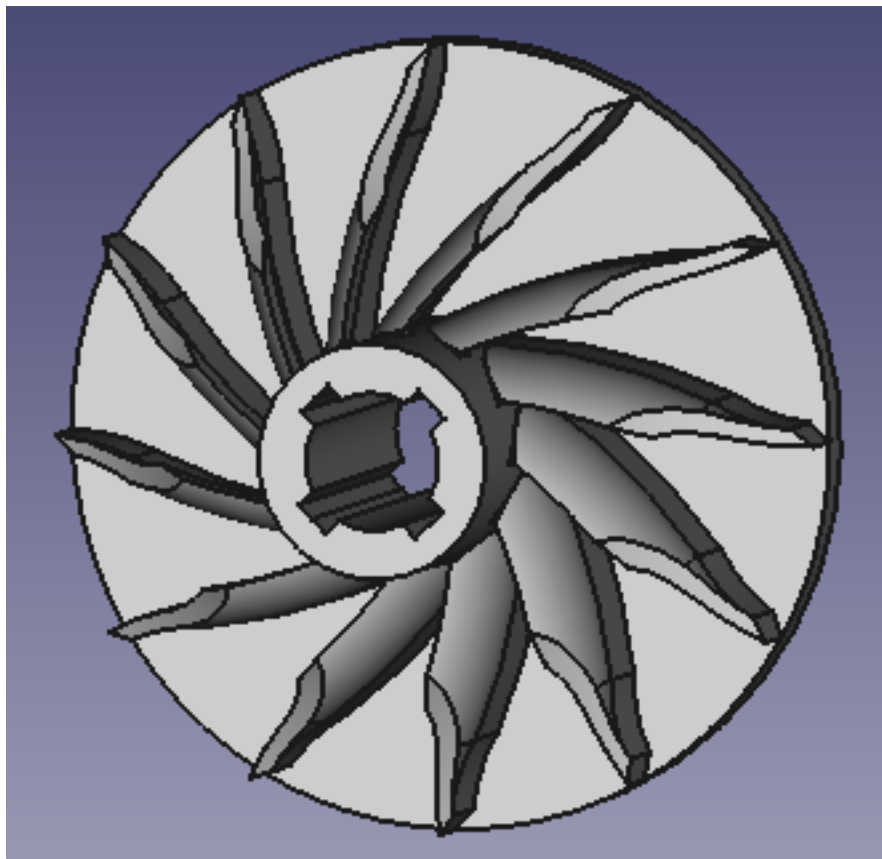


6.6. Gas turbine compressor

1) Compressor impeller



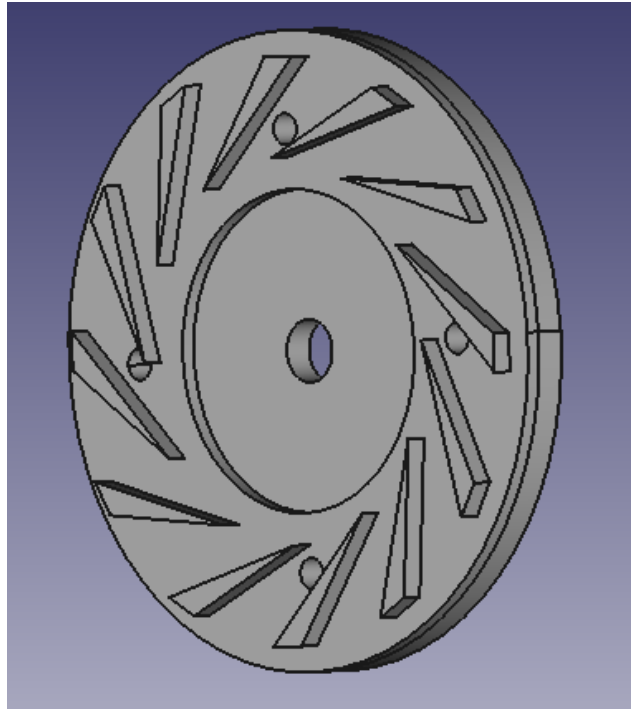
compressor.FCStd



2) Compressor diffuser



diffuser.FCStd

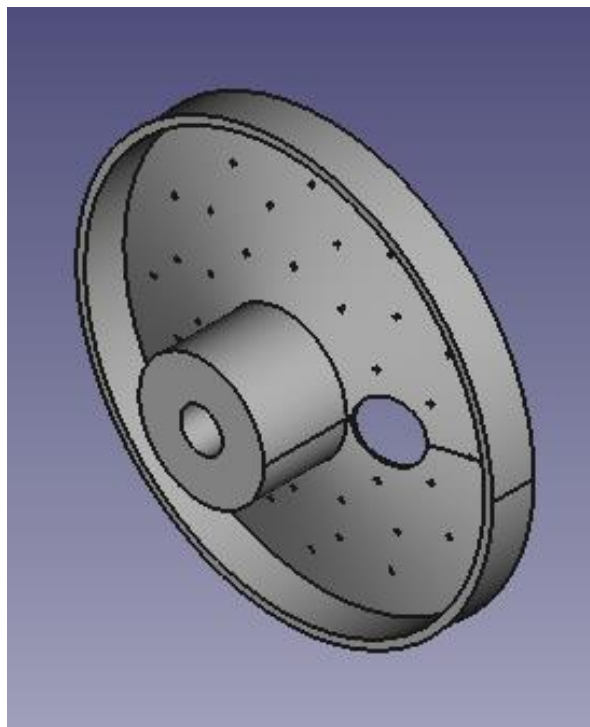


6.7. Combustion chamber parts With FreeCAD design

1) Cap



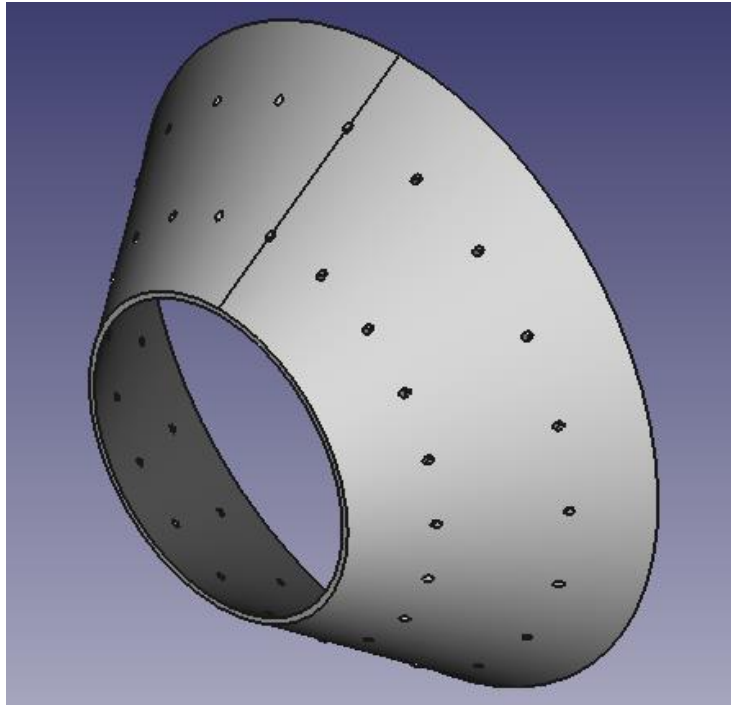
combustion
cap.FCStd



2) Primary zone



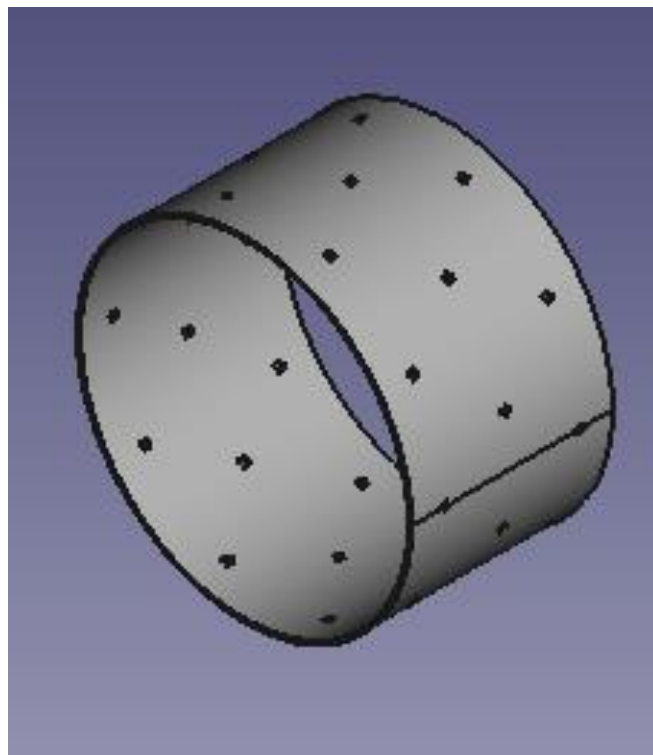
combustion primary
zone.FCStd



3) Intermediate zone

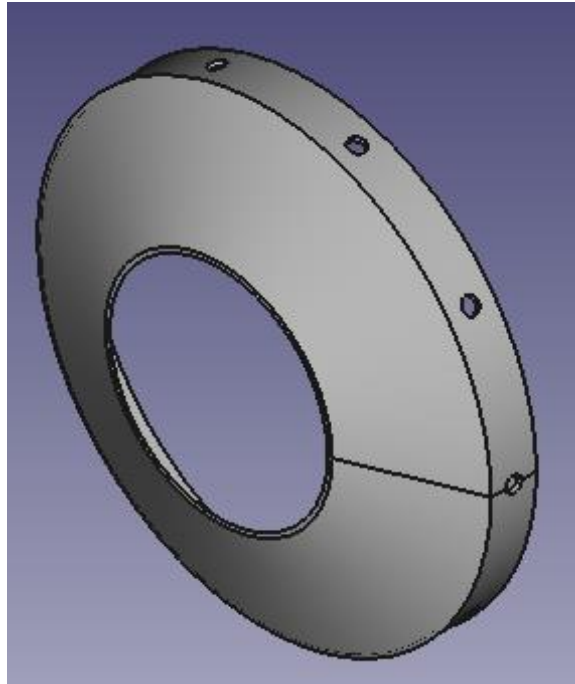


combustion
intermediate zone.FC



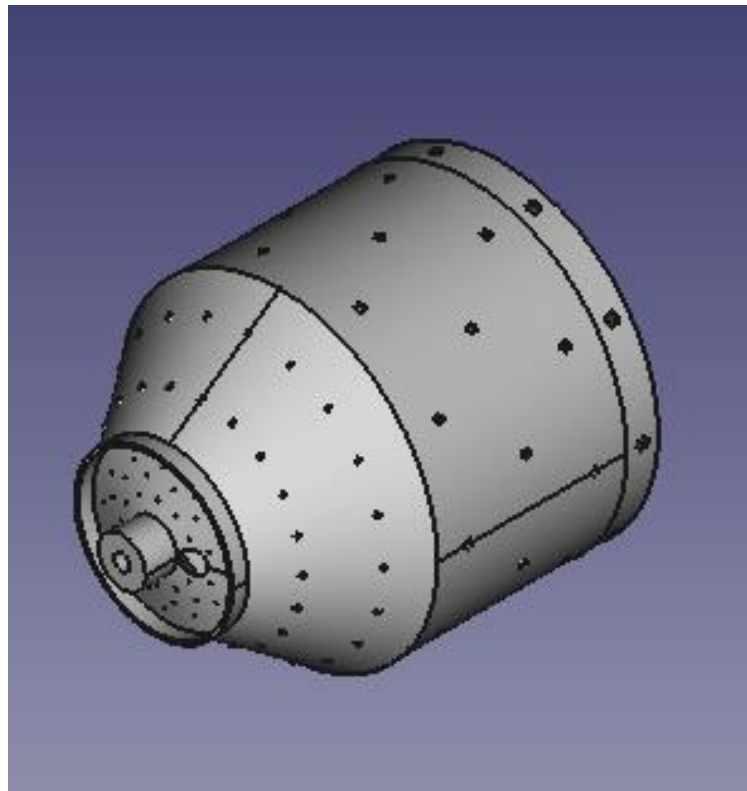
4) Dilution zone


combustion
dilution.FCStd

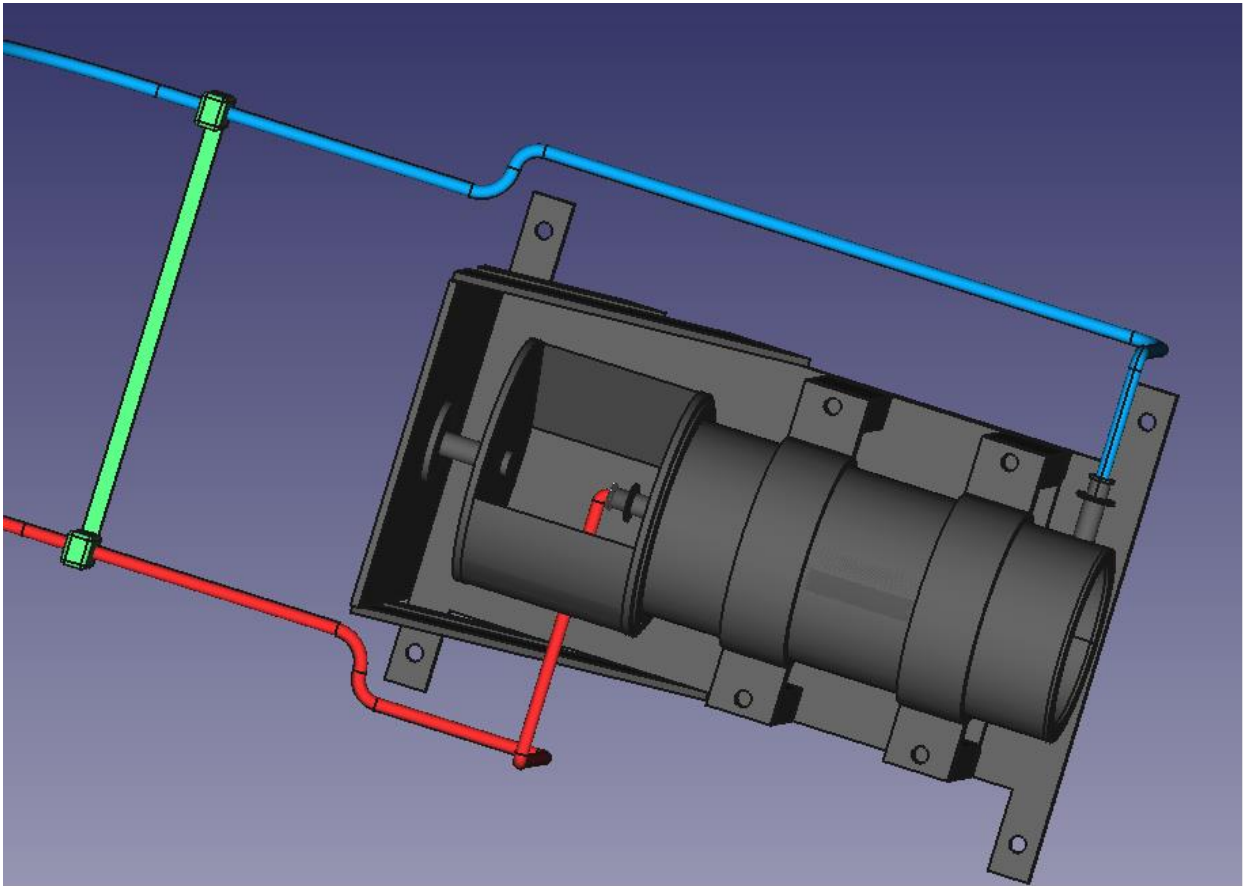


5) Combustion chamber


comb-chamb.FCStd



6) Alternative Fuel burner combustion chamber



6.8. What's next

To complete this project, we must select the type of metals and sensors suitable for the model, after that we can start manufacturing the turbine.

Project 7: Ashes Recycling (ICPT – AR)

7.1. Position of Ashes recycling project

Work on this project began in the past years. In this year (2022), the focus was on the control, as the PLC was added and operated on the project.

7.2. Ashes Recycling PCS Implementation

1) The process control system for the Ashes Recycling system

Graphical user interface



Modbus RS 485 Network

Control Panel



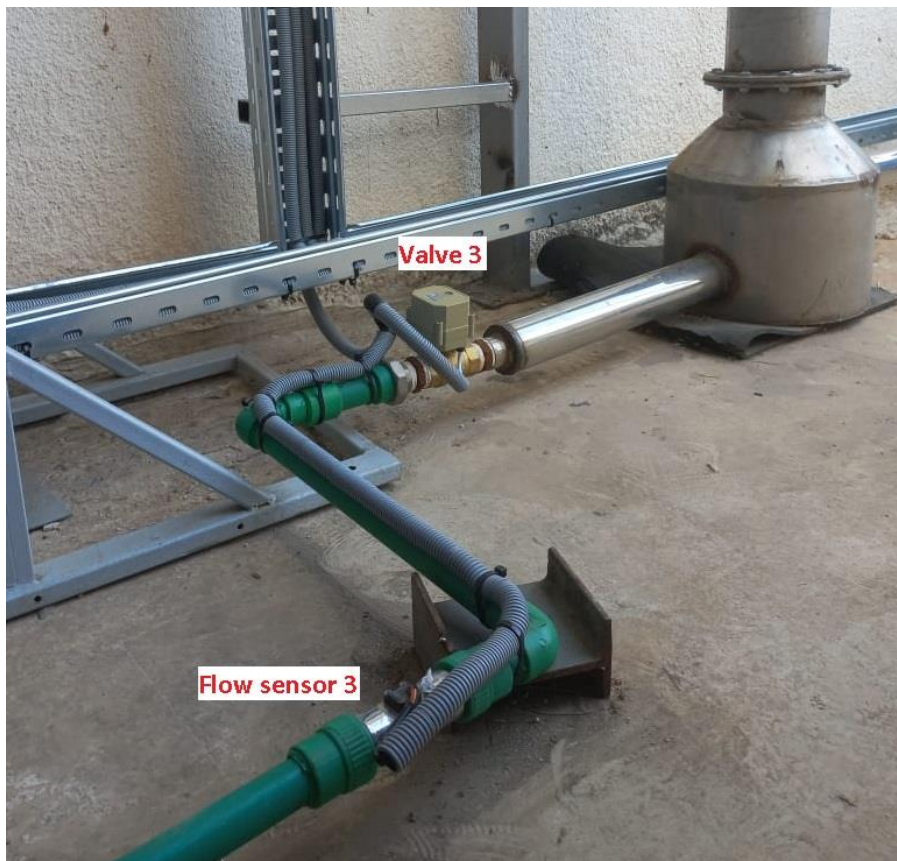
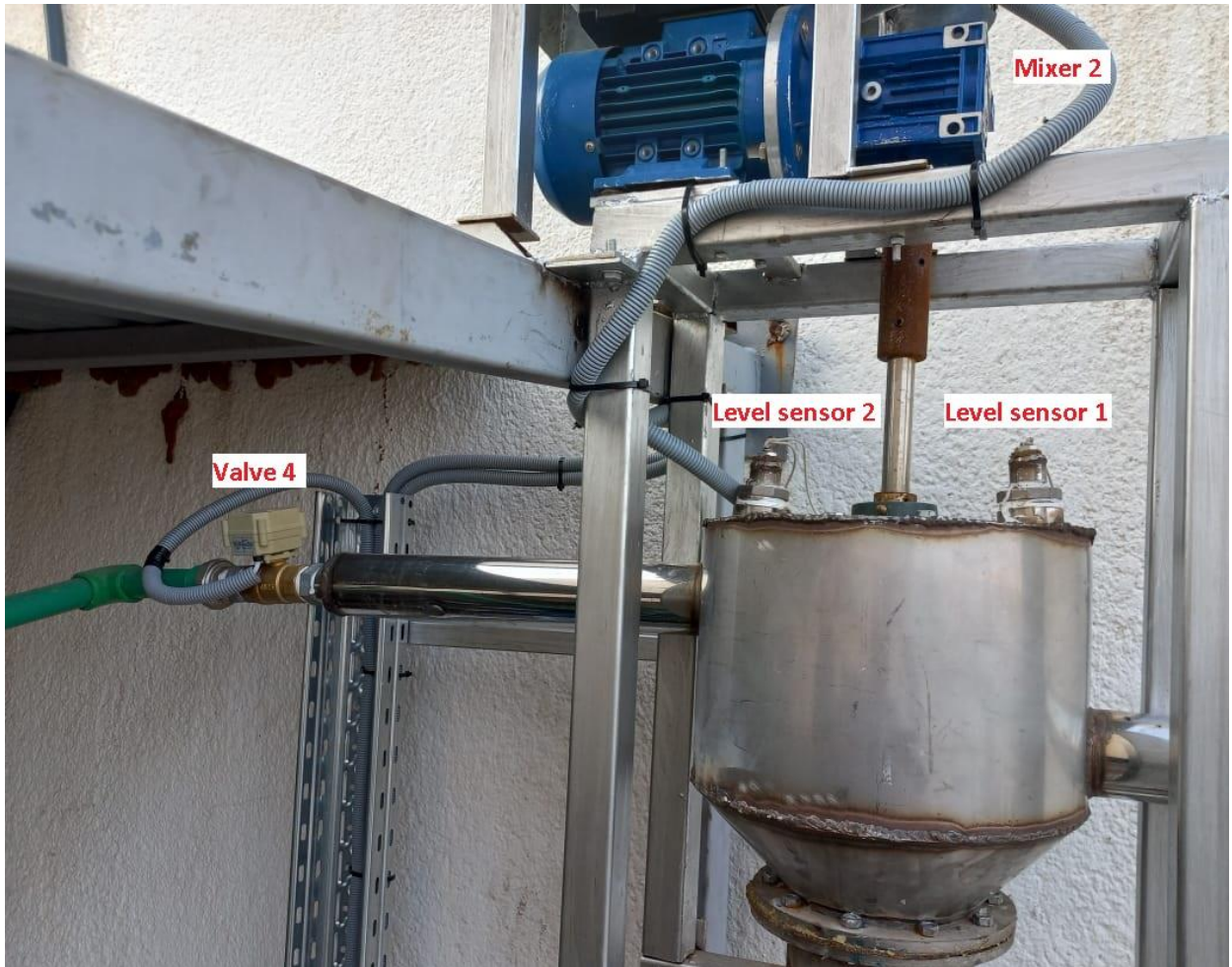
Electrical Cables

Sensor &
Actuator



2) The Ashes Recycling system



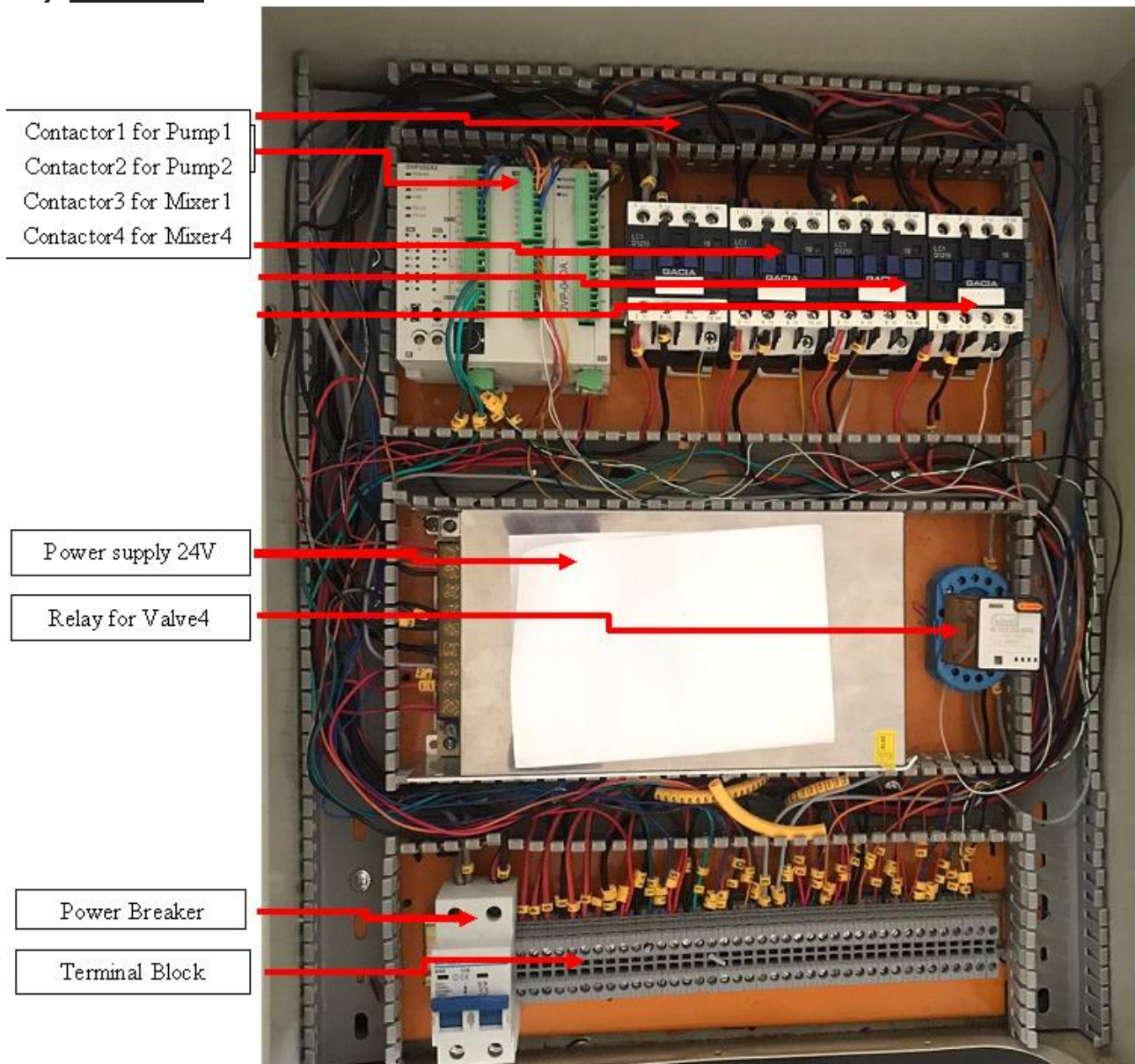




3) The Material Used

- 1-Proportional 2 way valve A20-M25-B2-C and Proportional 3 way valve A20-M25-B3-C (24VDC; input 0 to 10v) [1][2]
- 2-Motorize Valve A20-T25-B2-C (24VDC; CR301) [3][4]
- 3- Delta PLC DVP20SX21 1R [5]
- 4-Delta Module DVP04DA-S [6]
- 5- Water Flow Sensor USS-HS43TB (2-45L/M G3/4") [7]

4) PLC Panel



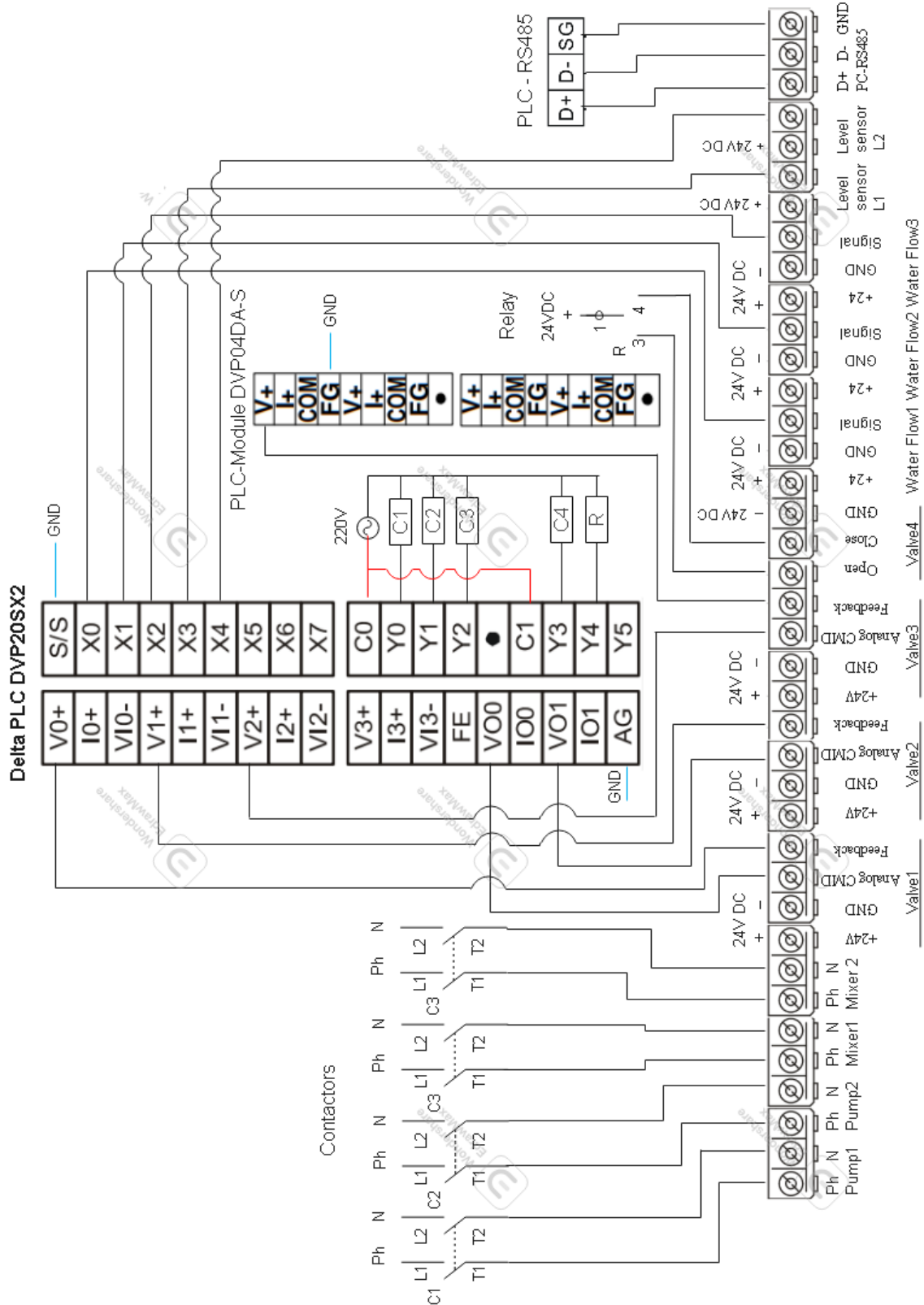
5) Terminal Block of Panel

1-Breaker	Power - Phase
2-Breaker	Power - Neutral
3-Terminal Block	Pump 1- Phase
4-Terminal Block	Pump 1- Neutral
5-Terminal Block	Pump 2- Phase
6-Terminal Block	Pump 2- Neutral
7-Terminal Block	Mixer 1- Phase
8-Terminal Block	Mixer 1- Neutral
9-Terminal Block	Mixer 2- Phase
10-Terminal Block	Mixer 2- Neutral
11-Terminal Block	Valve 1- 24VDC +
12-Terminal Block	Valve 1- 24VDC – (GND)
13-Terminal Block	Valve 1- Analog Command (0 to 10V)
14-Terminal Block	Valve 1- Feedback
15-Terminal Block	Valve 2- 24VDC +
16-Terminal Block	Valve 2- 24VDC – (GND)
17-Terminal Block	Valve 2- Analog Command (0 to 10V)
18-Terminal Block	Valve 2- Feedback
19-Terminal Block	Valve 3- 24VDC +
20-Terminal Block	Valve 3- 24VDC – (GND)
21-Terminal Block	Valve 3- Analog Command (0 to 10V)
22-Terminal Block	Valve 3- Feedback
23-Terminal Block	Valve 4- Open 24VDC +
24-Terminal Block	Valve 4- Close 24VDC +
25-Terminal Block	Valve 4- 24VDC – (GND)
26-Terminal Block	Water Flow 1- 24VDC +
27-Terminal Block	Water Flow 1- 24VDC – (GND)
28-Terminal Block	Water Flow 1- Signal
29-Terminal Block	Water Flow 2- 24VDC +
30-Terminal Block	Water Flow 2- 24VDC – (GND)
31-Terminal Block	Water Flow 2- Signal
32-Terminal Block	Water Flow 3- 24VDC +
33-Terminal Block	Water Flow 3- 24VDC – (GND)
34-Terminal Block	Water Flow 3- Signal
35-Terminal Block	Level sensor 1- 24VDC +
36-Terminal Block	Level sensor 1- Status
37-Terminal Block	Level sensor 2- 24VDC +
38-Terminal Block	Level sensor 2- Status
39-Terminal Block	RS485 Serial +
40-Terminal Block	RS485 Serial -
41-Terminal Block	RS485 Serial GND

6) Control Panel Wiring



200822Ashes
Recycling - Control I



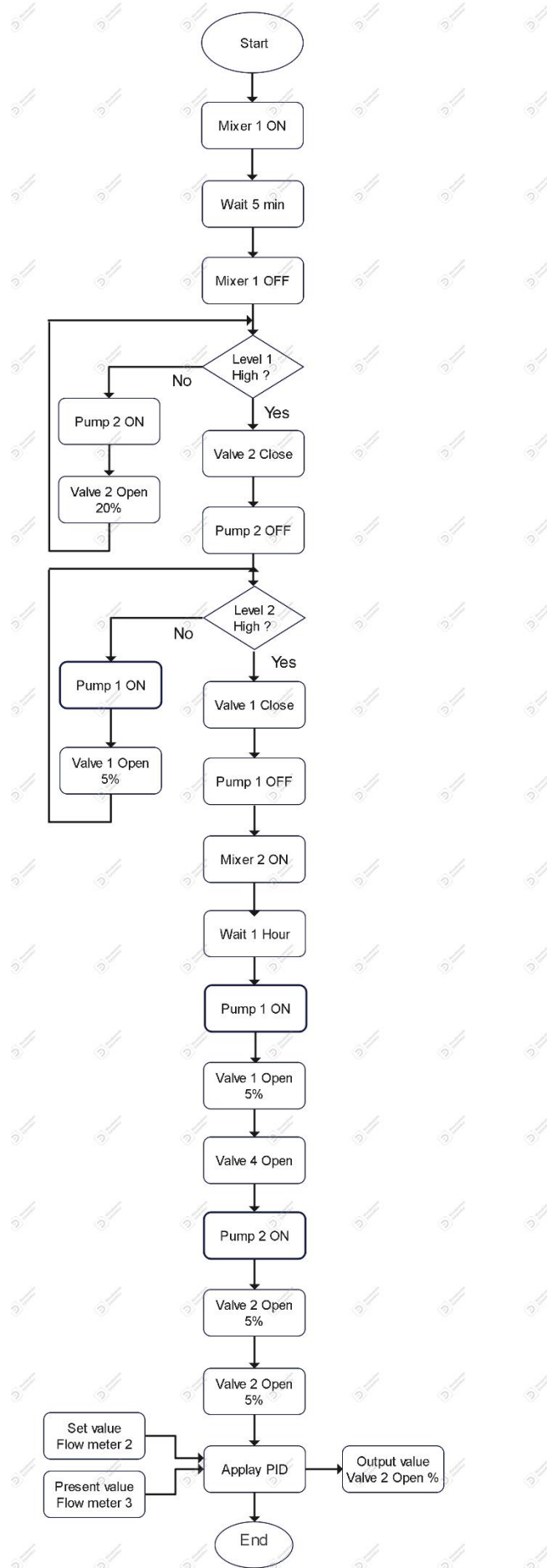
7) Operating steps

1. In the mixture put 338 Kg of Ashes with 1690 L of acid of 15.8 mol/l of concentration
2. Turn on the mixer (M1)
3. Open the Valve 2 and ON the pump (P2) to reach the column to the level (a) of ash mixed with nitric acid
4. When the level of liquid in the column reaches the top left nozzle (a), Turn Off the Pump (P2) and Close the Valve 2.
5. Turn on the mixer (M2)
6. Open the Valve 1 and Turn on the pump (P1) to put the solvent (LIX : LIX® 984N)
7. When the level of liquid reaches the top left nozzle (b), Turn Off the Pump and Close the Valve 1.
8. Wait Time ... min. Allow the interface to form between the top mesh (a) and the top left nozzle (b). The interface appears as an immiscible layer between acid and extractant with droplets
9. Turn On the Pump (P1) and Open the valves (V1) and (V4) to set the extractant (Solvent) flow rate (equal between the inputs and the output).
10. Turn On the Pump (P2) and Open the valves (V2) and (V3) to set the aqueous phase flow rate (equal between the inputs and the output).

8) Algorithm



030922Ashes
Recycling_PCS_Algo



9) Graphical user interface

- PLC code :



021222_ICPT-Ashes
Recycling_PCS_PLC C

- Graphical User Interface code (C#) :

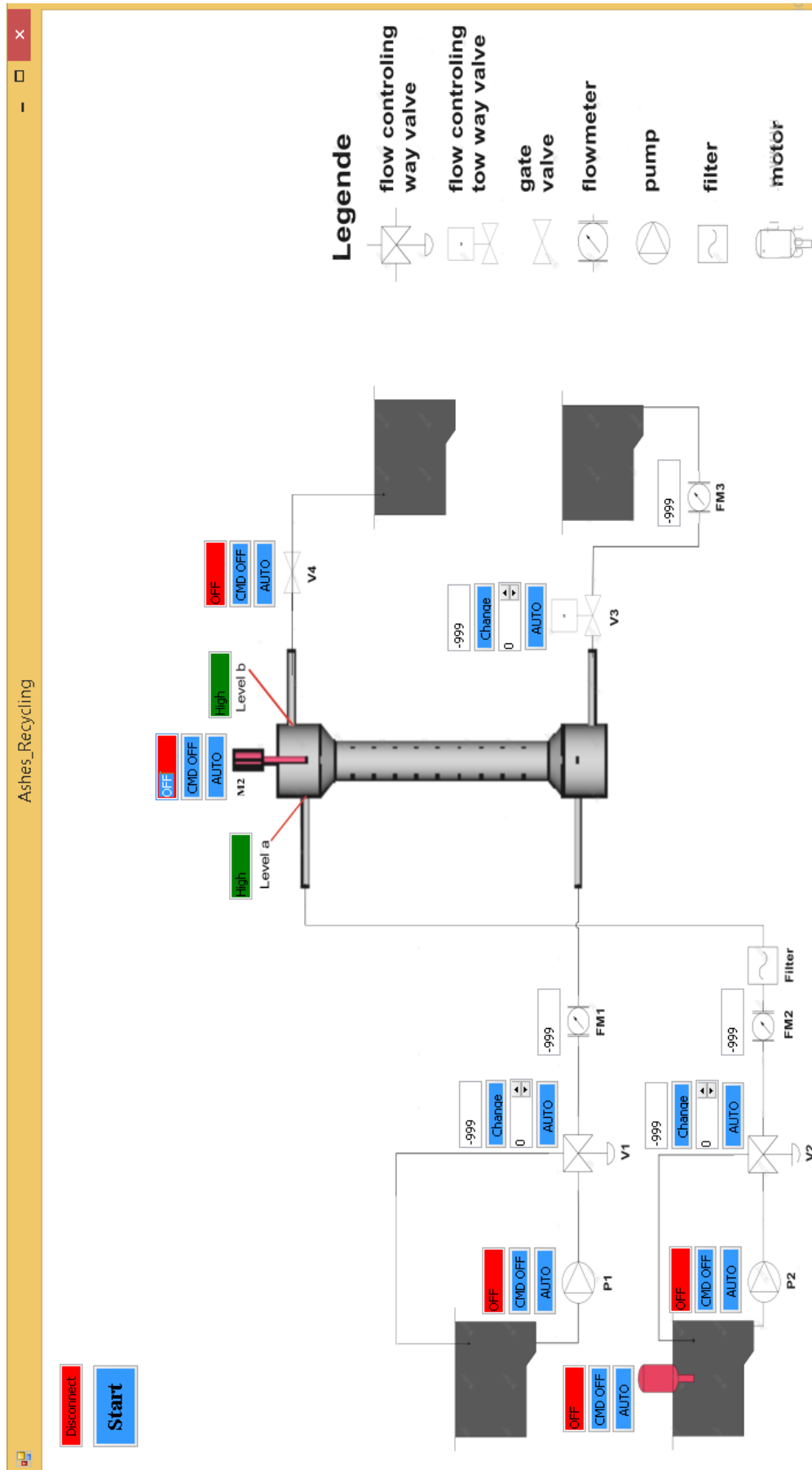


ICPT-Ashes
Recycling_PCS_GUI_!

- PLC Modbus Addresses :



090922_ICPT-Ashes
Recycling_PCS_PLC M



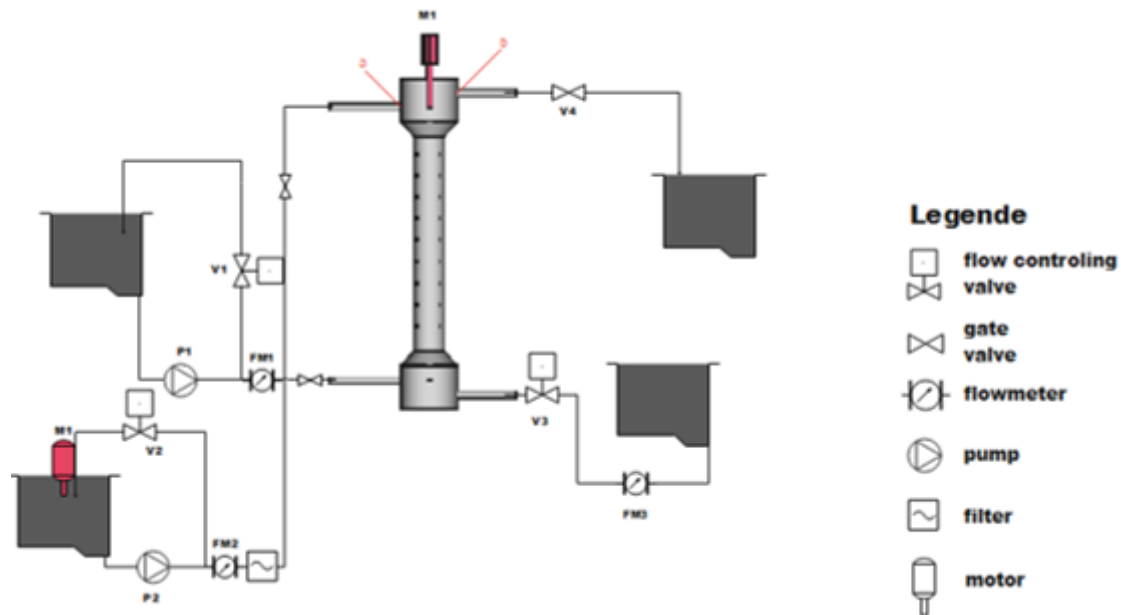
7.3. Ashes Recycling System Test Specifications



ICPT_WEDC-Testrigs_PCS2021_190122.zip

1) Before using

- All valves are turned off
- The motor is turned off



2) Follow these steps

1. Turn on the motor (M1)
2. In the mixture put 338 Kg of Ashes with 1 690 L Of acid of 15.8 mol/l of concentration
3. Turn on the motor (M2)
4. Open the pump (P2) to reach the column with 44 l of ash mixed with nitric acid
5. When the level of liquid in the column reaches the top left nozzle (a) . Turn on the valve (V2) to set the flow rate of the mixture
6. Turn on the pump (P1) to put the LIX (LIX® 984N)
7. When the level of liquid reaches the top left nozzle (b). Turn on the valve (V1) to set the extractant flowrate
8. Allow the interface to form between the top mesh (a) and the top left nozzle (b). The interface appears as an immiscible layer between acid and extractant with droplets
9. Once the interface is formed in the desired location, close the valve (V1) slowly until there are flowrates out of the column
10. To keep the flowrates equal between the inputs and the output 2, adjust the valve (V3) to set the output flowrate

7.4. Operation of ashes recycling system

List of Consumables for one batch run:

<u>Consumable</u>	<u>Quantity</u>	<u>Price</u>
Extractant	10L	
Nitric Acid	44L	

7.5. Requirements

A-Z : system requirements

1,2,3... : product requirements

A. The column system must be able to transfer the metallic salts from the solution to the solvent.

A.1. The rotator must be able to mix the two phases well enough to transfer the metal ions from the aqueous phase to the organic phase.

A.2. The solvent used shall be able to extract a specific ion from the solution (e.g. LIX® 984N for copper ions).

B. The mixer must be able to dissolve all solubles in the ash into the acid

C. The inflows and outflows of the fluids must be able to harmonise with each other.

C.1. The mixer shall rotate in x rpm

7.6. What's next

After completing the control of the applied model, in the future, this part must be started, and accordingly the required mixture – purchase or manufacture – must be provided to operate the model.

Project 8: Analytical Chemistry



Project 9: Metallurgical Lab

9.1. Position of Metallurgical Lab project

This project was designed to serve several projects under implementation or proposed. It is an implementation project that aims to form multiple types of mineral mixtures, where the type and quantity (percentage) of minerals combined with each other varies. Work on this project began this year (2022), and work on it will be completed when needed.

9.2. Iron melting Test

- Video 1:



WhatsApp Video
2022-12-24 at 14.03.

- Video 2:



WhatsApp Video
2022-12-24 at 14.04.





References

- Project 2 _ Water electrolysis references

[1] Straight-Parallel Electrodes and Variable Gap for Hydrogen and Oxygen Evolution Reactions

[2] <https://backend.orbit.dtu.dk/ws/portalfiles/portal/6368532/Electrical+conductivity+measurements.pdf>

- Project 4_ Liquefaction of Oxygen references

[1] <https://smstork.com/en/user-manuals>

[2] Jamshidi, N., Farhadi, M., Ganji, D.D., Sedighi, K., 2013. **Experimental analysis of heat transfer enhancement in shell and helical tube heat exchangers**. Appl. Thermal Eng. 51,644–652.

[3] S. Bahreghmand, A. Abbassi, 2016. **Heat transfer and performance analysis of nanofluid flow in helically coiled tube heat exchangers**. Chemical engineering research and design 109 (2016), 628–637.

[4] <https://manibhadrafittings.com/copper-pipe-weight-dimensions-chart-in-mm-kg/>

[5] <https://www.grainger.com/category/plumbing/insulation/pipe-insulation?attrs=Fits+Tube+Size%7C3%2F8+in&filters=attrs>

[6] <https://www.grainger.com/category/plumbing/insulation/pipe-insulation?attrs=Fits+Tube+Size%7C1%2F4+in~~Insulation+Temp.+Range%7C-297++Degrees+F+to+300++Degrees+F&filters=attrs&gwwRemoveElement=true>

[7] <https://whatispiping.com/cryogenic-piping/>

[8] https://www.techapps.com/hs-fs/hub/165629/file-18313511-pdf/documents/technical_paper_cost-efficient_storage_of_cryogens.pdf

[9] http://www.sah.rs/media/sah/techdocs/te-w_manual.pdf

[10] https://v1.cecdn.yun300.cn/100001_1908285038/HDP500%20Small%20Pressure%20Transmitter.pdf

[11] <https://smstork.com/uploads/files/urunlerimiz/S9610-EN.pdf>

- Project 7_ Ashes recycling references

[1] <http://www.tonheflow.com/product/detail/35>

[2] <http://www.tonheflow.com/uploads/soft/20211213/1639383694.pdf>

- [3] <http://www.tonheflow.com/product/detail/88>
- [4] <http://www.motorized-valve.com/brass-motorized-valve/A20-T25-B2-C-DN25-1-inch-DC12V-brass-NPT-motorized-ball-valves-electric-ball-valve.html>
- [5] http://www.technideal.com/uploads/Products/product_642/Automate_DVP-SX2.pdf
- [6] <https://datasheet.octopart.com/DVP04DA-S-Delta-Product-Groups-datasheet-13046264.pdf>
- [7] <http://www.ultisensor.com/product/30.html>

